

INFORMATION TO USERS

This manuscript has been reproduced from the microfilm master. UMI films the text directly from the original or copy submitted. Thus, some thesis and dissertation copies are in typewriter face, while others may be from any type of computer printer.

The quality of this reproduction is dependent upon the quality of the copy submitted. Broken or indistinct print, colored or poor quality illustrations and photographs, print bleedthrough, substandard margins, and improper alignment can adversely affect reproduction.

In the unlikely event that the author did not send UMI a complete manuscript and there are missing pages, these will be noted. Also, if unauthorized copyright material had to be removed, a note will indicate the deletion.

Oversize materials (e.g., maps, drawings, charts) are reproduced by sectioning the original, beginning at the upper left-hand corner and continuing from left to right in equal sections with small overlaps.

Photographs included in the original manuscript have been reproduced xerographically in this copy. Higher quality 6" x 9" black and white photographic prints are available for any photographs or illustrations appearing in this copy for an additional charge. Contact UMI directly to order.

Bell & Howell Information and Learning
300 North Zeeb Road, Ann Arbor, MI 48106-1346 USA
800-521-0600

UMI[®]

ENERGY SHAPING AND DISSIPATION:
UNDERWATER VEHICLE STABILIZATION
USING INTERNAL ROTORS

Craig Woolsey

A DISSERTATION
PRESENTED TO THE
FACULTY OF PRINCETON UNIVERSITY
IN CANDIDACY FOR THE DEGREE
OF DOCTOR OF PHILOSOPHY

RECOMMENDED FOR ACCEPTANCE BY THE
DEPARTMENT OF
MECHANICAL AND AEROSPACE ENGINEERING

JANUARY, 2001

UMI Number: 9995814

UMI[®]

UMI Microform 9995814

Copyright 2001 by Bell & Howell Information and Learning Company.

All rights reserved. This microform edition is protected against
unauthorized copying under Title 17, United States Code.

Bell & Howell Information and Learning Company
300 North Zeeb Road
P.O. Box 1346
Ann Arbor, MI 48106-1346

© Copyright by Craig Arthur Woolsey, 2001. All rights reserved.

Abstract

This dissertation concerns nonlinear feedback stabilization of mechanical systems using energy-based methods. Nonlinear techniques are appealing because they can yield large regions of attraction for feedback-stabilized equilibria. Energy-based methods are particularly attractive for mechanical systems because these methods preserve a physical view of a system's dynamics and because they yield Lyapunov functions. For conservative systems, proof of stability typically requires the existence of a Lyapunov function. For systems with damping, Lyapunov functions can be used to design feedback dissipation to ensure or enhance asymptotic stability and to obtain more global conclusions.

Both as a case study of a particular control methodology and as a practical contribution in the area of underwater vehicle control, we consider stabilization of an underwater vehicle using internal rotors as actuators. The methodology used to develop stabilizing control laws consists of three steps. The first step involves shaping the kinetic energy of the conservative dynamics. For the underwater vehicle, the control term in this step may be interpreted as modifying the system inertia. In the second step, feedback dissipation is designed based on a Lyapunov function developed in the first step. In the third step, it is verified that the effect of external damping due to viscous forces does not destroy the stability results. This method is applied first to a vehicle whose centers of gravity and buoyancy coincide and then to a vehicle with noncoincident centers of gravity and buoyancy.

The method of controlled Lagrangians, developed in recent years, is a generalization of the idea of kinetic energy shaping. The method applies to underactuated mechanical systems (systems with more degrees of freedom than independent actuators). Motivated

by the results of the investigation into the effect of external damping on an underwater vehicle with internal rotors, we study the effect of damping on more general systems which have been stabilized, in the conservative approximation, using the method of controlled Lagrangians. A significant result of this inquiry is that, for certain classes of systems, damping in the unactuated directions enhances stability by driving the unactuated dynamics to their desired equilibrium value. Damping in the controlled directions may be detrimental but can be directly compensated for through feedback. Thus, with an appropriate choice of feedback dissipation, these systems may be asymptotically stabilized even in the presence of physical damping.

for Sarah

*May your nightingale sing sweetly,
may your rainbow shine brightly,
and may every unicorn that you find
be joyful and content.*

Acknowledgements

I am deeply indebted to my adviser and mentor, Naomi Ehrich Leonard, for her free devotion of time and thought, her extraordinary patience, and her enduring optimism. I am blessed and honored to be her student.

I also wish to thank the faculty of the Mechanical and Aerospace Engineering Department, particularly the members of the Dynamics and Control Group. Thanks especially to Pat Curtiss, Phil Holmes, and Mike Littman for serving on my Ph.D. committee and for liberally sharing their time and ideas. Thanks also to Phil and to Jeremy Kasdin for their very helpful criticisms of this dissertation.

I owe special thanks to Jerry Marsden at CalTech and to Tony Bloch at the University of Michigan for helping to broaden the scope of my research. I also thank Richard Murray at CalTech and Francesco Bullo at the University of Illinois for the many enlightening discussions about locomotion of mechanical systems on Lie groups. And I thank Larry Jacobs at Georgia Tech for setting me on this course in the first place.

In the Dynamical Control Systems Laboratory, Ralf Bachmayer, Albert Chang, Eddie Fiorelli, Josh Graver, and Jeff Jenkins have been great friends and colleagues. I also thank John Schmitt for his friendship and for the "software support." For many valuable reading group discussions, I thank Dong Eui Chang, Monique Chyba, Dan Grossman, and Sunita Vatuk. Thanks also to Monique for her thorough review of parts of this dissertation.

Thanks to the many administrators and staff members who have helped me all these years. I especially thank George Miller, Glenn Northey, Bob Sorenson, and Mike Vocaturo for their help with the various experimental projects that I have pursued. Thanks also to the various Princeton alumnae and alumni who, as undergraduates, contributed to the progress of the Dynamical Control Systems Lab and to my own progress toward a degree.

In particular, I thank Sarah Bergbreiter, Stephen Lee, and Carl Riccadonna.

Finally, I thank my family for their love and encouragement, especially my parents, Carter and Joan, and my wife's parents, Dale and Cynthia. My sister Karen and her husband Steve continue to be my role models. More than anyone, I thank my wife Sarah for accompanying me on this adventure.

Contents

1	Introduction	1
2	Mathematical Preliminaries: Lie Groups in Mechanics	8
2.1	Basic Differential Geometry	9
2.2	Lie Groups and Group Actions	15
2.3	Reduction by Symmetry	26
2.4	Stability of Equilibria	36
2.5	Summary	40
3	Underwater Vehicle Dynamics	42
3.1	Underwater Vehicle Equations of Motion	43
3.1.1	Rigid Body in an Ideal Fluid	43
3.1.2	Internal Rotors	53
3.1.3	Viscous Forces	57
3.2	Stability of Relative Equilibria	58
3.2.1	Coincident Centers of Gravity and Buoyancy	59
3.2.2	Noncoincident Centers of Gravity and Buoyancy	62
3.3	Experimental Investigation of Stability	65

3.3.1	Viscous Flow Over a Prolate Spheroid	66
3.3.2	Experimental Setup	70
3.3.3	Experimental Results	75
4	Feedback Stabilization Using Internal Rotors	82
4.1	Coincident Centers of Gravity and Buoyancy	83
4.1.1	Stabilization of Steady Long Axis Translation	84
4.1.2	Asymptotic Stabilization	90
4.1.3	Viscous Forces and Global Asymptotic Stabilization	98
4.2	Noncoincident Centers of Gravity and Buoyancy	112
4.2.1	Asymptotically Stabilizing Steady Long Axis Translation	113
4.2.2	Viscous Forces and Asymptotic Stability	131
4.3	Simulations	138
5	Controlled Lagrangians and Dissipation	150
5.1	Review of the Method of Controlled Lagrangians	151
5.1.1	The Modified Lagrangian	151
5.1.2	The General Matching Conditions	156
5.1.3	Special Cases of Matching	161
5.2	Dissipation and General Matching Systems	164
5.2.1	The Effect of Generalized Forces on the Modified Energy	165
5.2.2	Example: The Pendulum on a Cart	173
5.2.3	Example: The Pendulum on a Rotor Arm	177
5.3	Dissipation and Euler-Poincaré Systems	184
5.3.1	The Effect of Generalized Forces on the Modified Energy	189

5.3.2	Example: The rigid spacecraft with one internal rotor	200
6	Conclusions and Future Work	212
6.1	Summary	213
6.2	Future Work	215
A	Discussion of Kirchhoff's Equations	218
B	Proof of Theorem 4.1.2	226
C	Translational Relative Equilibria: Noncoincident Centers	230
D	Dissipative Gains for Theorem 4.2.4	235
E	Identities Concerning the Method of Controlled Lagrangians	239
E.1	Modified Metric Under General Matching Conditions	239
E.2	Identities for $B_{\alpha\beta}$ and B_{ab}	241
E.3	Proof of Proposition 5.2.2.	242
F	Experimental Rotary Arm Pendulum	244
G	Computations for Spacecraft Example	247

List of Figures

2.1	Comparing a vector field at two points on G	17
3.1	Kinematics of a rigid body.	45
3.2	Vehicle with noncoincident CG and CB.	51
3.3	Vehicle with three internal rotors.	54
3.4	Bottom-heavy prolate spheroid with an internal rotor.	64
3.5	Subcritical flow (from left to right) over a 2.5:1 and 2:1 spheroid.	68
3.6	Asymmetrically separating flow.	69
3.7	Sample frame from experimental footage.	71
3.8	Experimental Internal Rotor.	74
3.9	Experimental data for the 4:1 ratio spheroid: $\gamma = 0$	75
3.10	Experimental data for the 4:1 ratio spheroid: $\gamma = \gamma_c$	76
3.11	Experimental data for the 4:1 ratio spheroid: $\gamma = 2\gamma_c$	78
3.12	Integral deviation e versus CG displacement.	79
3.13	Comparison of 3:1 spheroid experiments with an internal rotor.	80
4.1	Geometric view: $\dot{\mathbf{\Pi}} = \mathbf{0}$ and $\mathbf{\Pi} \times \mathbf{\Omega} \neq \mathbf{0}$	94
4.2	The negative semidefinite function V	102
4.3	Closed-loop system as a series connection.	123

4.4	Closed-loop response to a perturbation: $\mathbf{r} = \mathbf{0}$, no drag.	144
4.5	Closed-loop response to a perturbation: $\mathbf{r} = \mathbf{0}$, drag included.	145
4.6	Closed-loop state response to a perturbation: $\mathbf{r} \neq \mathbf{0}$, no drag.	146
4.7	Control torques and energy: $\mathbf{r} \neq \mathbf{0}$, no drag.	147
4.8	Closed-loop response to a perturbation: $\mathbf{r} \neq \mathbf{0}$, drag included.	148
4.9	Control torques and energy: $\mathbf{r} \neq \mathbf{0}$, drag included.	149
5.1	Decomposition of $T_q Q$ into horizontal and vertical subspaces.	153
5.2	Original and modified horizontal and vertical decompositions.	155
5.3	Pendulum on a cart.	174
5.4	Planar pendulum simulation with feedback dissipation.	176
5.5	Pendulum on a rotary arm.	178
5.6	Experimental apparatus.	182
5.7	Experimental results.	184
5.8	Closed-loop spacecraft response to an initial perturbation.	210
5.9	The Casimir and Lyapunov function.	210
6.1	First order approximation of a flexible pendulum.	217
A.1	Circulation.	218
A.2	Rigid body in a fluid.	221
C.1	Equilibrium values of \mathbf{P} given $\mathbf{\Pi}_e$, and C_1 with $C_3 = 0$	233
F.1	Elevation response to initial perturbation.	245
F.2	Azimuthal velocity response to initial perturbation.	246

Chapter 1

Introduction

Autonomous underwater vehicles are enjoying a great deal of attention from ocean scientists, who envision cost-effective mobile sensor arrays, and from control theorists, who see a rich test bed for advancing the art of control of mechanical systems. The work presented here is the result of pursuing two complementary goals:

1. to expand the performance capabilities for a class of underwater vehicles using a novel type of actuator, and
2. to demonstrate and augment the tools available from geometric mechanics for the design of stabilizing control laws for mechanical systems.

The former goal is a justified and challenging end unto itself. Traditional underwater vehicle actuators, such as propellers and fins, provide adequate control authority over a range of operating conditions. However, the increasingly ambitious requirements of the military, industry, and ocean scientists are pushing the conventional performance envelope. For example, the practical implementation of a proposed long-term, unmanned ocean sensing network [25] will require efficient, durable, and maneuverable vehicles which can resist or tolerate impairments which are often caused by the harsh ocean environment. Most current

vehicle prototypes use a traditional arrangement of a single thruster with four actuated tail fins. A drawback of this arrangement is that fin actuators lose their control authority at low velocity. While additional thrusters might be added to provide low-velocity control, these would increase the drag on the vehicle, reducing its efficiency and, therefore, its endurance. Furthermore, both actuated fins and thrusters are subject to corrosion and biological fouling. The inherent limitations of conventional actuators lead one to consider alternative or complementary means of actuation.

Internal actuators are an appealing complement to traditional thrusters and control surfaces. Controlled movable masses are already used to provide attitude control for a number of underwater vehicles, notably for underwater *gliders* such as SLOCUM [66] and ALBAC [36]. In [45], internal rotors were proposed for the purpose of stabilizing steady, long-axis translation of a slender vehicle. Movable masses and internal rotors do pose some design challenges, such as how to deal with saturation and how to size the actuators under internal space constraints. Previous successes in spacecraft and underwater vehicle applications help to allay these concerns. The potential benefits of using internal actuators are great enough to justify investigation.

Actuators which are internal to a vehicle are isolated from the ocean environment and are therefore less prone to damage, biological fouling, and decay than exposed actuators. Furthermore, internal actuators do not directly increase a vehicle's drag. Another practical benefit is that these actuators preserve the integrity of the vehicle housing; no wiring, cables, or drive shafts penetrate the hull. Finally, internal actuators do not use relative fluid motion to exert control and are thus useful at low and even zero velocity, thereby extending a vehicle's operating range.

To derive control laws for the underwater vehicle with internal rotors, one may use the expanding toolbox of nonlinear techniques available for controlling mechanical systems. Nonlinear control methods are appealing because, for example, they can lead to stabilizing control laws which are valid over large regions of phase space. Tools which preserve and exploit the nonlinear dynamics are particularly attractive. By retaining a physical view of the system dynamics, as opposed to the common technique of supplanting the dynamics with a linear system, one preserves prior insight into the uncontrolled dynamics. One might, for example, make use of stability-enhancing nonlinearities rather than attempt to cancel them.

For at least two decades, there has been a fecund interplay between nonlinear control theory and mechanics. Mechanical systems have enjoyed special focus because they are more readily analyzed than less structured systems. In [20], Brockett introduced the idea of a Hamiltonian control system. The idea of stabilizing unstable equilibria for such systems by using feedback to shape the potential energy was proposed in [63]. More recently, this idea has been extended to underactuated systems [34, 21]. In [43], symmetry-breaking potentials are used to stabilize a system with full configuration symmetry. Alternatively, one may consider shaping a system's kinetic energy in order to provide stability. The method of controlled Lagrangians is an algorithmic approach to kinetic energy shaping [17]. The technique is particularly appropriate for systems where there is insufficient control authority to shape the potential energy. The related method of interconnection and damping assignment, described in [57], builds on the authors' previous work on passivity-based control. Ideas based on passivity are appealing for control of mechanical systems since these systems are inherently passive. (See [56].) In contrast to the method of controlled Lagrangians, which is algorithmic for a system with admissible structure and inertia properties, the intercon-

nection and damping assignment approach produces a set of partial differential equations whose solution then implies an admissible control law. While there is no general guarantee of success, the technique has been applied to an underwater vehicle with the traditional fin and thruster arrangement [8].

Regardless of the approach to constructing a control law, the problem still remains to show Lyapunov stability. While there is no general approach to constructing Lyapunov functions for arbitrary nonlinear systems, there are a few techniques available for mechanical systems. Many of these techniques rely on or generalize the Lagrange-Dirichlet theorem on stability of equilibria of canonical Hamiltonian systems [50]. Briefly, the Lagrange-Dirichlet theorem states that an equilibrium which is either a local minimum or a local maximum of the Hamiltonian is stable. See [61] or [48] for a review of the available methods for proving stability of equilibria of mechanical systems. The primary stability analysis tool used in this dissertation is the energy-Casimir method, which is described in [50].

The basic underwater vehicle model used in this dissertation is ideal in the sense that the vehicle is treated as a rigid body immersed in an inviscid, irrotational, incompressible, fluid. Rotors spin within the vehicle under the influence of some control torque. The control problem considered is to define a state feedback control law which stabilizes steady, long-axis translation of an ellipsoidal vehicle. External forces such as viscous dissipation and thrust are appended to the conservative model in the last step of the control design process.

The ideal (conservative) model of an underwater vehicle generalizes the equations describing the motion of a spacecraft, a system which has long been a test bed for nonlinear control theory. In fact, the work of Krishnaprasad [40] and Bloch *et al* [13] on spacecraft stabilization using internal rotors inspired the kinetic energy shaping technique pursued in Chapter 4 for the underwater vehicle. These papers also led to the development of the

method of controlled Lagrangians. A crucial distinction between spacecraft and underwater vehicles is the presence of external damping. While a spacecraft is arguably free of external damping, an underwater vehicle's dynamics are distinctly affected by the viscosity of water. Since the ideal underwater vehicle model neglects viscous effects, analysis and control design based on this model is insufficient. In particular, one must be concerned that the effect of physical damping does not destabilize an equilibrium which has been stabilized for the conservative model [12]. In addition to the development and analysis of stabilizing feedback control laws for an underwater vehicle with internal rotors, a primary contribution of this dissertation is to consider the effect of physical damping on the closed-loop stability results obtained using the ideal model. This question of "robustness to dissipation" is then pursued for more general controlled Lagrangian systems.

Chapter 2 introduces the mathematical and physical fundamentals on which the results of the dissertation are based. First, a few basic ideas from differential geometry are introduced, such as smooth manifolds and vector fields. The Lie bracket of vector fields, which is also introduced, has played a primary role in the development of nonlinear control theory. The important idea of Poisson reduction allows one to express a canonical Hamiltonian system with configuration symmetry as a noncanonical Hamiltonian system on a lower-dimensional phase space. Similarly, Euler-Poincaré reduction may be applied in the Lagrangian framework. These techniques are relevant here because the underwater vehicle model used may be written as a reduced Hamiltonian (or reduced Lagrangian) system. The chapter also recalls certain results concerning stability of equilibria. The energy-Casimir method for proving Lyapunov stability and LaSalle's invariance principle are two important tools used throughout the work. To close the chapter, we summarize the tools and ideas which arise throughout the dissertation.

In Chapter 3, a model is introduced for an underwater vehicle with internal rotors. The model assumes an ellipsoidal vehicle, a very reasonable assumption for the types of vehicles currently being used to perform ocean sensing. We also introduce a general model of the viscous forces and torques that a vehicle might experience. A discussion of various uncontrolled relative equilibria and their stability properties is followed by the results of an experimental investigation intended to verify theoretical stability predictions and thereby validate the idealized model on which these predictions were based [42, 45]. In particular, the experimental results confirm stability predictions indicated for a bottom-heavy spheroid moving in the direction of gravity and for a spheroid with an internal rotor to provide gyroscopic stability.

Chapter 4 describes our approach and the results of active stabilization using internal rotors. We use a three-step approach to design a control law that stabilizes steady long-axis translation of an ellipsoidal vehicle [69, 68]. In the first step, the vehicle dynamics are treated as a Hamiltonian system, and a control law is proposed which stabilizes the desired motion by shaping the kinetic energy of the closed-loop system while preserving the underlying Hamiltonian structure. Constructive proof of Lyapunov stability relies on the Hamiltonian nature of the closed-loop system. The resulting Lyapunov function is used in the second step where we add feedback dissipation to ensure asymptotic stability of the desired steady motion. Using previous analysis of the uncontrolled dynamics [42, 31] and physical insight into the closed-loop system dynamics, we choose control gains that yield large regions of attraction. Finally, in the third step, we check that physical dissipation does not destroy the results. In fact, for the case where the vehicle's center of gravity and center of buoyancy coincide, viscous drag enhances stability of the feedback-stabilized system by providing global asymptotic stability (even without feedback dissipation). For

the case of noncoincident centers of gravity and buoyancy, the control design and analysis is understandably more complicated. The results are only local, but are similar in nature to the case of coincident centers; physical dissipation tends to enhance stability of the feedback-stabilized system.

Chapter 5 presents more recent and more general results on the effect of physical and feedback dissipation on systems stabilized using the method of controlled Lagrangians. For balance-type systems, such as the inverted pendulum on a cart, the key result is that generic linear damping in the unactuated directions is beneficial whereas damping in the controlled directions can be detrimental. Since drag in the controlled direction can be compensated for directly, appropriate feedback dissipation makes an equilibrium which is stable for the conservative model asymptotically stable in the presence of damping. A related result is given for relative equilibria of systems with symmetry.

Chapter 6 recapitulates the major contributions and suggests some avenues for future investigation.

Chapter 2

Mathematical Preliminaries:

Lie Groups in Mechanics

This section introduces concepts and tools which are used throughout the work and also serves to set notation. A coherent development requires some ideas from geometric mechanics and the theory of Lie groups. Ideas from differential geometry are already in general use among dynamicists and a growing community of nonlinear control theorists. However, the topic is not yet familiar to the larger control community. Common texts on differential geometry include those of Spivak [62] and Nomizu [55]. Boothby [19] gives a suitably thorough, but very readable introduction to the topic. In their development of geometric control theory, Nijmeijer and van der Schaft [54] review differential geometry with a convenient balance of brevity and rigor.

As for the use of differential geometry in physics, Arnold [6] gives an accessible review of classical mechanics from a geometric perspective. Abraham and Marsden [1] provide a detailed account of geometric mechanics while Marsden and Ratiu [50] focus on the important role of symmetry in simplifying and characterizing solutions to a broad range of mechanics

problems. Both of these latter two references explore various problems of mathematical physics in which Lie groups naturally arise and each includes a suitable introduction to the theory of Lie groups. For a more thorough introduction to Lie groups, one might refer to Warner [65], for example.

In Section 2.1, we introduce some machinery necessary to discuss control of dynamical systems on smooth manifolds. In Section 2.2, we consider the important special case where the smooth manifold is a Lie group. Mechanical systems on Lie groups possess a great deal of structure which can be exploited in control design and stability analysis. When such a system exhibits symmetry, or invariance under certain actions, the equations describing the system motion can simplify considerably. In Section 2.3, we describe the process of reduction by symmetry. Reduction can be performed in either the Hamiltonian or the Lagrangian setting; both perspectives arise throughout the dissertation. Section 2.4 reviews some well-known facts about stability of equilibria, notably Lyapunov's two methods for proving stability and LaSalle's invariance principle, which extends Lyapunov's results. The section also describes an important tool, the energy-Casimir method, for studying stability of equilibria of reduced Hamiltonian systems. The technique plays a central role in this work because it provides Lyapunov functions for feedback-stabilized equilibria. Section 2.5 reviews the ideas and techniques most relevant to the dissertation.

2.1 Basic Differential Geometry

This section presents a very brief introduction to differential geometry which parallels the development in Appendix A of Murray, Li, and Sastry [53]. Their treatment is in turn based on Boothby [19].

The configuration of a given dynamical system can often be described as a point in

a smooth manifold. An n -dimensional manifold M is a topological space¹ which looks locally like n -dimensional Euclidean space: there is a continuous map with a continuous inverse, a *homeomorphism*, from some open neighborhood of each point in M to an open neighborhood of \mathbb{R}^n . Let ϕ and ψ be two such homeomorphisms from two open sets U and V in M , respectively. Suppose that U and V overlap and define $W = U \cap V$. If $\psi^{-1} \circ \phi$ is a *diffeomorphism* (a smooth map with a smooth inverse) from $\psi(W)$ to $\phi(W)$, then the local coordinate charts (ϕ, U) and (ψ, V) are called C^∞ *related*. The manifold M is said to be *smooth* if it can be covered by a collection of C^∞ related charts. Such a collection of charts is called a *smooth atlas*.

In the special case that M is a submanifold embedded in a Euclidean space of higher dimension, the notion of a vector tangent to M is intuitive. Let $c(t)$ be a smooth curve in M parameterized over an interval $t \in (-\epsilon, \epsilon)$ where $\epsilon > 0$. If, for example, t represents time then $c(t)$ might describe a portion of a trajectory of a dynamical system whose configuration space is M . The velocity vector $\dot{c}(0)$ is a vector tangent to M at $c(0)$, where $\dot{c}(t)$ is the derivative of $c(t)$ taken in the ambient Euclidean space. More generally, without considering M as embedded in a Euclidean space, a tangent vector to M at a point p is given by an equivalence class of curves passing through p and tangent to each other at that point.

The set of all vectors tangent to M at a point $p \in M$ forms a vector space called the tangent space to M at p and denoted $T_p M$. While an element $X_p \in T_p M$ can certainly be thought of as a vector tangent to M in the sense described above, it plays a dual role as an operator. In fact, the tangent space to a manifold is often defined as a vector space of operators with the tangent vector defined simply as an element of that space, i.e., a particular operator. Toward this alternative description, let $C^\infty(p)$ denote the space of

¹Technically, one requires a Hausdorff topological space with a countable basis. See [2].

smooth functions defined in a neighborhood of a point $p \in M$. The *tangent space* $T_p M$ is the vector space of linear maps $X_p : C^\infty(p) \rightarrow \mathbb{R}$ which satisfy the Leibniz rule,

$$X_p(fg) = (X_p f)g(p) + f(p)(X_p g), \quad f, g \in C^\infty(p). \quad (2.1)$$

Such a map X_p is called a *derivation at p* . A derivation at p defines a unique *tangent vector* to M at p . Defining local coordinates (x_1, \dots, x_n) on M , one may write X_p in a corresponding basis $(\frac{\partial}{\partial x_1}, \dots, \frac{\partial}{\partial x_n})$ on $T_p M$ as

$$X_p = X_1 \frac{\partial}{\partial x_1} + \dots + X_n \frac{\partial}{\partial x_n}.$$

This conventional notation underscores the tangent vector's role as an operator; in coordinates, a derivation corresponds to a directional derivative. When the choice of coordinates is clear, the tangent vector X_p may be written simply as the column vector $[X_1, \dots, X_n]^T$.

The union of all tangent spaces to M forms a $2n$ -dimensional manifold TM , the *tangent bundle* of M . The term bundle reflects the broader geometric notion of a *vector bundle*. A vector bundle is a set which can be described as a collection of *fibers* over a lower-dimensional *base space*. Each fiber is a vector space whose elements project to a unique point in the base space. In the present example, $T_p M$ is the n -dimensional fiber over the point p in the base space M . If M represents the configuration space of a mechanical system, then TM represents the system's velocity phase space. An element $(p, X_p) \in TM$ is an admissible configuration/velocity pair.

Having defined the tangent space to a manifold M at a point p , we may define the cotangent space $T_p^* M$ as the dual space to $T_p M$. Thus, $T_p^* M$ is an n -dimensional vector space whose elements ω_p map tangent vectors X_p to the real numbers. This natural pairing

between tangent and cotangent vectors is denoted $\langle \cdot, \cdot \rangle: T_p^*M \times T_pM \rightarrow \mathbb{R}$. Given the above basis for T_pM , the dual basis on T_p^*M is denoted (dx_1, \dots, dx_n) where the basis elements are defined by the requirement

$$\langle dx_i, \frac{\partial}{\partial x_j} \rangle = \delta_{ij}, \quad i, j = 1, \dots, n.$$

A cotangent vector ω_p is written

$$\omega_p = \omega_1 dx_1 + \dots + \omega_n dx_n.$$

When the coordinate choice is clear, ω_p may simply be written as the row vector $[\omega_1, \dots, \omega_n]$.

The union of all cotangent spaces to M forms a $2n$ -dimensional manifold T^*M , the *cotangent bundle* of M . If M represents the configuration space of a mechanical system, then T^*M represents the system's momentum phase space. An element $(p, \omega_p) \in T^*M$ is an admissible configuration/momentum pair.

Example: The Simple Pendulum. The configuration of a simple planar pendulum is uniquely described by a point in the smooth manifold S^1 , the unit circle. The tangent space to S^1 at any given point is the real line \mathbb{R} . Each copy of \mathbb{R} defines a fiber above a point in S^1 . The tangent bundle is diffeomorphic to a cylinder $TS^1 = S^1 \times \mathbb{R}$. (See page 164 of [2].) Any point on the cylinder represents an admissible pendulum angle and velocity. The cotangent bundle T^*S^1 is also diffeomorphic to a cylinder; any point in T^*S^1 represents an admissible pendulum angle and momentum. \square

A *Riemannian metric* on a manifold M is a smooth map that associates an inner product $\ll \cdot, \cdot \gg_p$ to each tangent space T_pM . Endowed with such a metric, M is called a *Riemannian manifold*. The Riemannian metric provides a map between the tangent and

cotangent spaces at a given point $p \in M$ by identifying with each element $X_p \in T_p M$ a unique cotangent vector $\omega_p := \ll X_p, \cdot \gg \in T_p^* M$ defined by requiring

$$\ll X_p, Y_p \gg = \langle \omega_p, Y_p \rangle$$

for all $Y_p \in T_p M$. If M is the configuration space of a dynamical system, such a correspondence between $T_p M$ and $T_p^* M$ defines the relationship between velocity (X_p) and momentum (ω_p).

The *differential* of a function f at a point $p \in M$ is a cotangent vector defined by the identity

$$\langle df(p), X_p \rangle = X_p(f)$$

for all tangent vectors X_p at p . If x represents local coordinates (x_1, \dots, x_n) on M , then

$$df(x) = \left[\frac{\partial f}{\partial x_1}(x), \dots, \frac{\partial f}{\partial x_n}(x) \right].$$

If M is a Riemannian manifold, the *gradient* of the function f satisfies the identity

$$\ll \text{grad} f, X_p \gg = \langle df(p), X_p \rangle = X_p(f)$$

for all $X_p \in T_p M$. In the simplest case that M is a Euclidean space endowed with the standard Euclidean metric, one finds that $\text{grad} f(x) = df(x)^T$.

As stated previously, the equations describing the motion of a dynamical system may often be defined with respect to some smooth configuration manifold M . A *vector field* X on a manifold M assigns a tangent vector X_p to each point p in the manifold. The vector field is called *smooth* if X may be written locally as $X(x) = [X_1(x), \dots, X_n(x)]^T$ where each

component function is smooth. A curve $c(t)$ is called an *integral curve* of X if

$$\dot{c}(t) = X(c(t)). \quad (2.2)$$

Equation (2.2) defines the equations of motion for a dynamical system; any system trajectory is an integral curve of X . The *flow* of a vector field over an interval $t \in (-\epsilon, \epsilon)$ where $\epsilon > 0$ is a one-parameter family of maps $\phi_t : M \rightarrow M$ such that $\phi_t(x)$ is the unique integral curve of X passing through x at time $t = 0$. For a linear vector field, the flow is the familiar state transition matrix.

Let X be a vector field on M and define for a function $f \in C^\infty(M)$ the new function $\mathcal{L}_X f$ given by

$$\mathcal{L}_X f(p) = X_p(f).$$

The function $\mathcal{L}_X f$ is called the Lie derivative of f with respect to the vector field X . Given two smooth vector fields X and Y , one may take successive Lie derivatives of f , for example $\mathcal{L}_X(\mathcal{L}_Y f)$ or $\mathcal{L}_Y(\mathcal{L}_X f)$. In general, neither $\mathcal{L}_X(\mathcal{L}_Y f)(p)$ nor $\mathcal{L}_Y(\mathcal{L}_X f)(p)$ can be written as a derivation acting on f at the point $p \in M$. However, $\mathcal{L}_X(\mathcal{L}_Y f)(p) - \mathcal{L}_Y(\mathcal{L}_X f)(p)$ is a derivation at p . Therefore, the object $[X, Y]$ defined by the function

$$[X, Y](f) := \mathcal{L}_X(\mathcal{L}_Y f) - \mathcal{L}_Y(\mathcal{L}_X f) \quad (2.3)$$

is a vector field. The operation $[\cdot, \cdot]$ is called the *Lie bracket* of vector fields.

The space $\mathfrak{X}(M)$ of all smooth vector fields on a manifold M is a vector space. In fact, $\mathfrak{X}(M)$ together with the Lie bracket of vector fields forms a *Lie algebra*. A Lie algebra V is a vector space V endowed with a bilinear, skew-symmetric operator, the Lie bracket $[\cdot, \cdot]$

on V , which satisfies the Jacobi identity,

$$[[u, v], w] + [[w, u], v] + [[v, w], u] = 0 \quad \text{for all } u, v, w \in V.$$

In analogy to vector fields on M , there is the dual notion of a covector field, or more generally of a differential form. A smooth *differential one-form* α on M assigns a cotangent vector to each point in the manifold. Locally, $\alpha(x) = [\alpha_1(x), \dots, \alpha_n(x)]$ where each component is a smooth function. Considering the natural pairing between tangent vectors and cotangent vectors, one may think of α as an operator that maps a tangent vector to a real number. More generally, a differential n -form maps n tangent vectors to a real number.

2.2 Lie Groups and Group Actions

This section is primarily based on the discussion in Marsden and Ratiu [50]. The reader might refer to that text for a more thorough presentation as well as a number of illustrative examples of physical significance.

A *Lie group* G is a group which is also a smooth manifold and for which group multiplication and inversion are smooth operations. Only finite-dimensional Lie groups will be considered in this dissertation. It is helpful to consider the class of Lie groups whose elements are representable as matrices. The group operation for a matrix Lie group is simply matrix multiplication.

Since one group element $g \in G$ may act on another element $h \in G$ on the left or on the right, one defines *left* and *right translation*, respectively,

$$L_g : G \rightarrow G; \quad h \mapsto gh$$

$$R_g : G \rightarrow G; h \mapsto hg.$$

If every group element g commutes with every other element h , then $L_g = R_g$ for all $g \in G$ and the group is called *Abelian*. Given that (left or right) translation maps one point in the manifold G to another point, the action induces a natural map from the tangent space at one point to the tangent space at another point,

$$T_h L_g : T_h G \rightarrow T_{gh} G$$

$$T_h R_g : T_h G \rightarrow T_{hg} G.$$

These maps are referred to as the tangent lift of left and right translation, respectively, or more briefly as the left and right tangent map. To compute these maps explicitly, consider a smooth curve $c(t) \in G$ defined on an interval $t \in (-\epsilon, \epsilon)$ such that $c(0) = h$. Then $\dot{c}(0) \in T_h G$ and one finds that

$$T_h L_g(\dot{c}(0)) = \frac{d}{dt} [L_g(c(t))]_{t=0}$$

$$T_h R_g(\dot{c}(0)) = \frac{d}{dt} [R_g(c(t))]_{t=0}.$$

For obvious reasons, the tangent map is also referred to as the *derivative map*. For a matrix Lie group, the left (right) tangent map is given by left (right) matrix multiplication.

The left and right tangent maps provide a means of comparing vectors in different tangent spaces on the same manifold. A vector field X on G is called *left invariant* under the action of G if

$$T_h L_g(X(h)) = X(L_g(h))$$

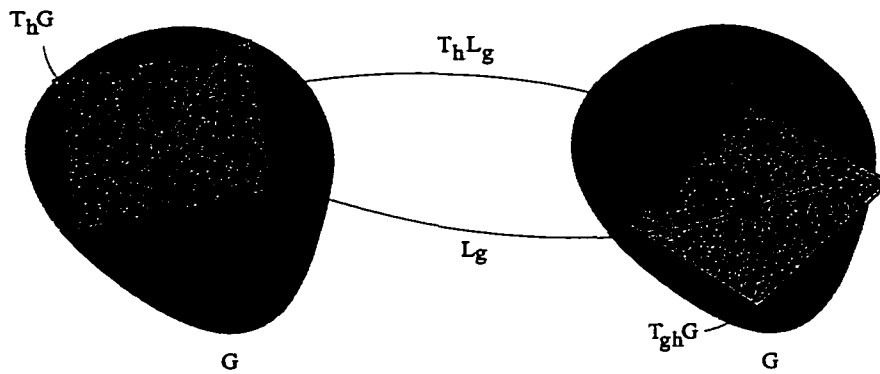


Figure 2.1: Comparing a vector field at two points on G .

for every $h \in G$. Figure 2.1 depicts left translation of a point h and the left tangent map of a vector $X(h)$. The vector field X is left invariant if the two vectors shown at the point gh coincide for every g and $h \in G$.

Right invariant vector fields are defined analogously. For a dynamical system, left or right invariance of the vector field defining the equations of motion reflects a symmetry in the system configuration. Such symmetries are advantageous since they typically allow one to simplify the dynamic equations.

A given left or right invariant vector field on a Lie group G can be entirely described by mapping a single vector at a single point to each tangent space using the left or right tangent map, respectively. For example, if X is a left invariant vector field, one may reproduce the entire vector field by applying the map $T_e L_g$ to the single vector $X(e)$ for each $g \in G$. (By convention, e denotes the identity element in G .) In fact, one may obtain any left or right invariant vector field on G by this same process. Given a vector $\xi \in T_e G$, define a left invariant vector field X_ξ on G as

$$X_\xi(g) = T_e L_g(\xi).$$

This procedure generates the entire set of left invariant vector fields on G . The set of left invariant vector fields on G is also a vector space, denoted $\mathfrak{X}_L(G)$, and is isomorphic to T_eG . The Lie bracket (2.3) of two left invariant vector fields is itself left invariant. Thus, $\mathfrak{X}_L(G)$ is a Lie algebra under the Lie bracket of vector fields. Similarly, the vector space $\mathfrak{X}_R(G)$ of right invariant vector fields on G is a Lie algebra. ($\mathfrak{X}_L(G)$ and $\mathfrak{X}_R(G)$ are Lie subalgebras of the Lie algebra $\mathfrak{X}(G)$ of all smooth vector fields on G .) Since both $\mathfrak{X}_L(G)$ and $\mathfrak{X}_R(G)$ are isomorphic to T_eG , each induces a Lie algebra there by providing a Lie bracket. In the left invariant case, one defines the Lie bracket of two elements $\xi, \eta \in T_eG$ by

$$[\xi, \eta] = [X_\xi, X_\eta](e) \quad (2.4)$$

where X_η is defined analogously to X_ξ . The vector space T_eG together with the operation (2.4) constitutes the *Lie algebra of G* which is denoted \mathfrak{g} . Elements of the Lie algebra of a matrix Lie group may also be represented by matrices. In this case, the Lie bracket is matrix commutation $[\xi, \eta] = \xi\eta - \eta\xi$.

Example: The Lie Algebra of $SO(3)$. The special orthogonal group

$$SO(3) = \{\mathbf{R} \in \mathbb{R}^{3 \times 3} \mid \mathbf{R}^{-1} = \mathbf{R}^T, \det(\mathbf{R}) = 1\}.$$

describes the set of proper rotations. This Lie group is well-studied within geometric mechanics. Besides providing a mathematically rich example, $SO(3)$ is of practical interest because it is the configuration space for the free rigid body.

To determine the Lie algebra associated with $SO(3)$, one examines the tangent space to the group at the identity. The identity element in $SO(3)$ is the 3×3 identity matrix which

is denoted \mathcal{I} . Differentiating the relationship $\mathbf{R}^T \mathbf{R} = \mathcal{I}$ gives

$$\dot{\mathbf{R}}^T \mathbf{R} + \mathbf{R}^T \dot{\mathbf{R}} = (\mathbf{R}^T \dot{\mathbf{R}})^T + \mathbf{R}^T \dot{\mathbf{R}} = \mathbf{0},$$

so $\mathbf{R}^T \dot{\mathbf{R}}$ is skew-symmetric. Evaluating at the identity, one finds that the Lie algebra corresponding to $SO(3)$ is the space of 3×3 skew-symmetric matrices,

$$\mathfrak{so}(3) = \{\mathbf{A} \in \mathbb{R}^{3 \times 3} \mid \mathbf{A}^T = -\mathbf{A}\}.$$

One may identify $\mathfrak{so}(3)$ with \mathbb{R}^3 by means of an operator $\hat{\cdot}$ defined by the identity $\hat{\mathbf{x}}\mathbf{y} = \mathbf{x} \times \mathbf{y}$ for $\mathbf{x}, \mathbf{y} \in \mathbb{R}^3$. Let $\hat{\mathbf{\Omega}} = \mathbf{R}^T \dot{\mathbf{R}}$. Emphasizing the connection between the group $SO(3)$ and rigid body dynamics, the matrix $\hat{\mathbf{\Omega}}$, or equivalently the vector $\mathbf{\Omega}$, is called the *body angular velocity*. Since $SO(3)$ is a matrix Lie group, the Lie bracket on $\mathfrak{so}(3)$ is matrix commutation, as mentioned previously.

A left invariant vector field on $SO(3)$ can be obtained by applying the tangent map to left translation to an element $\hat{\mathbf{\Omega}} \in \mathfrak{so}(3)$,

$$X_{\hat{\mathbf{\Omega}}}(\mathbf{R}) = T_{\mathcal{I}}L_{\mathbf{R}}\hat{\mathbf{\Omega}} = \mathbf{R}\hat{\mathbf{\Omega}}$$

for each $\mathbf{R} \in SO(3)$. This is the same vector field describing the time evolution of \mathbf{R} ,

$$\dot{\mathbf{R}} = X_{\hat{\mathbf{\Omega}}}(\mathbf{R}) = \mathbf{R}\hat{\mathbf{\Omega}}.$$

□

Notice that the Lie bracket of vector fields (2.3) is a differential computation whereas (2.4) is an algebraic computation. Thus, certain problems on $\mathfrak{X}_L(G)$ may be simplified by

“transferring” those problems to \mathfrak{g} . As an example, determining nonlinear controllability of a given system typically involves computing Lie brackets of the various vector fields describing the controlled system dynamics. However, if the configuration manifold is a Lie group and the vector fields are left invariant, the question of controllability can be answered through much simpler algebraic computations.

Since an element $\xi \in \mathfrak{g}$ induces a left invariant vector field X_ξ on G and this vector field induces a flow on G , there is a natural correspondence between elements in \mathfrak{g} and elements in G . Let $\phi_\xi(t)$ denote the integral curve of X_ξ which passes through e at time $t = 0$. The *exponential map* takes $t\xi \in \mathfrak{g}$ (for some $t \in \mathbb{R}$) and returns $\phi_\xi(t) \in G$. For a matrix Lie group, the exponential map is a matrix exponential,

$$\exp t\xi = \sum_{n=0}^{\infty} \frac{(t\xi)^n}{n!}.$$

The exponential map is a diffeomorphism between a neighborhood of $0 \in \mathfrak{g}$ and a neighborhood of $e \in G$. One may thus think of \mathfrak{g} as providing a local coordinate chart for G at the identity. But, by translation, any element in G can be reached from a neighborhood of the identity so this local chart extends to form an atlas on G . The inverse of the exponential map (where it is defined) is appropriately referred to as the *logarithmic map*.

Example: The Exponential Map from $\mathfrak{so}(3)$ to $SO(3)$. An element $\hat{\Omega} \in \mathfrak{so}(3)$ corresponds to the element of $SO(3)$

$$\exp(\hat{\Omega}) = \sum_{n=0}^{\infty} \frac{\hat{\Omega}^n}{n!}.$$

The exponential map of $\hat{\Omega}$ is a rotation about the vector Ω of magnitude $\|\Omega\|$. (See [53] for a proof as well as a simpler formula due to Rodrigues.) \square

It has already been shown how Lie groups act on themselves by translation. More generally, one may consider the action of a Lie group G on a smooth manifold M . A *left action* of G on M is a smooth mapping $\Phi : G \times M \rightarrow M$ such that $\Phi(e, x) = x$ and $\Phi(g, \Phi(h, x)) = \Phi(L_g h, x)$ for all $x \in M$ and all $g, h \in G$. A *right action* is defined analogously. The *orbit* of an action Φ through a point $x \in M$ is the subset of M which can be reached from x under the action Φ ,

$$\text{Orb}(x) = \{\Phi(g, x) \mid g \in G\}. \quad (2.5)$$

A group G_x of actions which leave a point $x \in M$ invariant is called an *isotropy group*,

$$G_x := \{g \in G \mid \Phi(g, x) = x\}. \quad (2.6)$$

The action Φ is called *free* if $G_x = \{e\}$ for every $x \in M$. That is, the action is free if $\Phi(g, x)$ leaves no point $x \in M$ fixed whenever $g \neq e$. The action is called *proper* if the corresponding map $\tilde{\Phi} : G \times M \rightarrow M \times M$ defined by $\tilde{\Phi}(g, x) = (x, \Phi(g, x))$ is proper. (If G and M are finite-dimensional, “properness” of $\tilde{\Phi}$ implies that $\tilde{\Phi}^{-1}(K)$ is compact for any compact subset $K \subset M \times M$.)

For finite-dimensional Lie groups, the set of orbits of a free and proper action Φ defines a bundle structure on M . In this case, each orbit is a fiber over a point in the base or *orbit space* M/G , which is itself a smooth submanifold of M . As a rather trivial example, suppose $M = G$ and the action is left translation. Then $\text{Orb}(g) = G$ since any other point $h \in G$ can be reached by the action $L_{hg^{-1}}$. In this case, $M/G = G/G$ is a single point. More interesting examples will follow in this and later sections.

Following are some important Lie group actions.

1. G acting on G : Left or right translation, L_g or R_g .
2. G acting on G : Conjugation, $I_g := L_g \circ R_{g^{-1}}$.
3. G acting on \mathfrak{g} : Adjoint action, $\text{Ad}_g := T_e I_g$.
4. G acting on \mathfrak{g}^* : Coadjoint action, $\text{Ad}_{g^{-1}}^* := (T_e I_{g^{-1}})^*$ where $*$ denotes the linear algebraic dual. That is, $\langle \text{Ad}_{g^{-1}}^* \alpha, \xi \rangle = \langle \alpha, \text{Ad}_{g^{-1}} \xi \rangle$ for all $\alpha \in \mathfrak{g}^*$ and $\xi \in \mathfrak{g}$.

Note that each of the actions 2 through 4 ultimately derives from simple translation. The conjugation operator 2, also called the *inner automorphism*, is a generalization of the similarity transformation in matrix algebra. Since I_g maps the identity element back to itself, the tangent map to I_g at the identity maps elements in \mathfrak{g} back into \mathfrak{g} . This map $T_e I_g$ defines the adjoint action on \mathfrak{g} . The coadjoint action of G on \mathfrak{g}^* is given by the dual of the adjoint action of g^{-1} on \mathfrak{g} for $g \in G$.

The adjoint action is particularly useful for computing the Lie bracket on \mathfrak{g} ; differentiating $\text{Ad}_g \eta$ with respect to g at the identity in the direction ξ gives the Lie bracket $[\xi, \eta]$. Given an element $\xi \in \mathfrak{g}$, one may define the operation

$$\text{ad}_\xi(\cdot) := [\xi, \cdot] : \mathfrak{g} \rightarrow \mathfrak{g}. \quad (2.7)$$

The notation underscores the relationship between the adjoint action and the Lie bracket on \mathfrak{g} . One may also define the operation

$$\text{ad}_\xi^*(\cdot) : \mathfrak{g}^* \rightarrow \mathfrak{g}^*$$

as the linear algebraic dual of ad_ξ :

$$\langle \text{ad}_\xi^*(p), \eta \rangle = \langle p, \text{ad}_\xi(\eta) \rangle \quad (2.8)$$

where $\xi, \eta \in \mathfrak{g}$ and $p \in \mathfrak{g}^*$

Example: The adjoint action of $SO(3)$ on $\mathfrak{so}(3)$. Let $\hat{\Omega}_1 \in \mathfrak{so}(3)$ and let $R_1(t)$ be a curve in $SO(3)$ such that $R_1(0) = \mathcal{I}$ and $\dot{R}_1(0) = \hat{\Omega}_1$. By the definition of the adjoint action on page 22,

$$\begin{aligned} \text{Ad}_R \hat{\Omega}_1 &= T_{\mathcal{I}}(L_R \circ R_{R^{-1}}) \hat{\Omega}_1 \\ &= \left. \frac{d}{dt} (R R_1(t) R^T) \right|_{t=0} \\ &= R \hat{\Omega}_1 R^T \end{aligned} \quad (2.9)$$

for an element $R \in SO(3)$.

To compute the Lie bracket on $\mathfrak{so}(3)$, suppose that $R_2(t) \in SO(3)$ satisfies $R_2(0) = \mathcal{I}$ and $\dot{R}_2(0) = \hat{\Omega}_2$. Differentiating $\text{Ad}_{R_2} \hat{\Omega}_1$ with respect to time at $t = 0$ gives the Lie bracket,

$$\begin{aligned} [\hat{\Omega}_2, \hat{\Omega}_1] = \text{ad}_{\hat{\Omega}_2}(\hat{\Omega}_1) &= \left. \frac{d}{dt} (R_2 \hat{\Omega}_1 R_2^T) \right|_{t=0} \\ &= \hat{\Omega}_2 \hat{\Omega}_1 - \hat{\Omega}_1 \hat{\Omega}_2. \end{aligned}$$

As anticipated, the Lie bracket on $\mathfrak{so}(3)$ is matrix commutation. More conventionally, one identifies $\mathfrak{so}(3)$ with \mathbb{R}^3 and defines the operator $\text{ad}_\Omega : \mathbb{R}^3 \rightarrow \mathbb{R}^3$. Recognizing that

$$[\hat{\Omega}_2, \hat{\Omega}_1] = \widehat{\Omega_2 \times \Omega_1},$$

it follows that

$$\text{ad}_{\Omega_2}(\Omega_1) = \Omega_2 \times \Omega_1 = \hat{\Omega}_2 \Omega_1$$

and therefore that

$$\text{ad}_{\Omega}(\cdot) = \hat{\Omega} \tag{2.10}$$

for $\Omega \in \mathbb{R}^3$. We can find ad_{Ω}^* from equation (2.8),

$$\begin{aligned} \langle \text{ad}_{\Omega_2}^* \Omega_1, \Omega_3 \rangle &= \langle \Omega_1, \text{ad}_{\Omega_2} \Omega_3 \rangle \\ &= \Omega_1 \cdot (\Omega_2 \times \Omega_3) \\ &= -(\Omega_2 \times \Omega_1) \cdot \Omega_3 \\ &= (-\hat{\Omega}_2 \Omega_1) \cdot \Omega_3. \end{aligned}$$

Thus, we find that

$$\text{ad}_{\Omega}^*(\cdot) = -\hat{\Omega}. \tag{2.11}$$

□

Orbits corresponding to the actions described on page 22 are also of interest. For certain conservative mechanical systems, for example, the system dynamics on the complete momentum phase space can be reduced to canonical Hamiltonian dynamics on the (smaller dimensional) coadjoint orbits. This process of *reduction* is discussed in Section 2.3.

Example: The coadjoint action of $SO(3)$ on $so(3)^*$ and the coadjoint orbits.

Using the definition 4 on page 22 and the identity

$$R\hat{x}R^T = \widehat{Rx}$$

for $R \in SO(3)$ and $\mathbf{x} \in \mathbb{R}^3$, one may compute that the coadjoint action of $SO(3)$ is

$$\text{Ad}_{R^{-1}}^*(\hat{\mathbf{\Pi}}) = R\hat{\mathbf{\Pi}}R^T \quad (2.12)$$

where $\hat{\mathbf{\Pi}} \in \mathfrak{so}(3)^*$, the dual of the Lie algebra $\mathfrak{so}(3)$.

Using the definition (2.5) of the orbit of an action, the *coadjoint orbit* of $SO(3)$ through the point $\hat{\mathbf{\Pi}} \in \mathfrak{so}(3)^*$ is the subset of $\mathfrak{so}(3)^*$ given by

$$\begin{aligned} \text{Orb}(\hat{\mathbf{\Pi}}) &= \{\text{Ad}_{R^{-1}}^*(\hat{\mathbf{\Pi}}) \mid R \in SO(3)\} \\ &= \{R\hat{\mathbf{\Pi}}R^T \mid R \in SO(3)\} \\ &= \{\widehat{R\mathbf{\Pi}} \mid R \in SO(3)\}. \end{aligned} \quad (2.13)$$

Identifying $\widehat{R\mathbf{\Pi}}$ with the vector $R\mathbf{\Pi}$, one finds that the coadjoint orbit through $\hat{\mathbf{\Pi}}$ comprises all rotations of the vector $\mathbf{\Pi}$. Thus, the coadjoint orbit through $\hat{\mathbf{\Pi}}$ is identified with the sphere of radius $\|\mathbf{\Pi}\|$. The orbit space $\mathfrak{so}(3)^*/SO(3)$ is the set of nonnegative real numbers, each of which corresponds to the radius of a sphere defining a coadjoint orbit. Marsden and Ratiu [50] are careful to point out that this orbit space is not a manifold and, in fact, that the coadjoint action of $SO(3)$ is not free since $\mathbf{0} \in \mathfrak{so}(3)^*$ is a fixed point under the coadjoint action. \square

As indicated before, an element $\xi \in \mathfrak{g}$ induces a one-parameter family of group elements by means of the exponential map $\exp t\xi$. In turn, the family $\exp t\xi$ induces a flow on M through the action Φ . Define for $\xi \in \mathfrak{g}$ the map $\Phi(\exp t\xi, \cdot) : M \rightarrow M$. This map is a flow on M . The vector field on M corresponding to this flow is called the *infinitesimal generator*

of the action corresponding to ξ and is denoted $\xi_M(x)$:

$$\xi_M(x) := \frac{d}{dt} \Phi(\exp t\xi, x)|_{t=0}. \quad (2.14)$$

Thus $\xi_M(x)$ gives the velocity of the integral curve $\Phi(\exp t\xi, x)$ at the point $x \in M$.

Example: Infinitesimal generator of right translation on $SO(3)$. Let $M = G = SO(3)$ and $\xi = \hat{\Omega} \in \mathfrak{so}(3)$. Consider the action of right translation on M so that $\Phi(g, h) = R_g h$ for $g, h \in G$. Then $\Phi(\exp t\hat{\Omega}, R) = R \exp t\hat{\Omega}$ and by the definition (2.14),

$$\xi_{SO(3)}(R) = \frac{d}{dt} \left[R \exp t\hat{\Omega} \right]_{t=0} = R\hat{\Omega}.$$

Thus the infinitesimal generator of right translation corresponding to $\hat{\Omega}$ is the left invariant vector field $X_{\hat{\Omega}}$. \square

2.3 Reduction by Symmetry

Suppose that the configuration of a system of interest corresponds to a point x in an n -dimensional manifold M . Then the system state is an element (x, v) in the velocity phase space TM . Locally, the configuration and velocity are given by the coordinate pair (q, \dot{q}) where $q = [q^1, \dots, q^n]^T$ is the vector of local coordinates. By definition, the system is a *Lagrangian dynamical system* with Lagrangian $\mathcal{L}(q, \dot{q})$ if any trajectory $(q(t), \dot{q}(t))$ over a time interval $t \in [t_0, t_1]$ satisfies Hamilton's principle,

$$0 = \delta \int_{t_0}^{t_1} \mathcal{L}(q, \dot{q}) dt$$

where the variations are smooth curves in M with fixed endpoints. In this case, the system dynamics are described by the *Euler-Lagrange equations*

$$\frac{d}{dt} \frac{\partial \mathcal{L}}{\partial \dot{q}^i} - \frac{\partial \mathcal{L}}{\partial q^i} = 0 \quad (2.15)$$

for $i = 1, \dots, n$. When speaking of mechanical systems, one is typically interested in so-called “natural Lagrangian systems” for which the Lagrangian is simply kinetic energy minus potential energy and the kinetic energy is quadratic in velocity. (Kinetic energy is given by a Riemannian metric on the configuration manifold.)

Equivalently, one may write the system dynamics in Hamiltonian form. First, define the momentum conjugate to \dot{q} ,

$$\mathbf{p}^T = \left[\frac{\partial \mathcal{L}}{\partial \dot{q}^1}, \dots, \frac{\partial \mathcal{L}}{\partial \dot{q}^n} \right]. \quad (2.16)$$

The pair $(\mathbf{q}, \mathbf{p}^T)$ is the coordinate representation of the system state expressed as an element in T^*M . More conventionally, one simply writes this pair (\mathbf{q}, \mathbf{p}) . If definition (2.16) can be solved uniquely for $\dot{\mathbf{q}}(\mathbf{q}, \mathbf{p})$, the Lagrangian is called *regular* or *nondegenerate*. Given a nondegenerate Lagrangian \mathcal{L} , the Hamiltonian $H(\mathbf{q}, \mathbf{p})$ is the Legendre transform of the Lagrangian

$$H(\mathbf{q}, \mathbf{p}) = (\mathbf{p}^T \dot{\mathbf{q}} - \mathcal{L}(\mathbf{q}, \dot{\mathbf{q}})) \Big|_{\dot{\mathbf{q}}(\mathbf{q}, \mathbf{p})}.$$

Hamilton’s equations are

$$\dot{p}_i = -\frac{\partial H}{\partial q^i}, \quad \dot{q}^i = \frac{\partial H}{\partial p_i} \quad \text{for } i = 1, \dots, n. \quad (2.17)$$

The $2n$ equations (2.17) are equivalent to the n Euler-Lagrange equations (2.15).

Equations (2.17) are a special case of a more general family of Hamilton's equations. This larger family is most easily described using the *Poisson bracket*. Let P denote a smooth manifold. A Poisson bracket $\{\cdot, \cdot\}$ on P is a Lie bracket on the vector space $C^\infty(P)$ which is also a derivation in each argument,

$$\{FG, H\} = \{F, H\}G + F\{G, H\}.$$

If such an operation exists, then P is referred to as a *Poisson manifold*.

Referring to equations (2.17), T^*M is a Poisson manifold under the Poisson bracket (given here in local coordinates)

$$\{F, G\} = \frac{\partial F}{\partial q^i} \frac{\partial G}{\partial p_i} - \frac{\partial F}{\partial p_i} \frac{\partial G}{\partial q^i}.$$

Alternatively, one may write

$$\{F, G\} = \begin{pmatrix} \nabla_q F \\ \nabla_p F \end{pmatrix} \cdot \mathbb{J} \begin{pmatrix} \nabla_q G \\ \nabla_p G \end{pmatrix}$$

where \mathbb{J} is the $2n$ -dimensional *symplectic matrix*

$$\mathbb{J} = \begin{pmatrix} \mathbf{0}_n & \mathcal{I}_n \\ -\mathcal{I}_n & \mathbf{0}_n \end{pmatrix}.$$

The symplectic matrix encodes all of the information defining the Hamiltonian structure on T^*M . The generalization of the symplectic matrix to a Poisson manifold P is a skew-symmetric 2-tensor Λ which may depend on the state $z \in P$. The *Poisson tensor* $\Lambda(z)$

defines the Poisson bracket

$$\{F, G\} = \Lambda^{ij}(z) \frac{\partial F}{\partial z^i} \frac{\partial G}{\partial z^j}.$$

Thus, all of the information describing the Hamiltonian structure on P is encoded in the single tensor $\Lambda(z)$. Alternatively, given a Poisson bracket one may compute the Poisson tensor by substituting the coordinate functions $F = z^i$ and $G = z^j$.

A Poisson bracket on a manifold P , together with a Hamiltonian H , defines a unique vector field X_H on P by the requirement that

$$X_H(F) = \{F, H\} \quad \text{for all } F \in C^\infty(P). \quad (2.18)$$

The vector field X_H is called the *Hamiltonian vector field* because it describes the Hamiltonian dynamics on P . In coordinates,

$$\dot{z}_i = X_H(z_i) = \{z_i, H\}.$$

For example, in the canonical case that $P = T^*M$ one may write equations (2.17) as

$$\dot{q}^i = \{q^i, H\} \quad \dot{p}_i = \{p_i, H\} \quad \text{for } i = 1, \dots, n. \quad (2.19)$$

More generally, the rate of change of any function $F \in C^\infty(P)$ along the flow of the Hamiltonian vector field is,

$$\dot{F} = X_H(F) = \{F, H\}.$$

If $\{F, H\} = 0$ then F is conserved along the flow. By skew-symmetry of the Poisson bracket, the Hamiltonian H is constant along trajectories of X_H . If $\{F, G\} = 0$ for any function

$G \in C^\infty(P)$ then the conserved quantity F is referred to as a *Casimir function*. As will be discussed shortly, conserved quantities play a crucial role in stability analysis.

There is an important connection between the Poisson bracket on P and the Lie bracket of vector fields. Referring to definition (2.18) of a Hamiltonian vector field, one may show

$$X_{\{F,G\}} = -[X_F, X_G].$$

Using this identity and the fact that $C^\infty(P)$ is a Lie algebra under the Poisson bracket, one may show that the set of Hamiltonian vector fields $\mathfrak{X}_{\text{Ham}}(P)$ is a Lie subalgebra of $\mathfrak{X}(P)$.

If a candidate Poisson bracket on a manifold \tilde{P} fails to satisfy the Jacobi identity, then $C^\infty(\tilde{P})$ is not a Lie algebra under this bracket and the bracket cannot be called a “Poisson bracket”. If the candidate bracket satisfies all other criteria for a Poisson bracket, then the Hamiltonian system defined by the bracket is called *almost Poisson* [22].

Many physically interesting systems can be described as systems on Lie groups. Consider the class of systems for which a configuration is given by an element in some Lie group G . A subclass of these systems is invariant under left or right translation and this invariance leads to a simplified set of dynamic equations. Even for those systems which do not exhibit invariance, or symmetry, greater insight into the dynamics often follows from considering an invariant system as a special case. Since a system which is invariant under right translation can be transformed into a left invariant system, there is no further loss of generality in considering only left invariant dynamics.

For a Lagrangian or a Hamiltonian system on a Lie group G , left invariance of the dynamics is equivalent to left invariance of the Lagrangian or the Hamiltonian. A function $F_L : TG \rightarrow \mathbb{R}$ is *left invariant* if the function evaluated at any point in TG is equal to the



function evaluated at any other point reachable by left translation, that is, if

$$F_L(L_g h, T_h L_g v) = F_L(h, v) \quad (2.20)$$

for all $g \in G$ and all $(h, v) \in TG$. Left invariant functions on T^*G are defined analogously. More generally, one may consider functions which are only invariant under the action of some subgroup of G .

The following theorem relates left invariant Lagrangian dynamics on the $2n$ -dimensional space TG to “reduced” dynamics on the n -dimensional space $TG/G \simeq \mathfrak{g}$.

Theorem 2.3.1 (Marsden and Ratiu [50]) *Let G be a Lie group and let $\mathcal{L} : TG \rightarrow \mathbb{R}$ be a left invariant Lagrangian. Let $l : \mathfrak{g} \rightarrow \mathbb{R}$ be its restriction to the identity. For a curve $g(t) \in G$, let $\xi(t) = T_{g(t)} L_{g(t)^{-1}} \cdot \dot{g}(t)$. Then the following are equivalent:*

1. $g(t)$ satisfies the Euler-Lagrange equations for \mathcal{L} on G ;
2. the variational principle

$$\delta \int \mathcal{L}(g(t), \dot{g}(t)) dt = 0$$

holds, for variations with fixed endpoints.

3. the Euler-Poincaré equations hold,

$$\frac{d}{dt} \frac{\delta l}{\delta \xi} = \text{ad}_\xi^* \frac{\delta l}{\delta \xi}, \quad (2.21)$$

where the functional derivative $\frac{\delta l}{\delta \xi}$ is the unique element of \mathfrak{g}^* satisfying

$$\left\langle \delta \xi, \frac{\delta l}{\delta \xi} \right\rangle = \lim_{\epsilon \rightarrow 0} \frac{1}{\epsilon} [l(\xi + \epsilon \delta \xi) - l(\xi)].$$

4. the variational principle

$$\delta \int l(\xi(t)) dt = 0$$

holds on \mathfrak{g} using variations of the form

$$\delta \xi = \dot{\eta} + [\xi, \eta],$$

where η vanishes at the endpoints.

Thus, left invariant Lagrangian dynamics on TG reduce to the Euler-Poincaré equations on \mathfrak{g} . These equations are obtained by restricting the variations $(\delta g, \delta \dot{g})$ on TG to $\delta \xi$ on \mathfrak{g} subject to the identity $\xi(t) = T_{g(t)} L_{g(t)^{-1}} \cdot \dot{g}(t)$.

Example: The free rigid body. Consider a rigid body whose orientation is described by a matrix $R \in SO(3)$ which maps a body-fixed coordinate frame to an inertial coordinate frame. In other words, R transforms a vector expressed in body coordinates into the corresponding vector expressed in inertial coordinates. Recall from Section 2.2 that

$$\dot{R} = R\hat{\Omega}$$

where Ω is the vector representing the body angular velocity.

Let I denote the positive definite, symmetric inertia tensor for the rigid body relative to the body-fixed coordinate frame. The matrix I maps $\mathfrak{so}(3)$ to $\mathfrak{so}(3)^*$,

$$\hat{\Pi} = \widehat{I\Omega} \in \mathfrak{so}(3)^*.$$

As a result, I induces a metric $\langle \cdot, \cdot \rangle$ on $\mathfrak{so}(3)$ by means of the pairing between $\mathfrak{so}(3)$

and $\mathfrak{so}(3)^*$ as follows,

$$\ll \hat{\Omega}, \hat{\Omega} \gg := \langle \hat{\Omega}, \widehat{I\Omega} \rangle = \Omega \cdot I\Omega.$$

The metric on $\mathfrak{so}(3)$ in turn induces a Riemannian metric on $SO(3)$. Recognizing that the kinetic energy of the rigid body is $\frac{1}{2} \ll \hat{\Omega}, \hat{\Omega} \gg$, the Lagrangian on $TSO(3)$ is simply

$$\mathcal{L}(\mathbf{R}, \dot{\mathbf{R}}) = \frac{1}{2} \ll \mathbf{R}^T \dot{\mathbf{R}}, \mathbf{R}^T \dot{\mathbf{R}} \gg$$

According to equation (2.20), \mathcal{L} is a left invariant function on $TSO(3)$. The restriction of $\mathcal{L}(\mathbf{R}, \dot{\mathbf{R}})$ to $T_{\mathcal{I}}SO(3)$ is

$$l(\hat{\Omega}) = \mathcal{L}(\mathcal{I}, \hat{\Omega}) = \frac{1}{2} \ll \hat{\Omega}, \hat{\Omega} \gg = \frac{1}{2} \Omega \cdot I\Omega. \quad (2.22)$$

By Theorem 2.3.1, the reduced equations of motion, the Euler-Poincaré equations, for the free rigid body are

$$\frac{d}{dt} \frac{\delta l}{\delta \Omega} = \text{ad}^*_{\Omega} \frac{\delta l}{\delta \Omega},$$

where we have identified $\mathfrak{so}(3)^*$ with \mathbb{R}^3 . Substituting from (2.22) and (2.11) gives the familiar Euler equations for the free rigid body,

$$\frac{d}{dt}(I\Omega) = (I\Omega) \times \Omega.$$

□

As described in Theorem 2.3.1, left invariant Lagrangian dynamics on TG reduce to dynamics on $TG/G \simeq \mathfrak{g}$. Similarly, canonical left invariant Hamiltonian dynamics on T^*G reduce to Poisson dynamics on $T^*G/G \simeq \mathfrak{g}^*$.

Theorem 2.3.2 (Marsden and Ratiu [50]) *Let G be a Lie group and let $H : T^*G \rightarrow \mathbb{R}$ be a left invariant Hamiltonian. Let $h : \mathfrak{g}^* \rightarrow \mathbb{R}$ be the restriction of H to T_e^*G . For a curve $p(t) \in T_{g(t)}^*G$, let $\mu(t) = (T_{g(t)}^*L_{g(t)^{-1}}) \cdot p(t)$ be the induced curve in \mathfrak{g}^* . Assuming that $g(t)$ satisfies the differential equation*

$$\dot{g} = T_e L_g \frac{\delta h}{\delta \mu}$$

where $\mu(0) = p(0)$, the following are equivalent:

1. $p(t)$ is an integral curve of X_H ; i.e., Hamilton's equations hold on T^*G ;
2. for any smooth function F defined on T^*G , $\dot{F} = \{F, H\}$ where $\{\cdot, \cdot\}$ is the canonical Poisson bracket on T^*G ;
3. $\mu(t)$ satisfies the Lie-Poisson equations

$$\frac{d\mu}{dt} = \text{ad}_{\delta h / \delta \mu}^* \mu; \quad (2.23)$$

4. for any smooth function f defined on \mathfrak{g}^* , we have

$$\dot{f} = \{f, h\}_{\mathfrak{g}^*}, \quad (2.24)$$

where the reduced Poisson bracket $\{\cdot, \cdot\}_{\mathfrak{g}^*}$ is defined by restricting the canonical bracket acting on left invariant functions on T^*G to the space \mathfrak{g}^* . Explicitly,

$$\{f, h\}_{\mathfrak{g}^*}(\mu) = - \left\langle \mu, \text{ad}_{\delta h / \delta \mu} \frac{\delta f}{\delta \mu} \right\rangle \quad (2.25)$$

for $\mu \in \mathfrak{g}^*$. (The minus sign is a consequence of left invariance. A right invariant Hamiltonian leads to a similarly defined bracket without the minus sign.)

The Euler-Poincaré equations are obtained by restricting the form of the variations used when Hamilton's principle is applied on \mathfrak{g} . The Lie-Poisson equations are obtained by restricting the canonical Poisson bracket on T^*G to \mathfrak{g}^* .

Example: The free rigid body. Consider once again the rigid body and recall the definition

$$\hat{\Pi} = \widehat{I\Omega} \in \mathfrak{so}(3)^*.$$

Just as I induces a metric on $\mathfrak{so}(3)$, its inverse induces a dual metric on $\mathfrak{so}(3)^*$,

$$\ll \hat{\Pi}, \hat{\Pi} \gg_{\mathfrak{so}(3)^*} := \langle \hat{\Pi}, \widehat{I^{-1}\Pi} \rangle = \Pi \cdot I^{-1}\Pi.$$

The Hamiltonian H on $T^*SO(3)$ may be computed directly from $\mathcal{L}(\mathbf{R}, \dot{\mathbf{R}})$ by choosing coordinates for $SO(3)$ and performing the Legendre transform. Furthermore, since \mathcal{L} is left invariant, the resulting Hamiltonian is necessarily left invariant. The restriction of H to $T_{\mathbf{I}}^*SO(3)$ is

$$h(\hat{\Pi}) = \frac{1}{2} \ll \hat{\Pi}, \hat{\Pi} \gg_{\mathfrak{so}(3)^*} = \frac{1}{2} \Pi \cdot I^{-1}\Pi$$

Identifying $\mathfrak{so}(3)^*$ with \mathbb{R}^3 , Theorem 2.3.2 indicates that the Lie-Poisson equations for the free rigid body are

$$\frac{d\Pi}{dt} = \text{ad}_{\hat{\Omega}}^* \Pi = -\hat{\Omega} \times \Pi = \Pi \times \Omega. \quad (2.26)$$

The dynamics (2.26) preserve the magnitude of Π ; the function $\frac{1}{2}\Pi \cdot \Pi$ is a Casimir for this system. This observation follows more easily if one considers the reduced Poisson bracket on $\mathfrak{so}(3)^*$. Continuing to identify $\mathfrak{so}(3)^*$ and \mathbb{R}^3 , one may write the Poisson bracket

$$\{F, G\} := \nabla_{\Pi} F \cdot \hat{\Pi} \nabla_{\Pi} G$$

for smooth functions F and G on $\mathfrak{so}(3)^*$. Since the gradient of $\frac{1}{2}\mathbf{\Pi} \cdot \mathbf{\Pi}$ is in the null space of the Poisson tensor $\hat{\mathbf{\Pi}}$, this function Poisson commutes with any other function. It can be shown that the three scalar equations (2.26) may be further reduced to symplectic dynamics on the 2-dimensional coadjoint orbit, the sphere of radius $\|\mathbf{\Pi}\|$, whenever $\mathbf{\Pi} \neq 0$. \square

It has been mentioned that a system defined on a Lie group G may be invariant under the action of some subgroup of G . In this case, the system does not exhibit full G -symmetry and one cannot fully reduce the dynamics from T^*G to \mathfrak{g}^* . However, some reduction may be possible by considering the full dynamics on an augmented space, a semidirect product of G with some other space. *Semidirect product reduction* is described in [51].

2.4 Stability of Equilibria

Of principal concern in the study of any dynamical system are the stability properties of its equilibria. Consider a system whose configuration is described by the manifold M and whose dynamics evolve according to a vector field X on M ,

$$\dot{z} = X(z), \quad z \in M. \quad (2.27)$$

A point $z_e \in M$ is an *equilibrium point* if $X(z_e) = 0$. An equilibrium z_e is called *stable* if trajectories starting near z_e remain close. This idea is made more precise by the following definition.

Definition 2.4.1 (Stability, Asymptotic Stability, Instability) *An equilibrium z_e of the dynamics (2.27) is*

- *stable if for any positive scalar ϵ there is a positive scalar δ such that any trajectory satisfying $\|z(0) - z_e\| \leq \delta$ also satisfies $\|z(t) - z_e\| \leq \epsilon$ for all time $t \geq 0$.*

- *asymptotically stable if it is stable and $z(t) \rightarrow z_e$ as $t \rightarrow \infty$.*
- *unstable if it is not stable (i.e., if there is a value ϵ for which no δ exists).*

In situations where the dynamics involve time explicitly, one must consider uniformness of stability (i.e., whether the stability properties depend on the initial time). Only autonomous systems are considered here.

Two methods for studying stability, both attributed to Lyapunov, are the so-called “indirect” and “direct” methods. The indirect method involves examining the spectrum of the linearization of X at z_e .

Theorem 2.4.2 (Lyapunov’s Indirect Method [37]) *An equilibrium z_e of the dynamics (2.27) is*

- *asymptotically stable if each point in the spectrum of the linearization of X at z_e lies in the open left half of the complex plane.*
- *unstable if any point in the spectrum of the linearization of X at z_e lies in the open right half of the complex plane.*

If each point in the spectrum lies in the closed left half plane, the equilibrium is called *spectrally stable*. If the linearized system is stable (i.e., spectrally stable with an independent eigenvector associated to each eigenvalue with zero real part), then z_e is called *linearly stable*. Linear stability is stronger than spectral stability but is not sufficient to prove stability of z_e . For example, the system $\dot{z} = z^3$ has a linearly stable equilibrium at $z = 0$. However, this equilibrium is actually unstable.

For a canonical Hamiltonian system, the eigenvalues of the linearized dynamics are distributed symmetrically in the complex plane under reflection about the real and imaginary

axes. Thus any given eigenvalue is either located at the origin of the complex plane or is a member of a real conjugate pair, a purely imaginary conjugate pair, or a symmetric quartet of eigenvalues. Linear analysis can therefore predict instability for an equilibrium of a Hamiltonian system but cannot predict stability.

Lyapunov's direct method involves finding an energy-like function V , called a *Lyapunov function*, which is positive definite and whose rate is negative semidefinite.

Theorem 2.4.3 (Lyapunov's Direct Method [37]) *Suppose there is a function V which has a strict minimum, say zero, in a neighborhood D of z_e . That is, suppose*

$$V(z) = 0 \quad \text{and} \quad V(z) > 0 \quad \text{for all } z \in D - \{z_e\}.$$

Then the equilibrium z_e is stable if

$$\dot{V}(z) \leq 0 \quad \text{for all } z \in D.$$

The equilibrium z_e is asymptotically stable if

$$\dot{V}(z) < 0 \quad \text{for all } z \in D - \{z_e\}.$$

An obvious challenge in applying Lyapunov's direct method is constructing the function V . There is no truly general procedure for constructing a Lyapunov function although, for physical systems, the energy is often a good candidate.

LaSalle's invariance principle extends Theorem 2.4.3 allowing one, in some cases, to conclude asymptotic stability even if \dot{V} is only negative semidefinite.

Theorem 2.4.4 (LaSalle's Invariance Principle [37]) *Let $\Omega \subset D$ be a compact set that is positively invariant with respect to the dynamics (2.27). Let $E = \{z \in \Omega \mid \dot{V}(z) = 0\}$ and let \mathcal{M} be the largest invariant set contained in E . Then all trajectories starting in Ω approach \mathcal{M} as time goes to infinity.*

Essentially, the proof involves observing that, since V is bounded below and nonincreasing, $\dot{V} \rightarrow 0$ as $t \rightarrow \infty$. But \dot{V} cannot remain zero unless $z \in \mathcal{M}$. Therefore, $z(t)$ must go to \mathcal{M} .

Corollary 2.4.5 *If $\mathcal{M} = \{z_e\}$ then z_e is asymptotically stable.*

In the reduced setting of an Euler-Poincaré or Lie-Poisson system, the term “equilibrium” is somewhat ambiguous since an equilibrium of the reduced equations corresponds to a nonequilibrium trajectory in the full phase space. This trajectory is actually a group orbit corresponding to an “equilibrium velocity”. The orbit, or rather any point on the orbit, is referred to as a *relative equilibrium*.

Since Euler-Poincaré and Lie-Poisson equations describe conservative dynamics, stability of a relative equilibrium cannot be proven using Lyapunov's indirect method. However, there are procedures for constructing Lyapunov functions for stable equilibria of these systems. In the Hamiltonian (Lie-Poisson) setting, one relevant technique is the *energy-Casimir method* described in [50]. The method involves the following steps:

1. Define the “augmented Hamiltonian” $H_\Phi = H + \Phi(C_i, c_i)$ where Φ is an arbitrary smooth function of its arguments. The constants C_i are Casimirs and the constants c_i are any remaining conserved quantities.
2. Impose conditions on the first derivative of Φ evaluated at the equilibrium such that the equilibrium is a critical point of H_Φ .

3. Impose conditions on the second derivative of Φ evaluated at the equilibrium such that H_Φ is definite.

Since H_Φ is definite about the equilibrium and is constant, stability of the equilibrium of the reduced dynamics follows by Theorem 2.4.3. (If the second variation of H_Φ evaluated at the equilibrium is negative definite, one may simply take $V = -H_\Phi$.) For the Hamiltonian system, stability of the equilibrium follows regardless of whether it is a maximum or a minimum of H_Φ . If the Hamiltonian system models a physical process, one must be more concerned about whether the equilibrium is a maximum or a minimum because of the effect of damping. If, for example, the equilibrium is a maximum and damping decreases the value of H_Φ , then dissipation actually destabilizes the equilibrium.

Having proven stability of the reduced dynamics, one may assert that the relative equilibrium of the unreduced dynamics is *relatively stable modulo G* . This means that while the dynamics are stable in the sense that momenta stay close to their equilibrium values, some drift may occur in the system configuration. The issue of drift in the study of stability of relative equilibria is addressed by Patrick [58] for the case where G is compact. His results are extended by Leonard and Marsden [44] to include systems on noncompact Lie groups.

2.5 Summary

A fundamental theme of this dissertation is Lyapunov-based stabilization. A Lyapunov function candidate encodes a system's dynamics in a single scalar function. Lyapunov's direct method reduces the problem of proving stability of the whole system to analyzing this one function. If the function is parameterized by control gains, the analysis yields conditions on the control parameters for closed-loop stability. One may use the resulting Lyapunov function to estimate the region of attraction of the feedback-stabilized equilib-

rium. Furthermore, if the Lyapunov function was constructed for a conservative system model, it can then be used to study the effect of additional forces, such as physical and feedback dissipation.

While Lyapunov techniques can be challenging for arbitrary systems, mechanical systems naturally lend themselves to Lyapunov-based control design. In Chapters 3 and 4, we treat an underwater vehicle as a Lie-Poisson (reduced Hamiltonian) system and use the energy-Casimir method to study stability of relative equilibria for the uncontrolled and feedback-controlled system. When considering feedback, the approach gives conditions on the control gains for closed-loop stability and the resulting Lyapunov function provides an estimate of the region of attraction. We then use the Lyapunov function to design feedback dissipation to provide asymptotic stability and to characterize the effect of physical damping. LaSalle's invariance principle plays an important role in this analysis. In Chapter 5, we use a similar approach to study a class of systems in the Lagrangian framework.

Chapter 3

Underwater Vehicle Dynamics

This chapter develops and discusses a dynamic model of a rigid body with internal rotors immersed in a fluid. Under certain assumptions on the fluid, the dynamic equations are Lie-Poisson. Stability of relative equilibria may be studied using the energy-Casimir method and we give a number of previous and new stability results based on this approach. We focus on stability of long-axis translation for an ellipsoidal vehicle.

One assumption underlying the Lie-Poisson model is that the fluid is inviscid. A real underwater vehicle is subject to viscous forces which can greatly affect the dynamics. It is important to understand the limitations of the Hamiltonian model and to not be misled by results based on conservative system analysis. For example, while one expects that a stable equilibrium of a Hamiltonian system will be asymptotically stable in the presence of damping, this is not necessarily the case. (America's first satellite, Explorer I, provides a spectacular example [47].) To demonstrate the applicability of our conservative underwater vehicle model for studying stability of steady translation, we present experimental results which verify theoretical predictions.

In Section 3.1, we describe the vehicle model, including a somewhat general model of

the viscous force and torque. Section 3.2 presents stability results for an immersed ellipsoid translating along a principal axis. Section 3.3 describes an experimental investigation of the stability criteria presented in Section 3.2.

3.1 Underwater Vehicle Equations of Motion

In this section, we describe the vehicle model and the open-loop equations of motion. Section 3.1.1 presents the equations of motion for a neutrally buoyant vehicle modeled as a rigid body immersed in an ideal fluid. In Section 3.1.2, internal rotors are included as actuators in the system model. In Section 3.1.3, a general model is presented for the forces and torques due to viscous drag.

3.1.1 Rigid Body in an Ideal Fluid

Rigid Body Kinematics. Consider a coordinate frame described by the orthonormal vectors (e_1, e_2, e_3) , which is fixed to a rigid body. The rigid body is oriented in some way with respect to an inertial coordinate frame, described by the orthonormal vectors (i, j, k) . The configuration space for the rigid body is the Euclidean group, $SE(3)$, of rigid transformations. An element in $SE(3)$ is given by the pair (R, b) where $R \in SO(3)$ is the proper rotation matrix that maps body coordinates into inertial coordinates and $b \in \mathbb{R}^3$ is the vector from the origin of the inertial frame to the origin of the body frame. (See Figure 3.1.) The pair (R, b) thus describes the vehicle's position and orientation in inertial space.

The left action of $SE(3)$ on itself is given by

$$L_{(R_1, b_1)}(R_2, b_2) = (R_1 R_2, R_1 b_2 + b_1) \quad (3.1)$$

where $(\mathbf{R}_1, \mathbf{b}_1)$ and $(\mathbf{R}_2, \mathbf{b}_2)$ are two elements in $SE(3)$. An element of $SE(3)$ may be represented as a matrix,

$$\begin{pmatrix} \mathbf{R} & \mathbf{b} \\ \mathbf{0} & 1 \end{pmatrix}$$

for $(\mathbf{R}, \mathbf{b}) \in SE(3)$.

To see how $SE(3)$ relates the inertial and body-fixed coordinate frames, let $\mathbf{x}_{\text{inertial}}$ be the position of a point in space with respect to the inertial coordinate frame. Let \mathbf{x}_{body} be the position of the same point with respect to the body-fixed coordinate frame. Then, using the matrix representation,

$$\begin{pmatrix} \mathbf{x}_{\text{inertial}} \\ 1 \end{pmatrix} = \begin{pmatrix} \mathbf{R} & \mathbf{b} \\ \mathbf{0} & 1 \end{pmatrix} \begin{pmatrix} \mathbf{x}_{\text{body}} \\ 1 \end{pmatrix}.$$

If $\boldsymbol{\Omega}$ and \mathbf{v} represent the angular and translational velocity of the rigid body expressed in body coordinates, then

$$\begin{pmatrix} \dot{\mathbf{R}} & \dot{\mathbf{b}} \\ \mathbf{0} & \mathbf{0} \end{pmatrix} = \begin{pmatrix} \mathbf{R} & \mathbf{b} \\ \mathbf{0} & 1 \end{pmatrix} \begin{pmatrix} \hat{\boldsymbol{\Omega}} & \mathbf{v} \\ \mathbf{0} & \mathbf{0} \end{pmatrix}. \quad (3.2)$$

Equation (3.2) describes the rigid body kinematics.

The pair $(\hat{\boldsymbol{\Omega}}, \mathbf{v})$ is an element in the Lie algebra $\mathfrak{se}(3)$ of the Euclidean group; the right-most matrix in equation (3.2) is its matrix representation. As pointed out in Section 2, the Lie bracket for a matrix Lie algebra is simply matrix commutation. Therefore, one may easily verify that

$$[(\hat{\boldsymbol{\Omega}}_1, \mathbf{v}_1), (\hat{\boldsymbol{\Omega}}_2, \mathbf{v}_2)] = (\hat{\boldsymbol{\Omega}}_1 \hat{\boldsymbol{\Omega}}_2 - \hat{\boldsymbol{\Omega}}_2 \hat{\boldsymbol{\Omega}}_1, \hat{\boldsymbol{\Omega}}_1 \mathbf{v}_2 - \hat{\boldsymbol{\Omega}}_2 \mathbf{v}_1) \quad (3.3)$$

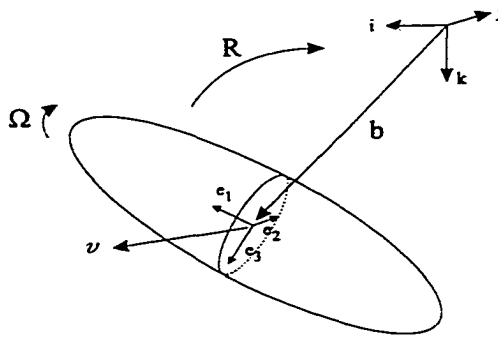


Figure 3.1: Kinematics of a rigid body.

for two elements $(\hat{\Omega}_1, v_1)$ and $(\hat{\Omega}_2, v_2)$ in $\mathfrak{se}(3)$. Physically, the Lie bracket on $\mathfrak{se}(3)$ expresses how infinitesimal rotations and infinitesimal translations commute.

The Reduced Dynamics and Kirchhoff's Equations. Kirchhoff's equations provide a finite-dimensional dynamic model of a neutrally buoyant rigid body translating and rotating in an infinite volume of fluid. A body is said to be neutrally buoyant when the weight of the displaced fluid is equal to the weight of the body. The fluid is assumed to be irrotational, incompressible, inviscid and at rest at the infinitely distant boundary. (Appendix A briefly reviews the derivation of Kirchhoff's equations, as given by Lamb [41].) While these assumptions are restrictive, there are situations where Kirchhoff's equations provide a useful model of the dynamics of an underwater vehicle. For example, the equations are particularly suitable when considering streamline motion of a slender vehicle. External forces such as viscous effects and external control inputs can be appended to this basic model as external forces.

Kirchhoff's key simplification was to treat the combined body/fluid system as a single dynamical system so that the fluid force acting on the body's surface need not be computed.

The kinetic energy of the combined body/fluid system is

$$T = \frac{1}{2} \begin{pmatrix} \boldsymbol{\Omega} \\ \mathbf{v} \end{pmatrix} \cdot \begin{pmatrix} \mathbf{I} & \mathbf{D} \\ \mathbf{D}^T & \mathbf{M} \end{pmatrix} \begin{pmatrix} \boldsymbol{\Omega} \\ \mathbf{v} \end{pmatrix}$$

where the 6×6 *generalized inertia matrix* is symmetric and positive definite. The component matrices of the generalized inertia represent the sum of contributions from the rigid body and from the fluid,

$$\mathbf{I} = \mathbf{I}_{rb} + \mathbf{I}_f, \quad \mathbf{M} = m\mathcal{I} + \mathbf{M}_f, \quad \mathbf{D} = m\hat{\mathbf{r}} + \mathbf{D}_f.$$

The matrix \mathbf{I}_{rb} is the vehicle inertia, computed with respect to the body-fixed coordinate frame, and \mathbf{I}_f is the *added inertia* from the potential flow model of the fluid dynamics. The scalar m is the vehicle mass, \mathcal{I} is the 3×3 identity matrix, and \mathbf{M}_f is the *added mass matrix* associated with the fluid. The vector \mathbf{r} is the location of the vehicle center of gravity (CG) in body coordinates and \mathbf{D}_f represents added inertial coupling terms which arise from asymmetries in the vehicle's external shape.

The added mass and inertia terms depend on the external shape of the vehicle, the density of the fluid, and the choice of body-fixed coordinate frame. These terms simplify tremendously for a body with three planes of symmetry. Throughout this dissertation, the underwater vehicle is modeled as an ellipsoid. The origin of the body coordinate frame is fixed at the center of buoyancy (CB), which is the center of mass of the fluid displaced by the ellipsoid. The body coordinate axes are fixed along the ellipsoid principal axes. For an ellipsoidal vehicle with this choice of body coordinates, \mathbf{I}_f and \mathbf{M}_f are diagonal and $\mathbf{D}_f = \mathbf{0}$. Let L_i be the length of the i th principal axis of the ellipsoid. For a nonaxisymmetric vehicle,

one may assume without loss of generality that $L_1 > L_2 > L_3$. Then, $\mathbf{M} = \text{diag}(m_1, m_2, m_3)$ where $m_1 < m_2 < m_3$. If the vehicle mass is uniformly distributed, then the CG coincides with the CB so that $\mathbf{r} = \mathbf{0}$. In this case, $\mathbf{I} = \text{diag}(I_1, I_2, I_3)$. The inertia elements may be ordered $I_3 > I_2 > I_1$ or $I_2 > I_3 > I_1$ or $I_2 > I_1 > I_3$, depending on the relative lengths of the ellipsoid axes [42, 31]. Throughout the dissertation, only vehicle configurations for which the inertia matrix \mathbf{I} of the vehicle is diagonal will be considered. However, cases where the CG and CB do not coincide will be considered.

When $\mathbf{r} = \mathbf{0}$, gravity plays no role in the dynamics. In the absence of external forces, the dynamics are given by the Euler-Lagrange equations on the 12-dimensional velocity phase space $TSE(3)$, the tangent bundle of $SE(3)$. The Lagrangian is the kinetic energy,

$$\mathcal{L}(\mathbf{R}, \mathbf{b}, \mathbf{R}\hat{\boldsymbol{\Omega}}, \mathbf{R}\mathbf{v}) = \frac{1}{2} \begin{pmatrix} \boldsymbol{\Omega} \\ \mathbf{v} \end{pmatrix} \cdot \begin{pmatrix} \mathbf{I} & \mathbf{0} \\ \mathbf{0} & \mathbf{M} \end{pmatrix} \begin{pmatrix} \boldsymbol{\Omega} \\ \mathbf{v} \end{pmatrix} \quad (3.4)$$

where $\dot{\mathbf{R}}$ and $\dot{\mathbf{b}}$ have been replaced according to equation (3.2).¹ Recalling the definition (2.20) of a left invariant function, one may verify that

$$\begin{aligned} \mathcal{L}(L_{(\bar{\mathbf{R}}, \bar{\mathbf{b}})}(\mathbf{R}, \mathbf{b}), T_{(\mathbf{R}, \mathbf{b})}L_{(\bar{\mathbf{R}}, \bar{\mathbf{b}})}(\mathbf{R}\hat{\boldsymbol{\Omega}}, \mathbf{R}\mathbf{v})) &= \mathcal{L}(\bar{\mathbf{R}}\mathbf{R}, \bar{\mathbf{R}}\mathbf{b} + \bar{\mathbf{b}}, \bar{\mathbf{R}}\mathbf{R}\hat{\boldsymbol{\Omega}}, \bar{\mathbf{R}}\mathbf{R}\mathbf{v}) \\ &= \mathcal{L}(\mathbf{R}, \mathbf{b}, \mathbf{R}\hat{\boldsymbol{\Omega}}, \mathbf{R}\mathbf{v}) \end{aligned}$$

for any $(\bar{\mathbf{R}}, \bar{\mathbf{b}}) \in SE(3)$ and thus \mathcal{L} is a left invariant Lagrangian. The system therefore exhibits full $SE(3)$ symmetry and the equations of motion reduce to Euler-Poincaré equations on the 6-dimensional space $\mathfrak{se}(3)$, the Lie algebra of $SE(3)$. Alternatively, one may

¹To write the Euler-Lagrange equations, one should choose “generalized coordinates” and write the Lagrangian in terms of these coordinates and their velocities. The body velocity $(\boldsymbol{\Omega}, \mathbf{v})$ does *not* represent the rate of change of a valid set of generalized coordinates.

define the reduced Hamiltonian and write Lie-Poisson equations on $\mathfrak{se}(3)^*$, the dual of $\mathfrak{se}(3)$.

Define the conjugate momenta to Ω and v , respectively, as

$$\mathbf{\Pi} = I\Omega$$

$$\mathbf{P} = Mv.$$

According to Lamb [41], Lord Kelvin identifies the components $\mathbf{\Pi}$ and \mathbf{P} as the impulsive couple and force necessary to generate the motion of the body-fluid system instantaneously from rest. The system impulse varies as the momentum of a finite dynamical system and will therefore be referred to simply as the system momentum.

The Hamiltonian (restricted to the cotangent space of $SE(3)$ at the identity) is

$$H = \frac{1}{2}\mathbf{\Pi} \cdot I^{-1}\mathbf{\Pi} + \frac{1}{2}\mathbf{P} \cdot M^{-1}\mathbf{P}. \quad (3.5)$$

Using Theorem 2.3.2, and computing the operator ad^* on $\mathfrak{se}(3)^*$ from its definition (2.8), the reduced equations are

$$\begin{pmatrix} \dot{\mathbf{\Pi}} \\ \dot{\mathbf{P}} \end{pmatrix} = \begin{pmatrix} \hat{\mathbf{\Pi}} & \hat{\mathbf{P}} \\ \hat{\mathbf{P}} & \mathbf{0} \end{pmatrix} \nabla H. \quad (3.6)$$

Equations (3.6) are a less familiar expression of Kirchhoff's equations,

$$\dot{\mathbf{\Pi}} = \mathbf{\Pi} \times \Omega + \mathbf{P} \times v$$

$$\dot{\mathbf{P}} = \mathbf{P} \times \Omega. \quad (3.7)$$

More generally, the Poisson bracket of two differentiable functions F and G on $\mathfrak{se}(3)^*$ is

$$\{F, G\}_{(\Pi, P)} = \nabla F \cdot \begin{pmatrix} \hat{\Pi} & \hat{P} \\ \hat{P} & 0 \end{pmatrix} \nabla G \quad (3.8)$$

Since the functions

$$C_1(\Pi, P) = \frac{1}{2} \|P\|^2 \quad \text{and}$$

$$C_2(\Pi, P) = \Pi \cdot P$$

Poisson commute with any other function, these are two independent Casimirs. When $P \neq 0$, the Poisson tensor in equation (3.8) has maximal rank (four). Its null space is spanned by ∇C_1 and ∇C_2 . Physically, the two Casimirs reflect the conservation of inertial linear and angular momentum. To make this observation more clear, let π denote the system's inertial angular momentum vector and let p denote the inertial translational momentum vector. As noted in [42], these vectors are related to the body coordinate momenta as follows,

$$\pi = R\Pi + b \times p$$

$$p = RP.$$

Assuming that no external forces or torques act on the body/fluid system, the equations of motion in inertial space are simply

$$\dot{\pi} = 0 \quad \dot{p} = 0. \quad (3.9)$$

Examining the Casimirs C_1 and C_2 , one finds that

$$C_1 = \frac{1}{2} \mathbf{P} \cdot \mathbf{P} = \frac{1}{2} \mathbf{p} \cdot \mathbf{R} \mathbf{R}^T \mathbf{p} = \frac{1}{2} \mathbf{p} \cdot \mathbf{p}$$

and that

$$C_2 = \mathbf{\Pi} \cdot \mathbf{P} = (\boldsymbol{\pi} - \mathbf{b} \times \mathbf{p}) \cdot \mathbf{R} \mathbf{R}^T \mathbf{p} = \boldsymbol{\pi} \cdot \mathbf{p}.$$

In the reduced system, only these two scalar conserved quantities remain from the vector conservation laws (3.9).

Allowing a Gravitational Torque. Typically, a vehicle's CG and CB do not coincide. In practical settings, an underwater vehicle is trimmed so that the CG is below the CB for stability. In the conservative model, the effect of gravity is to break the full $SE(3)$ symmetry so that the dynamics are no longer invariant under arbitrary translations and rotations. However, the dynamics remain invariant under translation and under rotations about the direction of gravity. Using semidirect product reduction, the equations of motion may once again be written on a reduced phase space. (See [42].)

Kirchhoff's equations describe the motion of a neutrally buoyant vehicle for which the (equilibrating) forces of buoyancy and gravity act at the same point. If the CG and the CB do not coincide, however, then the downward-pointing gravitational force and the upward pointing buoyant force create a gravitational torque. Let

$$\boldsymbol{\Gamma} = \mathbf{R}^T \mathbf{k}$$

be the unit vector pointing in the direction of gravity, expressed with respect to the body

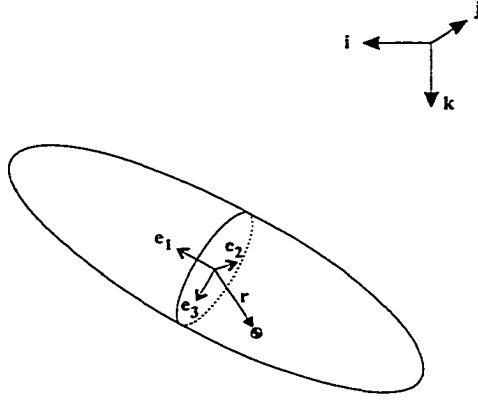


Figure 3.2: Vehicle with noncoincident CG and CB.

frame. The gravitational torque about the body coordinate origin is

$$\mathcal{T}_{\text{gravity}} = \mathbf{r} \times mg\mathbf{\Gamma}. \quad (3.10)$$

When $\mathbf{r} \neq \mathbf{0}$, the Lagrangian includes the effect of the gravitational torque (3.10), as well as the inertial coupling $\mathbf{D} = m\hat{\mathbf{r}}$,

$$\mathcal{L}(\mathbf{R}, \mathbf{b}, \dot{\mathbf{R}}, \dot{\mathbf{b}}) = \frac{1}{2} \begin{pmatrix} \boldsymbol{\Omega} \\ \mathbf{v} \end{pmatrix} \cdot \begin{pmatrix} \mathbf{I} & \mathbf{D} \\ \mathbf{D}^T & \mathbf{M} \end{pmatrix} \begin{pmatrix} \boldsymbol{\Omega} \\ \mathbf{v} \end{pmatrix} + \mathbf{r} \cdot (mg\mathbf{R}^T \mathbf{k}). \quad (3.11)$$

When $\mathbf{r} = \mathbf{0}$, this Lagrangian reduces to the original one (3.4). While \mathcal{L} given in (3.11) is not left invariant under the action of $SE(3)$, it is left invariant under the action of $SE(2) \times \mathbb{R}$, a Lie subgroup of $SE(3)$. As described in [42], the Hamiltonian dynamics on $T^*SE(3)$ can be reduced to Lie-Poisson dynamics on \mathfrak{s}^* , the dual of the Lie algebra of the semidirect product $S = SE(3) \times_{\rho} \mathbb{R}^3$. The 12-dimensional canonical Hamiltonian dynamics reduce to 9-dimensional Lie-Poisson dynamics.

The Hamiltonian restricted to \mathfrak{s}^* is

$$H(\mathbf{\Pi}, \mathbf{P}, \Gamma) = \frac{1}{2} \begin{pmatrix} \mathbf{\Pi} \\ \mathbf{P} \end{pmatrix} \cdot \begin{pmatrix} I & m\hat{r} \\ -m\hat{r} & M \end{pmatrix} \begin{pmatrix} \mathbf{\Pi} \\ \mathbf{P} \end{pmatrix} - \mathbf{r} \cdot mg\Gamma \quad (3.12)$$

and the Lie-Poisson equations on \mathfrak{s}^* are

$$\begin{pmatrix} \dot{\mathbf{\Pi}} \\ \dot{\mathbf{P}} \\ \dot{\Gamma} \end{pmatrix} = \begin{pmatrix} \hat{\mathbf{\Pi}} & \hat{\mathbf{P}} & \hat{\Gamma} \\ \hat{\mathbf{P}} & 0 & 0 \\ \hat{\Gamma} & 0 & 0 \end{pmatrix} \nabla H \quad (3.13)$$

In later sections concerning a vehicle with a noncoincident CG and CB, it will be assumed that $\mathbf{r} = \gamma\mathbf{e}_3$ where γ is a scalar parameter with units of length. It will also be assumed that the vehicle mass is distributed in such a way that the inertia matrix I remains diagonal. (Note, for example, that an ellipsoid with uniformly distributed mass and an additional point mass along a principal axis has a diagonal inertia matrix.)

There are three independent Casimirs for the system described by equations (3.13),

$$\begin{aligned} C_1(\mathbf{\Pi}, \mathbf{P}, \Gamma) &= \frac{1}{2}\|\mathbf{P}\|^2, \\ C_2(\mathbf{\Pi}, \mathbf{P}, \Gamma) &= \frac{1}{2}\|\Gamma\|^2, \quad \text{and} \\ C_3(\mathbf{\Pi}, \mathbf{P}, \Gamma) &= \mathbf{P} \cdot \Gamma. \end{aligned}$$

Notice that $\mathbf{\Pi} \cdot \mathbf{P} = \boldsymbol{\pi} \cdot \mathbf{p}$ is no longer conserved, as it is when $\mathbf{r} = \mathbf{0}$, because the gravitational torque destroys conservation of inertial angular momentum $\boldsymbol{\pi}$. The magnitude of \mathbf{P} is still constant, however. The vector Γ has unit magnitude by definition, so C_2 obviously must be conserved. The third Casimir, $C_3 = \mathbf{P} \cdot \Gamma = \mathbf{p} \cdot \mathbf{k}$, is the component of translational

momentum in the direction of gravity.

Equations (3.13) describe a conservative model of the system dynamics. More generally, one might be interested in the effect of external forces such as viscous drag or external controls. Such forces may be included as generalized forces as follows,

$$\begin{aligned}
 \dot{\mathbf{\Pi}} &= \mathbf{\Pi} \times \mathbf{\Omega} + \mathbf{P} \times \mathbf{v} + \mathbf{r} \times mg\mathbf{\Gamma} + \mathcal{T}_{\text{other}} \\
 \dot{\mathbf{P}} &= \mathbf{P} \times \mathbf{\Omega} + \mathcal{F}_{\text{other}} \\
 \dot{\mathbf{\Gamma}} &= \mathbf{\Gamma} \times \mathbf{\Omega}
 \end{aligned} \tag{3.14}$$

where $\mathcal{T}_{\text{other}}$ and $\mathcal{F}_{\text{other}}$ are external torques and forces not due to gravity or buoyancy.

3.1.2 Internal Rotors

In this section, the vehicle model is extended to include three internal rotors which serve as actuators. The configuration space for the underwater vehicle with three internal rotors is $SE(3) \times T^3$. The first factor describes the orientation of the vehicle and the second factor describes the relative spin angles of the internal rotors. Left translation is given by

$$L_{(\mathbf{R}_1, \mathbf{b}_1, \boldsymbol{\alpha}_1)}(\mathbf{R}_2, \mathbf{b}_2, \boldsymbol{\alpha}_2) = (\mathbf{R}_1\mathbf{R}_2, \mathbf{R}_1\mathbf{b}_2 + \mathbf{b}_1, \boldsymbol{\alpha}_1 + \boldsymbol{\alpha}_2)$$

for two elements $(\mathbf{R}_1, \mathbf{b}_1, \boldsymbol{\alpha}_1)$ and $(\mathbf{R}_2, \mathbf{b}_2, \boldsymbol{\alpha}_2)$ in $SE(3) \times T^3$.

Several simplifying assumptions are made concerning the rotor shape and configuration. Each rotor is axisymmetric and spins about its symmetry axis under the influence of a control torque. The rotors are mounted orthogonally within the vehicle so that each rotor's spin axis is aligned with a body coordinate axis. The CG of the three internal rotors is assumed to coincide with the vehicle CB. This assumption would be satisfied, for example,

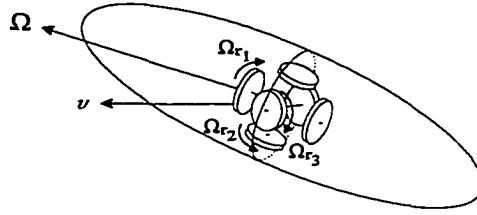


Figure 3.3: Vehicle with three internal rotors.

if each “rotor” is actually a balanced rotor pair, as shown in Figure 3.3.

Let the diagonal matrix with diagonal elements (J_1^i, J_2^i, J_3^i) be the inertia matrix of the rotor which spins about the i th body coordinate axis ($i = 1, 2,$ or 3). Define

$$\Lambda_j = I_j + J_j^1 + J_j^2 + J_j^3, \quad j = 1, 2, \text{ and } 3.$$

The inertia of the vehicle/fluid system with the rotors locked in place is $\Lambda = \text{diag}(\Lambda_1, \Lambda_2, \Lambda_3)$.

It is also convenient to define the matrix of rotor moments of inertia about their respective spin axes: $J_r = \text{diag}(J_1^1, J_2^2, J_3^3)$. Let $\bar{I} = \text{diag}(\bar{I}_1, \bar{I}_2, \bar{I}_3) = \Lambda - J_r$; this matrix represents the body/fluid portion of the locked inertia.

Suppose that the “spin angle” of the i th internal rotor relative to the body is α_i and define the vector of rotor spin angles $\alpha = [\alpha_1, \alpha_2, \alpha_3]^T$. Let $\Omega_r = [\Omega_{r1}, \Omega_{r2}, \Omega_{r3}]^T = \dot{\alpha}$ be the vector of rotor relative angular velocities, as depicted in Figure 3.3.

The Lagrangian for the body/fluid/rotor system is the total kinetic energy

$$\mathcal{L}(\mathbf{R}, \mathbf{b}, \alpha, \mathbf{R}\hat{\Omega}, \mathbf{R}\mathbf{v}, \Omega_r) = \frac{1}{2} \begin{pmatrix} \Omega \\ v \\ \Omega_r \end{pmatrix} \cdot \begin{pmatrix} \Lambda & m\hat{r} & J_r \\ -m\hat{r} & M & 0 \\ J_r & 0 & J_r \end{pmatrix} \begin{pmatrix} \Omega \\ v \\ \Omega_r \end{pmatrix}.$$

Here, we have redefined the vehicle mass m as the combined mass of the ellipsoid and the

three internal rotors. This mass m is still assumed to be equal to the mass of the displaced fluid, i.e., the vehicle is still neutrally buoyant. The Lagrangian is left invariant under the action of $SE(3) \times T^3$ so, in the absence of external forces or torques, the dynamics reduce to Lie-Poisson equations on the dual of the Lie algebra of this group. The reduced Lagrangian, defined on the 9-dimensional reduced velocity phase space, is

$$l(\Omega, v, \Omega_r) = \frac{1}{2} \begin{pmatrix} \Omega \\ v \\ \Omega_r \end{pmatrix} \cdot \begin{pmatrix} \Lambda & m\hat{r} & J_r \\ -m\hat{r} & M & 0 \\ J_r & 0 & J_r \end{pmatrix} \begin{pmatrix} \Omega \\ v \\ \Omega_r \end{pmatrix}.$$

We redefine the body coordinate momenta Π and P to reflect the contribution of the internal rotors and introduce l , the momentum conjugate to Ω_r :

$$\Pi = \Lambda\Omega + m\hat{r}v + J_r\Omega_r,$$

$$P = -m\hat{r}\Omega + Mv,$$

$$l = J_r(\Omega + \Omega_r).$$

Here, Π and P are the total angular and linear momentum vectors, respectively. The i th component of l is the total momentum of the i th rotor about its spin axis.

Using either Euler-Poincaré or Lie-Poisson reduction, one finds that

$$\begin{aligned} \dot{\Pi} &= \Pi \times \Omega + P \times v \\ \dot{P} &= P \times \Omega \\ \dot{l} &= 0. \end{aligned} \tag{3.15}$$

This system possesses five Casimirs: $C_1(\mathbf{\Pi}, \mathbf{P}, \mathbf{l}) = \frac{1}{2}\|\mathbf{P}\|^2$, $C_2(\mathbf{\Pi}, \mathbf{P}, \mathbf{l}) = \mathbf{\Pi} \cdot \mathbf{P}$, and each component of \mathbf{l} .

The rotor angular momenta, the components of \mathbf{l} , are coupled to the equations for $\dot{\mathbf{\Pi}}$ and $\dot{\mathbf{P}}$ through the body angular velocity

$$\mathbf{\Omega} = \bar{\mathbf{I}}^{-1}(\mathbf{\Pi} - \mathbf{l}).$$

We are interested in using the internal rotors to control the vehicle dynamics. Suppose that three motors mounted within the vehicle exert control torques on the internal rotors. Then the third equation of (3.15) becomes

$$\dot{\mathbf{l}} = \mathbf{u} \tag{3.16}$$

where $\mathbf{u} = (u_1, u_2, u_3)^T$ and u_i is the torque applied to the i th internal rotor about its spin axis. In general, \mathbf{l} will no longer be conserved, however C_1 and C_2 are conserved for *any* choice of \mathbf{u} . This observation reflects the fact that internal actuators cannot affect the total inertial momentum.

In the more general case that the vehicle CG and CB do not coincide, symmetry is partially broken. As in Section 3.1.1, the reduced dynamics may be obtained through semidirect product reduction:

$$\begin{aligned} \dot{\mathbf{\Pi}} &= \mathbf{\Pi} \times \mathbf{\Omega} + \mathbf{P} \times \mathbf{v} + \mathbf{r} \times m\mathbf{g}\mathbf{\Gamma} \\ \dot{\mathbf{P}} &= \mathbf{P} \times \mathbf{\Omega} \\ \dot{\mathbf{\Gamma}} &= \mathbf{\Gamma} \times \mathbf{\Omega} \\ \dot{\mathbf{l}} &= \mathbf{u}. \end{aligned} \tag{3.17}$$

The quantities $C_1(\mathbf{\Pi}, \mathbf{P}, l, \Gamma) = \frac{1}{2}\|\mathbf{P}\|^2$, $C_2(\mathbf{\Pi}, \mathbf{P}, l, \Gamma) = \frac{1}{2}\|\Gamma\|^2$, and $C_3(\mathbf{\Pi}, \mathbf{P}, l, \Gamma) = \mathbf{P} \cdot \Gamma$ are conserved for any choice of control \mathbf{u} .

3.1.3 Viscous Forces

This section describes a model for the viscous fluid forces. It is assumed that the torque due to viscous forces acting on the vehicle takes the form $\mathbf{f}_\Omega(\Omega, \mathbf{v})$ where $\mathbf{f}_\Omega(\cdot, \cdot)$ has continuous partial derivatives and $\mathbf{f}_\Omega(\Omega, \mathbf{v}) = \mathbf{0}$ if and only if $\Omega = \mathbf{0}$. Similarly, the damping force is given by $\mathbf{f}_v(\Omega, \mathbf{v})$ where $\mathbf{f}_v(\cdot, \cdot)$ is C^1 and $\mathbf{f}_v(\Omega, \mathbf{v}) = \mathbf{0}$ if and only if $\mathbf{v} = \mathbf{0}$. For example, a simple drag model which satisfies these assumptions is given in [29]:

$$\begin{aligned} \mathbf{e}_i \cdot \mathbf{f}_\Omega(\Omega, \mathbf{v}) &= -(a_i + \bar{a}_i|\Omega_i|)\Omega_i \\ \mathbf{e}_i \cdot \mathbf{f}_v(\Omega, \mathbf{v}) &= -(b_i + \bar{b}_i|v_i|)v_i \end{aligned} \tag{3.18}$$

where all of the coefficients are positive constants.

One expects that the force of drag will oppose velocity in the sense that

$$\begin{aligned} \Omega \cdot \mathbf{f}_\Omega(\Omega, \mathbf{v}) &< 0 & (\Omega \neq \mathbf{0}) \\ \mathbf{v} \cdot \mathbf{f}_v(\Omega, \mathbf{v}) &< 0 & (\mathbf{v} \neq \mathbf{0}) \end{aligned}$$

We make the stronger assumption that drag grows at least linearly with velocity,

$$\begin{aligned} \Omega_i \mathbf{e}_i \cdot \mathbf{f}_\Omega(\Omega, \mathbf{v}) &\leq -\underline{f}_{\Omega_i} \Omega_i^2 < 0 & (i = 1, 2, 3 \text{ and } \Omega_i \neq 0) \\ v_i \mathbf{e}_i \cdot \mathbf{f}_v(\Omega, \mathbf{v}) &\leq -\underline{f}_{v_i} v_i^2 < 0 & (i = 1, 2, 3 \text{ and } v_i \neq 0) \end{aligned} \tag{3.19}$$

where \underline{f}_{Ω_i} and \underline{f}_{v_i} are positive scalars. For the example drag model (3.18), one could choose any \underline{f}_{Ω_i} satisfying $0 < \underline{f}_{\Omega_i} \leq a_i$ and any \underline{f}_{v_i} satisfying $0 < \underline{f}_{v_i} \leq b_i$ for $i = 1, 2$, and 3 .

A vehicle which is symmetric about its 1-2 and 1-3 planes will experience no lift or side

force when translating steadily along its 1-axis (i.e., at zero angle-of-attack and zero sideslip angle). For any scalar c ,

$$\mathbf{e}_i \cdot \mathbf{f}_v(\mathbf{0}, c \mathbf{e}_1) = 0, \quad \text{for } i = 2 \text{ and } 3. \quad (3.20)$$

Note that the symmetry assumption does not prohibit a symmetric wing or empennage.

This chapter concerns stability of steady vehicle translation. In the presence of drag, steady translation requires a constant motive force. Therefore a constant, body-fixed force $\mathcal{F}_{\text{thrust}}$ is included to counter the drag force at equilibrium. The equations of motion, with viscous forces and thrust included explicitly, are

$$\begin{aligned} \dot{\mathbf{\Pi}} &= \mathbf{\Pi} \times \mathbf{\Omega} + \mathbf{P} \times \mathbf{v} + \mathbf{r} \times mg\mathbf{\Gamma} + \mathbf{f}_{\Omega}(\mathbf{\Omega}, \mathbf{v}) \\ \dot{\mathbf{P}} &= \mathbf{P} \times \mathbf{\Omega} + \mathbf{f}_v(\mathbf{\Omega}, \mathbf{v}) + \mathcal{F}_{\text{thrust}} \\ \dot{\mathbf{\Gamma}} &= \mathbf{\Gamma} \times \mathbf{\Omega} \\ \dot{\mathbf{i}} &= \mathbf{u}. \end{aligned} \quad (3.21)$$

3.2 Stability of Relative Equilibria

In this section, we review a number of published stability results for the underwater vehicle and we also present some new stability results. In previous work on underwater vehicle stability, Holmes *et al* [31] present a comprehensive investigation of stability of relative equilibria for an immersed ellipsoid with uniformly distributed mass. (They also show how one might use the global system dynamics to perform interesting maneuvers. The idea of using nonlinear dynamics to advantage is a major motivation for nonlinear control design.) Leonard [42] considers stability of a vehicle which is translating along and possibly

rotating about an ellipsoid principal axis; the paper introduces a Lie-Poisson model for a bottom-heavy underwater vehicle which is the basis for the model presented in Section 3.1.1. Pursuing questions regarding stability of a bottom-heavy underwater vehicle, Leonard and Marsden [44] consider the issue of drift in the configuration variables for Lie-Poisson systems on noncompact Lie groups. In particular, they consider cases where the Poisson tensor loses rank at the equilibrium. While the energy-Casimir method may be used to prove stability for such “nongeneric equilibria,” the nature of the stability must be carefully interpreted. Leonard and Marsden show for a bottom-heavy underwater vehicle that one may expect drift in the noncompact (translational) directions but not in the compact (rotational) directions. Other work on stability of bottom-heavy, immersed bodies includes that of Kozlov [38, 39], who considered a heavy, planar body falling under its own weight in a fluid with constant circulation, and Rubanovskii [60], who studied stability of precessional motions of a translating, bottom-heavy body.

Section 3.2.1 reviews the equilibria for an underwater vehicle with coincident centers of buoyancy and gravity as well as some stability results. Section 3.2.2 gives a similar review in the case that the center of gravity lies along the shortest ellipsoid principal axis.

3.2.1 Coincident Centers of Gravity and Buoyancy

This section discusses stability of relative equilibria for the uncontrolled underwater vehicle with the internal rotors locked in place. Assume that no viscous forces act on the vehicle and that the CG and CB coincide ($\mathbf{r} = \mathbf{0}$). Equivalently, consider the model (3.7) where the inertia matrix \mathbf{I} is replaced by $\mathbf{\Lambda}$. This system has several families of relative equilibria [31]. There are three two-parameter families of relative equilibria corresponding to steady translation along and rotation about vehicle principal axes. Following [31], we refer to these

as “pure mode” equilibria. For example, a pure 1 mode equilibrium is given by

$$\mathbf{\Pi}_e = \begin{pmatrix} \Pi_1^0 \\ 0 \\ 0 \end{pmatrix}, \quad \mathbf{P}_e = \begin{pmatrix} P_1^0 \\ 0 \\ 0 \end{pmatrix} \quad (3.22)$$

where the subscript “e” denotes an equilibrium value. If $(\boldsymbol{\Omega}_e, \mathbf{v}_e) = (\Omega_1^0 \mathbf{e}_1, v_1^0 \mathbf{e}_1)$, then $\Pi_1^0 = \Lambda_1 \Omega_1^0$ and $P_1^0 = m_1 v_1^0$.

It was shown in [31] that, depending on the ordering of moments of inertia, Λ_1, Λ_2 , and Λ_3 , there may also exist non-principal axis steady motions referred to as “mixed mode” equilibria. For example, when $\Lambda_2 > \Lambda_1 > \Lambda_3$ or $\Lambda_2 > \Lambda_3 > \Lambda_1$, a mixed 2-3 mode equilibrium is given by

$$\mathbf{\Pi}_e = \pm \rho \begin{pmatrix} 0 \\ \Lambda_2 P_2^0 \\ \Lambda_3 P_3^0 \end{pmatrix}, \quad \mathbf{P}_e = \begin{pmatrix} 0 \\ P_2^0 \\ P_3^0 \end{pmatrix}, \quad \rho = \sqrt{\frac{m_3 - m_2}{m_2 m_3 (\Lambda_2 - \Lambda_3)}}. \quad (3.23)$$

The equilibrium (3.23) describes translation along an axis in the body 2-3 plane and rotation about a different axis in the same plane.

Stability of relative equilibria can be studied using the energy-Casimir method [50]. Of particular interest is stability of the pure 1 mode equilibrium (3.22). Since the 1-axis is the longest vehicle axis, this equilibrium is a practical (streamlined) motion. Applying the energy-Casimir method with $P_1^0 \neq 0$ indicates that (3.22) is stable provided

$$\frac{1}{\Lambda_1} \left(\frac{1}{\Lambda_i} - \frac{1}{\Lambda_1} \right) \left(\frac{\Pi_1^0}{P_1^0} \right)^2 > \frac{1}{\Lambda_i} \left(\frac{1}{m_1} - \frac{1}{m_i} \right) \quad (3.24)$$

for both $i = 2$ and $i = 3$. (See [31] for the proof.) The right-hand side of (3.24) will always be positive and the left-hand side will always be negative for $i = 2$. Thus, the equilibrium will never satisfy these conditions. Indeed, Holmes, Jenkins, and Leonard [31] show by spectral analysis that the equilibrium is unstable for small magnitudes of the ratio $\frac{\Pi_1^0}{P_1^0}$.²

In fact, it is well known that steady translation of a non-rotating ellipsoid along its long axis through a fluid is unstable. This instability can be understood physically by considering the flow around the vehicle when it is slightly perturbed from the equilibrium motion. A pressure gradient results that tends to turn the vehicle so that its blunt side faces the flow.

In the special case of a prolate, axisymmetric ellipsoid, if the body rotates about its symmetry axis with sufficient angular velocity (with the internal rotors locked in place), the equilibrium will be stable. Consider a prolate spheroid with principal axis lengths $L_1 = L_2 < L_3$. As one would expect, the mass and inertia elements satisfy $m_1 = m_2 > m_3$ and $I_1 = I_2 > I_3$ and we assume that the rotors are identical so that $\Lambda_1 = \Lambda_2 > \Lambda_3$.

Proposition 3.2.1 (Leonard [42]) *The equilibrium defined by translational velocity $v = v_e = [0, 0, v_3^0]^T$ and angular velocity $\Omega = \Omega_e = [0, 0, \Omega_3^0]^T$ is stable provided*

$$\frac{(\Lambda_3 \Omega_3^0)^2}{4\Lambda_1} > \left(\frac{1}{m_3} - \frac{1}{m_1}\right)(m_3 v_3^0)^2. \quad (3.25)$$

Lamb [41] showed spectral stability under condition (3.25). However, spectral stability is only a necessary condition, not sufficient, for stability. The steady motion of Proposi-

²The authors also show that the equilibrium is linearly stable for a sufficiently high ratio $\frac{\Pi_1^0}{P_1^0}$ provided $\Lambda_3 > \Lambda_2 > \Lambda_1$ or $\Lambda_2 > \Lambda_3 > \Lambda_1$. If $\Lambda_2 > \Lambda_1 > \Lambda_3$, then, depending on the relative mass and inertia parameters, linear stability may or may not be possible for some range of nonzero $\frac{\Pi_1^0}{P_1^0}$. In any case, the energy-Casimir method fails to provide sufficient conditions for nonlinear stability.

tion 3.2.1 is unstable if the reverse of inequality (3.25) is satisfied.

Rather than spin the vehicle, as suggested by condition (3.25), one might place an axisymmetric rotor within the vehicle with its spin axis aligned with the body symmetry axis. let α denote the spin angle of such an internal rotor relative to the body. Let J_{rotor} be the moment of inertia of the rotor about its spin axis and let Λ represent the total body/fluid inertia with the internal rotor locked in place.

Proposition 3.2.2 (Leonard and Woolsey [45]) *Consider an axisymmetric vehicle with a single internal rotor driven to a constant angular rate $\dot{\alpha}$ and suppose that $\mathbf{r} = \mathbf{0}$. The equilibrium defined by translational velocity $\mathbf{v} = \mathbf{v}_e = [0, 0, v_3^0]^T$ and angular velocity $\boldsymbol{\Omega} = \boldsymbol{\Omega}_e = [0, 0, \Omega_3^0]^T$ is stable provided*

$$\frac{(\Lambda_3 \Omega_3^0 + J_{\text{rotor}} \dot{\alpha})^2}{4\Lambda_1} > \left(\frac{1}{m_3} - \frac{1}{m_1} \right) (m_3 v_3^0)^2. \quad (3.26)$$

Thus it is possible to stabilize long axis translation by spinning the body about its symmetry axis, by spinning an internal rotor, or by a combination of the two.

3.2.2 Noncoincident Centers of Gravity and Buoyancy

Here, we consider stability of relative equilibria for the uncontrolled system with $\mathbf{r} = \gamma \mathbf{e}_3$. For this vehicle configuration, the CG lies along the 3-axis of the body coordinate frame. If $\gamma > 0$, then the vehicle is “bottom-heavy,” meaning that the CG is below the CB when the body frame coincides with the inertial coordinate frame. The dynamics are described by the model (3.14) with $\mathcal{T}_{\text{other}} = \mathbf{0}$ and with $\mathcal{F}_{\text{other}} = \mathbf{0}$. The relative equilibria for this system and their stability properties are studied in some detail in [42]. For a nonaxisymmetric

ellipsoid, there are two categories of steady translational equilibria, those for which the vehicle spins about and translates along its 3-axis parallel to the direction of gravity, and those for which the vehicle translates (without spinning) along a direction in the body 1-3 or 2-3 plane.

When considering a vehicle with $\mathbf{r} \neq \mathbf{0}$, we will refer to an equilibrium of the form

$$\mathbf{\Pi}_e = \begin{pmatrix} 0 \\ \frac{m\gamma P_1^0}{m_1} \\ 0 \end{pmatrix}, \quad \mathbf{P}_e = \begin{pmatrix} P_1^0 \\ 0 \\ 0 \end{pmatrix}, \quad \mathbf{\Gamma}_e = \begin{pmatrix} 0 \\ 0 \\ 1 \end{pmatrix} \quad (3.27)$$

as a “pure 1 mode” equilibrium. The equilibrium (3.27) corresponds to pure translation (i.e., translation without rotation) along the body 1-axis: $(\mathbf{\Omega}_e, \mathbf{v}_e) = (\mathbf{0}, \frac{P_1^0}{m_1} \mathbf{e}_1)$. The pure 2 mode is defined likewise. Pure mode equilibria as defined here are a special subclass of a more general family of pure translation equilibria (4.68) described in Section 4.2.1. We will be particularly interested in pure 1 mode equilibria.

Recalling the axis length ordering $L_1 > L_2 > L_3$, it was shown in [42] via the energy-Casimir method that pure 2 mode equilibria can be made Lyapunov stable by setting

$$\gamma > \frac{1}{mg} \left(\frac{1}{m_2} - \frac{1}{m_3} \right) (P_2^0)^2 > 0.$$

Thus, by making the center of gravity sufficiently low relative to the center of buoyancy, *intermediate* axis translation in the horizontal plane can be stabilized. However, the pure 1 mode equilibrium is unstable for any choice of γ . While gravity stabilizes the vehicle in pitch and roll, the gravitational torque cannot counter the vertical component of fluid torque which tends to turn the vehicle (in the horizontal plane) away from the equilibrium.

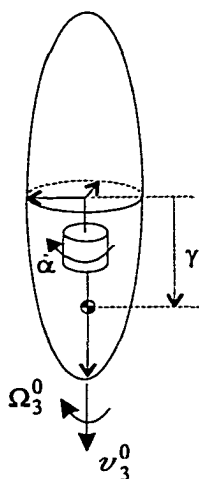


Figure 3.4: Bottom-heavy prolate spheroid with an internal rotor.

Considering once again the case of a prolate spheroid ($L_1 = L_2 < L_3$), motion parallel to the direction of gravity can be stabilized by spinning the vehicle or by placing the CG sufficiently low along the axis of symmetry or by a combination of both. Assume that $\mathbf{r} = \gamma \mathbf{e}_3$ so that the center of gravity is a distance $|\gamma|$ along the vehicle's symmetry axis.

Proposition 3.2.3 (Leonard and Marsden [44]) *The equilibrium defined by translational velocity $\mathbf{v} = \mathbf{v}_e = [0, 0, v_3^0]^T$ and angular velocity $\boldsymbol{\Omega} = \boldsymbol{\Omega}_e = [0, 0, \Omega_3^0]^T$ is stable provided*

$$mg\gamma + \frac{(\Lambda_3 \Omega_3^0)^2}{4 \left(\Lambda_1 - \frac{(m\gamma)^2}{m_1} \right)} > \left(\frac{1}{m_3} - \frac{1}{m_1} \right) (m_3 v_3^0)^2. \quad (3.28)$$

Note that it is possible to pick γ large enough that angular velocity is unnecessary for stability. That is, if the spheroid is sufficiently “bottom-heavy,” it can translate stably at speed v_3^0 parallel to the direction of gravity. In contrast, it is also possible to spin a top-heavy ($\gamma < 0$) vehicle fast enough that axial translation parallel to gravity is stable.

If necessary, the gyroscopic contribution to the vehicle's stability may be provided in whole or in part by an internal rotor. Spectral analysis gives the following intuitive result.

Proposition 3.2.4 *Suppose that an axisymmetric rotor aligned with the vehicle's symmetry axis is driven at a constant relative rate $\dot{\alpha}$. The equilibrium defined by translational velocity $v = v_e = [0, 0, v_3^0]^T$ and angular velocity $\Omega = \Omega_e = [0, 0, \Omega_3^0]^T$ with $\Gamma_e = e_3$ is spectrally stable provided*

$$mg\gamma + \frac{(\Lambda_3\Omega_3^0 + J_{\text{rotor}}\dot{\alpha})^2}{4\left(\Lambda_1 - \frac{(m\gamma)^2}{m_1}\right)} \geq \left(\frac{1}{m_3} - \frac{1}{m_1}\right)(m_3v_3^0)^2. \quad (3.29)$$

While spectral stability does not imply nonlinear stability, the results of [42] make it reasonable to conjecture that nonlinear stability would hold under condition (3.29) with strict inequality. Proposition 3.2.4 suggests that it is possible to stabilize long axis translation parallel to the direction of gravity by spinning the body about its symmetry axis, by spinning an internal rotor, by lowering the CG relative to the CB, or by a combination of all of these.

3.3 Experimental Investigation of Stability

While global dynamic models are indeed useful in developing nonlinear control strategies, underwater vehicle models based on potential flow analysis, such as Kirchhoff's model or slender body approximations, are accurate only for streamlined bodies moving near the streamline direction. For other motions, the effect of viscosity is significant if not dominant. Still, Kirchhoff's model accurately (and globally) describes the dynamics of a body in an inviscid, irrotational fluid and thus provides a useful starting point for control designers.

This section describes an experimental investigation of the stability predictions of Sections 3.2.1 and 3.2.2. In particular, we consider steady translation of a prolate spheroid (a slender, axisymmetric ellipsoid) along its symmetry axis. If the body's CB and CG coin-

cide, such a motion is an equilibrium of the dynamic equations regardless of the direction of travel. According to Proposition 3.2.1, stability of this motion depends on the body's fineness ratio (the ratio of length to diameter) and the equilibrium values of translational and angular momentum. If the CG is some distance $|\gamma|$ along the symmetry axis from the CB, then steady translation along the symmetry axis parallel to the direction of gravity is a steady motion. Stability of this equilibrium depends on the parameters above as well as the "bottom-heaviness" parameter γ , as described in Proposition 3.2.4.

Section 3.3.1 discusses the effect of viscosity on the flow over a prolate spheroid and on the stability predictions. Section 3.3.2 describes the experimental apparatus used to verify the stability predictions. In Section 3.3.3, we present some quantitative analysis of the experiments performed and discuss the results.

3.3.1 Viscous Flow Over a Prolate Spheroid

Kirchhoff's equations rely on the assumption of an inviscid fluid which "slips" along the body surface. In reality, viscosity requires that the fluid velocity match the velocity of the body at its surface. As a result of this so-called "no slip" condition, there develops over the body surface a boundary layer through which the fluid velocity changes from zero relative velocity at the surface to the relative free stream velocity. This boundary layer begins at the forward stagnation point (where the free stream has been brought to rest relative to the body) and grows along the surface to a point where it can no longer grow under the ambient conditions. The boundary layer then either "separates" from the body causing a turbulent wake or "transitions" into a turbulent boundary layer which continues to grow more or less as before. A turbulent boundary layer will also separate at some point but, for a streamlined body, typically leaves a much smaller wake than a separating laminar

boundary layer.

The two major mechanisms by which viscosity retards a body's motion through a fluid are skin friction and pressure drag. Skin friction refers to the viscous stress exerted directly on a body's surface. Pressure drag refers to a retardant force due to a lower fluid pressure in the body's wake. The lower pressure in the wake results from an energy loss to viscous dissipation. For a streamlined body, there is a tradeoff between these two drag mechanisms: while skin friction is greater for a turbulent boundary layer than for a laminar one, pressure drag decreases with the size of the wake. For very slender bodies, skin friction can be a dominant concern, but pressure drag is more important for less slender bodies.

An indicator of the tendency of a laminar boundary layer to transition into a turbulent one is the dimensionless Reynolds number, $Re = \frac{UL}{\nu}$ where U is the body velocity, L is the body's length, and ν is the kinematic viscosity of the fluid. For a slender spheroid, a turbulent boundary layer typically develops when $Re > 2.5 \times 10^6$ [67]. Of the two possibilities, a laminar-then-turbulent boundary layer or separating laminar flow, the former is closer to the ideal case of potential flow; because of the smaller wake, potential theory is valid in a larger region of the flow. In the experiments to be described in Section 3.3.2, Re is of order 10^4 so that we expect the less ideal case of a separating laminar boundary layer. If the theoretical stability predictions hold for the less ideal case of subcritical flow, one would expect them to hold for supercritical flow, as well. In this sense, the experiments give conservative results.

Figure 3.5 illustrates the development and separation of the boundary layer for two spheroids of different fineness ratio. (The fineness ratio is the ratio of the largest cross-sectional width to the length.) The spheroids are both 6 inches in length and are immersed in a channel of water flowing from left to right at 0.10 ± 0.03 m/s. Note the accumulation

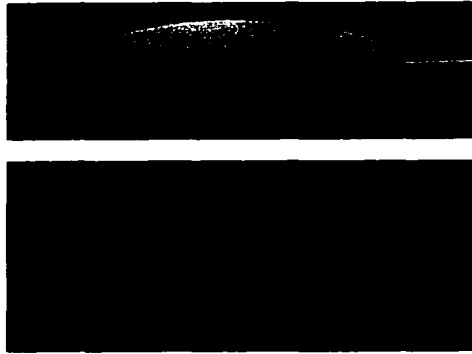


Figure 3.5: Subcritical flow (from left to right) over a 2.5:1 and 2:1 spheroid.

of dye tracer which indicates the line of separation. Separation occurs later on the more slender spheroid. This suggests that potential flow models streamlined motions of slender bodies better than bluff body motions. We therefore expect better agreement between theory and experiment for the spheroids with higher fineness ratios.

Note that the boundary layer shown in Figure 3.5 separates along a circular cross section of the spheroid. When the vehicle is slightly perturbed from axial translation, axial symmetry of the flow is broken and the boundary layer no longer separates along a circular perimeter of the spheroid. Nor does the boundary layer separate along an elliptical cross section of the body, as one might expect. Calculations and experiments described in [26] and [27] underscore the complexity of steady, laminar flow over a prolate spheroid whose symmetry axis is inclined at some “angle-of-attack” to a steady flow. The motion of a free spheroid in a fluid is more properly described by unsteady flow; unsteady flow over a maneuvering spheroid is a topic of current research. (See [67] and references therein.)

Putnam *et al* [59] describe two semiempirical models for the fluid forces and moments on a slender body of revolution at nonzero angle-of-attack. Both models, one due to Allen [3, 4] and the other due to Hopkins [32], combine the force and moment predictions from slender body theory with an additive “correction” which is based on a semiempirical model

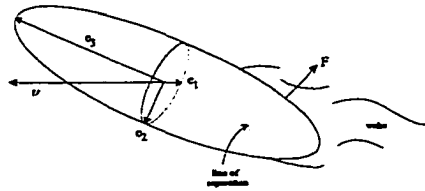


Figure 3.6: Asymmetrically separating flow.

of the drag on a cylinder in a cross flow. While neither model considers the full complexity of steady flow over an axisymmetric body at incidence, both models give good agreement with experimental measurements of the resulting forces and moments [59].

For the purpose of this investigation, it is chiefly important to note that the flow over an inclined spheroid separates earlier on the leeward side. The resulting asymmetric wake actually tends to stabilize axial translation because the lower pressure in the wake tends to realign the body's symmetry axis with the free stream [59]. The idea is illustrated in Figure 3.6, where the force F represents the net force on the spheroid due to the lower pressure aft of the line of separation. The force F imposes a torque which tends to realign the body's symmetry axis with the flow. Of course, Figure 3.6 is only a cartoon intended to depict the effect of the separating wake. It does not show the effect of the flow forward of the line of separation; the flow in this region is well-approximated by inviscid theory. The effect of separation will not generally dominate the destabilizing torque predicted by potential flow theory, but it will attenuate that effect. Further, it is reasonable to conjecture that viscous drag will enhance stability once the motion has been stabilized by lowering the CG and/or by spinning an internal rotor.

It is more difficult to describe the effect of viscosity on stability when the spheroid itself spins. The flow of a viscous fluid over an axisymmetric object spinning about its symmetry axis has been the subject of a number of theoretical and experimental investigations. Luthander and Rydberg [64], Hoskin [33], and Fadnis [28] studied the effect of spin rate on

boundary layer development over a sphere and the resulting effect on drag. The essential observation about the effect of spin rate on a spheroid's motion is that the boundary layer separates earlier with increasing angular velocity leading to an increasingly broad turbulent wake. Consequently, the drag is greater at increased spin rates. There are also more subtle concerns such as the influence of the Magnus effect on a spinning spheroid which is perturbed from axial translation. This phenomenon has been studied by Martin [52], for example. See Liberzon [46] and references therein for a discussion of the effect of the Magnus force on stability of a spinning and translating body of revolution.

3.3.2 Experimental Setup

To study the stability criteria presented in Section 3.2, several spheroids of varying fineness ratio were fabricated for testing in a 5 foot \times 3 foot \times 1.5 foot water tank. Two types of spheroid were created; the first type allows for variation of the CG while the second type contains an adjustable-speed internal rotor. A launch device was constructed to provide the experimental bodies with a desired initial axial velocity in the vertical direction. The launch device can also provide a desired initial spin rate about a spheroid's symmetry axis.

To quantify the experimental stability analysis, position and orientation were measured using an image-based tracking system. A commercial video camera was placed with the line of sight orthogonal to the tank's flat glass wall. The camera view included a direct view of the test trajectories and a side view reflected through a 45° mirror. Also contained within the camera view was a red light-emitting diode which was placed at a known location to serve as a fiduciary point for the analysis. Recorded test footage was digitized using a Silicon Graphics Indigo2 workstation and analyzed using an image-processing routine developed to measure the body's position. Figure 3.7 shows the negative of a sample image from an

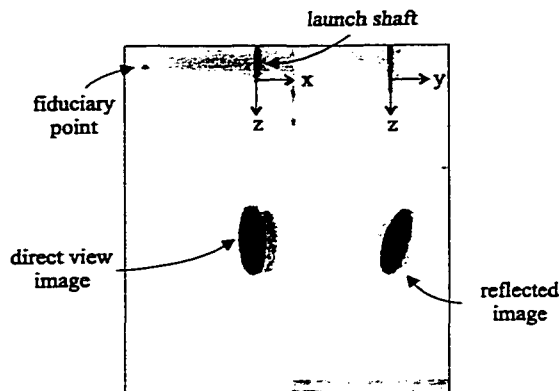


Figure 3.7: Sample frame from experimental footage.

experiment. For details about the tracking algorithm, see [35].

We first describe the experimental setup for the spheroids with an adjustable CG. We then describe the experimental setup for the spheroids with an internal rotor.

Spheroid with an Adjustable CG. Recall from condition (3.28) that two independent parameters affect stability for a given spheroid translating at speed v_3^0 along its long axis in the direction of gravity: the “bottom-heaviness” γ and the angular rate Ω_3^0 . When $\gamma = 0$, the critical angular rate $\Omega_3^0 = \Omega_c$ for a given velocity v_3^0 is given by

$$\Omega_c^2 = \frac{4I_2}{I_3^2} \left(\frac{1}{m_3} - \frac{1}{m_2} \right) (m_3 v_3^0)^2.$$

Proposition 3.2.3 implies that steady symmetry-axis translation will be stable provided $|\Omega_3^0| > |\Omega_c|$. When $\Omega_3^0 = 0$, the critical CG location $\gamma = \gamma_c$ is

$$\gamma_c = \frac{1}{mg} \left(\frac{1}{m_3} - \frac{1}{m_2} \right) (m_3 v_3^0)^2.$$

In this case, Proposition 3.2.3 indicates that steady symmetry-axis translation (without rotation about the symmetry axis) will be stable provided $\gamma > \gamma_c$. In principle, one could explore stability in terms of the two parameters γ and Ω_3^0 . In reality, such an investigation

Fineness	m (g)	m_{slug} (g)	m_1 (g)	m_3 (g)	I_1 (kg m ²)	I_3 (kg m ²)
4:1	116	25.0	215	125	2.0E-4	1.5E-5
3:1	206	31.7	372	232	3.7E-4	4.9E-5
2.5:1	322	38.1	520	346	5.3E-4	1.1E-4
2:1	463	45.6	789	560	8.1E-4	2.5E-4

Table 3.1: Mass and Inertia Properties.

is complicated by the problem of maintaining a steady spin rate. While experiments were performed at varying spin rates, it was found that the angular rate decayed too quickly to give credible stability results. We therefore consider only the case where $\Omega_3^0 = 0$ and explore stability in terms of the single parameter γ .

A series of experiments was performed using four spheroids of equal length but with differing fineness ratios. The spheroids were each 15 cm (6 in) in length with fineness ratios of 4:1, 3:1, 2.5:1, and 2:1. The spheroids were milled from machinable polyethylene using a computer-numerically controlled machine. They were bored and tapped along the symmetry axis and a slug of threaded stainless steel was inserted to trim the vehicles' mass and to allow for variation of the bottom-heaviness parameter γ . The relevant mass and inertia properties are given in Table 3.1 for the case of coincident CG and CB. The displaced mass is m and m_{slug} is the mass of the stainless steel slug. In reality, each spheroid was trimmed to be slightly heavy when submerged, i.e., the actual mass is slightly more than the displaced mass m .

A launch mechanism was constructed to provide the appropriate initial velocity and an adjustable spin rate. The mechanism consists of a keyed shaft spinning at the desired rate within a loose collar. The shaft mates to the end of a spheroid. A small permanent magnet embedded in the shaft tip attracts a ferrous tablet embedded in the spheroid holding the body in place before it is launched. When triggered, the shaft drops, accelerating towards

Fineness	$\gamma_c/(v_3^0)^2$ (s ² /cm)	v_3^0 (cm/s)	γ_c (cm)
4:1	0.00045	17 ± 1	0.13 ± 0.02
3:1	0.00043	21 ± 1	0.19 ± 0.02
2.5:1	0.00039	16 ± 1	0.10 ± 0.02
2:1	0.00035	17 ± 1	0.10 ± 0.02

Table 3.2: Critical Values of γ given v_3^0 .

a mechanical stop which is placed such that the shaft and spheroid approach the body's terminal velocity. The spheroid slides off of the shaft under its own momentum.

The spheroids were trimmed to be slightly heavy when submerged in order to obtain the terminal descent velocity indicated in Table 3.2. Also shown is the critical parameter value γ_c for the given equilibrium velocity v_3^0 . In general, the 2:1 ellipsoid is the "least unstable" in steady translation in the sense that γ_c is smallest for a given value of v_3^0 . The 4:1 ellipsoid is the most unstable.

Spheroid with an Internal Rotor. As mentioned, it was not possible to obtain steady or nearly steady motions for $\Omega_3^0 \neq 0$; the body angular rate decayed too quickly. One solution would be to use spin fins, as found, for example, on ballistic missile reentry vehicles. However, the effect of spin fins on an axisymmetric body in a flow is not limited to their contribution to the body's symmetry axis spin rate; it would be difficult to separate the stabilizing effect of spin rate from the viscous moment exerted by the fins and the validity of condition (3.28) would be obscured.

Rather than spin the body, one may provide angular momentum using an internal rotor. An actuated rotor overcomes the difficulty of maintaining a steady spin rate and also simplifies the viscous effects (at least to the extent that viscous flow over a non-spinning spheroid is "simple").

The experimental internal rotor (Figure 3.8) is a modified commercial yaw rate gyroscope



Figure 3.8: Experimental Internal Rotor.

Fineness	v_3^0 (cm/s)	γ (cm)	$\dot{\alpha}_c$ (rad/s)
3:1	25 ± 1	0.24 ± 0.04	240 ± 10
2.5:1	25 ± 1	0.24 ± 0.04	240 ± 10

Table 3.3: Critical values of $\dot{\alpha}$ given γ and v_3^0 .

designed for use with radio-controlled model aircraft. An adjustable voltage regulator allows for variation of the spin rate. The moment of inertia of this rotor about its spin axis is $J_{\text{rotor}} = 4.0\text{E} - 6 \text{ kgm}^2$. The mass and inertia characteristics of the spheroid with internal rotor are practically identical to those listed in Table 3.1. The 4:1 spheroid was not used in the internal rotor experiments because the rotor was too large to be contained within that body. The 2:1 spheroid was not used because the angular momentum range for the rotor was insufficient to resolve the critical condition for stability. (See the remarks concerning the 2.5:1 spheroid at the end of Section 3.3.3.)

The spheroids created for the rotor experiments allowed for very little CG variation, so γ was held constant. Table 3.3 gives the critical internal rotor spin rate $\dot{\alpha}_c$ for stability at the indicated speed and the indicated value of γ . The equilibrium velocity v_3^0 was chosen to place the critical spin rate within the physically realizable range of the internal rotor. The critical spin rate $\dot{\alpha}_c$ was computed for the two spheroids from condition (3.29) of Conjecture 3.2.4. As indicated in Table 3.3, the values of $\dot{\alpha}_c$ were essentially equal.

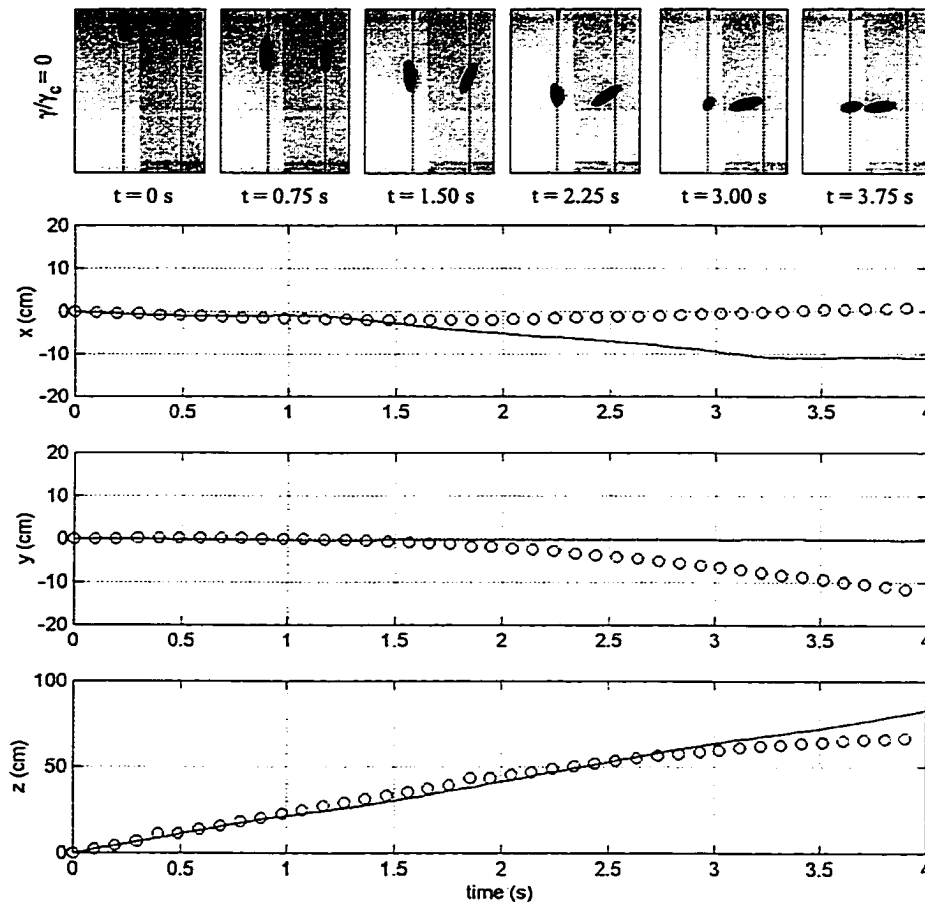


Figure 3.9: Experimental data for the 4:1 ratio spheroid: $\gamma = 0$.

3.3.3 Experimental Results

For each spheroid with an adjustable CG, a series of experiments was performed in which the parameter γ was varied. At each value of γ , at least three tests were recorded, digitized, and analyzed. The analysis involved using an image-based tracking algorithm to measure the spheroid position from experimental footage.

Figures 3.9, 3.10, and 3.11 show representative experimental data from tests of the 4:1 fineness ratio spheroid. At the top of each figure is a time series of images taken from the experimental footage. Below the series of images are three plots showing the estimated position of the spheroid center (shown as circles). Also shown in these plots is the position

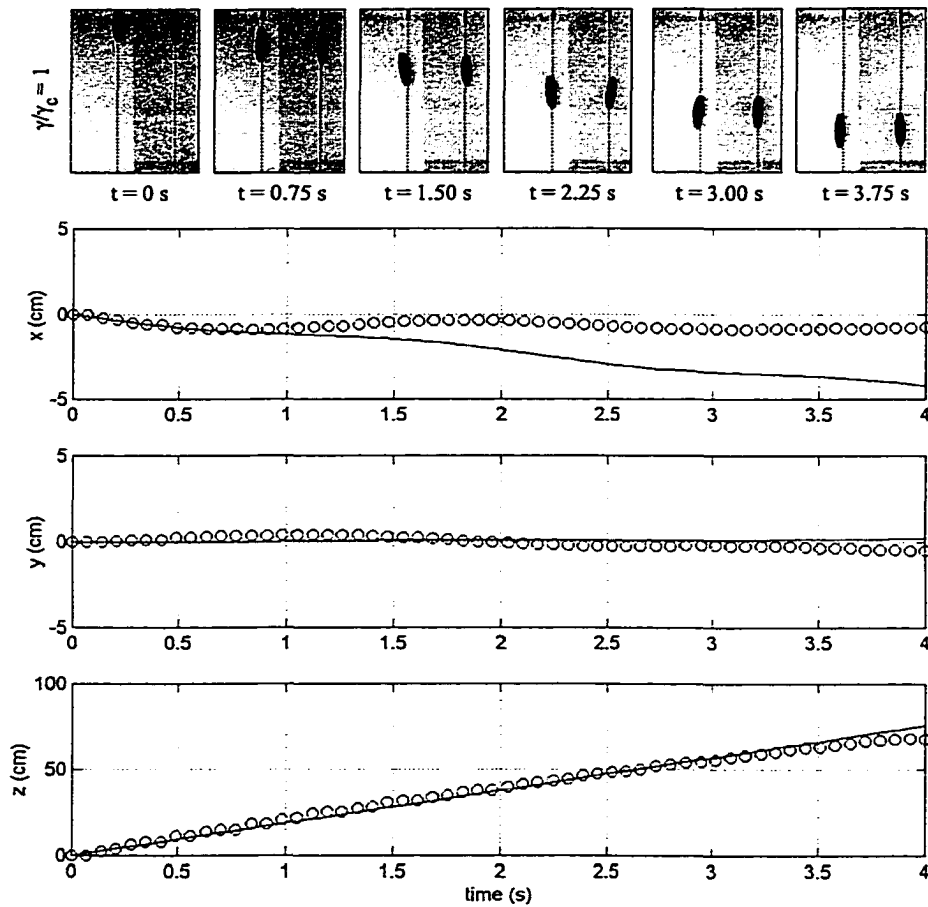


Figure 3.10: Experimental data for the 4:1 ratio spheroid: $\gamma = \gamma_c$.

predicted by simulation using the ideal (inviscid) equations of motion. The initial conditions for the simulations were estimated from experimental data. Because the image processing routine could not reliably predict the spheroid's orientation, only position data are shown.

Figure 3.9 shows an experiment in which the CG and CB coincide. The images at the top of the figure clearly show the spheroid diverging from the initial long-axis translation motion. The spheroid rotates to the point where it is translating more or less along a minor axis. Note from the comparison of actual and simulated data that the velocity of the spheroid decreases significantly and that simulations do not correctly predict the direction in which the spheroid motion diverges.

Figure 3.10 shows an experiment in which the value of γ is the critical value predicted from theory. The motion of the spheroid is obviously much less divergent than in Figure 3.9. (Note the much smaller scale on the plots of x and y .) The motion observed in this experiment appears stable. In fact, the critical value of γ was fairly difficult to resolve experimentally. Experiments with γ slightly smaller and slightly larger than γ_c were practically indistinguishable from the experiment shown in Figure 3.10. These motions were characterized by slight attitude oscillations about the desired equilibrium of steady long-axis translation. Note from the simulated data that inviscid theory over-predicts the lateral motion of the spheroid. This is consistent with the predictions of translational drift given in [31].

Figure 3.11 shows an experiment in which γ is twice the critical value predicted from theory. The motion of the spheroid is very close to the desired motion and the attitude oscillations are much smaller than those in Figure 3.10.

Quantitatively gauging stability of a motion from experimental data is somewhat subjective. Because of the finite extent of the test tank, there is a range of γ over which stable, critically stable, and unstable motions are practically indistinguishable. This observation impacts how finely the critical value of γ may be resolved through experiment.

Assuming that the initial condition is identical for each experiment, a reasonable measure of instability is the integral of the spheroid's lateral excursion from its launch point. Suppose that a spheroid is launched at time t_0 and that the spheroid nears the bottom of the tank at time t_f . Let

$$e = \frac{1}{L} \int_{t_0}^{t_f} \sqrt{x(\tau)^2 + y(\tau)^2} d\tau$$

where L is a characteristic length, say the length of the spheroid. An unstable motion will typically result in a large lateral excursion, and thus a large value of e , whereas a

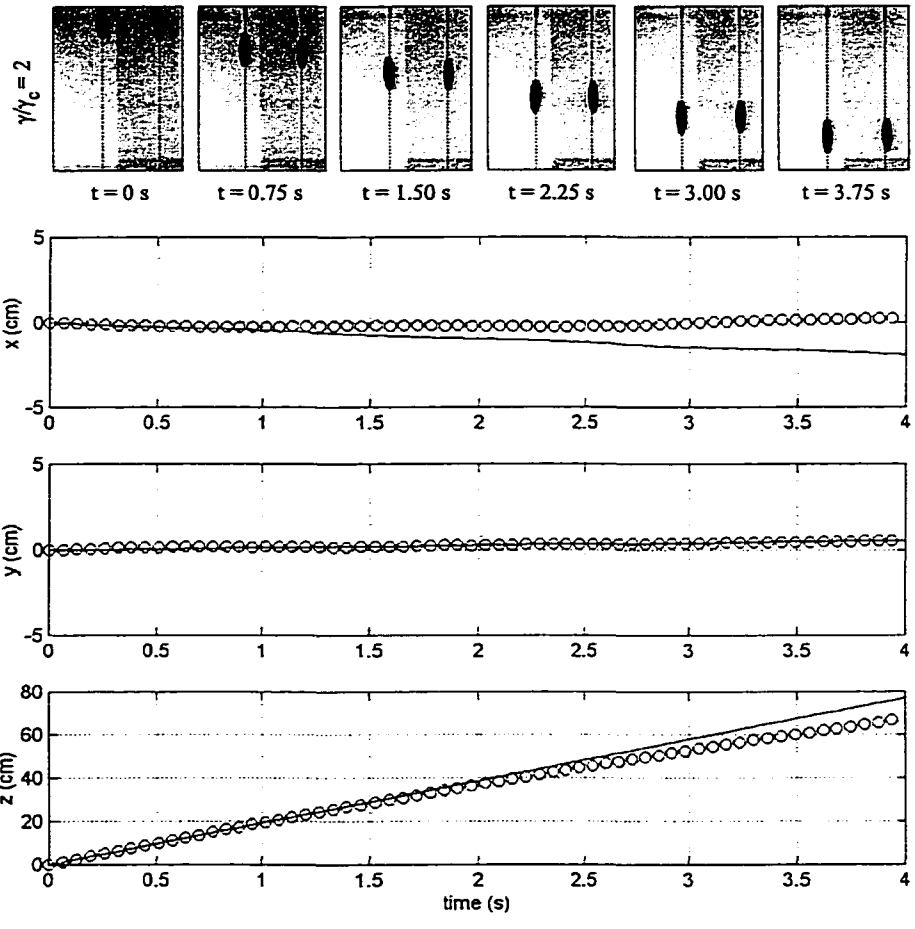


Figure 3.11: Experimental data for the 4:1 ratio spheroid: $\gamma = 2\gamma_c$.

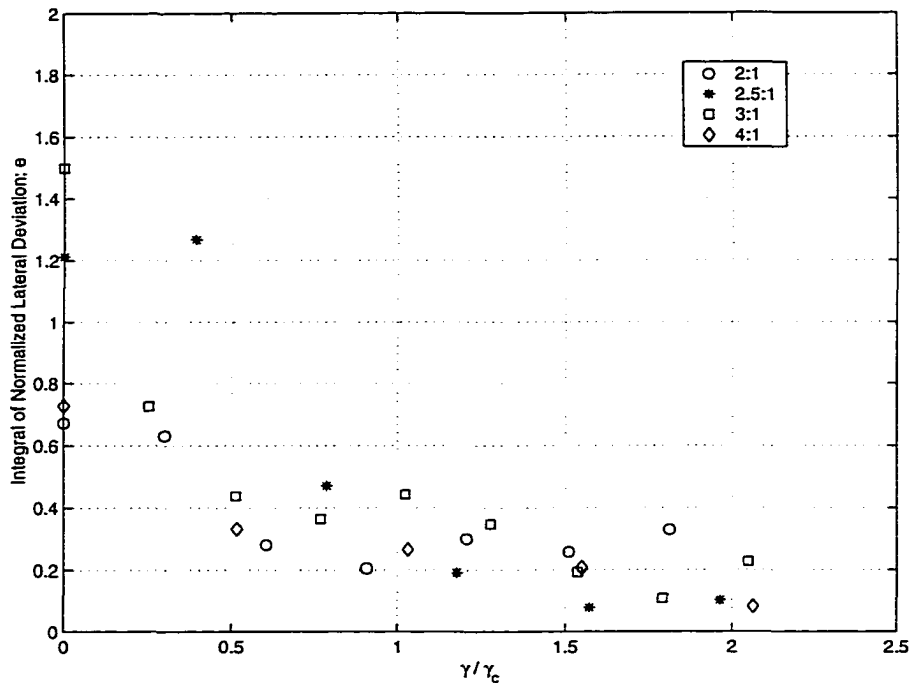


Figure 3.12: Integral deviation e versus CG displacement.

stable motion will not. The “metric” e is not a true measure of instability because it does not involve the complete vehicle state, including attitude and velocities. Measuring the complete state was not experimentally feasible and, in any case, the integral deviation e is a suitable indicator of the spheroid’s adherence to or divergence from equilibrium. Figure 3.12 shows the lateral deviation e for the indicated values of γ/γ_c for each spheroid tested. Each data point represents an average value of e for the set of tests performed at the indicated parameter value.

As one would expect, the deviation e generally diminishes as the CG is lowered relative to the CB (as γ/γ_c increases). This trend is particularly evident for the spheroid with a 4:1 fineness ratio. Once again, we note that potential flow theory, on which the stability results are based, is most applicable to a slender body moving in the streamline direction. It follows that the stability prediction should be most accurate for the most slender spheroid. It is certainly true for each spheroid tested that the steady translation is stable when $\gamma > \gamma_c$.

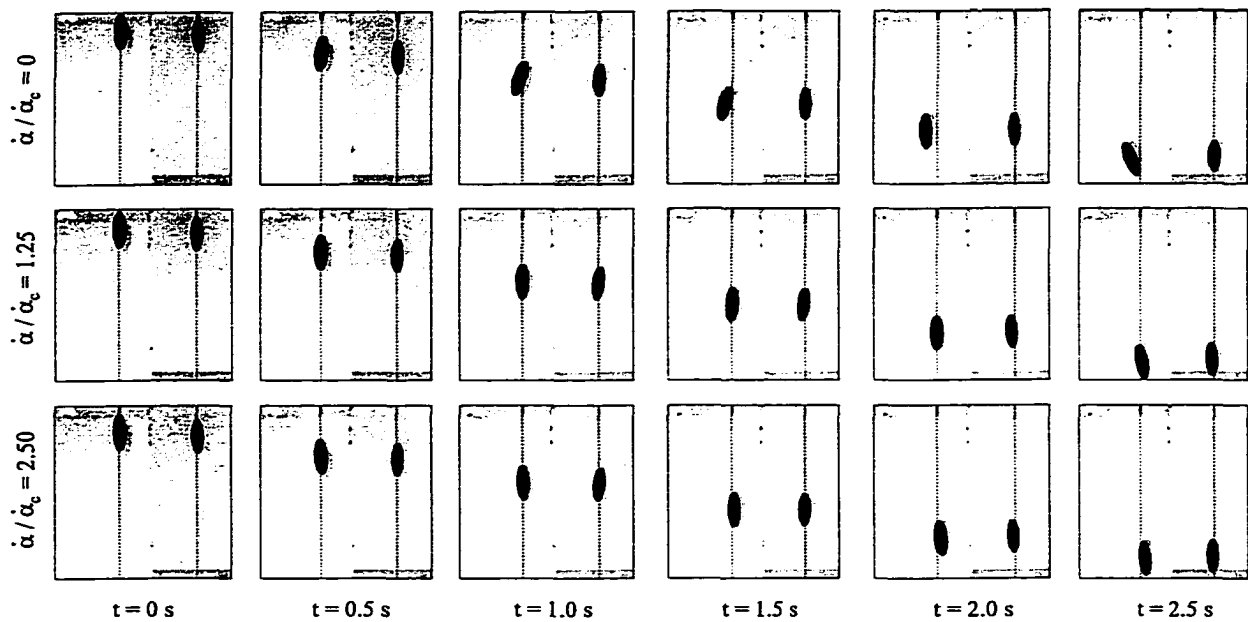


Figure 3.13: Comparison of 3:1 spheroid experiments with an internal rotor.

However, it is apparent in Figure 3.12 that the critical value of γ is not well-resolved and could be somewhat lower than that indicated by theory. In this sense, the potential flow analysis proves to give conservative stability estimates.

For the experiments involving an internal rotor, it proved more difficult to quantitatively gauge stability. The integral deviation e was roughly equal for a series of tests which were qualitatively quite distinct. Shown in Figure 3.13 are three series of images taken from the experimental footage of the 3:1 fineness ratio test series. In both the 3:1 and 2.5:1 tests, the CG was well below the CB. It was therefore necessary to launch the body at higher velocity than in the previous tests in order to place the critical rotor speed for stability within the achievable range. Figure 3.13 seems to indicate that the equilibrium is unstable when the internal rotor is not spinning. The body immediately diverges from the equilibrium, undergoing a comparatively large excursion. It is important to note that as the body diverges, it slows and begins to realign with the direction of gravity. This limiting behavior must not be confused with stability; the body does, in fact, diverge from

the equilibrium of steady long-axis translation. On the other hand, with sufficient angular momentum provided by the internal rotor, the body falls stably along its long axis (with a very minor pitch oscillation evident in the reflected view). For the 2.5:1 spheroid, the body's qualitative behavior is somewhat less varied over the range of internal rotor spin rates. While the internal rotor provided the same amount of angular momentum in both test series, there was a more marked effect on the dynamics of the more slender 3:1 spheroid. This is certainly reasonable, as the internal rotor represents a greater contribution to that spheroid's total inertia.

In conclusion, translation of a prolate spheroid along its symmetry axis can be stabilized in at least two distinct ways. In an inviscid fluid, the body may be gyroscopically stabilized by spinning it about the symmetry axis at a sufficiently high angular rate. This approach may not be feasible in a viscous fluid, however gyroscopic stability can be provided internally by means of a spinning rotor. If the spheroid moves in the direction of gravity, it may also be stabilized by lowering the CG relative to the CB. Experiments indicate that condition (3.28) gives a conservative estimate of the critical "bottom-heaviness" γ for stability.

These experiments also verify the intuition that physical damping should enhance stability by making it asymptotic. Pure long axis translation motions which are predicted to be stable using an ideal system model, are seen to be asymptotically stable in experiment. The intuition that damping enhances stability is certainly not always true, however. (See [47], for example.) The effect of damping on stability predictions based on conservative system analysis continues to be a concern in the following chapter, where we consider an alternative use of internal rotors for underwater vehicle stabilization. This alternative use of internal rotors does not involve gyroscopic stabilization, but rather provides stability through momentum exchange.

Chapter 4

Feedback Stabilization Using Internal Rotors

In this chapter, we consider active stabilization of underwater vehicle dynamics through feedback control of a set of internal rotors. As mentioned in Section 2.5, Lyapunov-based control design is a major theme of the dissertation, and it is the focus of this chapter in particular. We consider a Hamiltonian model of the underwater vehicle with internal rotors and prescribe feedback which preserves this Hamiltonian structure. The energy-Casimir method provides a control-parameterized Lyapunov function for steady long-axis translation as well as conditions on the gains for closed-loop stability. The Lyapunov function is then used to design asymptotically stabilizing feedback dissipation, to estimate the region of attraction, and to examine the effect of physical damping, which is ignored in the original design.

The approach comprises three steps:

1. Apply feedback to the conservative system which preserves the Hamiltonian structure and shapes the kinetic energy such that steady, long-axis translation is stable.
2. Using the Lyapunov function developed in Step 1, design feedback dissipation to asymptotically stabilize the equilibrium.
3. Examine the effect of physical damping on stability and, if necessary, modify the feedback dissipation from Step 2 to ensure asymptotic stability.

In Section 4.1, we apply this procedure to an ellipsoidal vehicle with coincident centers of gravity and buoyancy. In Section 4.2, we do the same but allow the CG to be located at any point along the shortest ellipsoid principal axis.

4.1 Coincident Centers of Gravity and Buoyancy

In this section, a feedback control law is developed for the three internal rotors in order to stabilize steady long axis translation for a vehicle with coincident centers of gravity and buoyancy. Following the method outlined above, the control law provides kinetic energy shaping and energy dissipation. The idea of stabilizing an underwater vehicle with internal rotors by shaping the kinetic energy was first proposed in [45]. Closed-loop stability is proven by using the modified energy to construct a Lyapunov function for which the equilibrium is a maximum. The second step is to add feedback dissipation to drive the value of the Lyapunov function to its maximum value and thereby asymptotic stabilize the equilibrium [69]. In this step, observations about the global dynamics inform the choice of control gains leading to a large estimated region of attraction. Finally, in the third step, viscous forces

are included in the model and their effect on stability is considered [68]. Although the equilibrium of interest is a maximum of the modified energy, viscous forces tend to increase this modified energy. Thus, drag serves to enhance stability. In fact, a family of equilibria corresponding to the desired steady motion (with the internal rotors spinning at arbitrary constant velocity) is shown to be globally attractive.

4.1.1 Stabilization of Steady Long Axis Translation

Bloch *et al* [13] showed, for a spacecraft with a single internal rotor, that angular momentum rate feedback yields Hamiltonian closed-loop dynamics. The closed-loop Hamiltonian is a modification of the Hamiltonian for the original uncontrolled system. The control gain appears as a factor in the closed-loop kinetic energy metric, so the control effectively shapes the inertia and, therefore, the kinetic energy. Since the closed-loop system is Hamiltonian, stability of equilibria can be studied using the energy-Casimir method. In this way, it was shown that steady intermediate axis rotation of a spacecraft can be stabilized using a single internal rotor spinning about the spacecraft's major axis.

With $\mathbf{r} = \mathbf{0}$ and neglecting viscous forces for now, the equations of motion for an underwater vehicle with internal rotors are

$$\begin{aligned}
 \dot{\mathbf{\Pi}} &= \mathbf{\Pi} \times \mathbf{\Omega} + \mathbf{P} \times \mathbf{v} \\
 \dot{\mathbf{P}} &= \mathbf{P} \times \mathbf{\Omega} \\
 \dot{\mathbf{i}} &= \mathbf{u}.
 \end{aligned}
 \tag{4.1}$$

With the goal of obtaining a closed-loop Hamiltonian system with control-modified inertia,

define the feedback control law

$$\begin{aligned} \mathbf{u} &= \mathbf{K}\dot{\boldsymbol{\Pi}} \\ &= \mathbf{K}((\Lambda\boldsymbol{\Omega} + \mathbf{J}_r\boldsymbol{\Omega}_r) \times \boldsymbol{\Omega} + \mathbf{M}\mathbf{v} \times \mathbf{v}) \end{aligned} \quad (4.2)$$

where \mathbf{K} is a 3×3 matrix of control gains. For reasons that will be made clear, we choose $\mathbf{K} = \mathbf{K}^T$ such that \mathbf{K} and $\bar{\mathbf{I}}$ commute. A simple choice that satisfies the requirements is $\mathbf{K} = \text{diag}(k_1, k_2, k_3)$.

Remark 4.1.1 *The idea of stabilizing an unstable motion by shaping the kinetic energy has evolved into a general procedure known as the method of controlled Lagrangians [14, 15, 17]. The control law given here, first proposed in [45], was conceived as a natural progression from the results of [13] on spacecraft spin stabilization. However, the control law can also be derived as an application of the method of controlled Lagrangians. The method of controlled Lagrangians for Euler-Poincaré systems is discussed briefly in Section 5.3 where the question of the effect of physical dissipation on closed-loop stability is addressed more generally. For an underwater vehicle with coincident CG and CB, equation (5.70) is precisely the control law (4.2).*

Since $\dot{\mathbf{l}} = \mathbf{u} = \mathbf{K}\dot{\boldsymbol{\Pi}}$, the vector quantity $\mathbf{l} - \mathbf{K}\boldsymbol{\Pi}$ is conserved. It is convenient to change variables from $(\boldsymbol{\Pi}, \mathbf{P}, \mathbf{l})$ to $(\boldsymbol{\Pi}, \mathbf{P}, \boldsymbol{\zeta})$ where

$$\boldsymbol{\zeta} = (\mathcal{I} - \mathbf{K})^{-1}(\mathbf{l} - \mathbf{K}\boldsymbol{\Pi}). \quad (4.3)$$

(The gain matrix \mathbf{K} will be chosen such that $k_i \neq 1$ for $i = 1, 2$, and 3 so that $\boldsymbol{\zeta}$ is

well-defined.) Define the “controlled inertia matrix”

$$\mathbf{I}_K = \text{diag}(I_{K_1}, I_{K_2}, I_{K_3}) = (\mathcal{I} - \mathbf{K})^{-1} \bar{\mathbf{I}}. \quad (4.4)$$

This matrix is symmetric, under the assumption that $\mathbf{K} = \mathbf{K}^T$ commutes with $\bar{\mathbf{I}}$, and it has units of inertia. Indeed, the matrix \mathbf{I}_K plays the role of inertia for the closed-loop system. Thus the effect of the control parameters is to modify the closed-loop inertia. From the definitions of $\mathbf{\Pi}$, \mathbf{l} , ζ , and \mathbf{I}_K ,

$$\mathbf{\Omega} = \mathbf{I}_K^{-1}(\mathbf{\Pi} - \zeta).$$

The closed-loop equations of motion are

$$\begin{aligned} \dot{\mathbf{\Pi}} &= \mathbf{\Pi} \times \mathbf{\Omega} + \mathbf{P} \times \mathbf{v} \\ \dot{\mathbf{P}} &= \mathbf{P} \times \mathbf{\Omega} \\ \dot{\zeta} &= \mathbf{0}. \end{aligned} \quad (4.5)$$

As intended, equations (4.5) describe Lie-Poisson dynamics,

$$\begin{pmatrix} \dot{\mathbf{\Pi}} \\ \dot{\mathbf{P}} \\ \dot{\zeta} \end{pmatrix} = \begin{pmatrix} \hat{\mathbf{\Pi}} & \hat{\mathbf{P}} & \mathbf{0} \\ \hat{\mathbf{P}} & \mathbf{0} & \mathbf{0} \\ \mathbf{0} & \mathbf{0} & \mathbf{0} \end{pmatrix} \nabla H_K. \quad (4.6)$$

The new Hamiltonian H_K depends on the control gains and is a modification of the kinetic

energy of the uncontrolled system:

$$H_K(\mathbf{\Pi}, \mathbf{P}, \zeta) = \frac{1}{2}(\mathbf{\Pi} - \zeta) \cdot \mathbf{I}_K^{-1}(\mathbf{\Pi} - \zeta) + \frac{1}{2}\mathbf{P} \cdot \mathbf{M}^{-1}\mathbf{P}. \quad (4.7)$$

Compare H_K , for example, with the Hamiltonian (3.5) for the vehicle without internal rotors. The functions $C_1(\mathbf{\Pi}, \mathbf{P}, \zeta) = \frac{1}{2}\|\mathbf{P}\|^2$ and $C_2(\mathbf{\Pi}, \mathbf{P}, \zeta) = \mathbf{\Pi} \cdot \mathbf{P}$, as well as each component of ζ , are five independent Casimirs for this system.

Observe that pure mode equilibria of the uncontrolled system, such as the equilibrium (3.22), are also equilibria of the closed-loop system with $\zeta_e \parallel \mathbf{\Pi}_e \parallel \mathbf{P}_e$. We focus on the three-parameter family of pure 1 mode equilibria

$$\mathbf{\Pi}_e = \begin{pmatrix} \Pi_1^0 \\ 0 \\ 0 \end{pmatrix}, \quad \mathbf{P}_e = \begin{pmatrix} P_1^0 \\ 0 \\ 0 \end{pmatrix}, \quad \zeta_e = \begin{pmatrix} \zeta_1^0 \\ 0 \\ 0 \end{pmatrix}. \quad (4.8)$$

If $\mathbf{\Omega}_e = \Omega_1^0 \mathbf{e}_1$ and $\mathbf{v}_e = v_1^0 \mathbf{e}_1$ are the equilibrium body angular and linear velocity vectors, then $\Pi_1^0 - \zeta_1^0 = I_{K_1} \Omega_1^0$ and $P_1^0 = m_1 v_1^0$. These equilibria correspond to vehicle translation along and rotation about the long axis with the 1-axis rotor spinning at a constant rate.

Since the closed-loop system is Lie-Poisson, the energy-Casimir method can be used to determine conditions for closed-loop stability of relative equilibria.

Theorem 4.1.2 (Coincident Centers - Lyapunov Stability.) *Let $\text{sign}(I_{K_2}) = \text{sign}(I_{K_3})$.*

Then, the relative equilibrium (4.8) with $P_1^0 \neq 0$ will be Lyapunov stable if for $i = 2$ and

$i = 3$

$$\frac{1}{I_{K_1}} \left(\frac{1}{I_{K_i}} - \frac{1}{I_{K_1}} \right) \left(\frac{\Pi_1^0 - \zeta_1^0}{P_1^0} \right)^2 + \frac{1}{I_{K_1} I_{K_i}} \frac{(\Pi_1^0 - \zeta_1^0) \zeta_1^0}{(P_1^0)^2} > \frac{1}{I_{K_i}} \left(\frac{1}{m_1} - \frac{1}{m_i} \right). \quad (4.9)$$

Proof: Define the Lyapunov function candidate

$$H_\Phi = H_K(\mathbf{\Pi}, \mathbf{P}, \zeta) + \Phi(C_1, C_2, \zeta_1, \zeta_2, \zeta_3) \quad (4.10)$$

where $\zeta_i = \zeta \cdot e_i$ for $i = 1, 2$, and 3 . To prove nonlinear stability, the function Φ should be chosen so that the equilibrium is a minimum or a maximum of H_Φ . That is, we require that the first variation DH_Φ be zero at the equilibrium and that the second variation D^2H_Φ , when evaluated at the equilibrium, be positive or negative definite. A straightforward calculation (see Appendix B) shows that, if the control gains are chosen so that $I_{K_2} > 0$ and $I_{K_3} > 0$ and the inequality (4.9) holds, then Φ can be found such that the equilibrium (4.8) is a minimum of H_Φ . By the energy-Casimir method, one may conclude that the equilibrium (4.8) is stable. If $I_{K_2} < 0$ and $I_{K_3} < 0$ and (4.9) holds, then Φ can be found such that (4.8) is a maximum of H_Φ . Again, one may conclude stability by the energy-Casimir method. In both cases, Φ can be chosen as a second order polynomial. The augmented Hamiltonian H_Φ should be interpreted as a Lyapunov function. \square

When $\zeta_1^0 = 0$, conditions (4.9) revert to conditions (3.24) with I replaced by I_K . Of course, since I_K is parameterized by the control, it may be modified such that conditions can be satisfied.

Practically, the case where $\zeta_1^0 = 0$ is less interesting than the case $\Omega_1^0 = (\Pi_1^0 - \zeta_1^0)/I_{K_1} = 0$; in the latter case the vehicle does not spin. If $\Omega_1^0 = 0$, the conditions (4.9) become

$$0 > \frac{1}{I_{K_i}} \left(\frac{1}{m_1} - \frac{1}{m_i} \right) \quad i = 2 \text{ and } 3. \quad (4.11)$$

Since $m_1 < m_2 < m_3$, conditions (4.11) will hold only when $I_{K_2} < 0$ and $I_{K_3} < 0$.

Corollary 4.1.3 Choose $k_i > 1$ so that $I_{K_i} < 0$ for $i = 2$ and 3 . Then steady translation along the vehicle long axis with zero body angular rate is Lyapunov stable.

Proof: The proof is a special case of the proof of Theorem 4.1.2 as applied to the equilibrium

(4.8) with $\Pi_1^0 = \zeta_1^0$. A Lyapunov function is:

$$\begin{aligned} \bar{H}_\Phi(\mathbf{\Pi}, \mathbf{P}, \zeta) = & H_K(\mathbf{\Pi}, \mathbf{P}, \zeta) - \frac{1}{m_1} C_1 + \frac{1}{2} \rho_1 (C_1 - \frac{1}{2} (P_1^0)^2)^2 + \rho_2 (C_2 - \Pi_1^0 P_1^0) (C_1 - \frac{1}{2} (P_1^0)^2) \\ & + \frac{1}{2} \rho_3 (C_2 - \Pi_1^0 P_1^0)^2 + \frac{1}{2} \rho_{3.5} (\zeta_1 - \Pi_1^0)^2 + \frac{1}{2} \rho_4 \zeta_2^2 + \frac{1}{2} \rho_5 \zeta_3^2 \end{aligned} \quad (4.12)$$

where the constants $\rho_1, \rho_2, \rho_3, \rho_{3.5}, \rho_4$, and ρ_5 are chosen to satisfy

$$\begin{aligned} \rho_1 &< -3\rho_3 \left(\frac{\Pi_1^0}{(P_1^0)} \right)^2, \\ \rho_2 &= -\rho_3 \left(\frac{\Pi_1^0}{P_1^0} \right), \\ \rho_3 &< -\frac{1}{I_{K_1} (P_1^0)^2}, \\ \rho_{3.5} &< \frac{\rho_3 (P_1^0)^2}{1 - \rho_3 I_{K_1} (P_1^0)^2}, \\ \rho_4 &< 0, \\ \rho_5 &< 0. \end{aligned}$$

The equilibrium is a *maximum* of \bar{H}_Φ . For details about the construction of this Lyapunov function, see Appendix B. \square

Note that the stability conditions (4.11) do not involve I_{K_1} . In fact, these conditions hold even if $k_1 = 0$ and $I_{K_1} = \Lambda_1 = I_1$, that is, even if there is no rotor about the 1-axis. Thus, for the conservative model, steady long-axis translation may be stabilized using only two internal rotors.

Remark 4.1.4 If, in addition to $I_{K_2} < 0$ and $I_{K_3} < 0$, one chooses $k_1 > 1$ so that $I_{K_1} < 0$

(and consequently $I_K < 0$), then one may choose

$$\rho_1 = -3\rho_3 \frac{1 + (\Pi_1^0)^2}{(P_1^0)^2}, \quad \rho_2 = -\rho_1 \left(\frac{\Pi_1^0}{P_1^0} \right), \quad \rho_3 = -\frac{1}{2I_{K_1}(P_1^0)^2}, \quad \rho_{3.5} = 0, \quad \rho_4 < 0, \quad \rho_5 < 0. \quad (4.13)$$

In later sections, for reasons concerning the effect of physical dissipation, it is assumed that $I_K < 0$. The Lyapunov function (4.12) with the constants ρ_i given by (4.13) is used to prove asymptotic stability under dissipative feedback.

Remark 4.1.5 For the control (4.2), the set

$$\mathcal{F}_1 = \{(\Pi, P, \zeta) \mid P_1 = \Pi_2 = \Pi_3 = \zeta_2 = \zeta_3 = 0\}$$

and its cyclic permutations are invariant. With $I_K < 0$, the pure 2 and pure 3 mode equilibria are unstable (saddle points). However, restricted to \mathcal{F}_1 , the pure 2 mode is stable. This observation is relevant in Section 4.1.2 where the region of attraction of an asymptotically stabilizing control law is considered.

4.1.2 Asymptotic Stabilization

Here, following step 2 in the method outlined on page 83, feedback dissipation is applied such that steady long-axis translation is stabilized in the absence of drag. The approach, first considered in [69], builds on the results of Section 4.1.1 in the sense that the Lyapunov function developed for the conservative system is used to generate the asymptotically stabilizing dissipative feedback control law. The proof of asymptotic stability relies on LaSalle's invariance principle. The approach gives an estimate of the region of attraction and conditions on the control parameters to broaden this estimated region.

By Corollary 4.1.3, choosing $I_{K_i} < 0$ ($i = 1, 2,$ and 3) stabilizes the equilibrium

$$\mathbf{\Pi}_e = \begin{pmatrix} \Pi_1^0 \\ 0 \\ 0 \end{pmatrix}, \quad \mathbf{P}_e = \begin{pmatrix} P_1^0 \\ 0 \\ 0 \end{pmatrix}, \quad \boldsymbol{\zeta}_e = \begin{pmatrix} \Pi_1^0 \\ 0 \\ 0 \end{pmatrix}. \quad (4.14)$$

Recall that the equilibrium (4.14) corresponds to vehicle translation along the body 1-axis without rotation but with the 1-axis rotor spinning. Since the closed-loop system (4.5) is Hamiltonian, stability is not asymptotic. To asymptotically stabilize the equilibrium (4.14), an undetermined dissipative feedback term is appended to the original control law. Returning to the equations of motion (4.1), replace \mathbf{u} with

$$\begin{aligned} \mathbf{u} &= \mathbf{u}_s + (\mathcal{I} - \mathbf{K})\mathbf{u}_d \\ &= \mathbf{K}\dot{\boldsymbol{\Pi}} + (\mathcal{I} - \mathbf{K})\mathbf{u}_d \end{aligned} \quad (4.15)$$

where $\mathbf{u}_s = \mathbf{K}\dot{\boldsymbol{\Pi}}$ is the stabilizing control law discussed in Section 4.1.1 and \mathbf{u}_d represents a dissipative control term which remains to be chosen. Again, make the change of variables $(\boldsymbol{\Pi}, \mathbf{P}, l) \rightarrow (\boldsymbol{\Pi}, \mathbf{P}, \boldsymbol{\zeta})$ with $\boldsymbol{\zeta} = (\mathcal{I} - \mathbf{K})^{-1}(l - \mathbf{K}\boldsymbol{\Pi})$. The equations of motion become

$$\begin{aligned} \dot{\boldsymbol{\Pi}} &= \boldsymbol{\Pi} \times \boldsymbol{\Omega} + \mathbf{P} \times \mathbf{v} \\ \dot{\mathbf{P}} &= \mathbf{P} \times \boldsymbol{\Omega} \\ \dot{\boldsymbol{\zeta}} &= \mathbf{u}_d. \end{aligned} \quad (4.16)$$

With $\mathbf{u}_d = \mathbf{0}$, the equations (4.16) reduce to the conservative equations (4.5). The function \bar{H}_Φ given by equation (4.12) with ρ_i given by (4.13) ($i = 1, 2, 3, 3.5, 4,$ and 5) is a

natural Lyapunov function candidate for studying stability of the equilibrium (4.14) of the dissipative equations (4.16). One may easily compute

$$\frac{d}{dt}\bar{H}_\Phi = \nabla\bar{H}_\Phi \cdot \begin{pmatrix} \dot{\mathbf{\Pi}} \\ \dot{\mathbf{P}} \\ \dot{\zeta} \end{pmatrix} = \frac{\partial\bar{H}_\Phi}{\partial\zeta} \cdot \mathbf{u}_d = \left(-I_K^{-1}(\mathbf{\Pi} - \zeta) + \begin{pmatrix} 0 \\ \rho_4\zeta_2 \\ \rho_5\zeta_3 \end{pmatrix} \right) \cdot \mathbf{u}_d$$

where ρ_4 and ρ_5 are the constants defined in the proof of Corollary 4.1.3. Taking

$$\mathbf{u}_d = K_d \left(-I_K^{-1}(\mathbf{\Pi} - \zeta) + \begin{pmatrix} 0 \\ \rho_4\zeta_2 \\ \rho_5\zeta_3 \end{pmatrix} \right) \quad (4.17)$$

with $K_d > 0$ makes $\frac{d}{dt}\bar{H}_\Phi \geq 0$.

Noting that $C_1 = \frac{1}{2}\|\mathbf{P}\|^2$ and $C_2 = \mathbf{\Pi} \cdot \mathbf{P}$ are conserved for equations (4.16) (regardless of the choice of \mathbf{u}_d), let $\mathcal{D}_\Phi = \{(\mathbf{\Pi}, \mathbf{P}, \zeta) \mid \frac{1}{2}\|\mathbf{P}\|^2 = C_1, \mathbf{\Pi} \cdot \mathbf{P} = C_2\}$ represent the invariant leaf on which the dynamics (4.16) evolve.¹ If ω_Φ is some compact, positively invariant subset of \mathcal{D}_Φ then, by LaSalle's invariance theorem, solutions starting in ω_Φ go to the largest invariant set \mathcal{M} contained in the set $E = \{(\mathbf{\Pi}, \mathbf{P}, \zeta) \in \omega_\Phi \mid \frac{d}{dt}\bar{H}_\Phi = 0\}$.

Lemma 4.1.6 *For any $\omega_\Phi \subset \mathcal{D}_\Phi$, the largest invariant set \mathcal{M} contained in the set $E = \{(\mathbf{\Pi}, \mathbf{P}, \zeta) \in \mathcal{D}_\Phi \mid \frac{d}{dt}\bar{H}_\Phi = 0\}$ contains only closed-loop equilibria.*

¹While the closed-loop equations (4.16) with feedback dissipation (4.17) are no longer Lie-Poisson, the two Casimirs $C_1(\mathbf{P}, \mathbf{\Pi})$ and $C_2(\mathbf{P}, \mathbf{\Pi})$ still define a subspace of the reduced phase space on which the dynamics evolve. The terminology reflects the observation that coadjoint orbits of a Lie-Poisson system are often symplectic leaves of a foliation of the reduced momentum phase space.

Proof: If $\frac{d}{dt}\bar{H}_\Phi = 0$ then $\mathbf{u}_d \equiv \mathbf{0}$ and

$$\mathbf{I}_K^{-1}(\mathbf{\Pi} - \zeta) = \mathbf{\Omega} = \begin{pmatrix} 0 \\ \rho_4 \zeta_2 \\ \rho_5 \zeta_3 \end{pmatrix}$$

which is constant since $\dot{\zeta} = \mathbf{u}_d = \mathbf{0}$. Therefore,

$$\dot{\mathbf{\Omega}} = (\mathcal{I} - \mathbf{K})^{-1}(\dot{\mathbf{\Pi}} - \dot{\zeta}) \equiv \mathbf{0},$$

so $\dot{\mathbf{\Pi}} \equiv \mathbf{0}$ and

$$\mathbf{P} \times \mathbf{v} = -\mathbf{\Pi} \times \mathbf{\Omega} = \text{constant}.$$

If $\mathbf{\Omega} = \mathbf{0}$, then $\dot{\mathbf{P}} = \mathbf{0}$ and the system is in equilibrium. Otherwise, the vectors \mathbf{P} , \mathbf{v} , $\mathbf{\Pi}$, and $\mathbf{\Omega}$ are coplanar. (See Figure 4.1.) Now, since $\mathbf{\Omega}$ is constant, the second equation of (4.16) implies

$$\mathbf{P}(t) = e^{-\hat{\mathbf{\Omega}}t} \mathbf{P}(0).$$

(The exponential map is discussed briefly on page 20.) Thus, $\mathbf{P}(t)$ is a rotation of $\mathbf{P}(0)$ about the vector $\mathbf{\Omega}$. Unless \mathbf{P} and $\mathbf{\Omega}$ are parallel, \mathbf{P} would rotate out of the plane containing \mathbf{P} , \mathbf{v} , $\mathbf{\Pi}$, and $\mathbf{\Omega}$. It follows from these observations that \mathbf{P} , \mathbf{v} , $\mathbf{\Pi}$, and $\mathbf{\Omega}$ are coplanar if and only if \mathbf{P} and $\mathbf{\Omega}$ are collinear, in which case $\dot{\mathbf{P}} = \mathbf{0}$. \square

The equilibrium conditions are

$$\mathbf{0} = \mathbf{\Pi} \times \mathbf{\Omega} + \mathbf{P} \times \mathbf{v} \tag{4.18}$$

$$\mathbf{0} = \mathbf{P} \times \mathbf{\Omega} \tag{4.19}$$

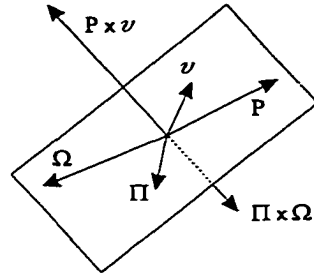


Figure 4.1: Geometric view: $\dot{\Pi} = 0$ and $\Pi \times \Omega \neq 0$.

$$\mathbf{0} = \mathbf{K}_d \left(-\Omega + \begin{pmatrix} 0 \\ \rho_4 \zeta_2 \\ \rho_5 \zeta_3 \end{pmatrix} \right) \quad (4.20)$$

From (4.19) we have $\Omega = \alpha P$ for some real α . Equation (4.18) then gives

$$\begin{aligned} \mathbf{0} &= (\mathbf{I}_K \Omega + \zeta) \times \Omega + P \times M^{-1} P \\ &= [(\alpha^2 \mathbf{I}_K - M^{-1})P + \alpha \zeta] \times P \end{aligned}$$

or

$$(\alpha^2 \mathbf{I}_K - M^{-1})P + \alpha \zeta = \beta P \quad (4.21)$$

for some real β . Using (4.20) to eliminate ζ_2 and ζ_3 from (4.21), one sees that the condition for an equilibrium of the closed-loop system is that real-valued parameters α and β exist such that

$$\begin{bmatrix} (-\alpha^2 I_{K_1} + \frac{1}{m_1} + \beta) P_1 \\ (-\alpha^2 (I_{K_2} + \frac{1}{\rho_4}) + \frac{1}{m_2} + \beta) P_2 \\ (-\alpha^2 (I_{K_3} + \frac{1}{\rho_5}) + \frac{1}{m_3} + \beta) P_3 \end{bmatrix} = \begin{bmatrix} \alpha \zeta_1 \\ 0 \\ 0 \end{bmatrix}. \quad (4.22)$$

From (4.20), $\Omega_1 = 0$ at equilibrium. Since $\Omega = \alpha P$, any equilibrium for which $P_1 \neq 0$

must have $\alpha = 0$, i.e., zero body angular velocity. For any such equilibrium,

$$\left(\frac{1}{m_i} + \beta\right)P_i = 0 \quad \text{for } i = 1, 2, \text{ and } 3. \quad (4.23)$$

Since $m_1 < m_2 < m_3$, equations (4.23) hold only when $\beta = -\frac{1}{m_1}$ and $P_2 = P_3 = 0$. Thus, pure long axis translation (4.14) is the only possible equilibrium for which $P_1 \neq 0$. Pure 2 mode and pure 3 mode equilibria also exist for the closed-loop system and are described in Remark 4.1.7 below. Note that, since (4.8) are the only equilibria for which $P_1 \neq 0$, there can be no mixed 1-2 or 1-3 mode equilibria. (See Section 3.2.1.)

Now suppose that $P_1 = 0$. Subtracting P_2 times the third equation from P_3 times the second equation of (4.22) indicates that an equilibrium satisfies

$$\left[-\alpha^2 \left((I_{K_2} + \frac{1}{\rho_4}) - (I_{K_3} + \frac{1}{\rho_5}) \right) + \left(\frac{1}{m_2} - \frac{1}{m_3} \right) \right] P_2 P_3 = 0.$$

If $P_2 \neq 0$ and $P_3 \neq 0$, there is a mixed 2-3 mode equilibrium provided

$$\alpha^2 = \frac{\left(\frac{1}{m_2} - \frac{1}{m_3} \right)}{\left((I_{K_2} + \frac{1}{\rho_4}) - (I_{K_3} + \frac{1}{\rho_5}) \right)} > 0.$$

The terms I_{K_2} , I_{K_3} , ρ_4 , and ρ_5 are all control parameters which we have required only to be negative. Choosing these parameters such that

$$I_{K_2} + \frac{1}{\rho_4} < I_{K_3} + \frac{1}{\rho_5} \quad (4.24)$$

prohibits a real solution for α and thus prohibits mixed 2-3 mode equilibria.

Remark 4.1.7 *If $\Omega \neq 0$, then the pure 2 mode equilibria are a two-parameter family of*

the form

$$\mathbf{\Pi}_e = (1 + \rho_4 I_{K_2}) \zeta_e = \Pi_2^0 \mathbf{e}_2, \quad \mathbf{P}_e = P_2^0 \mathbf{e}_2,$$

where $C_1 = \frac{1}{2}(P_2^0)^2$ and $C_2 = (\Pi_2^0 P_2^0)$. If $\Omega = \mathbf{0}$, the pure 2 mode equilibria satisfy $\mathbf{\Pi}_e = \zeta_e$ and $\mathbf{P}_e = P_2^0 \mathbf{e}_2$ where $C_1 = \frac{1}{2} \mathbf{P}_e \cdot \mathbf{P}_e$ and $C_2 = \mathbf{\Pi}_e \cdot \mathbf{P}_e$. But from equation (4.20), we know that $\zeta_2 = \zeta_3 = 0$ for equilibria with $\Omega = \mathbf{0}$. This means that $\mathbf{\Pi}_e \cdot \mathbf{P}_e = 0$, so these equilibria are possible only if $C_2 = 0$. In this degenerate case (i.e., when $C_2 = 0$), pure 2 mode equilibria lie in the union of the two-parameter family described above (for $\Omega \neq \mathbf{0}$) and the two-parameter family of the form

$$\mathbf{\Pi}_e = \zeta_e = \Pi_1^0 \mathbf{e}_1, \quad \mathbf{P}_e = P_2^0 \mathbf{e}_2.$$

Pure 3 mode equilibria are defined analogously.

Having found a dissipative control law and characterized the closed-loop equilibria, it remains to find a region of phase space within which trajectories converge to the desired equilibrium (4.14). The approach taken here is to define a compact, positively invariant set that contains no equilibria other than the desired one. Asymptotic stability may then be studied in the context of LaSalle's invariance principle. This approach was first applied in [69].

Define a constant $c_\Phi = -(\frac{1}{m_1} - \frac{1}{m_2})C_1 > 0$. Let

$$\omega_\Phi = \{(\mathbf{\Pi}, \mathbf{P}, \zeta) \in \mathcal{D}_\Phi | \bar{H}_\Phi \geq (1 - \epsilon)c_\Phi\} \quad (4.25)$$

where $0 < \epsilon \ll 1$. The set ω_Φ is positively invariant because $\bar{H}_\Phi < 0$ is nondecreasing. Furthermore, the equilibria $(\mathbf{\Pi}_e, \mathbf{P}_e, \zeta_e)$ and $(-\mathbf{\Pi}_e, -\mathbf{P}_e, -\zeta_e)$, with $\mathbf{\Pi}_e$, \mathbf{P}_e , and ζ_e given

by (4.14), are the only equilibria in ω_Φ . We also note that ω_Φ excludes states for which $P_1 = 0$ because $\bar{H}_\Phi \leq -(\frac{1}{m_1} - \frac{1}{m_2})C_1$ whenever $P_1 = 0$. In fact, ω_Φ is the disjoint union of two compact, positively invariant subsets. Let $\omega_{\Phi_+} = \{(\Pi, P, \zeta) \in \omega_\Phi \mid P_1 > 0\}$ and let $\omega_{\Phi_-} = \{(\Pi, P, \zeta) \in \omega_\Phi \mid P_1 < 0\}$. Then $\omega_\Phi = \omega_{\Phi_+} \cup \omega_{\Phi_-}$. Each of these two subsets is positively invariant since ω_Φ is positively invariant and no trajectory can pass through both ω_{Φ_+} and ω_{Φ_-} without leaving ω_Φ . Furthermore, each subset contains a single closed-loop equilibrium. For example, ω_{Φ_+} contains the equilibrium (Π_e, P_e, ζ_e) where $P_1^0 > 0$.

Theorem 4.1.8 (Coincident Centers - Asymptotic Stability) *Suppose $C_1 \neq 0$. Then any solution to the equations (4.16) which starts in ω_{Φ_+} at time $t = 0$ with \mathbf{u}_d given by (4.17) goes to*

$$\Pi_e = \begin{pmatrix} C_2/\sqrt{2C_1} \\ 0 \\ 0 \end{pmatrix}, \quad P_e = \begin{pmatrix} \sqrt{2C_1} \\ 0 \\ 0 \end{pmatrix}, \quad \zeta_e = \begin{pmatrix} C_2/\sqrt{2C_1} \\ 0 \\ 0 \end{pmatrix} \quad (4.26)$$

as $t \rightarrow \infty$. If the solution starts in ω_{Φ_-} , then it goes to $(-\Pi_e, -P_e, -\zeta_e)$ as $t \rightarrow \infty$.

Proof: The proof is an application of LaSalle's invariance theorem. \square

Theorem 4.1.8 indicates that the body angular velocity goes to zero as do the angular velocities of the 2-axis and 3-axis internal rotors. The vehicle goes to an equilibrium of the form (4.14) which corresponds to pure translation along the long axis with the 1-axis internal rotor spinning at some generically nonzero rate. The magnitudes of the equilibrium values of Π , P , and ζ are determined by the conservation laws.

Notice from the definition (4.12) of \bar{H}_Φ (with parameter values given by (4.13)) that the size of the regions ω_{Φ_+} and ω_{Φ_-} may be increased by appropriate choice of the control

parameters. Recall that ω_Φ is defined by a lower bound on the value of \bar{H}_Φ . Noting that

$$\begin{aligned} H_K &= \frac{1}{2}(\mathbf{\Pi} - \zeta) \cdot \mathbf{I}_K^{-1}(\mathbf{\Pi} - \zeta) + \frac{1}{2}\mathbf{P} \cdot \mathbf{M}^{-1}\mathbf{P} \\ &= \frac{1}{2}\mathbf{\Omega} \cdot \mathbf{I}_K\mathbf{\Omega} + \frac{1}{2}\mathbf{v} \cdot \mathbf{M}\mathbf{v}, \end{aligned}$$

choosing I_{K_i} (for $i = 1, 2$, and 3), ρ_4 , and ρ_5 to have small magnitude makes the magnitude of \bar{H}_Φ smaller at given values of $\mathbf{\Omega}$, ζ_2 , and ζ_3 . Thus, the range of values that $\mathbf{\Omega}$, ζ_2 , and ζ_3 can take within the sets $\omega_{\Phi+}$ and $\omega_{\Phi-}$ is larger. These guidelines, together with condition (4.24), indicate how to choose control parameters to shape the closed-loop phase space so that the asymptotically stable equilibrium (4.26) has a large region of attraction.

4.1.3 Viscous Forces and Global Asymptotic Stabilization

In this section, we perform step 3 of the method outlined on page 83, i.e., we consider the effect of physical damping on the previous stability results and modify the feedback dissipation as necessary to ensure asymptotic stability. We apply the control law (4.15) to an underwater vehicle model which includes viscous forces and torques. The open-loop equations of motion are given by (3.21) with $\mathbf{r} = \mathbf{0}$,

$$\begin{aligned} \dot{\mathbf{\Pi}} &= \mathbf{\Pi} \times \mathbf{\Omega} + \mathbf{P} \times \mathbf{v} + \mathbf{f}_\Omega(\mathbf{\Omega}, \mathbf{v}) \\ \dot{\mathbf{P}} &= \mathbf{P} \times \mathbf{\Omega} + \mathbf{f}_v(\mathbf{\Omega}, \mathbf{v}) + \mathcal{F}_{\text{thrust}} \\ \dot{\mathbf{i}} &= \mathbf{u}. \end{aligned} \tag{4.27}$$

(When $\mathbf{r} = \mathbf{0}$, $\mathbf{\Gamma}$ plays no role in the dynamics and may be ignored.) For the conservative system, as discussed in Section 4.1.1, the control law indicated by the method of controlled

Lagrangians is

$$\mathbf{u} = \mathbf{K}\dot{\boldsymbol{\Pi}} \quad (4.28)$$

$$= \mathbf{K}(\boldsymbol{\Pi} \times \boldsymbol{\Omega} + \mathbf{P} \times \mathbf{v}). \quad (4.29)$$

When considering the dissipative equations (4.27), the control law (4.28) becomes

$$\mathbf{u} = \mathbf{K}(\boldsymbol{\Pi} \times \boldsymbol{\Omega} + \mathbf{P} \times \mathbf{v} + \mathbf{f}_{\boldsymbol{\Omega}}(\boldsymbol{\Omega}, \mathbf{v})). \quad (4.30)$$

Again, this control law makes $l - \mathbf{K}\boldsymbol{\Pi}$ a conserved quantity. The conservation law is useful for proving nonlinear stability. This approach was considered in [68], where it was shown that the desired equilibrium of the resulting closed-loop system is destabilized by drag, as one might expect for an equilibrium which is an “energy maximum”. The detrimental effect of drag was compensated for by choosing an appropriate dissipative feedback control law.

Here, the original velocity feedback control law (4.29), developed for the conservative system model, is applied instead of (4.30). The desired closed-loop equilibrium is still a maximum of the function \bar{H}_{Φ} given by (4.12). In this case, however, drag tends to increase the modified energy, driving the state to the desired equilibrium asymptotically. In fact, one can view the compensatory feedback dissipation formulated in [68] as undoing the harm done by choosing the control law (4.30). (See Remark 4.1.11 at the end of this section.) Under the control law (4.29), physical dissipation naturally enhances stability. As an additional benefit, (4.29) requires neither acceleration measurements nor a model of physical damping.

The construction of the Lyapunov function \bar{H}_{Φ} relied on several conservation laws which are broken when physical dissipation is introduced. Neither the modified energy H_K nor the two Casimirs $C_1 = \frac{1}{2}\mathbf{P} \cdot \mathbf{P}$ and $C_2 = \boldsymbol{\Pi} \cdot \mathbf{P}$ are conserved in the presence of drag.

Furthermore, the choice of feedback (4.29) introduces no controlled conserved quantities, i.e., ζ is no longer conserved. In fact, $\frac{d}{dt}\bar{H}_\Phi$ becomes indefinite in the presence of viscous forces and thus \bar{H}_Φ can no longer serve as a Lyapunov function. Still, this function does provide a useful starting point for proving stability of the system with damping. In this section, a *semidefinite* Lyapunov function is formed by dropping some of the terms in \bar{H}_Φ which destroy the definiteness of $\frac{d}{dt}\bar{H}_\Phi$. This semidefinite function allows a characterization of a crucial portion of the system dynamics leading to a global asymptotic stability result.

Once again, let

$$\begin{aligned} \mathbf{u} &= \mathbf{u}_s + (\mathcal{I} - \mathbf{K})\mathbf{u}_d \\ &= \mathbf{K}(\boldsymbol{\Pi} \times \boldsymbol{\Omega} + \mathbf{P} \times \mathbf{v}) + (\mathcal{I} - \mathbf{K})\mathbf{u}_d \end{aligned} \quad (4.31)$$

and make the change of variables $(\boldsymbol{\Pi}, \mathbf{P}, l) \rightarrow (\boldsymbol{\Pi}, \mathbf{P}, \zeta)$ where $\zeta = (\mathcal{I} - \mathbf{K})^{-1}(l - \mathbf{K}\boldsymbol{\Pi})$. In these variables, the closed-loop equations of motion are

$$\begin{aligned} \dot{\boldsymbol{\Pi}} &= \boldsymbol{\Pi} \times \boldsymbol{\Omega} + \mathbf{P} \times \mathbf{v} + \mathbf{f}_\Omega(\boldsymbol{\Omega}, \mathbf{v}) \\ \dot{\mathbf{P}} &= \mathbf{P} \times \boldsymbol{\Omega} + \mathbf{f}_v(\boldsymbol{\Omega}, \mathbf{v}) + \mathcal{F}_{\text{thrust}} \\ \dot{\zeta} &= -(\mathcal{I} - \mathbf{K})^{-1}\mathbf{K}\mathbf{f}_\Omega(\boldsymbol{\Omega}, \mathbf{v}) + \mathbf{u}_d. \end{aligned} \quad (4.32)$$

Since steady translation along the vehicle long axis requires a propulsive force to counter drag, a constant body-fixed force $\mathcal{F}_{\text{thrust}}$ is introduced to maintain the desired equilibrium. Given a desired steady velocity $\mathbf{v}_e = \bar{v}_1 \mathbf{e}_1$ with $\boldsymbol{\Omega}_e = \mathbf{0}$, choose

$$\mathcal{F}_{\text{thrust}} = -\mathbf{f}_v(\mathbf{0}, \mathbf{v}_e). \quad (4.33)$$

This constant external force is equal and opposite to the drag at the desired equilibrium velocity. Assumption (3.20) implies that thrust is aligned with the vehicle 1-axis.

Given a desired equilibrium speed $\bar{v}_1 > 0$, a crucial requirement is that thrust and drag equilibrate (when $\boldsymbol{\Omega} \equiv \mathbf{0}$ and $v_2 \equiv v_3 \equiv 0$) in such a way that $v_1 \rightarrow \bar{v}_1$. This requirement leads to the restriction that \bar{v}_1 satisfy

$$(v_1 - \bar{v}_1)\mathbf{e}_1 \cdot (\mathbf{f}_v(\mathbf{0}, v_1\mathbf{e}_1) - \mathbf{f}_v(\mathbf{0}, \bar{v}_1\mathbf{e}_1)) \leq 0 \quad (4.34)$$

with equality if and only if $v_1 = \bar{v}_1$. Assumption (4.34) requires that, when the vehicle translates along its long axis, the magnitude of drag is larger (smaller) than the magnitude of thrust when the vehicle moves faster (slower) than \bar{v}_1 . For the example drag model (3.18), condition (4.34) places no restriction on the choice of \bar{v}_1 . More generally, one might expect a small range of inadmissible equilibrium speeds in the neighborhood of the critical speed for boundary layer transition, where the drag force can *decrease* with increasing speed [30].

Because the terms in \bar{H}_Φ (given in (4.12)) which are quadratic make the rate $\frac{d}{dt}\bar{H}_\Phi$ indefinite when drag is introduced, we truncate these terms to obtain the negative semidefinite function

$$V(\boldsymbol{\Pi}, \mathbf{P}, \zeta) = H_K(\boldsymbol{\Pi}, \mathbf{P}, \zeta) - \frac{1}{m_1}C_1 = \frac{1}{2}(\boldsymbol{\Pi} - \zeta)^T \mathbf{I}_K^{-1}(\boldsymbol{\Pi} - \zeta) + \frac{1}{2}\mathbf{P}^T(\mathbf{M}^{-1} - \frac{1}{m_1}\mathbf{I})\mathbf{P}. \quad (4.35)$$

This is the function one would obtain by applying steps 1 and 2 of the energy-Casimir method, outlined on page 39, to the equilibrium (4.14). The desired equilibrium is a critical point of V but is not a strict maximum.

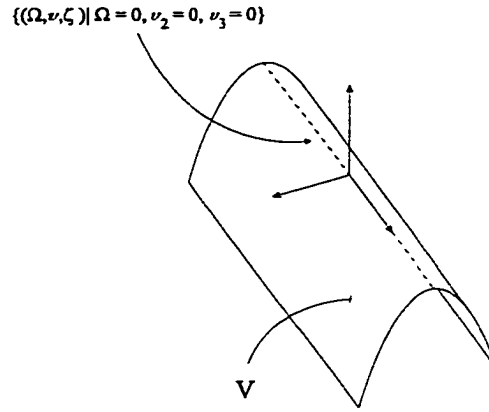


Figure 4.2: The negative semidefinite function V .

Written in $(\Omega, \mathbf{v}, \zeta)$ coordinates, the function V is

$$V(\Omega, \mathbf{v}, \zeta) = \frac{1}{2} \Omega \cdot \mathbf{I}_K \Omega + \frac{1}{2} \left(\frac{1}{m_2} - \frac{1}{m_1} \right) (m_2 v_2)^2 + \frac{1}{2} \left(\frac{1}{m_3} - \frac{1}{m_1} \right) (m_3 v_3)^2.$$

Since $\mathbf{I}_K < \mathbf{0}$ and $m_1 < m_2 < m_3$, V is negative definite in the coordinate directions corresponding to $\Omega_1, \Omega_2, \Omega_3, v_2$ and v_3 . The function is depicted in Figure 4.2 where the “line” of maxima corresponds to $\Omega_1 = \Omega_2 = \Omega_3 = v_2 = v_3 = 0$ (i.e., to $V = 0$).

Differentiating (4.35) gives

$$\begin{aligned} \dot{V} &= \frac{\partial V}{\partial \Pi} \cdot \dot{\Pi} + \frac{\partial V}{\partial \mathbf{P}} \cdot \dot{\mathbf{P}} + \frac{\partial V}{\partial \zeta} \cdot \dot{\zeta} \\ &= \Omega \cdot \dot{\Pi} + \left(\mathbf{v} - \frac{1}{m_1} \mathbf{P} \right) \cdot \dot{\mathbf{P}} - \Omega \cdot \dot{\zeta} \\ &= \Omega \cdot ((\mathcal{I} - \mathbf{K})^{-1} \mathbf{f}_\Omega(\Omega, \mathbf{v}) - \mathbf{u}_d) + \sum_{i=2}^3 \frac{(m_1 - m_i)}{m_1} v_i \mathbf{e}_i \cdot (\mathbf{f}_v(\Omega, \mathbf{v}) - \mathbf{f}_v(\mathbf{0}, \mathbf{v}_e)). \end{aligned}$$

Define the dissipative feedback

$$\mathbf{u}_d = -\mathbf{K}_d \Omega, \quad \mathbf{K}_d \geq 0. \quad (4.36)$$

Under assumptions (3.19) and (3.20) on the form of drag, \dot{V} is positive semidefinite:

$$\dot{V} \geq \sum_{i=1}^3 \left(-\frac{1}{1-k_i} f_{\Omega_i} \Omega_i^2 + \Omega \cdot \mathbf{K}_d \Omega + \frac{(m_i - m_1)}{m_1} f_{v_i} v_i^2 \right) \geq 0 \quad (4.37)$$

and $\dot{V} = 0$ if and only if Ω , v_2 , and v_3 are all zero. Since V is bounded above and nondecreasing, $\dot{V} \rightarrow 0$ asymptotically in time. In fact, V converges even with $\mathbf{K}_d = \mathbf{0}$.

It can further be shown that V converges to zero exponentially. Define the nondimensional vector $\bar{\sigma}^T = [\frac{L_1}{\bar{v}_1} \Omega^T, \frac{v_2}{\bar{v}_1}, \frac{v_3}{\bar{v}_1}]$. Then $V = \frac{1}{2} \bar{\sigma}^T \Sigma \bar{\sigma}$ where

$$\Sigma = \begin{pmatrix} \left(\frac{\bar{v}_1}{L_1}\right)^2 \mathbf{I}_K & & & \mathbf{0} \\ & (m_2 \bar{v}_1)^2 \left(\frac{1}{m_2} - \frac{1}{m_1}\right) & & 0 \\ & \mathbf{0} & & (m_3 \bar{v}_1)^2 \left(\frac{1}{m_3} - \frac{1}{m_1}\right) \end{pmatrix} < \mathbf{0}.$$

Therefore

$$0 \geq V \geq -b \|\bar{\sigma}\|^2 \quad \text{where} \quad b = -\frac{1}{2} \min_i \Sigma_{ii} \quad (4.38)$$

and Σ_{ii} is the i th diagonal element of Σ . From equation (4.37), $\dot{V} \geq \bar{\sigma}^T \Upsilon \bar{\sigma}$, where

$$\Upsilon = \begin{pmatrix} \left(\frac{\bar{v}_1}{L_1}\right)^2 \left(\text{diag}\left(-\frac{f_{\Omega_1}}{1-k_1}, -\frac{f_{\Omega_2}}{1-k_2}, -\frac{f_{\Omega_3}}{1-k_3}\right) + \mathbf{K}_d \right) & & & \mathbf{0} \\ & \mathbf{0} & & \frac{(m_2 - m_1) \bar{v}_1^2}{m_1} f_{v_2} \\ & & & 0 \\ & & & \frac{(m_3 - m_1) \bar{v}_1^2}{m_1} f_{v_3} \end{pmatrix}.$$

Thus, $\Upsilon > \mathbf{0}$ and it follows that

$$V \geq a \|\bar{\sigma}\|^2 \geq 0 \quad \text{where} \quad a = \min_i \Upsilon_{ii} \quad (4.39)$$

and Υ_{ii} is the i th diagonal element of Υ . From equations (4.38) and (4.39),

$$\dot{V} \geq \frac{a}{b} (b\|\bar{\sigma}\|^2) \geq -\left(\frac{a}{b}\right) V.$$

So V decays to zero exponentially,

$$0 \geq V(t) \geq V(0)e^{-\frac{a}{b}t}. \quad (4.40)$$

Having bounded V one may bound $\|\bar{\sigma}\|$, and thereby bound $\|\Omega\|$, $|v_2|$ and $|v_3|$. Let

$$d = -\frac{1}{2} \max_i \Sigma_{ii}.$$

Then,

$$\|\bar{\sigma}\|^2 \leq \frac{1}{d}|V| \leq \frac{1}{d}|V(0)|e^{-\frac{a}{b}t}$$

and $\|\bar{\sigma}\|$ decays exponentially,

$$\|\bar{\sigma}\| \leq X e^{-\frac{1}{2}\left(\frac{a}{b}\right)t} \quad (4.41)$$

where $X = \sqrt{|V(0)|/d}$.

It must be shown that the remaining dynamics are well-behaved. In fact, v_1 goes to the desired speed \bar{v}_1 and the rotor velocities remain bounded. To establish the first observation, define the set $\mathcal{M}_{\text{viscous}} = \{(\mathbf{\Pi}, \mathbf{P}, \zeta) \mid \Omega = \mathbf{0}, v_2 = v_3 = 0\}$. Referring to the equations of motion (4.32) with $\mathcal{F}_{\text{thrust}}$ defined by (4.33) and \mathbf{u}_d defined by equation (4.36), it should be clear that the rotor velocities are constant on $\mathcal{M}_{\text{viscous}}$ since $\mathbf{\Pi}$ and ζ are constant there.

In fact, the only nontrivial dynamics on $\mathcal{M}_{\text{viscous}}$ are governed by the following equation,

$$\dot{v}_1 = \frac{1}{m_1} \mathbf{e}_1 \cdot (\mathbf{f}_v(\mathbf{0}, v_1 \mathbf{e}_1) - \mathbf{f}_v(\mathbf{0}, \bar{v}_1 \mathbf{e}_1)). \quad (4.42)$$

But under assumption (4.34), when $\boldsymbol{\Omega} = \mathbf{0}$ and $v_2 = v_3 = 0$, the drag and thrust forces equilibrate in such a way that $v_1 \rightarrow \bar{v}_1$. More precisely, $\frac{1}{2}(v_1 - \bar{v}_1)^2$ is a Lyapunov function on $\mathcal{M}_{\text{viscous}}$ so, for trajectories contained in $\mathcal{M}_{\text{viscous}}$, v_1 goes to \bar{v}_1 asymptotically.

It has been shown that all trajectories go to $\mathcal{M}_{\text{viscous}}$ and that all trajectories within $\mathcal{M}_{\text{viscous}}$ go to an equilibrium of the desired form (4.14). As trajectories approach $\mathcal{M}_{\text{viscous}}$, $\boldsymbol{\Omega} \rightarrow \mathbf{0}$, $v_2 \rightarrow 0$, and $v_3 \rightarrow 0$ and the rate of change of v_1 is well-approximated by equation (4.42). One may conclude that $\boldsymbol{\Omega} \rightarrow \mathbf{0}$ and $\mathbf{v} \rightarrow \mathbf{v}_e$ asymptotically. Furthermore, this is true *globally*.

Remark 4.1.9 *If, instead of the constant thrust $\mathcal{F}_{\text{thrust}} = -\mathbf{f}_v(\mathbf{0}, \bar{v}_1 \mathbf{e}_1)$, one were to choose*

$$\mathcal{F}_{\text{thrust}}(v_1) = \mathbf{f}_v(\mathbf{0}, v_1 \mathbf{e}_1) - \kappa(v_1 - \bar{v}_1) \mathbf{e}_1$$

with some positive constant κ , then v_1 would converge to \bar{v}_1 exponentially on $\mathcal{M}_{\text{viscous}}$. For this choice of thrust, $(\boldsymbol{\Omega}, \mathbf{v})$ is globally exponentially stable to $(\mathbf{0}, \mathbf{v}_e)$. Implementing this propulsive force requires exact knowledge of the vehicle drag when $(\boldsymbol{\Omega}, \mathbf{v}) = (\mathbf{0}, v_1 \mathbf{e}_1)$. For streamline motions such as the equilibrium considered here, accurate drag models can be obtained experimentally [30].

It remains only to show that $\|\boldsymbol{\Omega}_r\|$ is bounded. Since $\boldsymbol{\Omega} \rightarrow \mathbf{0}$ exponentially, both $\boldsymbol{\Pi}$ and ζ go to $\mathbf{J}_r \boldsymbol{\Omega}_r$ exponentially. Thus, it is sufficient to show that $\|\boldsymbol{\Pi}\|$ or $\|\zeta\|$ is bounded.

Consider the following inequality

$$\begin{aligned}
\frac{d}{dt} \left(\frac{1}{2} \|\zeta\|^2 \right) &= \|\zeta\| \frac{d}{dt} \|\zeta\| = \zeta \cdot \dot{\zeta} \\
&= \zeta \cdot \left(-(\mathcal{I} - \mathbf{K})^{-1} \mathbf{K} \mathbf{f}_\Omega(\Omega, \mathbf{v}) + \mathbf{K}_d \Omega \right) \\
&\leq \|\zeta\| \left(\|\mathbf{K}_d\| \|\Omega\| + \|(\mathcal{I} - \mathbf{K})^{-1} \mathbf{K}\| \|\mathbf{f}_\Omega(\Omega, \mathbf{v})\| \right) \quad (4.43)
\end{aligned}$$

For the feedback-stabilized system, there is a positive constant N (which depends on the initial conditions) such that

$$\|\mathbf{f}_\Omega(\Omega, \mathbf{v})\| \leq N \|\Omega\|. \quad (4.44)$$

To define N , observe that $\mathbf{f}_\Omega(\Omega, \mathbf{v})$ is continuous and is therefore bounded on a compact set $B \subset \{(\Omega, \mathbf{v}) \mid \Omega \neq \mathbf{0}\}$. Let

$$N = \sup_B \frac{\|\mathbf{f}_\Omega(\Omega, \mathbf{v})\|}{\|\Omega\|}. \quad (4.45)$$

In addition to being compact, the set B should be positively invariant to ensure that condition (4.44) remains valid as (Ω, \mathbf{v}) converges. To define a suitable set B , begin with the set $B_1 = \{(\Omega, \mathbf{v}) \mid V \geq -c_{B_1}\}$ where $c_{B_1} > 0$ is a scalar constant. Since V is nondecreasing, B_1 is positively invariant. However, V does not involve v_1 , so B_1 is not compact. Instead, B is defined as the intersection of B_1 with another positively invariant set described below.

Consider the effect of thrust and drag on the translational momentum. The rate of change of $C_1 = \frac{1}{2} \|\mathbf{P}\|^2$ is

$$\frac{d}{dt} \left(\frac{1}{2} \|\mathbf{P}\|^2 \right) = \mathbf{P} \cdot \dot{\mathbf{P}} = \mathbf{P} \cdot (\mathbf{f}_v(\Omega, \mathbf{v}) - \mathbf{f}_v(\mathbf{0}, \mathbf{v}_e)).$$

Using the conditions (3.19), it follows that

$$\begin{aligned} \frac{d}{dt} \left(\frac{1}{2} \|\mathbf{P}\|^2 \right) &\leq - \sum_{i=1}^3 m_i f_{v_i} v_i^2 - \mathbf{P} \cdot \mathbf{f}_v(\mathbf{0}, \mathbf{v}_e) \\ &\leq - \min_i \left(\frac{f_{v_i}}{m_i} \right) \|\mathbf{P}\|^2 + \|\mathbf{f}_v(\mathbf{0}, \mathbf{v}_e)\| \|\mathbf{P}\|. \end{aligned}$$

Thus, if $\|\mathbf{P}\|$ is large, C_1 is decreasing. In other words, there is some maximum speed which the vehicle can sustain. Choose a scalar constant c_{B_2} satisfying

$$c_{B_2} \geq \frac{1}{2} \left(\frac{\|\mathbf{f}_v(\mathbf{0}, \mathbf{v}_e)\|}{\min_i \left(\frac{f_{v_i}}{m_i} \right)} \right)^2.$$

Another positively invariant set is therefore

$$B_2 = \left\{ \mathbf{P} \mid \frac{1}{2} \|\mathbf{P}\|^2 \leq \max \{c_{B_2}, \frac{1}{2} \|\mathbf{P}(\mathbf{0})\|^2\} \right\}.$$

$B = B_1 \cap B_2$ is a compact, positively invariant set on which equation (4.45) holds. Furthermore, by choice of the constant c_{B_1} , B may be chosen to contain any given initial condition.

By the inequality (4.43),

$$\frac{d}{dt} \|\zeta\| \leq (\|(\mathcal{I} - \mathbf{K})^{-1} \mathbf{K}\| N + \|\mathbf{K}_d\|) \|\Omega\| \quad \text{when } \|\zeta\| \neq 0.$$

Using the bound on $\|\Omega\|$ and integrating the above inequality from 0 to $t \geq 0$, one obtains an explicit bound on $\|\zeta\|$,

$$\|\zeta(t)\| \leq 2(\|(\mathcal{I} - \mathbf{K})^{-1} \mathbf{K}\| N + \|\mathbf{K}_d\|) \left(\frac{b}{a} \right) X + \|\zeta(0)\|$$

$$= 2(\|(\mathcal{I} - \mathbf{K})^{-1}\mathbf{K}\|N + \|\mathbf{K}_d\|) \left(\frac{b}{a}\right) \sqrt{V(0)/d} + \|\zeta(0)\|.$$

To minimize the bound on $\|\zeta\|$ for a given drag model, we should choose control gain matrices \mathbf{K} and \mathbf{K}_d such that

$$(\|(\mathcal{I} - \mathbf{K})^{-1}\mathbf{K}\|N + \|\mathbf{K}_d\|) \left(\frac{b}{a}\right) \frac{1}{\sqrt{d}}$$

is small. Furthermore, choosing the control such that b/a is as small as possible maximizes the rate at which $\|\sigma\|$ converges to zero. From the definitions of b and a in (4.38) and (4.39), respectively, the definition of \mathbf{I}_K in (4.4), and recalling that $m_1 < m_2 < m_3$, the ratio b/a is smallest when

$$|I_{K_i}| < \left(\frac{1}{m_1} - \frac{1}{m_3}\right) (m_3 L_1)^2 \quad i = 1, 2, 3 \quad (4.46)$$

and

$$\lambda_{\min}(\mathbf{K}_d) \geq \frac{L_1^2 \min_{i=2,3} \left\{ \left(\frac{1}{m_1} - \frac{1}{m_i}\right) m_i f_{v_i} \right\}}{\max_{i=1}^3 \left\{ -\frac{1}{1-k_i} f_{\Omega_i} \right\}} \quad (4.47)$$

where $\lambda_{\min}(\cdot)$ denotes the smallest eigenvalue. Contrary to conditions (4.46) and (4.47),

$$\frac{1}{\sqrt{d}} (\|(\mathcal{I} - \mathbf{K})^{-1}\mathbf{K}\|N + \|\mathbf{K}_d\|)$$

is smallest when we choose \mathbf{K}_d small and \mathbf{I}_K large. A reasonable compromise is to choose the control so that conditions (4.46) and (4.47) are just satisfied. This choice will ensure that the bound on $\|\zeta(t)\|$ is as small as possible, subject to the requirement that $\|\sigma\|$ converge as rapidly as possible (with the convergence rate governed by the fluid drag).

The closed-loop equations of motion under the feedback control law

$$\mathbf{u} = \mathbf{K}(\boldsymbol{\Pi} \times \boldsymbol{\Omega} + \mathbf{P} \times \mathbf{v}) - (\mathcal{I} - \mathbf{K})\mathbf{K}_d\boldsymbol{\Omega} \quad (4.48)$$

are

$$\begin{aligned} \dot{\boldsymbol{\Pi}} &= \boldsymbol{\Pi} \times \boldsymbol{\Omega} + \mathbf{P} \times \mathbf{v} + \mathbf{f}_\Omega(\boldsymbol{\Omega}, \mathbf{v}) \\ \dot{\mathbf{P}} &= \mathbf{P} \times \boldsymbol{\Omega} + \mathbf{f}_v(\boldsymbol{\Omega}, \mathbf{v}) - \mathbf{f}_v(\mathbf{0}, \mathbf{v}_e) \\ \dot{\boldsymbol{\zeta}} &= -(\mathcal{I} - \mathbf{K})^{-1}\mathbf{K}\mathbf{f}_\Omega(\boldsymbol{\Omega}, \mathbf{v}) - \mathbf{K}_d\boldsymbol{\Omega}. \end{aligned} \quad (4.49)$$

Theorem 4.1.10 (Coincident Centers with Viscosity - Global Asymptotic Stability) *Equations (4.49) with $(\mathcal{I} - \mathbf{K}) < 0$, \mathbf{K} diagonal, and $\mathbf{K}_d \geq 0$ describe a system for which the state remains bounded and asymptotically approaches an equilibrium*

$$\boldsymbol{\Pi}_e = \tilde{\boldsymbol{\Pi}}, \quad \mathbf{P}_e = m_1\tilde{v}_1\mathbf{e}_1, \quad \boldsymbol{\zeta}_e = \tilde{\boldsymbol{\Pi}} \quad (4.50)$$

regardless of initial condition.

The vehicle's translational and angular velocity will always approach the desired values $\mathbf{v}_e = \tilde{v}_1\mathbf{e}_1$ and $\boldsymbol{\Omega}_e = \mathbf{0}$, although the final equilibrium value of $\boldsymbol{\Pi}$ and $\boldsymbol{\zeta}$ will vary with initial condition. When $\boldsymbol{\Omega}$ is zero, $\boldsymbol{\zeta}$ corresponds to the rotor angular momentum. While it is not expected that the internal rotors will each be driven to zero angular velocity with this choice of control, at least these angular velocities will be bounded.

Remark 4.1.11 *The control law $\mathbf{u} = \mathbf{K}\dot{\boldsymbol{\Pi}}$ with $\mathcal{I} - \mathbf{K} < 0$ effectively changes the sign of the vehicle inertia. Physically, this means that external torques will tend to turn the vehicle in the opposite sense. The effect of any torque which would drive the uncontrolled*

vehicle away from the desired (unstable) equilibrium is reversed by the feedback control law. If $\dot{\mathbf{\Pi}}$ includes a contribution from viscosity, which ordinarily tends to decrease the vehicle's angular velocity, the feedback control law reverses its effect as well so that drag tends to increase angular velocity. If the viscous torque is simply excluded from the feedback control law, as in equation (4.29), its effect will not be reversed and drag will continue to decrease angular velocity.

Remark 4.1.12 Recall from equations (3.7) that

$$\dot{\mathbf{\Pi}} = \mathbf{\Pi} \times \mathbf{\Omega} + \mathbf{P} \times \mathbf{v}.$$

Comparing this with Euler's equations for a freely rotating rigid body, one may view the term $\mathbf{P} \times \mathbf{v}$ as a torque due to the fluid. Were the vehicle not immersed in a fluid, the mass matrix \mathbf{M} would become a scalar (times the identity), $\mathbf{P} \times \mathbf{v}$ would be zero, and one would recover the unforced Euler's equations. In fact, the "fluid torque" $\mathbf{P} \times \mathbf{v}$ is the source of instability for long axis translation; it tends to turn the vehicle away from the desired equilibrium. Suppose we choose a control law to reverse this effect. Consider the feedback control

$$\mathbf{u} = k\mathbf{P} \times \mathbf{v} \tag{4.51}$$

where k is a scalar control gain. Define the change of variables from $(\mathbf{\Pi}, \mathbf{P}, l)$ to $(\mathbf{\Pi}, \mathbf{P}, \xi)$ where

$$\xi = \frac{1}{1-k}(l - k\mathbf{\Pi}) \tag{4.52}$$

with $k \neq 1$. The definition of ξ follows the definition of ζ in (4.3) with the gain matrix \mathbf{K}

replaced by a scalar gain k . Define

$$I_k = \frac{1}{1-k} \bar{I}.$$

The closed-loop equations of motion are

$$\begin{aligned} \dot{\Pi} &= \Pi \times \Omega + P \times v \\ \dot{P} &= P \times \Omega \\ \dot{\xi} &= -\frac{k}{1-k} \Pi \times \Omega. \end{aligned} \tag{4.53}$$

Since $\dot{l} = u \neq k\dot{\Pi}$, the new momentum ξ is not conserved. Still, equations (4.53) describe Hamiltonian dynamics. Define the Hamiltonian

$$H_k(\Pi, P, \xi) = \frac{1}{2}(\Pi - \xi)I_k^{-1}(\Pi - \xi) + \frac{1}{2}P \cdot M^{-1}P. \tag{4.54}$$

Then

$$\begin{pmatrix} \dot{\Pi} \\ \dot{P} \\ \dot{\xi} \end{pmatrix} = \begin{pmatrix} \hat{\Pi} & \hat{P} & 0 \\ \hat{P} & 0 & 0 \\ 0 & 0 & \frac{k}{1-k} \hat{\Pi} \end{pmatrix} \nabla H_k. \tag{4.55}$$

Since the bracket operation implied by equation (4.55) does not satisfy the Jacobi identity, this system is not Lie-Poisson. Rather, it is "almost Poisson" as discussed in [70, 22]. The functions $C_1(\Pi, P, \xi) = \frac{1}{2}\|P\|^2$ and $C_2(\Pi, P, \xi) = \Pi \cdot P$ are Casimirs for this system (i.e., the gradients of these functions are in the null space of the tensor in equation (4.55)). Choosing the control gain $k > 1$ along with suitable feedback dissipation asymptotically stabilizes steady long axis translation when drag is absent [70]. Analogous to the results of

this section, it can also be shown that asymptotic stability is enhanced by viscous forces so that dissipative feedback is unnecessary in the presence of drag.

4.2 Noncoincident Centers of Gravity and Buoyancy

This section treats the more general case of an underwater vehicle whose CG lies along the shortest ellipsoid principal axis. In particular, it is assumed that $\mathbf{r} = \gamma \mathbf{e}_3$ with γ a scalar constant; in this case, the CG lies along the body coordinate 3-axis. As in Section 3.2.2, we are principally interested in steady translation of the vehicle along its long axis. This equilibrium is of practical interest and is unstable for the uncontrolled system. Even though a low CG ($\gamma > 0$) can provide a restoring torque in pitch and roll, the fluid tends to cause the vehicle to yaw away from the equilibrium.

Following the method outlined in the introductory comments to Chapter 4, we break the control design into steps. In the first step, we shape the kinetic energy in much the same way as in Section 4.1.1. While the approach leads to satisfiable stability conditions, the control law does not preserve the naturally stabilizing effect of a low CG. (Recall that the gravity torque on a bottom-heavy vehicle ordinarily tends to stabilize the vehicle in pitch and roll.) We therefore modify the control law slightly to take advantage of the stabilizing gravity torque. The resulting closed-loop system can be interpreted as a Hamiltonian system with a modified kinetic energy, a modified potential energy, and a modified structure. The system is almost Poisson.

We break this system into a series of two subsystems, the first of which is Lie-Poisson. We use the energy-Casimir method to find conditions for stability of this first subsystem and then design feedback dissipation to asymptotically stabilize it. We then verify that the remaining subsystem is well-behaved in some sense. Finally, we move on to step 3 of the

procedure on page 83 and consider the effect of physical damping.

Section 4.2.1 treats the system without physical damping. Section 4.2.2 extends the analysis to include the effect of drag.

4.2.1 Asymptotically Stabilizing Steady Long Axis Translation

Recall from Section 3.1.1 that gravity breaks the full $SE(3)$ symmetry for a bottom-heavy underwater vehicle. The reduced dynamics no longer evolve on $\mathfrak{se}(3)^*$, but may be obtained through semidirect product reduction as described in [42]. The method of controlled Lagrangians for systems with full configuration symmetry, such as the underwater vehicle with coincident CG and CB, can be extended to systems with semidirect product symmetry. This is also carried out by Chang and Marsden [24] for the reasonably simple example of a heavy top with internal rotors. In that example, gravity breaks the system symmetry exactly as it does for a bottom-heavy underwater vehicle. The uncontrolled dynamics evolve on a reduced semidirect product space and the method of controlled Lagrangians carries through essentially as described in [10]. See Section 5.3 for a brief review of the method of controlled Lagrangians as it applies to Euler-Poincaré systems.

Recall from equation (3.21) that the conservative dynamics for an underwater vehicle with noncoincident CG and CB are described by the equations

$$\begin{aligned}
 \dot{\Pi} &= \Pi \times \Omega + P \times v + r \times mg\Gamma \\
 \dot{P} &= P \times \Omega \\
 \dot{\Gamma} &= \Gamma \times \Omega \\
 \dot{i} &= u.
 \end{aligned} \tag{4.56}$$

Define the matrices \mathbf{A} , \mathbf{B} , and \mathbf{C} as the block components of the inverse generalized inertia for the rigid body (see Section 3.1.1),

$$\begin{pmatrix} \mathbf{A} & \mathbf{B}^T \\ \mathbf{B} & \mathbf{C} \end{pmatrix} = \begin{pmatrix} \bar{\mathbf{I}} & m\hat{\mathbf{r}} \\ -m\hat{\mathbf{r}} & \mathbf{M} \end{pmatrix}^{-1}.$$

(The notation follows that of [42].) One may easily verify that

$$\begin{aligned} \mathbf{A} &= \mathbf{A}^T = (\bar{\mathbf{I}} + (m\hat{\mathbf{r}})\mathbf{M}^{-1}(m\hat{\mathbf{r}}))^{-1} \\ \mathbf{B} &= \mathbf{C}(m\hat{\mathbf{r}})\bar{\mathbf{I}}^{-1} \\ &= \mathbf{M}^{-1}(m\hat{\mathbf{r}})\mathbf{A} \\ \mathbf{C} &= \mathbf{C}^T = (\mathbf{M} + (m\hat{\mathbf{r}})\bar{\mathbf{I}}^{-1}(m\hat{\mathbf{r}}))^{-1}. \end{aligned} \quad (4.57)$$

If the CG is located along a body principal axis, \mathbf{A} and \mathbf{C} are diagonal. When $\mathbf{r} = \gamma\mathbf{e}_3$,

$$\mathbf{A} = \text{diag}\left(a_1, a_2, \frac{1}{I_3}\right) \quad \text{and} \quad \mathbf{C} = \text{diag}\left(c_1, c_2, \frac{1}{m_3}\right). \quad (4.58)$$

where

$$\begin{aligned} a_1 &= \frac{m_2}{m_2 I_1 - (m\gamma)^2} > 0 & \text{and} & & c_1 &= \frac{I_2}{m_1 I_2 - (m\gamma)^2} > 0 \\ a_2 &= \frac{m_1}{m_1 I_2 - (m\gamma)^2} > 0 & & & c_2 &= \frac{I_1}{m_2 I_1 - (m\gamma)^2} > 0. \end{aligned}$$

Referring ahead to Section 5.3, the method of controlled Lagrangians provides the kinetic energy shaping feedback control law (5.70) for systems such as the underwater vehicle with internal rotors. Using notation to be introduced in Chapter 5, the control law (5.70) for an

underwater vehicle with noncoincident CG and CB is

$$\begin{aligned} \mathbf{u} = [u_a] &= \left[k_{a\alpha}^{\text{ca}} \left(\frac{d}{dt} \frac{\partial l}{\partial \eta^\alpha} \right) \right] = \left[D_{ab} \sigma^{bc} g_{c\beta} B^{\beta\alpha} \right] \begin{pmatrix} \dot{\Pi} \\ \dot{P} \end{pmatrix} \\ &= (\tilde{\mathbf{K}}, \mathbf{0}) \begin{pmatrix} \mathbf{A} & \mathbf{B}^T \\ \mathbf{B} & \mathbf{C} \end{pmatrix} \begin{pmatrix} \dot{\Pi} \\ \dot{P} \end{pmatrix}. \end{aligned}$$

Disregarding the notation for now, it is important only to note that the matrix $\tilde{\mathbf{K}}$ may be freely chosen. Substituting for \mathbf{B} from (4.57),

$$\begin{aligned} \mathbf{u} &= \tilde{\mathbf{K}} (\mathbf{A}\dot{\Pi} + \mathbf{B}^T\dot{P}) \\ &= \tilde{\mathbf{K}} \mathbf{A} (\dot{\Pi} - (m\hat{r})M^{-1}\dot{P}) \\ &= \mathbf{K} ((\Pi \times \Omega + P \times v + r \times mg\Gamma) - (m\hat{r})M^{-1}(P \times \Omega)). \end{aligned} \quad (4.59)$$

Define the control gain matrix $\mathbf{K} = \tilde{\mathbf{K}} \mathbf{A}$. As in Section 4.1, the control effectively modifies the kinetic energy metric. Because the closed-loop energy metric must be symmetric, we once again choose $\mathbf{K} = \mathbf{K}^T$ to commute with $\bar{\mathbf{I}}$. We also require that \mathbf{K} commutes with \mathbf{A} . A simple choice which satisfies these requirements is $\mathbf{K} = \text{diag}(k_1, k_2, k_3)$. Note that when $\mathbf{r} = \mathbf{0}$, (4.59) reduces to the control law (4.2) chosen in Section 4.1.1.

Define the change of variables $(\Pi, P, \Gamma, l) \rightarrow (\Pi, P, \Gamma, \zeta)$ where

$$\zeta = (\mathcal{I} - \mathbf{K})^{-1} (l - \mathbf{K}(\Pi - m\hat{r}M^{-1}P)). \quad (4.60)$$

There should be no notational confusion since ζ defined in equation (4.60) reduces to the previous definition (4.3) when $\mathbf{r} = \mathbf{0}$. The body angular and translational velocity are

related to Π , P , and ζ by

$$\begin{pmatrix} \Omega \\ v \end{pmatrix} = \begin{pmatrix} A & B^T \\ B & C \end{pmatrix} \begin{pmatrix} \mathcal{I} - K & K(m\hat{r})M^{-1} \\ 0 & \mathcal{I} \end{pmatrix} \begin{pmatrix} \Pi - \zeta \\ P \end{pmatrix}. \quad (4.61)$$

Define the control-modified matrix components of the generalized inertia,

$$\begin{aligned} A_K &= A(\mathcal{I} - K) \\ B_K &= M^{-1}(m\hat{r})A_K \\ C_K &= C(M + (m\hat{r})\bar{\Gamma}^{-1}K(m\hat{r}))M^{-1}. \end{aligned} \quad (4.62)$$

Then, for $r = \gamma e_3$, equation (4.61) may be written more compactly as

$$\begin{pmatrix} \Omega \\ v \end{pmatrix} = \begin{pmatrix} A_K & B_K^T \\ B_K & C_K \end{pmatrix} \begin{pmatrix} \Pi - \zeta \\ P \end{pmatrix}. \quad (4.63)$$

The closed-loop equations of motion are

$$\begin{aligned} \dot{\Pi} &= \Pi \times \Omega + P \times v + r \times mg\Gamma \\ \dot{P} &= P \times \Omega \\ \dot{\Gamma} &= \Gamma \times \Omega \\ \dot{\zeta} &= 0. \end{aligned} \quad (4.64)$$

These equations describe Lie-Poisson dynamics with respect to a new Hamiltonian H_K ,

which includes a control-modified kinetic energy term:

$$H_K(\mathbf{\Pi}, \mathbf{P}, \mathbf{\Gamma}, \zeta) = \frac{1}{2} \begin{pmatrix} \mathbf{\Pi} - \zeta \\ \mathbf{P} \end{pmatrix} \cdot \begin{pmatrix} \mathbf{A}_K & \mathbf{B}_K^T \\ \mathbf{B}_K & \mathbf{C}_K \end{pmatrix} \begin{pmatrix} \mathbf{\Pi} - \zeta \\ \mathbf{P} \end{pmatrix} - \mathbf{r} \cdot m\mathbf{g}\mathbf{\Gamma}. \quad (4.65)$$

Equations (4.64) may be written

$$\begin{pmatrix} \dot{\mathbf{\Pi}} \\ \dot{\mathbf{P}} \\ \dot{\mathbf{\Gamma}} \\ \dot{\zeta} \end{pmatrix} = \begin{pmatrix} \hat{\mathbf{\Pi}} & \hat{\mathbf{P}} & \hat{\mathbf{\Gamma}} & \mathbf{0} \\ \hat{\mathbf{P}} & \mathbf{0} & \mathbf{0} & \mathbf{0} \\ \hat{\mathbf{\Gamma}} & \mathbf{0} & \mathbf{0} & \mathbf{0} \\ \mathbf{0} & \mathbf{0} & \mathbf{0} & \mathbf{0} \end{pmatrix} \nabla H_K. \quad (4.66)$$

There should be no confusion between this Hamiltonian H_K and the one defined in Section 4.1.1 since (4.65) reduces to (4.7) when $\mathbf{r} = \mathbf{0}$. There are six independent Casimirs,

$$C_1(\mathbf{\Pi}, \mathbf{P}, \mathbf{\Gamma}, \zeta) = \frac{1}{2} \|\mathbf{P}\|^2, \quad C_2(\mathbf{\Pi}, \mathbf{P}, \mathbf{\Gamma}, \zeta) = \frac{1}{2} \|\mathbf{\Gamma}\|^2, \quad C_3(\mathbf{\Pi}, \mathbf{P}, \mathbf{\Gamma}, \zeta) = \mathbf{P} \cdot \mathbf{\Gamma},$$

and each component of ζ .

The dynamics (4.66), and the original open-loop dynamics (4.56), are very rich, exhibiting several families of relative equilibria which were first identified by Leonard [42]. Anticipating a control law which drives the body angular rate to zero, we review only the equilibria for which $\mathbf{\Omega} \equiv \mathbf{0}$. These equilibria satisfy

$$\mathbf{P}_e \times \mathbf{v}_e + \mathbf{r} \times m\mathbf{g}\mathbf{\Gamma}_e = \mathbf{0}. \quad (4.67)$$

Equation (4.67) can be used to solve for Γ_e in terms of v_e and r ,

$$\Gamma_e = \delta r + \frac{1}{m g r \cdot r} r \times (M v_e \times v_e)$$

where $|\delta|$ is determined from the identity $\|\Gamma\|^2 = 1$. As discussed in Appendix C, choosing $r = \gamma e_3$ gives two five-parameter families of relative equilibria for which $\Omega \equiv 0$. The five equilibrium parameters are $\zeta_1^0, \zeta_2^0, \zeta_3^0$ and P_i^0 and P_3^0 where the two families correspond to $i = 1$ or 2 . The remaining component of the equilibrium momentum P_e is zero. Explicitly, the two families are given by

$$\Pi_e = (m\hat{r})M^{-1}P_e + \zeta_e, \quad P_e = P_i^0 e_i + P_3^0 e_3, \quad \zeta_e = \begin{pmatrix} \zeta_1^0 \\ \zeta_2^0 \\ \zeta_3^0 \end{pmatrix}, \quad \text{and}$$

$$\Gamma_e = \pm \sqrt{1 - \left(\left(\frac{1}{m_3} - \frac{1}{m_i} \right) \frac{P_i^0 P_3^0}{m g \gamma} \right)^2} e_3 + \left(\frac{1}{m_3} - \frac{1}{m_i} \right) \frac{P_i^0 P_3^0}{m g \gamma} e_i, \quad i = 1 \text{ or } 2 \quad (4.68)$$

where it is assumed that

$$1 - \left(\left(\frac{1}{m_3} - \frac{1}{m_i} \right) \frac{P_i^0 P_3^0}{m g \gamma} \right)^2 \geq 0.$$

Of particular interest is the family of equilibria for which the vehicle translates along its

long axis in the horizontal plane,

$$\mathbf{\Pi}_e = \begin{pmatrix} 0 \\ \frac{m\gamma}{m_1}\sqrt{2C_1} \\ 0 \end{pmatrix} + \begin{pmatrix} \zeta_1^0 \\ \zeta_2^0 \\ \zeta_3^0 \end{pmatrix}, \quad \mathbf{P}_e = \begin{pmatrix} \sqrt{2C_1} \\ 0 \\ 0 \end{pmatrix}, \quad \mathbf{\Gamma}_e = \begin{pmatrix} 0 \\ 0 \\ 1 \end{pmatrix}, \quad \zeta_e = \begin{pmatrix} \zeta_1^0 \\ \zeta_2^0 \\ \zeta_3^0 \end{pmatrix}. \quad (4.69)$$

Since the equilibrium (4.69) corresponds to the particular case that $C_3 = 0$, we assume that

$$\mathbf{\Gamma} \perp \mathbf{P}.$$

Because C_3 is conserved regardless of the control law, the assumption implies that $C_3 = 0$ for all time. Even when $C_3 = 0$, relative equilibria may exist for which the vehicle translates in a body principal plane but not along a body principal axis. As it is shown in Appendix C, these “gliding equilibria” exist only under certain conditions on the magnitude of γ . Since we are interested in making the equilibrium (4.69) asymptotically stable within as large a region of attraction as possible, we choose γ to eliminate these other equilibria. Specifically, we choose γ such that

$$(mg\gamma)^2 \geq 4C_1^2 \left(\frac{1}{m_3} - \frac{1}{m_i} \right)^2 \quad \text{for } i = 1 \text{ and } 2. \quad (4.70)$$

In this case, the only equilibria for which $\mathbf{\Omega} = \mathbf{0}$ correspond to pure translation along a vehicle principal axis.

Applying the energy-Casimir method to the equilibrium (4.69) gives conditions on \mathbf{K} and γ for stability.

Theorem 4.2.1 *Let $k_i > 1$ for $i = 1, 2$, and 3 and let $\gamma < 0$. Then the relative equilibrium*

(4.69) with $C_1 \neq 0$ is Lyapunov stable.

Proof: A Lyapunov function, which is negative definite about the equilibrium, is

$$\begin{aligned} H_\Psi &= H_K(\mathbf{\Pi}, \mathbf{P}, \mathbf{\Gamma}, \zeta) + \Psi(C_1, C_2, C_3, \zeta_1, \zeta_2, \zeta_3) \\ &= H_K(\mathbf{\Pi}, \mathbf{P}, \mathbf{\Gamma}, \zeta) - \frac{1}{m_1} C_1 + mg\gamma C_2 + \frac{1}{2} \Psi_{11|e} (C_1 - \frac{1}{2} (P_1^0)^2)^2 + \\ &\quad \frac{1}{2} \Psi_{44|e} (\zeta_1 - \zeta_1^0)^2 + \frac{1}{2} \Psi_{55|e} (\zeta_2 - \zeta_2^0)^2 + \frac{1}{2} \Psi_{66|e} (\zeta_3 - \zeta_3^0)^2 \end{aligned}$$

where $\Psi_{jj|e} < 0$ for $j = 2, 4, 5$, and 6 . To verify this statement, observe that the desired equilibrium (4.69) is a critical point of H_Ψ :

$$\begin{aligned} (DH_\Psi)_e \cdot (\delta\mathbf{\Pi}, \delta\mathbf{P}, \delta\mathbf{\Gamma}, \delta\zeta) &= (\mathbf{\Omega})_e \cdot \delta\mathbf{\Pi} + (v - \frac{1}{m_1} \mathbf{P} + \Psi_{11|e} (C_1 - \frac{1}{2} (P_1^0)^2) \mathbf{P})_e \cdot \delta\mathbf{P} \\ &\quad + (-mgr + mg\gamma\mathbf{\Gamma})_e \cdot \delta\mathbf{\Gamma} + \left(-\mathbf{\Omega} + \begin{pmatrix} \Psi_{44|e} (\zeta_1 - \zeta_1^0) \\ \Psi_{55|e} (\zeta_2 - \zeta_2^0) \\ \Psi_{66|e} (\zeta_3 - \zeta_3^0) \end{pmatrix} \right)_e \cdot \delta\zeta = 0 \end{aligned}$$

for all variations $\delta\mathbf{\Pi}$, $\delta\mathbf{P}$, $\delta\mathbf{\Gamma}$, and $\delta\zeta$. Since H_Ψ is conserved in the absence of physical or feedback dissipation, Lyapunov stability follows if (4.69) is a maximum or a minimum of H_Ψ . The matrix of the second variation of H_Ψ , evaluated at the equilibrium, is

$$\begin{pmatrix} \mathbf{A}_k & \mathbf{B}_k^T & \mathbf{0} & -\mathbf{A}_k \\ \mathbf{B}_k & \mathbf{C}_k - \frac{1}{m_1} \mathcal{I} + \Psi_{22|e} \mathbf{P}_e \mathbf{P}_e^T & \mathbf{0} & \mathbf{0} \\ \mathbf{0} & \mathbf{0} & mg\gamma \mathcal{I} & \mathbf{0} \\ -\mathbf{A}_k & \mathbf{0} & \mathbf{0} & \mathbf{A}_k + \text{diag}(\Psi_{44|e}, \Psi_{55|e}, \Psi_{66|e}) \end{pmatrix}.$$

This matrix is negative definite provided $\gamma < 0$, $k_i > 1$ for $i = 1, 2$, and 3 , and $\Psi_{jj|e} < 0$ for $j = 2, 4, 5$, and 6 . \square

Interestingly, the stability proof requires that the CG be *above* the CB (i.e., that $\gamma < 0$). This is somewhat counterintuitive; one would ordinarily expect stability to be at least partially improved when the CG is *below* the CB. For example, it was shown in [42] that steady translation of the vehicle along its intermediate axis in the horizontal plane is stable without control so long as $\gamma > 0$. That stability under the given control law might require a relatively high CG implies the internal rotors will be “balancing the inverted vehicle” as well as stabilizing steady translation. Intuitively, this seems rather inefficient and impractical.

There is, however, a simple physical explanation for the odd stability result of Theorem 4.2.1. It is related to the observations of Remark 4.1.11. Since the control \mathbf{u} represents a torque applied to the internal rotors, a reaction torque $-\mathbf{u}$ acts on the vehicle (less the rotors). Consider the control law (4.59) with $k_i > 1$. One may interpret this control law as tending to reverse the effect of torques acting on the vehicle. In particular, the destabilizing effect of the term $\mathbf{P} \times \mathbf{v}$ is reversed. However, the effect of gravity (i.e., the torque $\mathbf{r} \times mg\mathbf{\Gamma}$) is also reversed, even though gravity ordinarily plays a useful role when the CG is below the CB.

Accordingly, rather than pursue the control law (4.59) further, consider the following modified version,

$$\mathbf{u} = k \left((\mathbf{\Pi} \times \mathbf{\Omega} + \mathbf{P} \times \mathbf{v}) - m\hat{\mathbf{r}}\mathbf{M}^{-1}(\mathbf{P} \times \mathbf{\Omega}) \right) + (1 - k)(\zeta \times \mathbf{\Omega} - \tilde{\mathbf{u}}) \quad (4.71)$$

where k is a scalar gain and the term $\tilde{\mathbf{u}}$ represents a dissipative feedback term to be determined. The control law (4.71) is a modification of (4.59) that does not involve the gravitational torque $\mathbf{r} \times mg\mathbf{\Gamma}$. The resulting closed-loop system is

$$\dot{\mathbf{\Pi}} = \mathbf{\Pi} \times \mathbf{\Omega} + \mathbf{P} \times \mathbf{v} + \mathbf{r} \times mg\mathbf{\Gamma}$$

$$\begin{aligned}
\dot{\mathbf{P}} &= \mathbf{P} \times \boldsymbol{\Omega} \\
\dot{\boldsymbol{\Gamma}} &= \boldsymbol{\Gamma} \times \boldsymbol{\Omega} \\
\dot{\boldsymbol{\zeta}} &= \boldsymbol{\zeta} \times \boldsymbol{\Omega} - \frac{mgk}{1-k} \mathbf{r} \times \boldsymbol{\Gamma} - \tilde{\mathbf{u}}
\end{aligned} \tag{4.72}$$

The equilibria (4.69) of the original closed-loop system (4.64) are also equilibria of the system (4.72) when $\tilde{\mathbf{u}} = \mathbf{0}$.

Remark 4.2.2 *Let $\tilde{\mathbf{u}} = \mathbf{0}$. While equations (4.72) do not describe Lie-Poisson dynamics, the closed-loop system is almost Poisson (see Remark 4.1.12):*

$$\begin{pmatrix} \dot{\boldsymbol{\Pi}} \\ \dot{\mathbf{P}} \\ \dot{\boldsymbol{\Gamma}} \\ \dot{\boldsymbol{\zeta}} \end{pmatrix} = \begin{pmatrix} \hat{\boldsymbol{\Pi}} & \hat{\mathbf{P}} & (1-k)\hat{\boldsymbol{\Gamma}} & \mathbf{0} \\ \hat{\mathbf{P}} & \mathbf{0} & \mathbf{0} & \mathbf{0} \\ (1-k)\hat{\boldsymbol{\Gamma}} & \mathbf{0} & \mathbf{0} & -k\hat{\boldsymbol{\Gamma}} \\ \mathbf{0} & \mathbf{0} & -k\hat{\boldsymbol{\Gamma}} & -\boldsymbol{\zeta} \end{pmatrix} \nabla H_k \tag{4.73}$$

where the new Hamiltonian H_k is

$$H_k(\boldsymbol{\Pi}, \mathbf{P}, \boldsymbol{\Gamma}, \boldsymbol{\zeta}) = \frac{1}{2} \begin{pmatrix} \boldsymbol{\Pi} - \boldsymbol{\zeta} \\ \mathbf{P} \end{pmatrix} \cdot \begin{pmatrix} \mathbf{A}_k & \mathbf{B}_k^T \\ \mathbf{B}_k & \mathbf{C}_k \end{pmatrix} \begin{pmatrix} \boldsymbol{\Pi} - \boldsymbol{\zeta} \\ \mathbf{P} \end{pmatrix} - \frac{mg}{1-k} \mathbf{r} \cdot \boldsymbol{\Gamma}. \tag{4.74}$$

\mathbf{A}_k , \mathbf{B}_k , and \mathbf{C}_k are defined as in equations (4.62) with \mathbf{K} replaced by $k\mathbf{I}$. Here the control parameter k appears in both the kinetic and potential energy terms. Thus, we may view the control as shaping the potential energy as well as the kinetic energy. Potential shaping for underwater vehicles is discussed in [43].

The functions

$$C_1(\boldsymbol{\Pi}, \mathbf{P}, \boldsymbol{\Gamma}, \boldsymbol{\zeta}) = \frac{1}{2} \|\mathbf{P}\|^2, \quad \text{and} \quad C_2(\boldsymbol{\Pi}, \mathbf{P}, \boldsymbol{\Gamma}, \boldsymbol{\zeta}) = \frac{1}{2} \|\boldsymbol{\Gamma}\|^2$$

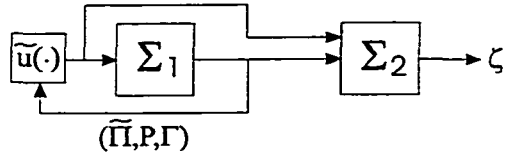


Figure 4.3: Closed-loop system as a series connection.

are two Casimirs. In addition, $P \cdot \Gamma$ and $\Gamma \cdot \zeta$ are conserved, although these are not Casimirs. Unfortunately, applying the energy-Casimir method to the equilibrium (4.69) using the Hamiltonian (4.74) does not easily provide conditions on k and γ for nonlinear stability.

A useful way to analyze the system (4.72) is to consider it as a series of two subsystems which may be studied in sequence. The first subsystem corresponds to the vehicle dynamics while the second describes some combination of the vehicle and internal rotor dynamics.

Let

$$\tilde{\Pi} = \Pi - \zeta. \quad (4.75)$$

Then

$$\begin{pmatrix} \Omega \\ v \end{pmatrix} = \begin{pmatrix} A_k & B_k^T \\ B_k & C_k \end{pmatrix} \begin{pmatrix} \tilde{\Pi} \\ P \end{pmatrix}. \quad (4.76)$$

The closed-loop equations of motion become

$$\begin{aligned} \dot{\tilde{\Pi}} &= \tilde{\Pi} \times \Omega + P \times v + \frac{mg}{1-k} r \times \Gamma + \tilde{u} \\ \dot{P} &= P \times \Omega \\ \dot{\Gamma} &= \Gamma \times \Omega \\ \dot{\zeta} &= \zeta \times \Omega - \frac{mgk}{1-k} r \times \Gamma - \tilde{u}. \end{aligned} \quad (4.77)$$

The dissipative feedback control law for \tilde{u} will be chosen as a function only of $\tilde{\Pi}$, P , and

Γ . The closed-loop system may therefore be broken into two subsystems, Σ_1 and Σ_2 , which are interconnected in series as shown in Figure 4.3. The subsystem dynamics are given by

$$\Sigma_1 : \begin{pmatrix} \dot{\tilde{\Pi}} \\ \dot{P} \\ \dot{\Gamma} \end{pmatrix} = \begin{pmatrix} \tilde{\Pi} \times \Omega + P \times v + \frac{mg}{1-k} r \times \Gamma + \tilde{u} \\ P \times \Omega \\ \Gamma \times \Omega \end{pmatrix} \quad (4.78)$$

and

$$\Sigma_2 : \quad \dot{\zeta} = \zeta \times \Omega - \frac{mgk}{1-k} r \times \Gamma - \tilde{u}. \quad (4.79)$$

The subsystem Σ_1 is a forced Lie-Poisson system and Σ_2 is a forced, linear time-varying system. To show stability of the desired equilibrium (4.69), we first define asymptotically stabilizing dissipative feedback for the corresponding equilibrium of Σ_1 . We then show that the resulting control law is, in fact, locally exponentially stabilizing and therefore does not cause the Σ_2 states to become unbounded.

Asymptotic Stability of Σ_1 . Here, we essentially pursue step 2 of the method described on page 83 for the subsystem Σ_1 . We add a dissipative feedback term $\tilde{u}(\tilde{\Pi}, P, \Gamma)$ to the control law (4.71) to ensure asymptotic stability of Σ_1 .

Equations (4.78) may also be written

$$\begin{pmatrix} \dot{\tilde{\Pi}} \\ \dot{P} \\ \dot{\Gamma} \end{pmatrix} = \begin{pmatrix} \hat{\tilde{\Pi}} & \hat{P} & \hat{\Gamma} \\ \hat{P} & 0 & 0 \\ \hat{\Gamma} & 0 & 0 \end{pmatrix} \nabla H_k + \begin{pmatrix} \mathcal{I} \\ 0 \\ 0 \end{pmatrix} \tilde{u}, \quad (4.80)$$

where H_k has been redefined in terms of $\tilde{\Pi}$, P , and Γ ,

$$H_k(\tilde{\Pi}, P, \Gamma) = \frac{1}{2} \begin{pmatrix} \tilde{\Pi} \\ P \end{pmatrix} \cdot \begin{pmatrix} A_k & B_k^T \\ B_k & C_k \end{pmatrix} \begin{pmatrix} \tilde{\Pi} \\ P \end{pmatrix} - \frac{mg}{1-k} r \cdot \Gamma. \quad (4.81)$$

Three independent Casimirs of the unforced system are

$$C_1(\tilde{\Pi}, P, \Gamma) = \frac{1}{2} \|P\|^2, \quad C_2(\tilde{\Pi}, P, \Gamma) = \frac{1}{2} \|\Gamma\|^2, \quad \text{and} \quad C_3(\tilde{\Pi}, P, \Gamma) = P \cdot \Gamma.$$

In fact, these quantities are conserved regardless of the choice of \tilde{u} . Choosing $\tilde{u} = 0$, for the moment, one may use the energy-Casimir method to find conditions on the parameter γ and the control gain k such that the equilibrium (corresponding to (4.69))

$$\tilde{\Pi}_e = \begin{pmatrix} 0 \\ \frac{m\gamma}{m_1} \sqrt{2C_1} \\ 0 \end{pmatrix}, \quad P_e = \begin{pmatrix} \sqrt{2C_1} \\ 0 \\ 0 \end{pmatrix}, \quad \Gamma_e = \begin{pmatrix} 0 \\ 0 \\ 1 \end{pmatrix} \quad (4.82)$$

is Lyapunov stable. Of course, the Lyapunov function constructed for Σ_1 will not prove stability of the entire system because we have ignored the ζ dynamics. However, one may use this Lyapunov function to develop a dissipative control law which drives Σ_1 to the equilibrium (4.82) asymptotically. With convergence of Σ_1 assured, it can then be verified that Σ_2 is well-behaved.

Define the augmented Hamiltonian

$$H_\psi(\tilde{\Pi}, P, \Gamma) = H_k + \psi(C_1, C_2, C_3),$$

where H_k is given by (4.81) and ψ is a function to be determined. Applying the energy-

Casimir method shows that, for $k > 1$, $\gamma > 0$, and $\psi_e^{11} < 0$, the function

$$H_\psi(\bar{\mathbf{\Pi}}, \mathbf{P}, \Gamma) = H_k - \frac{1}{m_1} C_1 + \frac{m\gamma\gamma}{1-k} \left(C_2 + \frac{1}{2} \right) + \frac{1}{2} \psi_e^{11} \left(C_1 - \frac{1}{2} (P_1^0)^2 \right)^2 \quad (4.83)$$

has a strict maximum at the equilibrium (4.82). Thus (4.82) is a stable equilibrium of Σ_1 .

Now suppose $\bar{\mathbf{u}} \neq \mathbf{0}$. Then

$$\frac{d}{dt} H_\psi = \Omega \cdot \bar{\mathbf{u}}. \quad (4.84)$$

Choosing

$$\begin{aligned} \bar{\mathbf{u}} &= \mathbf{K}_d \Omega \\ &= \mathbf{K}_d (\mathbf{A}_k \bar{\mathbf{\Pi}} + \mathbf{B}_k^T \mathbf{P}) \end{aligned} \quad (4.85)$$

with $\mathbf{K}_d > \mathbf{0}$ makes $\frac{d}{dt} H_\psi \geq 0$. Since H_ψ is bounded above and nondecreasing, $\frac{d}{dt} H_\psi \rightarrow 0$ as $t \rightarrow \infty$.

Lemma 4.2.3 $\frac{d}{dt} H_\psi \equiv 0$ if and only if Σ_1 is at equilibrium with $\Omega \equiv \mathbf{0}$.

Proof: From equations (4.84) and (4.85), $\Omega \equiv \mathbf{0}$ when $\frac{d}{dt} H_\psi \equiv 0$ and therefore $\dot{\mathbf{P}} = \mathbf{0}$ and $\dot{\mathbf{\Gamma}} = \mathbf{0}$. Also, since

$$\dot{\Omega} \equiv \mathbf{0} = \mathbf{A}_k \dot{\bar{\mathbf{\Pi}}} + \mathbf{B}_k^T \dot{\mathbf{P}},$$

it follows that $\dot{\bar{\mathbf{\Pi}}} = \mathbf{0}$. \square

Along the lines of the development in Section 4.1.2, one may find a compact, positively invariant set which contains only the desired equilibrium. Define a constant

$$c_\psi = \max \left\{ H_\psi \left(-\frac{m\gamma}{m_2} \mathbf{e}_1, \sqrt{2C_1} \mathbf{e}_2, \mathbf{e}_3 \right), H_\psi \left(\frac{m\gamma}{m_1} \mathbf{e}_2, \sqrt{2C_1} \mathbf{e}_1, -\mathbf{e}_3 \right) \right\}.$$

The former argument in the definition of c_ψ is the value of H_ψ when the vehicle translates purely along the 2-axis. The latter argument is the value of H_ψ when the vehicle translates “upside-down” along the 1-axis. Neither of these equilibria is desirable and neither is contained in the compact, positively invariant set

$$\omega_\psi = \left\{ (\tilde{\Pi}, \mathbf{P}, \Gamma) \mid C_3 = 0, H_\psi(\tilde{\Pi}, \mathbf{P}, \Gamma) \geq (1 - \epsilon)c_\psi \right\}$$

where $0 < \epsilon \ll 1$. In fact, ω_ψ contains only two equilibria for which $\Omega = \mathbf{0}$. These correspond to “forward” and “reverse” 1-axis translation (with the CG below the CB).

The set ω_ψ is actually the union of two compact, positively invariant subsets

$$\omega_{\psi_+} = \{(\tilde{\Pi}, \mathbf{P}, \Gamma) \in \omega_\psi \mid \mathbf{P} \cdot \mathbf{e}_1 > 0\}$$

and

$$\omega_{\psi_-} = \{(\tilde{\Pi}, \mathbf{P}, \Gamma) \in \omega_\psi \mid \mathbf{P} \cdot \mathbf{e}_1 < 0\}.$$

The proof of this observation follows similarly to the discussion preceding Theorem 4.1.8. The only equilibrium for which $\Omega = \mathbf{0}$ that is contained in ω_{ψ_+} is the desired equilibrium (4.82). By LaSalle’s invariance principle, (4.82) is asymptotically stable.

It still remains to show that the system Σ_2 is well-behaved. While $\dot{\zeta}$ certainly goes to zero as $(\tilde{\Pi}, \mathbf{P}, \Gamma) \rightarrow (\frac{m\gamma}{m_1}\mathbf{e}_2, \sqrt{2C_1}\mathbf{e}_1, \mathbf{e}_3)$, one would prefer an explicit bound on the states ζ . Such a bound can be obtained locally by linearizing the dynamics (4.78) and checking that (4.82) is locally exponentially stable. Given an exponential convergence rate for $(\tilde{\Pi}, \mathbf{P}, \Gamma)$, an explicit bound on ζ may be computed as in Section 4.1.3.

Linearizing the closed-loop system Σ_1 (i.e., the system (4.78) with the dissipative control

law (4.85)) about the equilibrium (4.82) gives

$$\begin{aligned}\delta\dot{\hat{\Pi}} &= \hat{\Pi}_e\delta\Omega + \hat{P}_e\delta v - \widehat{M^{-1}P_e}\delta P + \frac{mg\gamma}{1-k}\widehat{e_3}\delta\Omega + K_d\delta\Omega \\ \delta\dot{P} &= \hat{P}_e\delta\Omega \\ \delta\dot{\Gamma} &= \hat{\Gamma}_e\delta\Omega\end{aligned}$$

where δx represents the difference between x and its equilibrium value. Define

$$\sigma = [\Omega^T, v^T, \Gamma^T]^T \quad (4.86)$$

The linearized dynamics written in terms of the body velocity are

$$\delta\dot{\sigma} = \begin{pmatrix} A_k \left((m\gamma\widehat{e_3})\widehat{M^{-1}P_e} + K_d \right) + B_k^T \hat{P}_e & A_k(\hat{P}_e - \widehat{M^{-1}P_e}M) & A_k \left(\frac{mg\gamma}{1-k}\widehat{e_3} \right) \\ B_k \left((m\gamma\widehat{e_3})\widehat{M^{-1}P_e} + K_d \right) + C_k \hat{P}_e & B_k(\hat{P}_e - \widehat{M^{-1}P_e}M) & B_k \left(\frac{mg\gamma}{1-k}\widehat{e_3} \right) \\ \hat{\Gamma}_e & 0 & 0 \end{pmatrix} \delta\sigma \quad (4.87)$$

For simplicity, let $K_d = \text{diag}(k_{d1}, k_{d2}, k_{d3})$. Then the characteristic polynomial of the linearized system is

$$\lambda^3(\lambda^2 + \mu_1\lambda + \mu_2)(\lambda^4 + \mu_3\lambda^3 + \mu_4\lambda^2 + \mu_5\lambda + \mu_6) \quad (4.88)$$

where

$$\begin{aligned}\mu_1 &= -a_2(1-k)k_{d2} \\ \mu_2 &= a_2 \left(mg\gamma - (1-k) \left(\frac{1}{m_1} - \frac{1}{m_3} \right) (P_1^0)^2 \right)\end{aligned}$$

$$\begin{aligned}
\mu_3 &= -(1-k) \left(\frac{k_{d_3}}{I_3} + a_1 k_{d_1} \right) \\
\mu_4 &= -\frac{1-k}{I_3} \left(\frac{1}{m_1} - \frac{1}{m_2} \right) (P_1^0)^2 + a_1 m g \gamma \\
&\quad + a_1 \frac{(1-k)^2}{I_3} \left((m\gamma)^2 \left(\frac{1}{m_1} - \frac{1}{m_2} \right)^2 (P_1^0)^2 + k_{d_1} k_{d_3} \right) \\
\mu_5 &= -a_1 \frac{1-k}{I_3} \left(-(1-k) k_{d_1} \left(\frac{1}{m_1} - \frac{1}{m_2} \right) (P_1^0)^2 + (m g \gamma) k_{d_3} \right) \\
\mu_6 &= -\frac{(1-k) a_1}{I_3} (m g \gamma) \left(\frac{1}{m_1} - \frac{1}{m_2} \right) (P_1^0)^2.
\end{aligned}$$

The three zero roots of (4.88) correspond to the Casimirs C_1, C_2 , and C_3 , which are conserved under any choice of control $\tilde{u}(\tilde{\Pi}, P, \Gamma)$.

Since it has already been required that $k > 1$, $\gamma > 0$, and $k_{d_i} > 0$ for $i = 1, 2$, and 3, the quadratic term

$$(\lambda^2 + \mu_1 \lambda + \mu_2)$$

has roots with negative real part. Using the Routh-Hurwitz stability criterion (see [23] and references therein), one may find a compatible range of control parameters k, k_{d_1}, k_{d_3} , and γ such that the roots of the quartic term

$$(\lambda^4 + \mu_3 \lambda^3 + \mu_4 \lambda^2 + \mu_5 \lambda + \mu_6)$$

also have negative real part. In addition to requiring that each coefficient μ_3, μ_4, μ_5 , and μ_6 be positive, the Routh-Hurwitz criterion requires that

$$\mu_3 \mu_4 - \mu_5 > 0 \tag{4.89}$$

$$\mu_3 \mu_4 \mu_5 - \mu_5^2 - \mu_6 \mu_3^2 > 0. \tag{4.90}$$

One may check that condition (4.89) is satisfied when $k > 1$, $\gamma > 0$, and $k_{d_i} > 0$ for $i = 1$

and 3. Condition (4.90) is investigated in Appendix D where explicit conditions on the dissipative control gains k_{d_i} are obtained. Under these conditions, the six nonzero roots of the characteristic polynomial (4.88) have negative real part. Thus, one may ensure that when $C_3 = 0$, the equilibrium (4.82) is locally exponentially stable.

Define the dimensionless vector $\bar{\sigma} = [\frac{L}{v_1}\Omega^T, \frac{1}{v_1}v^T, \Gamma^T]^T$ and let $\bar{\sigma}_e$ denote the equilibrium value of $\bar{\sigma}$ corresponding to the equilibrium (4.82). Then, there exist positive constants X and λ_0 such that, locally

$$\|\delta\bar{\sigma}\| = \|\bar{\sigma} - \bar{\sigma}_e\| \leq X e^{-\lambda_0 t}. \quad (4.91)$$

The convergence rate $-\lambda_0$ is determined by the nonzero roots of (4.88). These roots depend on the parameters k , γ , and K_d . One might be tempted to choose the parameters such that λ_0 is as large as possible so that $\bar{\sigma}$ converges quickly. However, such a choice could adversely affect the rotor dynamics; it could lead to large steady-state rotor velocities.

Asymptotic Stability of Σ_2 . Referring to equation (4.79),

$$\begin{aligned} \frac{d}{dt} \left(\frac{1}{2} \|\zeta\|^2 \right) &= \|\zeta\| \frac{d}{dt} \|\zeta\| = \zeta \cdot \dot{\zeta} \\ &= \zeta \cdot \left(\zeta \times \Omega - \frac{mgk}{1-k} \mathbf{r} \times \Gamma - K_d \Omega \right) \\ &\leq \|\zeta\| \left(\left| \frac{mg\gamma k}{1-k} \right| \|\mathbf{e}_3 \times \Gamma\| + \|K_d\| \|\Omega\| \right) \end{aligned} \quad (4.92)$$

The term in parentheses on the right-hand side of (4.92) converges to zero exponentially for small values of $\|\bar{\sigma} - \bar{\sigma}_e\|$. Inequality (4.91) gives a bounding envelope on $\|\mathbf{e}_3 \times \Gamma\|$ and $\|\Omega\|$. Thus, whenever $\|\zeta\| \neq 0$,

$$\frac{d}{dt} \|\zeta\| \leq \left(\left| \frac{mg\gamma k}{1-k} \right| \|\mathbf{e}_3 \times \Gamma\| + \|K_d\| \|\Omega\| \right) \leq \bar{X} e^{-\lambda_0 t}. \quad (4.93)$$

where $\bar{X} > 0$ depends on X in equation (4.91) and on the terms $|mg\gamma k / (1-k)|$ and $\|K_d\|$.

Along the lines of the analysis in Section 4.1.3, the inequality (4.93) may be integrated to give the bound

$$\|\zeta(t)\| \leq \frac{\bar{X}}{\lambda_0}.$$

Clearly one would like to have \bar{X} small and λ_0 large. However, these goals may be contradictory and a trade-off might have to be made as in Section 4.1.3.

Theorem 4.2.4 *Consider the closed-loop system (4.77) with $\bar{u} = K_d\Omega$ where $K_d = \text{diag}(k_{d_1}, k_{d_2}, k_{d_3})$. Suppose $k > 1$, $\gamma > 0$, and $k_{d_i} > 0$ ($i = 1, 2$, and 3) have been chosen to satisfy (4.70) and (4.90), as in Appendix D. Assume that $C_3 = 0$. Then the equilibrium*

$$\bar{\Pi}_e = \begin{pmatrix} 0 \\ \frac{m\gamma}{m_1}\sqrt{2C_1} \\ 0 \end{pmatrix}, \quad P_e = \begin{pmatrix} \sqrt{2C_1} \\ 0 \\ 0 \end{pmatrix}, \quad \Gamma_e = \begin{pmatrix} 0 \\ 0 \\ 1 \end{pmatrix}$$

of the subsystem Σ_1 is asymptotically stable within ω_{ψ_+} . Furthermore, the equilibrium is locally exponentially stable and ζ is bounded and goes to a constant.

4.2.2 Viscous Forces and Asymptotic Stability

Here, viscous forces are included in the system model as described in Section 3.1.3. Under the control law (4.71), the equations of motion become

$$\begin{aligned} \dot{\bar{\Pi}} &= \bar{\Pi} \times \Omega + P \times v + \frac{mg}{1-k} r \times \Gamma + \frac{1}{1-k} f_{\Omega}(\Omega, v) \\ &\quad - \frac{k}{1-k} (m\hat{r}) M^{-1} (f_v(\Omega, v) - f_v(0, v_e)) + \bar{u} \\ \dot{P} &= P \times \Omega + f_v(\Omega, v) - f_v(0, v_e) \end{aligned}$$

$$\begin{aligned}
\dot{\Gamma} &= \Gamma \times \Omega \\
\dot{\zeta} &= \zeta \times \Omega - \frac{k}{1-k} \left(\mathbf{r} \times mg\Gamma + \mathbf{f}_\Omega(\Omega, \mathbf{v}) \right. \\
&\quad \left. - m\hat{r}M^{-1}(\mathbf{f}_v(\Omega, \mathbf{v}) - \mathbf{f}_v(\mathbf{0}, \mathbf{v}_e)) \right) - \bar{\mathbf{u}}.
\end{aligned} \tag{4.94}$$

where $\mathbf{v}_e = \bar{v}_1 \mathbf{e}_1$ is the desired velocity. We thus consider stability of the equilibrium

$$\mathbf{\Pi}_e = \begin{pmatrix} 0 \\ m\bar{v}_1 \\ 0 \end{pmatrix} + \begin{pmatrix} \zeta_1^0 \\ \zeta_2^0 \\ \zeta_3^0 \end{pmatrix}, \quad \mathbf{P}_e = \begin{pmatrix} m_1 \bar{v}_1 \\ 0 \\ 0 \end{pmatrix}, \quad \mathbf{\Gamma}_e = \begin{pmatrix} 0 \\ 0 \\ 1 \end{pmatrix}, \quad \zeta_e = \begin{pmatrix} \zeta_1^0 \\ \zeta_2^0 \\ \zeta_3^0 \end{pmatrix}. \tag{4.95}$$

As in Section 4.2.1, we break the system into subsystems Σ_1 and Σ_2 and consider the two subsystems separately. Σ_1 corresponds to the first nine equations of (4.94) while Σ_2 corresponds to the last three equations.

Asymptotic Stability of Σ_1 . Recall the modified Hamiltonian for the conservative system (4.80),

$$H_k(\tilde{\mathbf{\Pi}}, \mathbf{P}, \mathbf{\Gamma}) = \frac{1}{2} \begin{pmatrix} \tilde{\mathbf{\Pi}} \\ \mathbf{P} \end{pmatrix} \cdot \begin{pmatrix} \mathbf{A}_k & \mathbf{B}_k^T \\ \mathbf{B}_k & \mathbf{C}_k \end{pmatrix} \begin{pmatrix} \tilde{\mathbf{\Pi}} \\ \mathbf{P} \end{pmatrix} - \frac{mg\gamma}{1-k} \mathbf{e}_3 \cdot \mathbf{\Gamma}.$$

Recall that the feedback control law (4.71), with dissipative feedback term (4.85), locally asymptotically stabilizes the equilibrium (4.82) for the Σ_1 subsystem without external damping provided

$$k > 1, \quad \gamma > 0 \quad \text{and} \quad \mathbf{K}_d > \mathbf{0}.$$

In that case, the function H_ψ given by (4.83) is a Lyapunov function for the subsystem Σ_1 . When viscous forces are included, the Lyapunov rate $\frac{d}{dt}H_\psi$ becomes indefinite. To

circumvent this problem, define the negative semidefinite function

$$\bar{H}_\psi(\bar{\mathbf{\Pi}}, \mathbf{P}, \Gamma) = H_k - \frac{1}{m_1} C_1 + \frac{mg\gamma}{1-k} \left(C_2 + \frac{1}{2} \right) \quad (4.96)$$

by omitting the term in H_ψ which is quadratic in C_1 . The rate of change of \bar{H}_ψ is

$$\begin{aligned} \frac{d}{dt} \bar{H}_\psi &= \boldsymbol{\Omega} \cdot \dot{\bar{\mathbf{\Pi}}} + \left(\mathbf{v} - \frac{1}{m_1} \mathbf{P} \right) \cdot \dot{\mathbf{P}} + \frac{mg\gamma}{1-k} (\boldsymbol{\Gamma} - \mathbf{e}_3) \cdot \dot{\boldsymbol{\Gamma}} \\ &= \boldsymbol{\Omega} \cdot \left(\frac{1}{1-k} \mathbf{f}_\Omega(\boldsymbol{\Omega}, \mathbf{v}) - \frac{k}{1-k} (m\hat{\mathbf{r}}) \mathbf{M}^{-1} (\mathbf{f}_\mathbf{v}(\boldsymbol{\Omega}, \mathbf{v}) - \mathbf{f}_\mathbf{v}(\mathbf{0}, \mathbf{v}_e)) + \tilde{\mathbf{u}} \right) \\ &\quad + \left(\mathbf{v} - \frac{1}{m_1} \mathbf{P} \right) \cdot (\mathbf{f}_\mathbf{v}(\boldsymbol{\Omega}, \mathbf{v}) - \mathbf{f}_\mathbf{v}(\mathbf{0}, \mathbf{v}_e)). \end{aligned}$$

Substituting $\mathbf{P} = (-m\hat{\mathbf{r}})\boldsymbol{\Omega} + \mathbf{M}\mathbf{v}$ and defining

$$\boldsymbol{\varphi} = (-m\hat{\mathbf{r}}) \left(\frac{k}{1-k} \mathbf{M}^{-1} + \frac{1}{m_1} \mathcal{I} \right) (\mathbf{f}_\mathbf{v}(\boldsymbol{\Omega}, \mathbf{v}) - \mathbf{f}_\mathbf{v}(\mathbf{0}, \mathbf{v}_e)) \quad (4.97)$$

gives

$$\frac{d}{dt} \bar{H}_\psi = \boldsymbol{\Omega} \cdot \left(\frac{1}{1-k} \mathbf{f}_\Omega(\boldsymbol{\Omega}, \mathbf{v}) + \tilde{\mathbf{u}} \right) + \left(\mathbf{v} - \frac{1}{m_1} \mathbf{M}\mathbf{v} \right) \cdot (\mathbf{f}_\mathbf{v}(\boldsymbol{\Omega}, \mathbf{v}) - \mathbf{f}_\mathbf{v}(\mathbf{0}, \mathbf{v}_e)) + \boldsymbol{\Omega} \cdot \boldsymbol{\varphi} \quad (4.98)$$

Suppose that

$$\tilde{\mathbf{u}} = \mathbf{K}_d \boldsymbol{\Omega} + \varsigma \operatorname{sign}(\boldsymbol{\Omega} \cdot \boldsymbol{\varphi}) \boldsymbol{\varphi} \quad (4.99)$$

with $\mathbf{K}_d > \mathbf{0}$ and $\varsigma > 1$. The former term of (4.99) dissipates rotational kinetic energy while the latter term is intended to dominate the last term of (4.98) ensuring that $\frac{d}{dt} \bar{H}_\psi \geq 0$. To see this, recall the conditions on $\mathbf{f}_\Omega(\boldsymbol{\Omega}, \mathbf{v})$ and $\mathbf{f}_\mathbf{v}(\boldsymbol{\Omega}, \mathbf{v})$ given in Section 3.1.3,

$$\frac{d}{dt} \bar{H}_\psi = \boldsymbol{\Omega} \cdot \left(\frac{1}{1-k} \mathbf{f}_\Omega(\boldsymbol{\Omega}, \mathbf{v}) + \mathbf{K}_d \boldsymbol{\Omega} \right) + \left(\mathbf{v} - \frac{1}{m_1} \mathbf{M}\mathbf{v} \right) \cdot (\mathbf{f}_\mathbf{v}(\boldsymbol{\Omega}, \mathbf{v}) - \mathbf{f}_\mathbf{v}(\mathbf{0}, \mathbf{v}_e))$$

$$\begin{aligned}
& + (\boldsymbol{\Omega} \cdot \boldsymbol{\varphi} + \varsigma |\boldsymbol{\Omega} \cdot \boldsymbol{\varphi}|) \\
\geq & -\frac{1}{1-k} \sum_{i=1}^3 f_{\Omega_i} \Omega_i^2 - \sum_{j=2}^3 \left(1 - \frac{m_j}{m_1}\right) f_{v_j} v_j^2 + (\varsigma - 1) |\boldsymbol{\Omega} \cdot \boldsymbol{\varphi}| \geq 0.
\end{aligned}$$

Assume, as in Section 4.1.3, that the equilibrium speed \bar{v}_1 is chosen such that

$$(v_1 - \bar{v}_1) \mathbf{e}_1 \cdot (\mathbf{f}_v(\mathbf{0}, v_1 \mathbf{e}_1) - \mathbf{f}_v(\mathbf{0}, \bar{v}_1 \mathbf{e}_1)) \leq 0 \quad (4.100)$$

with equality if and only if $v_1 = \bar{v}_1$. (Recall that, for typical underwater vehicle flight conditions, this requirement essentially restricts the choice of \bar{v}_1 to exclude speeds in the range of the critical speed for boundary layer transition.) Then the following proposition holds.

Proposition 4.2.5 $\frac{d}{dt} \bar{H}_\psi = 0$ if and only if

$$\bar{\mathbf{\Pi}} = (m\hat{r})\mathbf{v}_e, \quad \mathbf{P} = \mathbf{M}\mathbf{v}_e, \quad \text{and} \quad \boldsymbol{\Gamma} = \pm \mathbf{e}_3.$$

Proof: From equation (4.98) with $\tilde{\mathbf{u}}$ given by (4.99), one finds that $\frac{d}{dt} \bar{H}_\psi = 0$ if and only if $\boldsymbol{\Omega} \equiv \mathbf{0}$ and $v_2 = v_3 \equiv 0$. Therefore, by assumption (3.20),

$$\dot{v}_1 = \frac{1}{m_1} (\mathbf{f}_v(\boldsymbol{\Omega}, \mathbf{v}) - \mathbf{f}_v(\mathbf{0}, \mathbf{v}_e)) \cdot \mathbf{e}_1. \quad (4.101)$$

Since $\boldsymbol{\Omega} \equiv \mathbf{0}$, we must have

$$\begin{aligned}
\dot{\boldsymbol{\Omega}} = 0 &= \mathbf{A}_k \left(\frac{mg\gamma}{1-k} \mathbf{e}_3 \times \boldsymbol{\Gamma} - \frac{k}{1-k} (m\gamma \widehat{\mathbf{e}}_3) \mathbf{M}^{-1} (\mathbf{f}_v(\boldsymbol{\Omega}, \mathbf{v}) - \mathbf{f}_v(\mathbf{0}, \mathbf{v}_e)) \right) \\
& \quad + \mathbf{B}_k^T (\mathbf{f}_v(\boldsymbol{\Omega}, \mathbf{v}) - \mathbf{f}_v(\mathbf{0}, \mathbf{v}_e)) \\
&= \frac{1}{1-k} \mathbf{A}_k (mg\gamma \mathbf{e}_3 \times \boldsymbol{\Gamma} - (m\gamma \widehat{\mathbf{e}}_3) \mathbf{M}^{-1} (\mathbf{f}_v(\boldsymbol{\Omega}, \mathbf{v}) - \mathbf{f}_v(\mathbf{0}, \mathbf{v}_e))). \quad (4.102)
\end{aligned}$$

But Γ is constant when $\Omega = \mathbf{0}$, so from (4.102)

$$\begin{aligned}
 m\gamma e_3 \times \Gamma = \text{constant} &= m\gamma e_3 \times M^{-1}(f_v(\Omega, v) - f_v(\mathbf{0}, v_e)) \\
 &= \frac{m\gamma}{m_1} ((f_v(\Omega, v) - f_v(\mathbf{0}, v_e)) \cdot e_1) e_2 \\
 &= m\gamma \dot{v}_1 e_2.
 \end{aligned} \tag{4.103}$$

It follows from (4.101) and (4.103) that \dot{v}_1 is constant. But, by assumption on the choice of equilibrium speed \bar{v}_1 , one finds that $\frac{d}{dt}(v_1 - \bar{v}_1)^2 \leq 0$. Since $(v_1 - \bar{v}_1)^2$ is bounded below and nonincreasing, it follows that \dot{v}_1 is constant if and only if it is zero, in which case $v_1 = \bar{v}_1$.

Equation (4.103) then implies that $\Gamma \parallel e_3$. \square

Once again, it remains to show that the system Σ_2 is well-behaved. First, it is shown that the desired equilibrium

$$\tilde{\Pi}_e = (m\hat{r})(\bar{v}_1 e_1), \quad P_e = m_1 \bar{v}_1 e_1, \quad \text{and} \quad \Gamma = e_3 \tag{4.104}$$

of Σ_1 is locally exponentially stable. This result is then used to obtain a bound on ζ .

Exponential stability of Σ_1 is shown by linearizing the closed-loop system (4.94) about the equilibrium (4.104). A few definitions will be convenient. Let σ be as defined in (4.86) and let

$$f_0(\sigma) = \begin{pmatrix} \tilde{\Pi} \times \Omega + P \times v + \frac{mg}{1-k} r \times \Gamma + K_d \Omega \\ P \times \Omega \\ \Gamma \times \Omega \end{pmatrix}.$$

The vector field $f_0(\sigma)$ expresses the system dynamics in the absence of viscous forces and

moments. The additional viscous effects are expressed by the vector field

$$f_1(\sigma) = \begin{pmatrix} \frac{1}{1-k} f_{\Omega}(\Omega, v) - \frac{k}{1-k} (m\hat{r}) M^{-1} (f_v(\Omega, v) - f_v(0, v_e)) + \varsigma \operatorname{sign}(\Omega \cdot \varphi) \varphi \\ f_v(\Omega, v) - f_v(0, v_e) \\ 0 \end{pmatrix}.$$

where φ is as defined in (4.97). The linearization of the dynamics (4.94) is then

$$\delta \dot{\sigma} = \left(\frac{\partial f_0}{\partial \sigma} + \frac{\partial f_1}{\partial \sigma} \right)_e \delta \sigma \quad (4.105)$$

where $\frac{\partial f_0}{\partial \sigma}|_e$ is the state matrix in equation (4.87). Assuming that the parameter conditions described in Section 4.2.1 are satisfied, $\frac{\partial f_0}{\partial \sigma}|_e$ has three zero eigenvalues, corresponding to the Casimirs C_1, C_2 , and C_3 of the inviscid dynamics, and six eigenvalues with negative real part.

Now consider the vector field $f_1(\sigma)$. Its linearization involves the linear approximations of the viscous moment and force. Since $f_{\Omega}(\Omega, v)$ and $f_v(\Omega, v)$ are C^1 ,

$$\begin{aligned} f_{\Omega}(\Omega, v) &= \left. \frac{\partial f_{\Omega}(\Omega, v)}{\partial \Omega} \right|_e \delta \Omega + \left. \frac{\partial f_{\Omega}(\Omega, v)}{\partial v} \right|_e \delta v + \text{h.o.t.} \quad \text{and} \\ f_v(\Omega, v) &= f_v(0, v_e) + \left. \frac{\partial f_v(\Omega, v)}{\partial \Omega} \right|_e \delta \Omega + \left. \frac{\partial f_v(\Omega, v)}{\partial v} \right|_e \delta v + \text{h.o.t.} \end{aligned}$$

By assumption, $f_{\Omega}(0, v) = 0$ for all v , so

$$\left. \frac{\partial f_{\Omega}(\Omega, v)}{\partial v} \right|_e = 0.$$

Furthermore, assumption (3.19) implies that

$$\left. \frac{\partial f_{\Omega}(\Omega, v)}{\partial \Omega} \right|_e < \mathbf{0} \quad \text{and} \quad \left. \frac{\partial f_v(\Omega, v)}{\partial v} \right|_e < \mathbf{0}.$$

Note that the term in $f_1(\sigma)$ involving φ must disappear in the linearization. (To circumvent smoothness problems, one may replace the discontinuous signum function with a C^1 approximation, for example, a very steep sigmoid.)

Proceeding with the linearization, one finds that

$$\left. \frac{\partial f_1}{\partial \sigma} \right|_e = \begin{pmatrix} \begin{pmatrix} \mathbf{A} & \mathbf{B}^T \\ \mathbf{B} & \mathbf{C} \end{pmatrix} \begin{pmatrix} \left. \frac{\partial f_{\Omega}(\Omega, v)}{\partial \Omega} \right|_e & \mathbf{0} \\ \left. \frac{\partial f_v(\Omega, v)}{\partial \Omega} \right|_e & \left. \frac{\partial f_v(\Omega, v)}{\partial v} \right|_e \end{pmatrix} & \mathbf{0} \\ \mathbf{0} & \mathbf{0} \end{pmatrix} \quad (4.106)$$

It can be shown that the upper left submatrix in the state matrix of (4.106) is Hurwitz under the assumptions on $f_{\Omega}(\Omega, v)$ and $f_v(\Omega, v)$. Thus $\left. \frac{\partial f_1}{\partial \sigma} \right|_e$ has three zero eigenvalues and six eigenvalues with negative real part.

In the presence of viscous forces, C_1 and C_3 are no longer conserved. Therefore, one expects that two of the zero eigenvalues from $\left. \frac{\partial f_0}{\partial \sigma} \right|_e$ will disappear in the presence of damping. On the other hand, C_2 is always conserved since $\|\Gamma\| = 1$ by definition. If the spectrum of the state matrix for the linear system (4.105) has a single zero eigenvalue (corresponding to conservation of $\|\Gamma\|$) and eight eigenvalues with negative real part, then the desired equilibrium (4.104) is locally exponentially stable. Local boundedness of ζ then follows by a similar argument to the one used at the end of Section 4.2.1.

Theorem 4.2.6 (Noncoincident Centers with Viscosity - Exponential Stability)

Consider the closed-loop system (4.94) with \tilde{u} given by (4.99). Suppose $k > 1$, $\gamma > 0$, and

$k_{d_i} > 0$ ($i = 1, 2,$ and 3) have been chosen to satisfy (4.90). Furthermore, suppose that the state matrix for the linear system (4.105) has all eigenvalues with negative real part save for a single zero eigenvalue. Then the equilibrium

$$\boldsymbol{\Omega}_e = \begin{pmatrix} 0 \\ 0 \\ 0 \end{pmatrix}, \quad \mathbf{v}_e = \begin{pmatrix} \tilde{v}_1 \\ 0 \\ 0 \end{pmatrix}, \quad \boldsymbol{\Gamma}_e = \begin{pmatrix} 0 \\ 0 \\ 1 \end{pmatrix}$$

of the subsystem Σ_1 is locally exponentially stable while ζ is bounded and goes to a constant.

It is notable that the simple drag model (3.18) satisfies the requirement on the spectrum of the state matrix in (4.105). Exponential stability of steady long-axis translation under this drag model is evident in the simulations shown in the next section.

4.3 Simulations

Numerical simulations were performed for a vehicle modeled as a neutrally buoyant ellipsoid with axis lengths $L_1 = 0.4572$ m (18 inches), $L_2 = 0.3048$ m (12 inches), and $L_3 = 0.1524$ m (6 inches). Given the density of water $\rho = 1000$ kg/m³, the elements of M are $m_1 = 13.2$ kg, $m_2 = 15.2$ kg and $m_3 = 25.6$ kg. Each internal rotor is modeled as a pair of rigidly coupled thin disks each of mass $m_{disk} = 0.25$ kg and radius $r = 0.0254$ m (1 inch) spinning about a given principal axis. Each disk is located a distance $d = .0381$ m (1.5 inches) along the principal axis from the vehicle CB in either direction. (See Figure 3.3 in Section 3.1.2.)

First, consider the results of Section 4.1. Assume that the vehicle mass is uniformly distributed (except for the internal rotors) so that the CG and CB coincide ($\mathbf{r} = \mathbf{0}$). It is desired to stabilize the vehicle in steady translation ($\boldsymbol{\Omega}_e = \mathbf{0}$ rad/s) along its long axis with

the equilibrium velocity $\mathbf{v}_e = 0.1 \mathbf{e}_1$ m/s.

As shown in Section 4.1, the desired equilibrium may be stabilized by the feedback control law

$$\mathbf{u} = \mathbf{K}(\boldsymbol{\Pi} \times \boldsymbol{\Omega} + \mathbf{P} \times \mathbf{v}) + (\mathcal{I} - \mathbf{K})\mathbf{u}_d \quad (4.107)$$

with \mathbf{u}_d given by equation (4.17):

$$\mathbf{u}_d = \mathbf{K}_d \left(-\mathbf{I}_K^{-1}(\boldsymbol{\Pi} - \boldsymbol{\zeta}) + \begin{pmatrix} 0 \\ \rho_4 \zeta_2 \\ \rho_5 \zeta_3 \end{pmatrix} \right).$$

The control gain matrix $\mathbf{K} = \text{diag}(4.3, 8.5, 10)$ so that $\mathbf{I}_K = \text{diag}(-0.0176, -0.0171, -0.0169)$ kg-m². The dissipative control gain matrix is $\mathbf{K}_d = \text{diag}(0.1, 0.1, 0.05)$. We also choose $\rho_4 = -2$ and $\rho_5 = -5$. One may verify that these choices satisfy the requirements derived in the preceding analysis.

Figure 4.4 on page 144 shows the closed-loop response to an initial perturbation from the desired equilibrium:

$$\begin{aligned} \boldsymbol{\Omega}(0) &= (0.01, 0.01, 0.01)^T \text{ rad/s,} \\ \mathbf{v}(0) &= (0.09, 0.02, 0.02)^T \text{ m/s and,} \\ \boldsymbol{\Omega}_r(0) &= (1, 1, 1)^T \text{ rad/s.} \end{aligned} \quad (4.108)$$

For the given initial velocities, $H_\Phi = -0.0053$ J initially. Since $\omega = \{(\boldsymbol{\Pi}, \mathbf{P}, \boldsymbol{\zeta}) \in \mathcal{D} \mid H_\Phi \geq (1 - \epsilon)c_\Phi\}$ where $c_\Phi = -(\frac{1}{m_1} - \frac{1}{m_2})C_1 = -0.0090$ J and $0 < \epsilon \ll 1$, the initial state is in the compact, positively invariant set $\omega_{\Phi_+} = \{(\boldsymbol{\Pi}, \mathbf{P}, \boldsymbol{\zeta}) \in \omega \mid P_1 > 0\}$ for ϵ small enough.

Figure 4.4 shows \mathbf{v} approaching the desired velocity. Because $P_1(0) > 0$, v_1 approaches

$+\sqrt{2C_1}/m_1 = 0.1$ m/s. Recall that the system asymptotically approaches an equilibrium corresponding to pure long-axis translation but that the final magnitude of v_1 depends on the (constant) value of C_1 . In this simulation, the final value of v_1 is as desired only because C_1 is the appropriate value for that equilibrium speed. On the other hand, $C_2 = \mathbf{\Pi} \cdot \mathbf{P}$ is not zero, so there will always be some nonzero angular momentum in the direction of the translational momentum \mathbf{P} . As can be seen in Figure 4.4, all components of the body and rotor angular velocity approach zero except for Ω_{r_1} which takes the appropriate magnitude dictated by the value of C_2 .

Simulations suggest that the region of attraction estimate ω_{ϕ_+} is conservative. Generically, trajectories beginning outside ω converge either to the equilibrium contained in ω_{ϕ_+} or the equilibrium contained in ω_{ϕ_-} .

Drag is modeled according to the example model (3.18) in Section 3.1.3. The drag coefficients are $a_i = 10^{-6}$ Ns, $\bar{a}_i = 1$ Ns², $b_i = 10^{-6}$ Ns/m, and $\bar{b}_i = 1$ Ns²/m for $i = 1, 2$, and 3. These values are somewhat arbitrary, although they yield moments and forces that are of the appropriate order for a vehicle of the given size moving at 0.1 m/s. Additionally, these coefficients reflect the expectation that the dominant effect of drag is quadratic in velocity at moderate vehicle speeds.

Choosing the control law (4.107), with \mathbf{u}_d given by (4.36), stabilizes steady translation for the vehicle subject to drag. Figure 4.5 on page 145 shows the closed-loop response to the initial condition (4.108) under the given control parameter choices. The velocities \mathbf{v} and $\mathbf{\Omega}$ approach the desired values while each rotor's angular velocity approaches a nonzero constant. This last observation is in contrast to the results shown in Figure 4.4 where the 2 and 3-axis rotor velocities returned to zero (and the 1-axis rotor velocity approached a constant dictated by the initial angular momentum). With drag present, the rotor velocities

do not approach zero. Furthermore, the magnitude of the excursion in rotor velocity is larger in the case where drag is present. (This is especially evident in the plot of Ω_{r_2} .) One way to reduce the rotor velocities would be to increase the rotor inertia. Perhaps more important than observations about rotor velocity is the observation that the control torques are all quite small. Figure 4.5 also shows the value of the semidefinite function V given in (4.35). As expected, V converges monotonically to its maximum value. A key observation is that drag does not destabilize the desired equilibrium. In fact, the body velocity (Ω, \mathbf{v}) would converge as desired even if $\mathbf{K}_d = \mathbf{0}$.

Turning now to the results of Section 4.2, the vehicle model is modified by setting $\mathbf{r} = \gamma \mathbf{e}_3$ where $\gamma > 0$. That is, the vehicle CG is a distance γ below the CB. The drag-free case is considered first. The “bottom-heaviness” parameter $\gamma = 0.002$ m. The feedback control law is given by (4.71)

$$\mathbf{u} = k \left((\mathbf{\Pi} \times \boldsymbol{\Omega} + \mathbf{P} \times \mathbf{v}) - m \hat{\mathbf{r}} \mathbf{M}^{-1} (\mathbf{P} \times \boldsymbol{\Omega}) \right) + (1 - k) (\boldsymbol{\zeta} \times \boldsymbol{\Omega} - \bar{\mathbf{u}})$$

where $\bar{\mathbf{u}} = \mathbf{K}_d \boldsymbol{\Omega}$. The control gains are $k = 1.5$ and $\mathbf{K}_d = \text{diag}(0.12, 0.11, 0.10)$. The initial conditions are the same as above with the additional condition $\boldsymbol{\Gamma}(0) = (-0.19, -0.60, 0.78)^T$ which corresponds to an initial “pitch angle” of roughly 11° and an initial “roll angle” of -37° . The initial value of $\boldsymbol{\Gamma}$ was chosen to be consistent with the assumption that $C_3 = \mathbf{P} \cdot \boldsymbol{\Gamma} = 0$.

Figures 4.6 and 4.7 show the simulation results. Note that the initial condition is outside the set $\omega_{\psi+}$; the boundary of this region is denoted by the line $H_\psi = c_\psi$. The value c_ψ is the energy H_ψ for pure 2-mode translation (at the same values of C_1, C_2 , and C_3). The region of attraction estimate is clearly conservative.

Figures 4.8 and 4.9 show the results of a simulation which includes the viscous force model. Once again, the control law used is (4.71). However, $\bar{\mathbf{u}}$ is chosen according to (4.99),

$$\bar{\mathbf{u}} = K_d \boldsymbol{\Omega} + \varsigma \operatorname{sign}(\boldsymbol{\Omega} \cdot \boldsymbol{\varphi}) \boldsymbol{\varphi}$$

where $\varsigma = 2$ and $\boldsymbol{\varphi}$ is given by (4.97). In the presence of drag and thrust, 2-mode translational equilibria disappear, although the inverted 1-mode equilibrium remains, limiting the obtainable region of attraction. The value of the Lyapunov function at this equilibrium is denoted by the line $H_\psi = c_\psi$.

The response shown in Figure 4.8 is more damped than that in Figure 4.6, which is understandable given the presence of physical damping in the latter case. Otherwise, the two simulations are quite similar. This similarity is due in part to the identical choice of initial conditions. If C_3 were different from zero, there would be a marked difference in the two closed-loop responses. Since C_3 is conserved for the system without external damping, the system state would not converge to pure long-axis translation. The angular velocity would approach zero, but the system would approach a “controlled equilibrium” corresponding to non-principal axis translation. The equilibrium would be a controlled equilibrium in the sense that a constant, nonzero control torque would be required to sustain the motion with the result that at least one rotor would continually accelerate.

When viscous forces are included in the model, they destroy conservation of C_3 so that it is no longer necessary to restrict attention to motions for which $C_3 = 0$ (Theorem 4.2.4). Steady long-axis translation in the horizontal plane for the closed-loop system subject to viscous dissipation is indeed locally exponentially stable. For this reason, the assumption that $C_3 = 0$ in our treatment of the conservative system model was not overly restric-

tive. Locally, physical damping drives the closed-loop system to a state for which $C_3 = 0$ regardless of the initial condition.

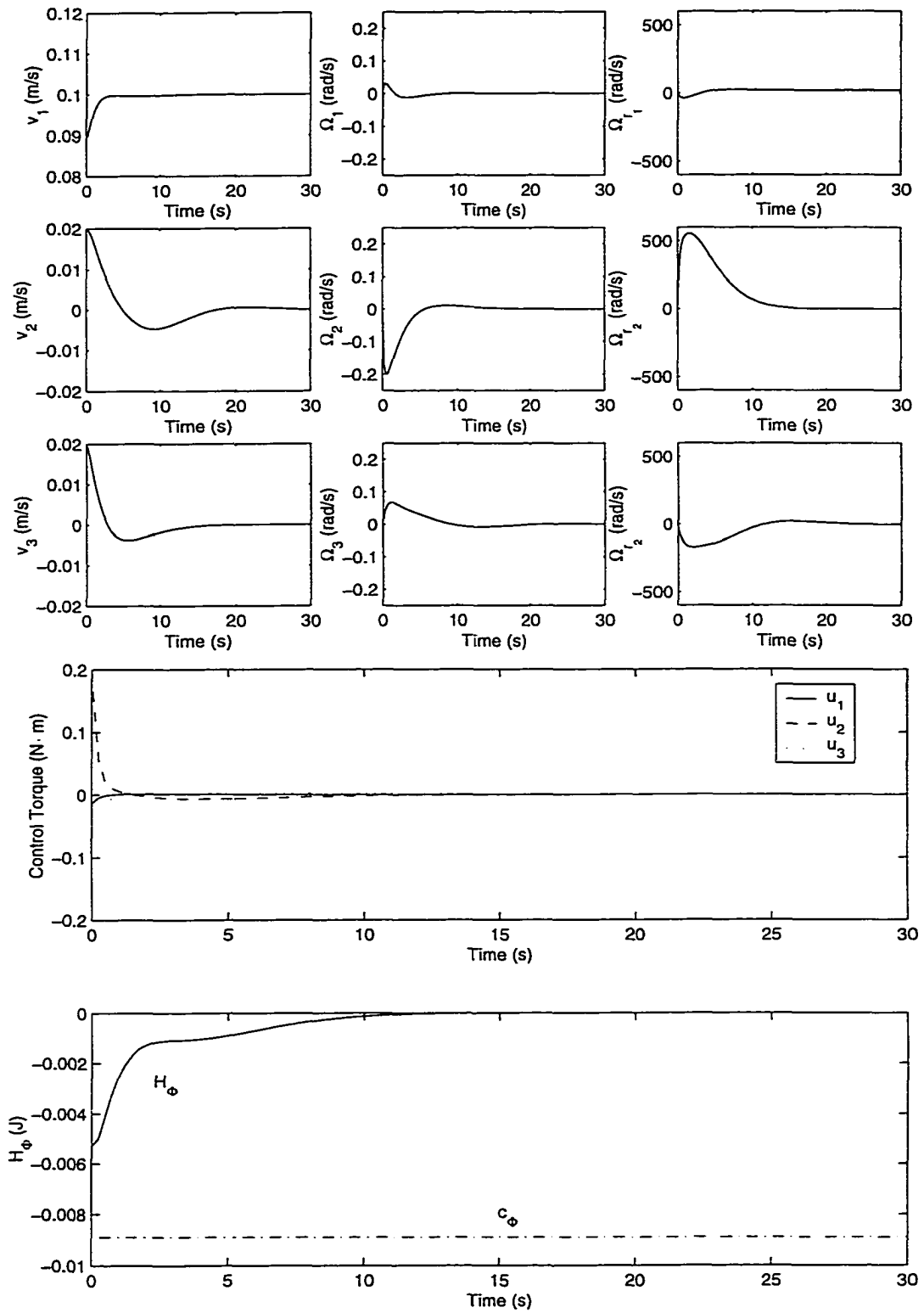


Figure 4.4: Closed-loop response to a perturbation: $r = 0$, no drag.

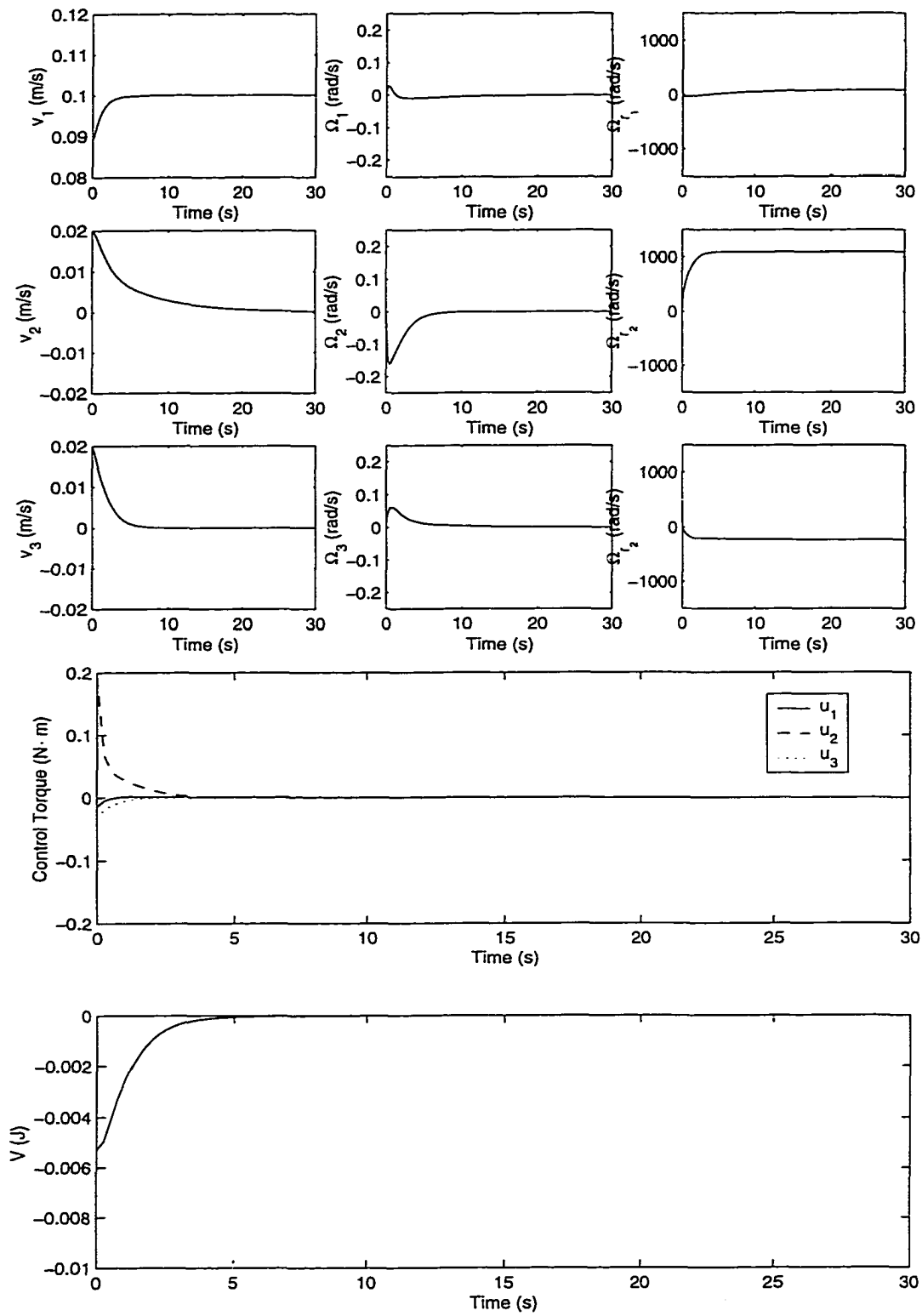


Figure 4.5: Closed-loop response to a perturbation: $r = 0$, drag included.

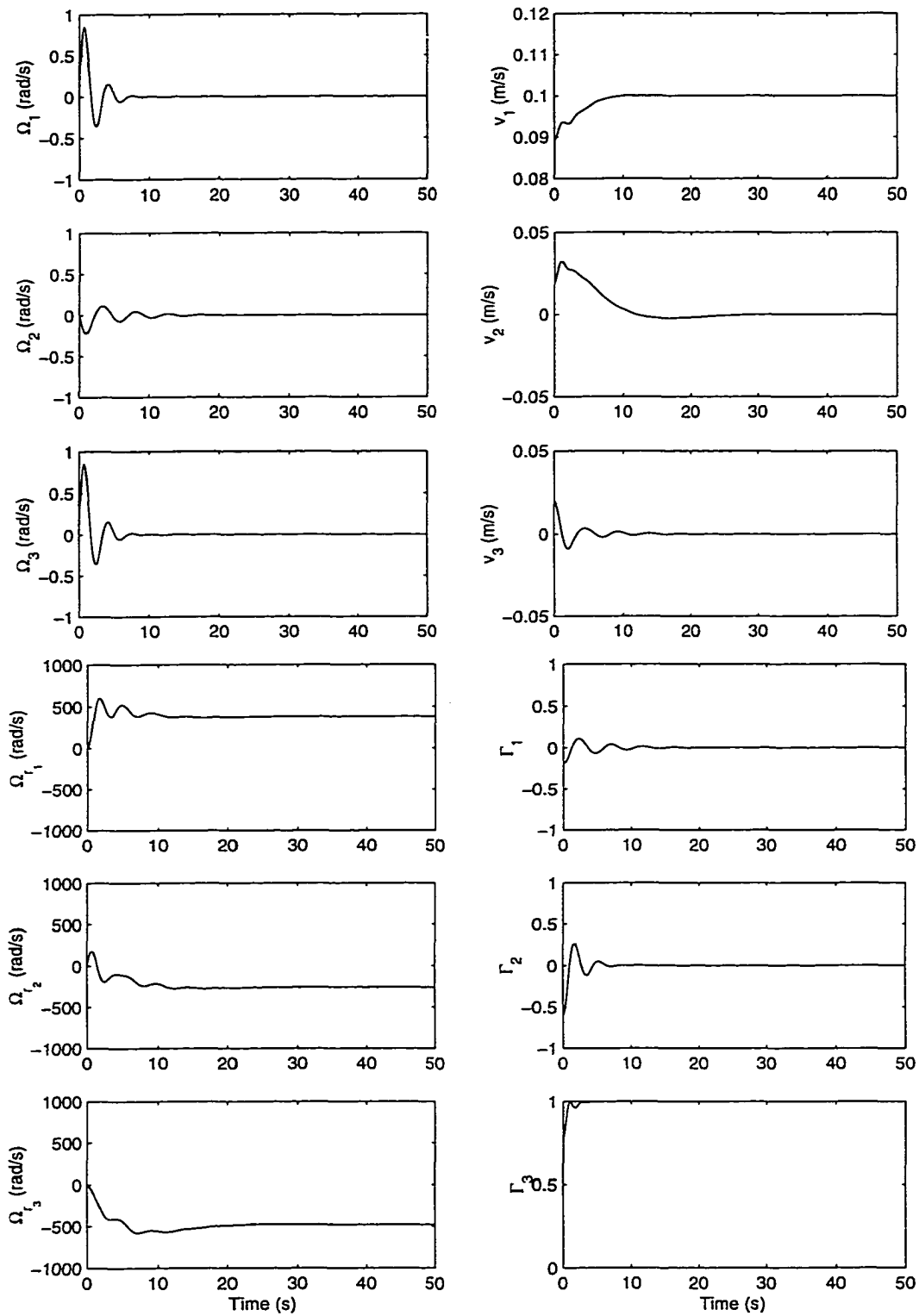


Figure 4.6: Closed-loop state response to a perturbation: $r \neq \mathbf{0}$, no drag.

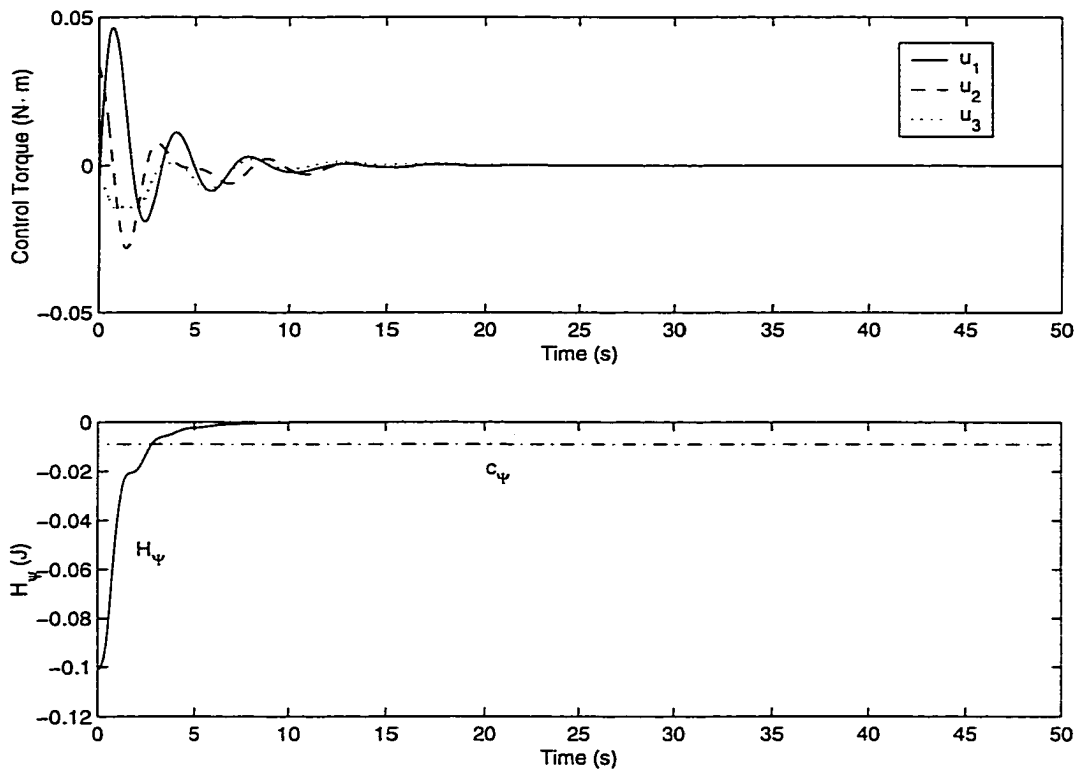


Figure 4.7: Control torques and energy: $\tau \neq 0$, no drag.

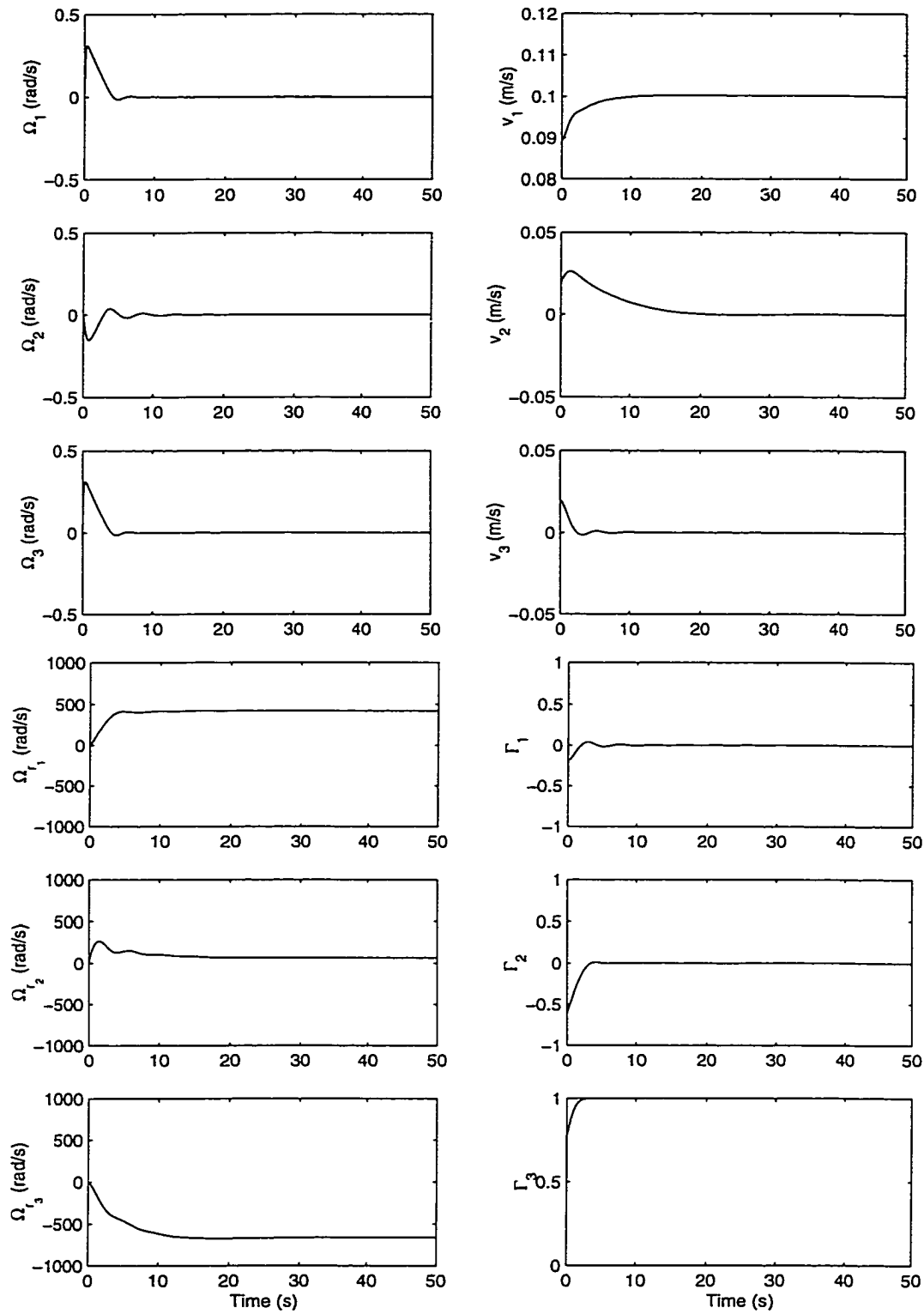


Figure 4.8: Closed-loop response to a perturbation: $r \neq 0$, drag included.

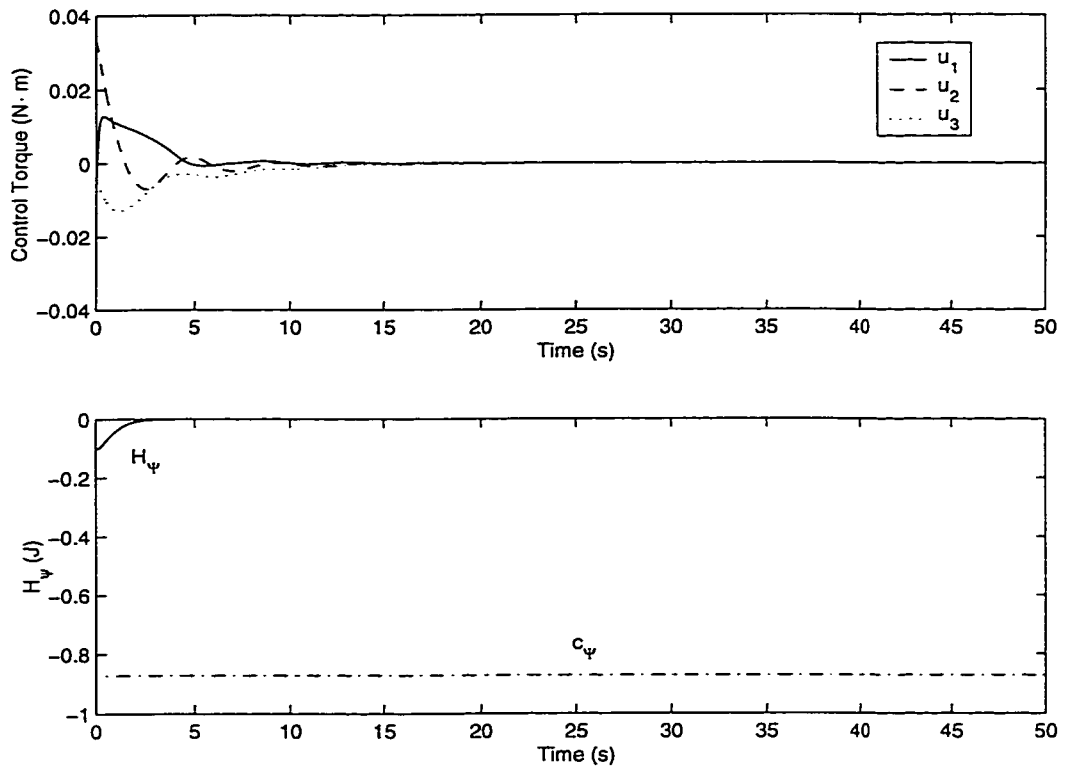


Figure 4.9: Control torques and energy: $r \neq 0$, drag included.

Chapter 5

Controlled Lagrangians and Dissipation

Chapter 4 concerned feedback stabilization of an underwater vehicle with internal rotors by kinetic energy shaping. The control law introduced for a vehicle modeled by Kirchhoff's equations was based on an idea proposed by Bloch *et al* [13] for a spacecraft with an internal rotor. Their idea of modifying the kinetic energy metric through feedback was generalized in [17] and the resulting technique was dubbed the method of controlled Lagrangians. The technique is an algorithmic approach to stabilization by kinetic energy shaping.

While Kirchhoff's model of an underwater vehicle is a very useful starting point for control design, practical application demands that one consider the effect of viscous damping on the resulting closed-loop system. Concern over the effect of dissipation on the feedback-stabilized underwater vehicle in Chapter 4 led to an investigation of the effect of damping on more general controlled Lagrangian systems. In this chapter, we analyze the effect of physical damping on controlled Lagrangian systems. We give conditions under which appropriate feedback dissipation can asymptotically stabilize an equilibrium which is stable for the conservative, closed-loop model.

In Section 5.1, we review the key ideas of the method of controlled Lagrangians and

introduce some new terminology which is useful for understanding the effect of external forces other than the control (i.e., physical and feedback dissipation forces). In Section 5.2, we consider the effect of damping on a class of controlled Lagrangian systems which includes “balance” problems such as the inverted pendulum on a cart. We also present numerical and experimental results. In Section 5.3, we consider the effect of damping on Euler-Poincaré systems.

5.1 Review of the Method of Controlled Lagrangians

The method of controlled Lagrangians is a technique for stabilizing a class of underactuated Lagrangian mechanical systems with symmetry [10, 11, 14, 15, 16, 17, 18]. The method provides a feedback control law which preserves the Lagrangian structure but which shapes the kinetic energy of the closed-loop system. Because the closed-loop system is constructed so that it has Lagrangian dynamics, any of a variety of stability analysis techniques can then be used to find conditions on control gains for closed-loop stability. Energy methods are particularly attractive for this purpose since they can provide Lyapunov functions which are useful for estimating regions of attraction and for studying robustness.

This section reviews the method of controlled Lagrangians as developed by Bloch, Leonard, and Marsden. Where relevant, we make observations or introduce expressions which simplify the analysis of physical and feedback dissipation.

5.1.1 The Modified Lagrangian

Suppose that a Lagrangian mechanical system is defined on an $(n + r)$ -dimensional configuration space Q and that the uncontrolled system dynamics are invariant under the action of an n -dimensional Abelian Lie group G . More specifically, we assume that G acts freely

and properly on Q and that the Lagrangian is invariant under this action. Locally, the system state can be described by an element in G and an element in the complementary space Q/G , referred to as the *shape space*. (It is perhaps helpful to consider the case of a trivial fiber bundle $Q = S \times G$, although the setting is more general.) If the control forces enter in the symmetry (G) direction, the method of controlled Lagrangians provides a choice of control such that the closed-loop system derives from a new Lagrangian (called the controlled Lagrangian) whose kinetic energy metric is a parameterization of the original metric. Choosing the parameters effectively shapes the kinetic energy. (See [10] for a discussion of potential energy shaping in this context.)

To understand the nature of the controlled Lagrangian, it is helpful to first recall some facts about velocity and kinetic energy. At any point $q \in Q$, one may decompose a tangent vector $v_q \in T_q Q$ into a component which is tangent to $\text{Orb}(q)$, the G -orbit through the point q , and a component which is the metric orthogonal to this first component. The space $T_q \text{Orb}(q)$ is referred to as the vertical space at q , Ver_q , and its metric orthogonal complement is the horizontal space at q , Hor_q . The projections of a tangent vector v_q onto Ver_q and Hor_q are denoted $\text{Ver } v_q$ and $\text{Hor } v_q$, respectively. The decomposition is uniquely defined in terms of the kinetic energy metric $g(\cdot, \cdot)$ by requiring that

$$g(v_q, w_q) = g(\text{Hor } v_q, \text{Hor } w_q) + g(\text{Ver } v_q, \text{Ver } w_q). \quad (5.1)$$

for every $v_q, w_q \in T_q Q$. The decomposition may be thought of as a splitting of the velocity vector into a component in the group direction and a component in the shape direction.

Define local coordinates θ^a for G ($a = 1, \dots, n$) and x^α for Q/G ($\alpha = 1, \dots, r$) so that

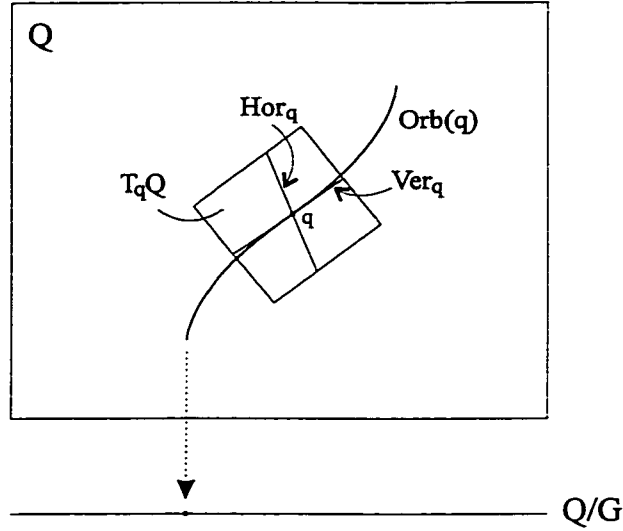


Figure 5.1: Decomposition of $T_q Q$ into horizontal and vertical subspaces.

$v = (\dot{x}^\alpha, \dot{\theta}^a)$ is the local expression for velocity. The kinetic energy is given locally by

$$T = \frac{1}{2}g_{\alpha\beta}\dot{x}^\alpha\dot{x}^\beta + g_{\alpha b}\dot{x}^\alpha\dot{\theta}^b + \frac{1}{2}g_{ab}\dot{\theta}^a\dot{\theta}^b$$

where $g_{\alpha\beta}$, $g_{\alpha b}$, and g_{ab} are the local components of the kinetic energy metric $g(\cdot, \cdot)$. According to the requirement (5.1), the velocity v decomposes as follows,

$$\text{Ver } v = (0, \dot{\theta}^a + g^{ab}g_{\alpha b}\dot{x}^\alpha) \quad (5.2)$$

$$\text{Hor } v = (\dot{x}^\alpha, -g^{ab}g_{\alpha b}\dot{x}^\alpha) \quad (5.3)$$

where, according to convention, g^{ab} represents the inverse of g_{ab} . Note that $\text{Ver } v = (0, \dot{\theta}^a)$ and $\text{Hor } v = (\dot{x}^\alpha, 0)$ if and only if there is no kinetic energy coupling between G and Q/G .

The decomposition can be thought of as block diagonalization or “completing the square,”

$$\begin{aligned} & \frac{1}{2}g_{\alpha\beta}\dot{x}^\alpha\dot{x}^\beta + g_{\alpha b}\dot{x}^\alpha\dot{\theta}^b + \frac{1}{2}g_{ab}\dot{\theta}^a\dot{\theta}^b \\ &= \frac{1}{2}g_{\alpha\beta}\dot{x}^\alpha\dot{x}^\beta - \frac{1}{2}g_{ab}(g^{ac}g_{c\alpha}\dot{x}^\alpha)(g^{bd}g_{d\beta}\dot{x}^\beta) \end{aligned}$$

$$\begin{aligned}
& +g_{ab} \left(\frac{1}{2} \dot{\theta}^a \dot{\theta}^b + g^{ac} g_{c\alpha} \dot{x}^\alpha \dot{\theta}^a + \frac{1}{2} (g^{ac} g_{c\alpha} \dot{x}^\alpha) (g^{bd} g_{d\beta} \dot{x}^\beta) \right) \\
= & \frac{1}{2} (g_{\alpha\beta} - g_{\alpha a} g^{ab} g_{b\beta}) \dot{x}^\alpha \dot{x}^\beta + \frac{1}{2} g_{ab} (\dot{\theta}^a + g^{ac} g_{c\alpha} \dot{x}^\alpha) (\dot{\theta}^b + g^{bd} g_{d\beta} \dot{x}^\beta). \quad (5.4)
\end{aligned}$$

Equation (5.4) is simply the coordinate expression of equation (5.1).

The decomposition of the tangent space can also be understood in the context of the *mechanical connection* [49]. The mechanical connection α is a Lie-algebra valued, horizontal one-form, i.e., a map from TQ to \mathfrak{g} which annihilates the vertical component of velocity,

$$\alpha(\mathbf{v}_q) = \alpha(\text{Hor } \mathbf{v}_q) \in \mathfrak{g}.$$

In local coordinates, the infinitesimal generator $[\alpha(\mathbf{v}_q)]_Q$ corresponds to $(0, g^{ab} g_{ab} \dot{x}^\alpha)$. This term appears as a velocity “shift” in the expressions (5.2) and (5.3).

The first step in defining the controlled Lagrangian involves shifting the horizontal space. Specifically, one defines a new connection by appending a Lie-algebra valued, horizontal one-form τ to the mechanical connection α giving a new horizontal space Hor_τ . Thus, one obtains a new decomposition

$$\begin{aligned}
\mathbf{v}_q & = \text{Hor}_\tau \mathbf{v}_q + \text{Ver}_\tau \mathbf{v}_q \\
& = (\text{Hor } \mathbf{v}_q - \tau(\mathbf{v}_q)) + (\text{Ver } \mathbf{v}_q + \tau(\mathbf{v}_q)).
\end{aligned}$$

Figure 5.2 depicts the role of α in the original decomposition and the analogous role of τ in defining the new decomposition.

The controlled Lagrangian is defined as

$$L_{\tau,\sigma,\rho}(\mathbf{v}) = \frac{1}{2} (g_\sigma(\text{Hor}_\tau \mathbf{v}_q, \text{Hor}_\tau \mathbf{v}_q) + g_\rho(\text{Ver}_\tau \mathbf{v}_q, \text{Ver}_\tau \mathbf{v}_q)) - V(q) \quad (5.5)$$

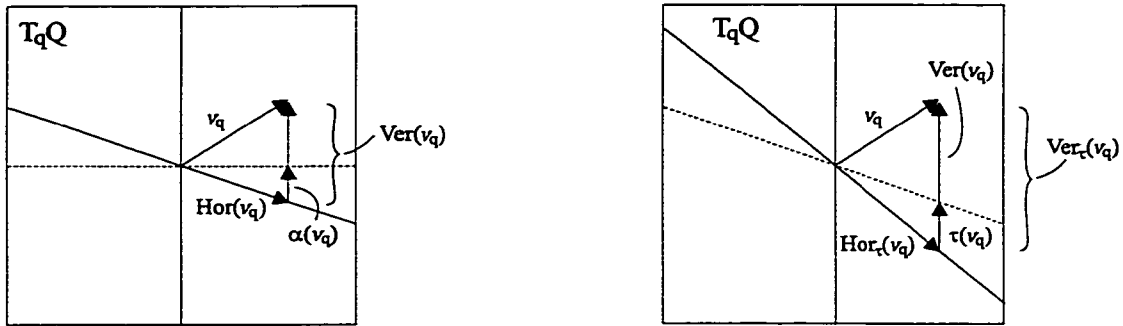


Figure 5.2: Original and modified horizontal and vertical decompositions.

where g_σ and g_ρ are parameterized modifications of the kinetic energy metric on horizontal and vertical vectors, respectively, and $V(q)$ is the potential energy. Under certain conditions on the parameters τ , σ , and ρ , the closed-loop equations are simply Lagrange's equations for $L_{\tau,\sigma,\rho}$. The conditions are referred to as “matching” conditions. They ensure that no additional inputs are necessary in uncontrolled directions in order to effect the closed-loop dynamics. These conditions typically leave freedom in some of the parameters τ , σ , and ρ , which then play the role of control gains.

Two assumptions are made in order to give the controlled Lagrangian a useful and manageable structure. First, it is assumed that $g_\sigma = g$ on the original horizontal space,

$$g_\sigma(\text{Hor } v_q, \text{Hor } w_q) = g(\text{Hor } v_q, \text{Hor } w_q).$$

Second, g_σ is chosen such that the original horizontal and vertical spaces are orthogonal,

$$g_\sigma(v_q, w_q) = g_\sigma(\text{Hor } v_q, \text{Hor } w_q) + g_\sigma(\text{Ver } v_q, \text{Ver } w_q).$$

Under these conditions, as shown in [17], the controlled Lagrangian (5.5) becomes

$$L_{\tau,\sigma,\rho}(v) = L(v + [\tau(v)]_Q) + \frac{1}{2}g_\sigma([\tau(v)]_Q, [\tau(v)]_Q) + \frac{1}{2}\varpi(\text{Ver}_\tau(v), \text{Ver}_\tau(v)) \quad (5.6)$$

where $\varpi = (g_\rho - g)$. In Section 5.1.2, we review the general criteria for matching and stabilization as discussed in [16, 17, 18].

A subclass of systems which are eligible for the method of controlled Lagrangians can be treated under the simplifying assumption that $\rho^{ab} + \sigma^{ab} = g^{ab}$ where ρ_{ab} and σ_{ab} are local components of g_ρ and g_σ , respectively. This assumption is appropriate, for example, for the rotary inverted pendulum and for a class of Euler-Poincaré systems [16, 18]. For another subclass, one may choose $g_\rho = g$ and the last term of (5.6) vanishes. This latter special case is treated by the First Matching Theorem of [17]. Matching and stabilization for both of these cases are reviewed in Section 5.1.3.

5.1.2 The General Matching Conditions

Assume that the Euler-Lagrange equations hold for a mechanical system with Lagrangian

$$L(x^\alpha, \dot{x}^\alpha, \dot{\theta}^a) = \frac{1}{2}g_{\alpha\beta}\dot{x}^\alpha\dot{x}^\beta + g_{\alpha b}\dot{x}^\alpha\dot{\theta}^b + \frac{1}{2}g_{ab}\dot{\theta}^a\dot{\theta}^b - V(x^\alpha). \quad (5.7)$$

with g independent of θ^a . A control effort u_a enters in this symmetry direction so that the equations of motion are

$$\begin{aligned} \frac{d}{dt} \frac{\partial L}{\partial \dot{x}^\alpha} - \frac{\partial L}{\partial x^\alpha} &= 0 \\ \frac{d}{dt} \frac{\partial L}{\partial \dot{\theta}^a} &= u_a. \end{aligned} \quad (5.8)$$

The method of controlled Lagrangians provides a technique for stabilizing an equilibrium

$$(x^\alpha, \dot{x}^\alpha, \dot{\theta}^a)_e = (x_e^\alpha, 0, c) \quad (5.9)$$

for the uncontrolled system (5.8), where c is a constant. We will be particularly interested in the case where $c = 0$. For balance systems such as inverted pendula, one typically finds that x_c^α is a local maximum of the potential $V(x^\alpha)$. Because the control does not enter in the x^α direction, it is not possible to shape the potential energy in such a way that the equilibrium becomes a potential minimum. The approach then is to shape the kinetic energy in such a way that the equilibrium becomes a kinetic maximum. There naturally arises a concern over the effect of physical damping in such a scheme and this question is the focus of Section 5.2.

Under certain conditions, the method of controlled Lagrangians provides a control law u_a and a modified Lagrangian $L_{\tau,\sigma,\rho}(x^\alpha, \dot{x}^\alpha, \dot{\theta}^a)$ for which the closed-loop equations become

$$\begin{aligned} \frac{d}{dt} \frac{\partial L_{\tau,\sigma,\rho}}{\partial \dot{x}^\alpha} - \frac{\partial L_{\tau,\sigma,\rho}}{\partial x^\alpha} &= 0 \\ \frac{d}{dt} \frac{\partial L_{\tau,\sigma,\rho}}{\partial \dot{\theta}^a} &= 0. \end{aligned} \quad (5.10)$$

The conditions under which this is possible ensure that the open-loop system matches the closed-loop system in the sense that no unavailable control authority is required to effect equations (5.10).

In coordinates, equation (5.6) for the controlled Lagrangian becomes

$$\begin{aligned} L_{\tau,\sigma,\rho}(x^\alpha, \dot{x}^\alpha, \dot{\theta}^a) &= L(x^\alpha, \dot{x}^\alpha, \dot{\theta}^a + \tau_\alpha^a \dot{x}^\alpha) + \frac{1}{2} \sigma_{ab} \tau_\alpha^a \tau_\beta^b \dot{x}^\alpha \dot{x}^\beta \\ &\quad + \frac{1}{2} \varpi_{ab} \left(\dot{\theta}^a + (g^{ac} g_{c\alpha} + \tau_\alpha^a) \dot{x}^\alpha \right) \left(\dot{\theta}^b + (g^{bd} g_{d\beta} + \tau_\beta^b) \dot{x}^\beta \right) \\ &= \frac{1}{2} (g_{\tau,\sigma,\rho})_{\alpha\beta} \dot{x}^\alpha \dot{x}^\beta + (g_{\tau,\sigma,\rho})_{\alpha b} \dot{x}^\alpha \dot{\theta}^b + \frac{1}{2} (g_{\tau,\sigma,\rho})_{ab} \dot{\theta}^a \dot{\theta}^b - V(x^\alpha). \end{aligned} \quad (5.11)$$

where $\varpi_{ab} = \rho_{ab} - g_{ab}$. The tensors σ_{ab} and ρ_{ab} and the one-form τ_α^a provide freedom in

modifying the Lagrangian. Some freedom is removed by requiring that the closed-loop equations be consistent with the open-loop control authority. After the “matching conditions” are satisfied, the modified Lagrangian can be used to derive closed-loop stability criteria. Any remaining freedom in the parameters can then be used to satisfy these criteria.

Equation (5.11) defines the coordinate form of the modified kinetic energy metric $g_{\tau,\sigma,\rho}$. To simplify notation, define the matrix forms of g and $g_{\tau,\sigma,\rho}$,

$$\mathbb{M} = \begin{pmatrix} [g_{\alpha\beta}] & [g_{\alpha b}] \\ [g_{a\beta}] & [g_{ab}] \end{pmatrix} \quad \text{and} \quad \mathbb{M}_{\tau,\sigma,\rho} = \begin{pmatrix} [(g_{\tau,\sigma,\rho})_{\alpha\beta}] & [(g_{\tau,\sigma,\rho})_{\alpha b}] \\ [(g_{\tau,\sigma,\rho})_{a\beta}] & [(g_{\tau,\sigma,\rho})_{ab}] \end{pmatrix}.$$

The matching conditions are derived by comparing equations (5.8) and (5.10) and choosing u_a, τ, g_σ , and g_ρ so that (5.8) and (5.10) are identical. Since the control u_a appears in the open-loop equations (5.8), this process not only gives conditions under which the equations match but also gives the feedback control law. For notational convenience, we define an “Euler-Lagrange operator” \mathcal{E} : for a state variable y^A and a Lagrangian L , let

$$\mathcal{E}_{y^A}(L) = \frac{d}{dt} \frac{\partial L}{\partial \dot{y}^A} - \frac{\partial L}{\partial y^A}.$$

The open-loop equations, written explicitly in coordinates, are

$$\begin{pmatrix} [\mathcal{E}_{x^\alpha}(L)] \\ [\mathcal{E}_{\theta^a}(L)] \end{pmatrix} = \frac{d}{dt}(\mathbb{M}) \begin{pmatrix} [\dot{x}^\beta] \\ [\dot{\theta}^b] \end{pmatrix} + \mathbb{M} \begin{pmatrix} [\ddot{x}^\beta] \\ [\ddot{\theta}^b] \end{pmatrix} - \begin{pmatrix} \left[\frac{\partial}{\partial x^\alpha} \left(\frac{1}{2} g_{\gamma\beta} \dot{x}^\gamma \dot{x}^\beta + g_{\gamma b} \dot{x}^\gamma \dot{\theta}^b + \frac{1}{2} g_{cb} \dot{\theta}^c \dot{\theta}^b - V(x^\gamma) \right) \right] \\ \mathbf{0} \end{pmatrix} = \begin{pmatrix} \mathbf{0} \\ [u_a] \end{pmatrix}. \quad (5.12)$$

Solving for acceleration and substituting into the desired closed-loop equations (5.10) gives

$$\begin{aligned}
& \begin{pmatrix} [\mathcal{E}_{x^\alpha}(L_{\tau,\sigma,\rho})] \\ [\mathcal{E}_{\theta^a}(L_{\tau,\sigma,\rho})] \end{pmatrix} = \frac{d}{dt}(\mathbb{M}_{\tau,\sigma,\rho}) \begin{pmatrix} [\dot{x}^\beta] \\ [\dot{\theta}^b] \end{pmatrix} + \mathbb{M}_{\tau,\sigma,\rho} \mathbb{M}^{-1} \cdot \\
& \left\{ -\frac{d}{dt}(\mathbb{M}) \begin{pmatrix} [\dot{x}^\beta] \\ [\dot{\theta}^b] \end{pmatrix} + \begin{pmatrix} \left[\frac{\partial}{\partial x^\alpha} \left(\frac{1}{2}g_{\gamma\beta}\dot{x}^\gamma\dot{x}^\beta + g_{\gamma b}\dot{x}^\gamma\dot{\theta}^b + \frac{1}{2}g_{cb}\dot{\theta}^c\dot{\theta}^b - V(x^\gamma) \right) \right] \\ [u_a] \end{pmatrix} \right\} \\
& - \begin{pmatrix} \left[\frac{\partial}{\partial x^\alpha} \left(\frac{1}{2}(g_{\tau,\sigma,\rho})_{\gamma\beta}\dot{x}^\gamma\dot{x}^\beta + (g_{\tau,\sigma,\rho})_{\gamma b}\dot{x}^\gamma\dot{\theta}^b + \frac{1}{2}(g_{\tau,\sigma,\rho})_{cb}\dot{\theta}^c\dot{\theta}^b - V(x^\gamma) \right) \right] \\ \mathbf{0} \end{pmatrix}. \quad (5.13)
\end{aligned}$$

As stated in [16], four conditions which, for the appropriate choice of control law, make the right-hand side of (5.13) zero are

Assumption GM-1. $\tau_\alpha^b = -\sigma^{ab}g_{b\alpha}$.

Assumption GM-2. $\sigma^{bd}(\sigma_{ad,\alpha} + g_{ad,\alpha}) = 2g^{bd}g_{ad,\alpha}$.

Assumption GM-3. $\varpi_{ab,\alpha} = 0$.

Assumption GM-4. Letting $\zeta_\alpha^a = g^{ac}g_{c\alpha}$,

$$\tau_{\alpha,\delta}^b - \tau_{\delta,\alpha}^b + \rho^{ba}\varpi_{ac}(\zeta_{\alpha,\delta}^c - \zeta_{\delta,\alpha}^c) - \rho^{ba}g_{ac,\delta}\rho^{cd}\varpi_{da}\zeta_\alpha^a - \rho^{ba}g_{ac,\alpha}\tau_\delta^a = 0.$$

According to convention, commas in subscripts denote partial derivatives. Conditions GM-1 through GM-4 are referred to as the “general matching conditions” to distinguish them from a set of simplified conditions which will be introduced shortly. Using condition GM-1, the coordinate form of the modified kinetic energy metric becomes

$$\begin{aligned}
(g_{\tau,\sigma,\rho})_{\alpha\beta} &= g_{\alpha\beta} + g_{\alpha c}\sigma^{cd}(g_{de} - \sigma_{de})\sigma^{ef}g_{f\beta} + g_{\alpha c}(g^{cd} - \sigma^{cd})(\rho_{de} - g_{de})(g^{ef} - \sigma^{ef})g_{f\beta} \\
(g_{\tau,\sigma,\rho})_{\alpha b} &= g_{\alpha c}(g^{cd} - \sigma^{cd})\rho_{db} \quad (5.14)
\end{aligned}$$

$$(g_{\tau,\sigma,\rho})_{ab} = \rho_{ab}.$$

Using the fact that the closed-loop momentum conjugate to θ^a is conserved by construction, and referring to (5.11), one may compute the control law as follows,

$$\begin{aligned} u_a &= \frac{d}{dt} \frac{\partial L}{\partial \dot{\theta}^a} \\ &= \frac{d}{dt} \left\{ \frac{\partial L_{\tau,\sigma,\rho}}{\partial \dot{\theta}^a} + (g_{ab} \dot{\theta}^b + g_{a\beta} \dot{x}^\beta) - (\rho_{ab} \dot{\theta}^b + \rho_{ac} (g^{cd} - \sigma^{cd}) g_{d\beta} \dot{x}^\beta) \right\} \\ &= -\frac{d}{dt} \left\{ (\rho_{ab} - g_{ab}) \dot{\theta}^b + (\rho_{ac} (g^{cd} - \sigma^{cd}) g_{d\beta} - g_{a\beta}) \dot{x}^\beta \right\}. \end{aligned} \quad (5.15)$$

Equation (5.15) gives the control in terms of velocities and accelerations. Alternatively, setting (5.13) to zero and solving for u_a eliminates the accelerations giving the control law in terms of the coordinate velocities. It is assumed throughout that the basic control law is in this velocity form. Thus, this part of the control law will be unaffected when additional forces such as physical and feedback dissipation are included.

The principal goal of the method of controlled Lagrangians is to stabilize equilibria. Because conserved quantities are useful in studying stability of equilibria, we define the controlled conserved quantity

$$\bar{J}_a = \frac{\partial L_{\tau,\sigma,\rho}}{\partial \dot{\theta}^a} = \rho_{ab} \left(\dot{\theta}^b + (g^{bc} - \sigma^{bc}) g_{c\alpha} \dot{x}^\alpha \right). \quad (5.16)$$

The desired equilibrium (5.9) will be stable under the control law (5.15) provided the control-modified energy

$$E_{\tau,\sigma,\rho}(x^\alpha, \dot{x}^\alpha; \bar{J}_a) = \frac{1}{2} A_{\alpha\beta} \dot{x}^\alpha \dot{x}^\beta + \frac{1}{2} \rho^{ab} \bar{J}_a \bar{J}_b + V(x^\alpha) \quad (5.17)$$

is definite as a function of x^α and \dot{x}^α . Since x_e^α is typically a local maximum of the amended potential

$$V_\mu(x^\alpha; \tilde{J}_a) = \frac{1}{2}\rho^{ab}\tilde{J}_a\tilde{J}_b + V(x^\alpha),$$

one usually requires that $A_{\alpha\beta}$ be negative definite at the equilibrium (see the discussion on page 157). In this case, the equilibrium (5.9) is a local maximum of the control-modified energy $E_{\tau,\sigma,\rho}$.

The tensor $A_{\alpha\beta}$ is the coordinate form of the modified horizontal kinetic energy metric g_σ . As shown in Appendix E.1,

$$A_{\alpha\beta} = g_{\alpha\beta} - g_{\alpha a}(g^{ab} - \sigma^{ab})g_{b\beta}. \quad (5.18)$$

The energy $E_{\tau,\sigma,\rho}$ is simply the Routhian corresponding to $L_{\tau,\sigma,\rho}$. It is treated as a function of the x^α variables alone because the \tilde{J}_a dynamics are trivial in the conservative setting and can be ignored. When generalized forces representing physical and feedback dissipation are introduced, however, \tilde{J}_a will no longer be conserved and $E_{\tau,\sigma,\rho}$ will be treated as a function of \tilde{J}_a , as well.

5.1.3 Special Cases of Matching

As mentioned at the end of Section 5.1.1, there are subclasses of systems which are eligible for the method of controlled Lagrangians for which the matching conditions simplify. Two such simplifying cases are considered in this section. In both cases, the modification to g_ρ , the vertical component of the modified kinetic energy metric, is restricted. The first simplifying case is relevant to Euler-Poincaré systems and also to a benchmark nonlinear control example, the pendulum on a rotor arm. The second simplifying case is also applicable to a

number of systems of physical interest.

Case 1: $\rho^{ab} = g^{ab} - \sigma^{ab}$.

In this case, the feedback control law (5.15) simplifies to

$$u_a = \frac{d}{dt} \left((\rho_{ab} - g_{ab}) \dot{\theta}^b \right). \quad (5.19)$$

Substituting for σ_{ab} in equation (5.14), the modified energy metric defining the controlled Lagrangian (5.11) becomes

$$\mathbb{M}_{\tau, \sigma, \rho} = \begin{pmatrix} [g_{\alpha\beta}] & [g_{\alpha b}] \\ [g_{a\beta}] & [\rho_{ab}] \end{pmatrix}. \quad (5.20)$$

To verify (5.20), it is helpful to note that

$$g_{ab} - \sigma_{ab} = g_{ac}(\sigma^{cd} - g^{cd})\sigma_{db} = -g_{ac}\rho^{cd}\sigma_{db}.$$

This simplifying case applies to the particular example of a pendulum on a rotor arm, which was considered in [16]. It is also appropriate for Euler-Poincaré systems as discussed in [18]. For Euler-Poincaré systems, symmetry implies that the components of the original kinetic energy metric are constant. To preserve this symmetry in the closed-loop system, the parameter ρ_{ab} must also be chosen constant. In this case, the general matching conditions GM-1 through GM-4 reduce to the two “Euler-Poincaré matching conditions”

Assumption EP-1. $\tau_\alpha^b = -\sigma^{ab}g_{b\alpha}$.

Assumption EP-2. $\sigma^{ab} + \rho^{ab} = g^{ab}$.

Case 2: $\rho_{ab} = g_{ab}$.

This class of systems is the subject of the First Matching Theorem given in [17]. In this case, conditions GM-1 through GM-4 reduce to the following three matching conditions.

1. $\tau_\alpha^a = -\sigma^{ab}g_{b\alpha}$,
2. $\sigma^{ab}(\sigma_{bc,\alpha} + g_{bc,\alpha}) = 2g^{ab}g_{bc,\alpha}$,
3. $\tau_{\alpha,\beta}^a - \tau_{\beta,\alpha}^a - g^{ab}g_{bc,\alpha}\tau_\beta^c = 0$.

Under these conditions, the control law

$$u_a = -\frac{d}{dt} \left(g_{ab}\sigma^{bc}g_{c\alpha}\dot{x}^\alpha \right) \quad (5.21)$$

gives the desired Euler-Lagrange equations with

$$\begin{aligned} L_{\tau,\sigma}(x^\alpha, \dot{x}^\alpha, \dot{\theta}^a) &= L(x^\alpha, \dot{x}^\alpha, \dot{\theta}^a - \sigma^{ab}g_{b\alpha}\dot{x}^\alpha) + \frac{1}{2}g_{\alpha a}\sigma^{ab}g_{b\beta}\dot{x}^\alpha\dot{x}^\beta - V(x^\alpha) \\ &= \frac{1}{2}(g_{\tau,\sigma})_{\alpha\beta}\dot{x}^\alpha\dot{x}^\beta + (g_{\tau,\sigma})_{\alpha b}\dot{x}^\alpha\dot{\theta}^b + \frac{1}{2}(g_{\tau,\sigma})_{ab}\dot{\theta}^a\dot{\theta}^b - V(x^\alpha) \end{aligned} \quad (5.22)$$

where the components of the controlled kinetic energy metric are

$$\begin{aligned} (g_{\tau,\sigma})_{\alpha\beta} &= g_{\alpha\beta} + g_{\alpha a}\sigma^{ab}(g_{bc} - \sigma_{bc})\sigma^{cd}g_{\beta d} \\ (g_{\tau,\sigma})_{\alpha b} &= g_{\alpha c}(g^{cd} - \sigma^{cd})g_{db} \\ (g_{\tau,\sigma})_{ab} &= g_{ab}. \end{aligned} \quad (5.23)$$

Under certain assumptions on the parameters σ_{ab} and τ_α^a and on the original kinetic energy metric, the matching conditions simplify further. The “simplified matching conditions” are

Assumption SM-1 $\sigma_{ab} = \sigma g_{ab}$ for constant σ ,

Assumption SM-2 $g_{ab,\alpha} = 0$,

Assumption SM-3 $\tau_\alpha^a = -\frac{1}{\sigma}g^{ab}g_{\alpha a}$,

Assumption SM-4 $g_{\alpha a,\beta} = g_{\beta a,\alpha}$.

Under the simplified matching conditions, the components of the controlled kinetic energy metric in equation (5.22) reduce to

$$\begin{aligned}
 (g_{\tau,\sigma})_{\alpha\beta} &= g_{\alpha\beta} + \frac{1-\sigma}{\sigma^2} g_{\alpha a} g^{ab} g_{\beta b} \\
 (g_{\tau,\sigma})_{ab} &= -\frac{1-\sigma}{\sigma} g_{ab} \\
 (g_{\tau,\sigma})_{ab} &= g_{ab}.
 \end{aligned}
 \tag{5.24}$$

Example systems which are subject to the simplified matching conditions include the planar pendulum on a cart and the spherical pendulum on a hockey puck [17].

5.2 Dissipation and General Matching Systems

In this section, we consider the impact of damping on “balance” type controlled Lagrangian systems, i.e., systems for which the desired equilibrium is a maximum of the potential energy. It is assumed that the equilibrium is stable for the conservative, closed-loop system. An important negative result concerning the effect of generic physical damping shows that one may not simply use a Lyapunov function developed for the conservative system model and expect to prove asymptotic stability. However, a semidefinite modification of the Lyapunov function indicates that asymptotic stabilization may be possible in cases, an observation which is verified through local analysis.

5.2.1 The Effect of Generalized Forces on the Modified Energy

To determine how physical and feedback dissipation affect the feedback-controlled system (5.8) with u_a defined by (5.15), consider the more general open-loop equations:

$$\begin{aligned}\frac{d}{dt} \frac{\partial L}{\partial \dot{x}^\alpha} - \frac{\partial L}{\partial x^\alpha} &= F_\alpha \\ \frac{d}{dt} \frac{\partial L}{\partial \dot{\theta}^a} &= u_a + F_a.\end{aligned}\tag{5.25}$$

The generalized forces F_α and F_a might represent physical dissipation, propulsive forces, etc. We consider stability of the equilibrium (5.9) with $c = 0$:

$$(x^\alpha, \dot{x}^\alpha, \dot{\theta}^a)_e = (x_e^\alpha, 0, 0).$$

We also assume that $F_\alpha = F_a = 0$ at equilibrium.

Since $E_{\tau,\sigma,\rho}$ is a Lyapunov function in the conservative setting, it is worthwhile to continue to study stability using this control-modified energy. However, when generalized forces are present, the controlled Lagrangian $L_{\tau,\sigma,\rho}$ no longer yields the correct closed-loop equations. To find the correct closed-loop equations (in terms of $L_{\tau,\sigma,\rho}$) and the effect of dissipation on stability, it is convenient to first express the accelerations \ddot{x}^α and $\ddot{\theta}^a$ explicitly.

Define

$$\begin{aligned}B_{\alpha\beta} &= g_{\alpha\beta} - g_{\alpha b} g^{ab} g_{a\beta} > 0 \\ B_{ab} &= g_{ab} - g_{a\alpha} g^{\alpha\beta} g_{\beta b} > 0\end{aligned}$$

so that the inverse of the kinetic energy metric may be written

$$\mathbb{M}^{-1} = \begin{pmatrix} [B^{\alpha\beta}] & [-B^{\alpha\gamma}g_{\gamma c}g^{cb}] \\ [-B^{ac}g_{c\gamma}g^{\gamma\beta}] & [B^{ab}] \end{pmatrix}. \quad (5.26)$$

Solving the open-loop equations (5.25) for acceleration gives

$$\begin{pmatrix} [\ddot{x}^\alpha] \\ [\ddot{\theta}^a] \end{pmatrix} = \mathbb{M}^{-1} \left\{ -\frac{d}{dt}(\mathbb{M}) \begin{pmatrix} [\dot{x}^\beta] \\ [\dot{\theta}^b] \end{pmatrix} + \begin{pmatrix} \left[\frac{\partial}{\partial x^\alpha} \left(\frac{1}{2}g_{\gamma\beta}\dot{x}^\gamma\dot{x}^\beta + g_{\gamma b}\dot{x}^\gamma\dot{\theta}^b + \frac{1}{2}g_{cb}\dot{\theta}^c\dot{\theta}^b - V(x^\gamma) \right) \right] \\ \mathbf{0} \end{pmatrix} + \begin{pmatrix} [F_\beta] \\ [u_b + F_b] \end{pmatrix} \right\}. \quad (5.27)$$

When F_α and F_a are zero, the closed-loop dynamics, under the control implied by the method of controlled Lagrangians, correspond to unforced Euler-Lagrange equations for $L_{\tau,\sigma,\rho}$. More generally, under this same control law, the closed-loop equations become

$$\begin{aligned} \begin{pmatrix} [\mathcal{E}_{x^\alpha}(L_{\tau,\sigma,\rho})] \\ [\mathcal{E}_{\theta^a}(L_{\tau,\sigma,\rho})] \end{pmatrix} &= \mathbb{M}_{\tau,\sigma,\rho} \begin{pmatrix} [\ddot{x}^\beta] \\ [\ddot{\theta}^b] \end{pmatrix} + \frac{d}{dt}(\mathbb{M}_{\tau,\sigma,\rho}) \begin{pmatrix} [\dot{x}^\beta] \\ [\dot{\theta}^b] \end{pmatrix} \\ &\quad - \begin{pmatrix} \left[\frac{\partial}{\partial x^\alpha} \left(\frac{1}{2}(g_{\tau,\sigma,\rho})_{\gamma\beta}\dot{x}^\gamma\dot{x}^\beta + (g_{\tau,\sigma,\rho})_{\gamma b}\dot{x}^\gamma\dot{\theta}^b + \frac{1}{2}(g_{\tau,\sigma,\rho})_{cb}\dot{\theta}^c\dot{\theta}^b - V(x^\gamma) \right) \right] \\ \mathbf{0} \end{pmatrix} \\ &= \mathbb{M}_{\tau,\sigma,\rho}\mathbb{M}^{-1} \begin{pmatrix} F_\gamma \\ F_c \end{pmatrix} \end{aligned} \quad (5.28)$$

Here, we have observed that in the presence of the generalized forces F_α and F_a , the only nonzero contribution on the right will be due to those forces. The forces enter via the accelerations \ddot{x}^α and $\ddot{\theta}^a$.

Recall that an equilibrium of the conservative, closed-loop dynamics is stable provided

$$E_{\tau,\sigma,\rho}(x^\alpha, \dot{x}^\alpha) = \frac{1}{2}A_{\alpha\beta}\dot{x}^\alpha\dot{x}^\beta + \frac{1}{2}\rho^{ab}\tilde{J}_a\tilde{J}_b + V(x^\alpha)$$

is definite about the equilibrium (5.9). When dissipation is introduced, \tilde{J}_a is no longer conserved and so its dynamics must also be considered. Assume that there is a function $\Psi(\tilde{J}_a)$ such that

$$E_{\tau,\sigma,\rho,\Psi}(x^\alpha, \dot{x}^\alpha, \tilde{J}_a) = \frac{1}{2}A_{\alpha\beta}\dot{x}^\alpha\dot{x}^\beta + \frac{1}{2}\rho^{ab}\tilde{J}_a\tilde{J}_b + V(x^\alpha) + \Psi(\tilde{J}_a)$$

is definite. Without loss of generality, assume that $E_{\tau,\sigma,\rho,\Psi}$ is negative definite. Then, for stability in the presence of dissipation, we require that $\frac{d}{dt}E_{\tau,\sigma,\rho,\Psi}$ be at least positive semidefinite. Using the accelerations computed in (5.27) and the fact that \tilde{J}_a is conserved when dissipation is absent, one finds

$$\begin{aligned} \frac{d}{dt}\tilde{J}_a &= \frac{d}{dt}\left(\rho_{ab}\dot{\theta}^b + \rho_{ab}(g^{bc} - \sigma^{bc})g_{c\alpha}\dot{x}^\alpha\right) \\ &= \rho_{ab}B^{bc}\left(-g_{c\alpha}g^{\alpha\beta}F_\beta + F_c\right) + \rho_{ab}(g^{bc} - \sigma^{bc})g_{c\alpha}B^{\alpha\beta}\left(F_\beta - g_{\beta d}g^{de}F_e\right) \\ &= \rho_{ab}\left(-B^{bc}g_{c\alpha}g^{\alpha\beta} + (g^{bc} - \sigma^{bc})g_{c\alpha}B^{\alpha\beta}\right)F_\beta \\ &\quad + \rho_{ab}\left(B^{be} - (g^{bc} - \sigma^{bc})g_{c\alpha}B^{\alpha\beta}g_{\beta d}g^{de}\right)F_e. \end{aligned}$$

As in [16], we simplify notation by defining the quantities

$$D^{ab} = g^{ab} + \sigma^{ac}g_{c\alpha}B^{\alpha\beta}g_{\beta e}g^{eb} \quad (5.29)$$

$$k_a^\beta = D_{ab}\sigma^{bc}g_{c\alpha}B^{\alpha\beta}. \quad (5.30)$$

Using these definitions and identities (E.4) and (E.5) from Appendix E.2, one finds that

$$\frac{d}{dt}\bar{J}_a = \rho_{ab}D^{bc}(F_c - k_c^\alpha F_\alpha). \quad (5.31)$$

Therefore,

$$\begin{aligned} \frac{d}{dt}E_{\tau,\sigma,\rho,\Psi} &= \frac{d}{dt}\left(\frac{1}{2}A_{\alpha\beta}\dot{x}^\alpha\dot{x}^\beta + \rho^{ab}\bar{J}_a\bar{J}_b\right) + \frac{\partial V}{\partial x^\alpha}\dot{x}^\alpha + \frac{\partial\Psi}{\partial\bar{J}_a}\dot{\bar{J}}_a \\ &= \dot{x}^\alpha A_{\alpha\beta}B^{\beta\gamma}\left(F_\gamma - g_{\gamma b}g^{bc}F_c\right) + \left(\bar{J}_a + \rho_{ab}\frac{\partial\Psi}{\partial\bar{J}_b}\right)D^{ac}\left(F_c - k_c^\beta F_\beta\right) \\ &= \dot{x}^\alpha A_{\alpha\beta}B^{\beta\gamma}F_\gamma - \dot{x}^\alpha g_{\alpha a}D^{ab}F_b + \left(\bar{J}_a + \rho_{ab}\frac{\partial\Psi}{\partial\bar{J}_b}\right)D^{ac}\left(F_c - k_c^\beta F_\beta\right) \end{aligned} \quad (5.32)$$

where we note without proof that

$$A_{\alpha\beta}B^{\beta\gamma}g_{\gamma a}g^{ab} = g_{\alpha a}D^{ab}. \quad (5.33)$$

Remark 5.2.1 Feedback dissipation with no physical damping. *Suppose that $F_\alpha = 0$ and that F_a can be specified. Choosing*

$$F_a = k_{ab}^{\text{diss}}D^{bc}\left(-g_{c\gamma}\dot{x}^\gamma + \bar{J}_c + \rho_{cd}\frac{\partial\Psi}{\partial\bar{J}_d}\right) \quad (5.34)$$

with $k_{ab}^{\text{diss}} > 0$ makes $\frac{d}{dt}E_{\tau,\sigma,\rho,\Psi} \geq 0$ and stability can be studied using LaSalle's invariance principle.

This observation is consistent with previous results concerning asymptotic stabilization using feedback dissipation (and in the absence of physical damping) [17]. Notice that the function Ψ appears in the dissipative feedback control law. Thus, freedom in choosing Ψ may be exploited in shaping the closed-loop dynamics.

When the system is subject to physical damping, asymptotic stabilization is more subtle.

The following proposition illustrates one of the difficulties.

Proposition 5.2.2 *Assume that the system is subject to physical dissipation in the unactuated directions and that the dissipative force opposes velocity,*

$$\dot{x}^\alpha F_\alpha \quad \begin{cases} < 0 & (\dot{x} \neq 0), \\ = 0 & (\dot{x} = 0). \end{cases}$$

Then there is no force F_a which makes $\frac{d}{dt}E_{\tau,\sigma,\rho,\Psi}$ nonnegative.

Proof. To prove the proposition, rewrite equation (5.32) as

$$\frac{d}{dt}E_{\tau,\sigma,\rho,\Psi} = \left(\dot{x}^\alpha A_{\alpha\beta} B^{\beta\gamma} - \left(\bar{J}_a + \rho_{ab} \frac{\partial \Psi}{\partial \bar{J}_b} \right) D^{ac} k_c^\gamma \right) F_\gamma + \left(-\dot{x}^\alpha g_{\alpha a} + \bar{J}_a + \rho_{ab} \frac{\partial \Psi}{\partial \bar{J}_b} \right) D^{ac} F_c. \quad (5.35)$$

Suppose that, at an instant,

$$\bar{J}_a = g_{\alpha a} \dot{x}^\alpha - \rho_{ab} \frac{\partial \Psi}{\partial \bar{J}_b} \quad (5.36)$$

where $\dot{x}^\alpha \neq 0$. Then, at that instant, the latter term of (5.35) is zero and

$$\begin{aligned} \frac{d}{dt}E_{\tau,\sigma,\rho,\Psi} &= \dot{x}^\alpha \left(A_{\alpha\beta} - g_{\alpha a} \sigma^{ab} g_{b\beta} \right) B^{\beta\gamma} F_\gamma \\ &= \dot{x}^\alpha F_\alpha < 0. \end{aligned}$$

□

Proposition 5.2.2 indicates that $E_{\tau,\sigma,\rho,\Psi}$ cannot be a Lyapunov function when there is physical dissipation of this sort. However, it may be possible to obtain stability results using a semidefinite function based on $E_{\tau,\sigma,\rho,\Psi}$. If ρ_{ab} is constant (as in the case of simplified

matching and Euler-Poincaré matching), then the second and fourth terms of

$$E_{\tau,\sigma,\rho,\Psi} = \frac{1}{2}A_{\alpha\beta}\dot{x}^\alpha\dot{x}^\beta + \frac{1}{2}\rho^{ab}\bar{J}_a\bar{J}_b + V(x^\alpha) + \Psi(\bar{J}_a),$$

are conserved when $F_a = F_\alpha = 0$. Thus, the function

$$\bar{E}_{\tau,\sigma,\rho} = \frac{1}{2}A_{\alpha\beta}\dot{x}^\alpha\dot{x}^\beta + V(x^\alpha) \quad (5.37)$$

is also conserved when $F_a = F_\alpha = 0$. Furthermore, by assumption, this function is negative semidefinite at the equilibrium. For nonzero F_a and F_α , one finds that

$$\frac{d}{dt}\bar{E}_{\tau,\sigma,\rho} = \dot{x}^\alpha A_{\alpha\beta}B^{\beta\gamma}F_\gamma - \dot{x}^\alpha g_{\alpha a}D^{ab}F_b. \quad (5.38)$$

Suppose that there is no damping in the actuated directions ($F_a = 0$) but that the unactuated directions are subject to linear dissipation $F_\alpha = -d_{\alpha\beta}\dot{x}^\beta$ where $d_{\alpha\beta}$ is positive definite. From equation (5.38),

$$\frac{d}{dt}\bar{E}_{\tau,\sigma,\rho} = -\dot{x}^\alpha A_{\alpha\beta}B^{\beta\gamma}d_{\gamma\psi}\dot{x}^\psi. \quad (5.39)$$

Since $(-A_{\alpha\beta})B^{\beta\gamma}d_{\gamma\psi}$ is a product of positive definite matrices, one expects that $\frac{d}{dt}\bar{E}_{\tau,\sigma,\rho}$ is non-negative. Assuming this is so, $\frac{d}{dt}\bar{E}_{\tau,\sigma,\rho}$ must converge to zero, since $\bar{E}_{\tau,\sigma,\rho}$ is bounded above. Therefore, \dot{x}^α converges to zero and, referring to equation (5.31), \bar{J}_a goes to a constant. Furthermore, the rate of convergence can be modified by choosing

$$F_a = -D_{ab}d_x^{bc}g_{c\beta}\dot{x}^\beta \quad (5.40)$$

where \tilde{d}_x^{ab} is a dissipative feedback gain matrix. Choosing \tilde{d}_x^{ab} positive definite augments the rate $\frac{d}{dt}\bar{E}_{\tau,\sigma,\rho}$, potentially yielding faster convergence of \dot{x}^α to zero.

Local analysis yields a much more definitive stability result. Changing coordinates from $(x^\alpha, \dot{x}^\alpha, \dot{\theta}^a)$ to $(x^\alpha, \dot{x}^\alpha, \tilde{J}_a)$, we now consider the equilibrium

$$(x^\alpha, \dot{x}^\alpha, \tilde{J}_a)_e = (x_e^\alpha, 0, 0). \quad (5.41)$$

The linearized dynamics are

$$\begin{aligned} \delta\ddot{x}^\alpha &= -\left(A^{\alpha\gamma} \frac{\partial^2 V}{\partial x^\gamma \partial x^\beta}\right)_e \delta x^\beta + B^{\alpha\beta} (\delta F_\beta - g_{\beta c} g^{cb} \delta F_b) \\ \delta\dot{\tilde{J}}_a &= \rho_{ac} D^{cb} (\delta F_b - k_b^\beta \delta F_\beta) \end{aligned}$$

We assume that $\delta F_\alpha = -d_{\alpha\beta} \delta \dot{x}^\beta$ where $d_{\alpha\beta} > 0$. We also assume that any physical damping in the actuated directions can be exactly cancelled so that δF_a may be specified. Suppose

$$\delta F_a = g_{ab} \tilde{d}_x^{bc} g_{c\beta} \delta \dot{x}^\beta - D_{ab} \rho^{bc} g_{cd} \tilde{d}_J^{de} \delta \tilde{J}_e. \quad (5.42)$$

where \tilde{d}_x^{ab} and \tilde{d}_J^{ab} are control parameters. The complete closed-loop linear dynamics are

$$\begin{pmatrix} [\delta \dot{x}^\alpha] \\ [\delta \ddot{x}^\alpha] \\ [\delta \dot{\tilde{J}}_a] \end{pmatrix} = \begin{pmatrix} \mathbf{0} & \mathcal{I} & \mathbf{0} \\ \mathbf{A} & \mathbf{B} & \mathbf{C} \\ \mathbf{0} & \mathbf{D} & \mathbf{E} \end{pmatrix} \begin{pmatrix} [\delta x^\alpha] \\ [\delta \dot{x}^\alpha] \\ [\delta \tilde{J}_a] \end{pmatrix}. \quad (5.43)$$

where

$$\mathbf{A} = \left[-A^{\alpha\gamma} \frac{\partial^2 V}{\partial x^\gamma \partial x^\beta} \right]_e$$

$$\begin{aligned}
\mathbf{B} &= \left[-B^{\alpha\gamma} (d_{\gamma\beta} + g_{\gamma c} \bar{d}_x^{cd} g_{d\beta}) \right]_e \\
\mathbf{C} &= \left[B^{\alpha\gamma} g_{\gamma c} g^{cd} D_{de} \rho^{ef} g_{fh} \bar{d}_J^{hb} \right]_e \\
\mathbf{D} &= \left[\rho_{ac} D^{cd} (k_d^\gamma d_{\gamma\beta} + g_{de} \bar{d}_x^{ef} g_{f\beta}) \right]_e \\
\mathbf{E} &= \left[-g_{ac} \bar{d}_J^{cb} \right]_e.
\end{aligned}$$

Since we have assumed that the equilibrium is a maximum of the potential and that control parameters have therefore been chosen such that $A_{\alpha\beta}|_e < 0$, we expect that $\mathbf{A} < 0$. Also, if $\bar{d}_x^{cd} \geq 0$ then we expect $\mathbf{B} < 0$. The characteristic polynomial of the submatrix

$$\begin{pmatrix} \mathbf{0} & \mathbf{I} \\ \mathbf{A} & \mathbf{B} \end{pmatrix} \tag{5.44}$$

is

$$|\lambda^2 \mathbf{I} - \lambda \mathbf{B} - \mathbf{A}|.$$

A corollary of a theorem due to Bellman [9] indicates that (5.44) is Hurwitz when $\bar{d}_x^{ab} \geq 0$.

Proposition 5.2.3 (Bellman) *Consider three square matrices $\bar{\mathbf{A}}$, $\bar{\mathbf{B}}$, and $\bar{\mathbf{C}}$ of equal dimension. If $\bar{\mathbf{A}} > 0$, $\bar{\mathbf{B}} > 0$, and $\bar{\mathbf{C}} > 0$, then the only root of the polynomial*

$$|\lambda^2 \bar{\mathbf{A}} + 2\lambda \bar{\mathbf{B}} + \bar{\mathbf{C}}| = 0$$

with nonnegative real part is $\lambda = 0$.

Thus, assuming that $\mathbf{A} < 0$ and $\mathbf{B} < 0$, the matrix (5.44) is Hurwitz. This result follows from Proposition 5.2.3 and the observation that, because \mathbf{A} is invertible, the matrix (5.44) is invertible and thus has no zero eigenvalues. Conditions on \bar{d}_J^{ab} must now be found under

which the entire closed-loop state matrix given in (5.43) is Hurwitz. One common approach to this sort of problem is to use the Routh-Hurwitz method [23].

Theorem 5.2.4 (Local Exponential Stability) *Consider the equilibrium (5.41) and the linearized dynamics (5.43). Suppose that $\mathbf{A} < 0$ and $\mathbf{B} < 0$. Choosing \bar{d}_J^{de} to make the state matrix Hurwitz yields local exponential stability of the equilibrium (5.41).*

Remark 5.2.5 *One might reasonably expect that a necessary condition for the state matrix to be Hurwitz is that \mathbf{E} be Hurwitz and therefore that \bar{d}_J^{ab} should be chosen positive definite. In the examples considered here, such a choice of \bar{d}_J^{ab} corresponds to positive \bar{J}_a feedback. The conditions on control parameters for stability require that $-D_{ab}\rho^{bc}g_{cd} > 0$. Therefore, when $\bar{d}_J^{ab} > 0$, the net result of the latter term of the dissipative control law (5.42) is to feed back \bar{J}_a with a positive gain. Feeding back \bar{J}_a with a positive gain effectively counters the dissipation in the controlled directions.*

Remark 5.2.6 *The group variable θ^a does not approach a specified value because the control law preserves the system symmetry. Adding an appropriate symmetry-breaking potential control law (i.e., a fictitious spring force) would presumably yield local exponential stability to a particular point [10].*

In Section 5.2.2, the approach described here is applied in simulation to the example of a planar pendulum on a cart. Section 5.2.3 presents the results of an experimental application to a variant of this problem, the pendulum on a rotor arm.

5.2.2 Example: The Pendulum on a Cart

The classic problem of a planar pendulum on a cart was treated in [17] under the simplified matching conditions described in Section 5.1.3. There it was shown that, in the conservative

setting, the inverted equilibrium is stabilized by the control law indicated by the method of controlled Lagrangians. Furthermore, feedback dissipation can be applied to asymptotically stabilize the equilibrium. Here, we show that one may asymptotically stabilize the inverted equilibrium even when the pendulum/cart system is subject to generic physical damping.

Using the same notation as in [17], the Lagrangian is

$$L = \frac{1}{2} \begin{pmatrix} \dot{\theta} \\ \dot{s} \end{pmatrix} \cdot \begin{pmatrix} ml^2 & ml \cos \theta \\ ml \cos \theta & M + m \end{pmatrix} \begin{pmatrix} \dot{\theta} \\ \dot{s} \end{pmatrix} - mgl \cos \theta,$$

where s represents the cart location and θ represents the pendulum angle. The configuration space is $\mathbb{R} \times S^1$ where \mathbb{R} represents the cart location and S^1 represents the pendulum angle. This system exhibits symmetry under the action of $G = \mathbb{R}$, that is, under translations of the cart.

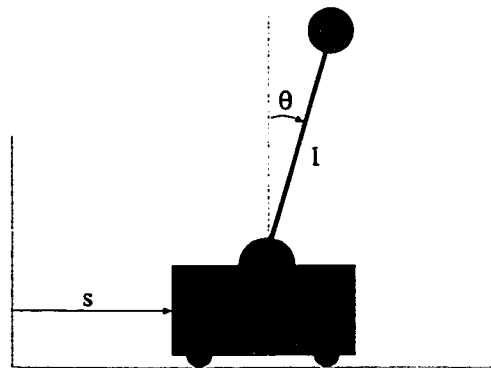


Figure 5.3: Pendulum on a cart.

In the conservative setting, the open-loop equations of motion for this system are

$$\begin{aligned} \frac{d}{dt} \frac{\partial L}{\partial \dot{\theta}} - \frac{\partial L}{\partial \theta} &= 0 \\ \frac{d}{dt} \frac{\partial L}{\partial \dot{s}} &= u \end{aligned}$$

where u represents a control force applied to the cart. It was shown in [17] that when

$$u = u_{cL} = \frac{1}{\sigma} \left(\frac{ml \sin \theta (\frac{q}{l} \cos \theta - \dot{\theta}^2)}{1 - \frac{m}{M+m} (1 - \frac{1}{\sigma}) \cos^2 \theta} \right), \quad (5.45)$$

the closed-loop dynamics derive from the controlled Lagrangian

$$L_{\tau,\sigma} = \frac{1}{2} \begin{pmatrix} \dot{\theta} \\ \dot{s} \end{pmatrix} \cdot \begin{pmatrix} ml^2 + \frac{(1-\sigma)(ml \cos \theta)^2}{\sigma^2(M+m)} & -\frac{1-\sigma}{\sigma} ml \cos \theta \\ -\frac{1-\sigma}{\sigma} ml \cos \theta & M+m \end{pmatrix} \begin{pmatrix} \dot{\theta} \\ \dot{s} \end{pmatrix} - mgl \cos \theta.$$

(This example corresponds to the case of simplified matching in which one may choose

$$\rho_{ab} = g_{ab}.)$$

Define the (conserved) momentum conjugate to s ,

$$\tilde{J} = \frac{\partial L_{\tau,\sigma}}{\partial \dot{s}} = (M+m)\dot{s} - \frac{1-\sigma}{\sigma} ml \cos \theta \dot{\theta}.$$

Choosing σ to satisfy

$$-\frac{m}{M} < \sigma < 0$$

stabilizes the inverted equilibrium $(\theta, \dot{\theta})_e = (0, 0)$ for any value of momentum \tilde{J} .

Stability can be proven with a Lyapunov function developed from the modified energy.

A negative definite Lyapunov function for the inverted equilibrium is

$$E_{\tau,\sigma}(\theta, \dot{\theta}; \tilde{J}) = \frac{1}{2} [A_{\alpha\beta}] \dot{\theta}^2 + \frac{1}{2} \frac{\tilde{J}^2}{M+m} + mgl \cos \theta \quad (5.46)$$

where

$$[A_{\alpha\beta}] = ml^2 + \frac{(1-\sigma)(ml \cos \theta)^2}{\sigma(M+m)} \quad (5.47)$$

is the modified horizontal energy metric.

Now assume that the system is subject to dissipation as described in Section 5.2,

$$\begin{aligned}\frac{d}{dt} \frac{\partial L}{\partial \dot{\theta}} - \frac{\partial L}{\partial \theta} &= -d_{\theta} \dot{\theta} \\ \frac{d}{dt} \frac{\partial L}{\partial \dot{s}} &= u_{cL} + u_{diss},\end{aligned}$$

where $d_{\theta} > 0$ and u_{cL} is given by equation (5.45). Following (5.42),

$$\begin{aligned}u_{diss} &= \left[g_{ab} \bar{d}_{bc}^{\bar{}} g_{c\beta} \dot{x}^{\beta} - D_{ab} \rho^{bc} g_{cd} \bar{d}_J^{de} \bar{J}_e \right] \\ &= \left[g_{ab} \bar{d}_{bc}^{\bar{}} g_{c\beta} \dot{x}^{\beta} - D_{ab} \bar{d}_J^{de} \bar{J}_e \right] \\ &= (M+m) \left(\frac{\bar{d}_{\theta}}{M+m} \right) (ml \cos \theta) \dot{\theta} - \left(\frac{(M+m)(M+m \sin^2 \theta)}{M+m - (1 - \frac{1}{\sigma})m \cos^2 \theta} \right) \left(\frac{\bar{d}_J}{M+m} \right) \bar{J} \\ &= \bar{d}_{\theta} (ml \cos \theta) \dot{\theta} - \bar{d}_J \left(\frac{M+m \sin^2 \theta}{M+m - (1 - \frac{1}{\sigma})m \cos^2 \theta} \right) \bar{J}.\end{aligned}\tag{5.48}$$

The parameters \bar{d}_{θ} and \bar{d}_J represent dissipative control gains.

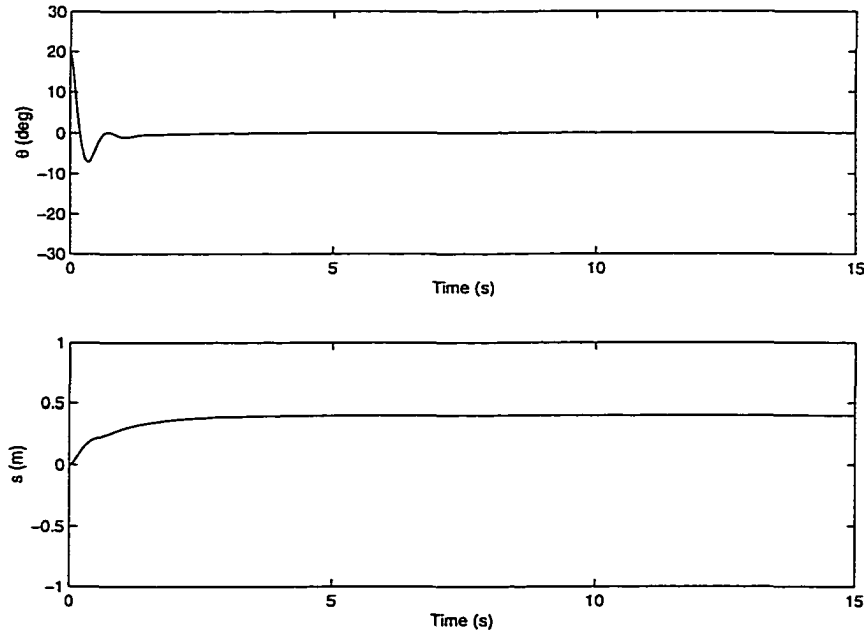


Figure 5.4: Planar pendulum simulation with feedback dissipation.

Figure 5.4 shows a simulation of the closed-loop system response. The physical properties are

$$M = 1 \text{ kg}, \quad m = 0.5 \text{ kg}, \quad l = 0.1 \text{ m}, \quad d_\theta = 0.01 \text{ Nms.}$$

The control parameters are

$$\sigma = -0.2, \quad \bar{d}_\theta = 10 \text{ s}^{-1}, \quad \bar{d}_J = 1 \text{ s}^{-1}.$$

The initial condition is a static pendulum angle of 20 degrees.

As can be seen in Figure 5.4, the pendulum approaches vertical and the cart comes to rest. Thus, the system with physical dissipation is asymptotically stabilized by the method of controlled Lagrangians and appropriate dissipative feedback.

Remark 5.2.7 *Cancelling the dissipation in the actuated direction and superimposing \bar{J} dissipation as prescribed effectively reverses the natural physical damping in the vertical (cart) direction. Such an approach is necessary for stability; uncompensated physical damping in the controlled direction (i.e., damping which opposes the cart velocity) destabilizes the desired equilibrium.*

5.2.3 Example: The Pendulum on a Rotor Arm

In this section, we consider the pendulum on a rotor arm. This problem was treated in [16], where it was noted that the simplified matching conditions cannot be used to stabilize the inverted equilibrium. The model used here differs slightly from the model of [16] in order to better approximate an experimental apparatus. Figure 5.5 depicts the device and the choice of coordinates. Assuming that the cylindrical links have small diameters and uniformly distributed mass (instead of massless links, as assumed in [16]), the Lagrangian

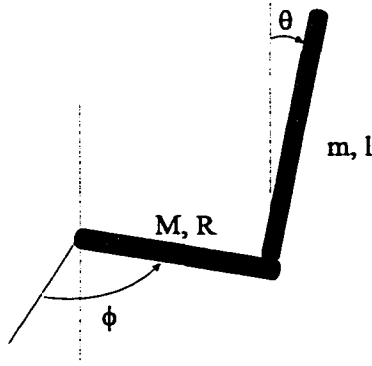


Figure 5.5: Pendulum on a rotary arm.

for the uncontrolled system is

$$L(\theta, \dot{\theta}, \dot{\phi}) = \frac{1}{2} \begin{pmatrix} \dot{\theta} \\ \dot{\phi} \end{pmatrix} \cdot \begin{pmatrix} \frac{1}{3}ml^2 & \frac{1}{2}mlR \cos \theta \\ \frac{1}{2}mlR \cos \theta & (\frac{1}{3}M + m)R^2 + \frac{1}{3}ml^2 \sin^2 \theta \end{pmatrix} \begin{pmatrix} \dot{\theta} \\ \dot{\phi} \end{pmatrix} - mgl(\cos \theta - 1). \quad (5.49)$$

A control torque is applied to the horizontal link about the vertical axis. The kinetic energy metric decomposes as shown,

$$[g_{\alpha\beta}] = \frac{1}{3}ml^2, \quad [g_{\alpha b}] = \frac{1}{2}mlR \cos \theta, \quad [g_{ab}] = \left(\frac{1}{3}M + m\right)R^2 + \frac{1}{3}ml^2 \sin^2 \theta.$$

Assuming that no external forces act, other than the control torque u , the Euler-Lagrange equations are

$$\begin{aligned} \frac{d}{dt} \frac{\partial L}{\partial \dot{\theta}} - \frac{\partial L}{\partial \theta} &= 0 \\ \frac{d}{dt} \frac{\partial L}{\partial \dot{\phi}} &= u. \end{aligned} \quad (5.50)$$

In [16], the matching conditions were satisfied by choosing

$$\sigma_{ab} = g_{ac} k^{cd} g_{db} + g_{ab}$$

$$\rho_{ab} = g_{ab} + k_{ab}$$

where k_{ab} represents a constant gain. In the following derivation, the same choices are made and $[k_{ab}]$ is replaced by k for brevity. The conditions on σ and ρ are consistent with the assumption that

$$g^{ab} = \rho^{ab} + \sigma^{ab},$$

as discussed in Section 5.1.3.

In the conservative setting, the feedback control law

$$\begin{aligned} u = u_{cL} &= -k\ddot{\phi} \\ &= -k \frac{\frac{1}{2}mlR \sin \theta \dot{\theta}^2 - \sin 2\theta \left(\frac{1}{3}ml^2 \dot{\theta} \dot{\phi} + \frac{1}{4}mRl(\cos \theta \dot{\phi}^2 + \frac{g}{l}) \right)}{\left(\frac{1}{3}M + \frac{1}{4}m \right) R^2 + m \left(\frac{3}{4}R^2 + \frac{1}{3}l^2 \right) \sin^2 \theta + k} \end{aligned} \quad (5.51)$$

leads to the modified Euler-Lagrange equations

$$\begin{aligned} \frac{d}{dt} \frac{\partial L_{\tau,\sigma,\rho}}{\partial \dot{\theta}} - \frac{\partial L_{\tau,\sigma,\rho}}{\partial \theta} &= 0 \\ \frac{d}{dt} \frac{\partial L_{\tau,\sigma,\rho}}{\partial \dot{\phi}} &= 0 \end{aligned} \quad (5.52)$$

with controlled Lagrangian

$$L_{\tau,\sigma,\rho}(\theta, \dot{\theta}, \dot{\phi}) = L(\theta, \dot{\theta}, \dot{\phi}) + \frac{1}{2}k\dot{\phi}^2. \quad (5.53)$$

While the control law (5.51) is quite complicated, it can easily be implemented using microprocessor-based control hardware.

Define \bar{J} to be the controlled momentum conjugate to ϕ ,

$$\bar{J} = \frac{\partial L_{\tau,\sigma,\rho}}{\partial \dot{\phi}} = \left(\left(\frac{1}{3}M + m \right) R^2 + \frac{1}{3}ml^2 \sin^2 \theta + k \right) \dot{\phi} + \frac{1}{2}mlR \cos \theta \dot{\theta}.$$

Then the modified system energy, the Routhian corresponding to $L_{\tau,\sigma,\rho}$, is

$$E_{\tau,\sigma,\rho}(\theta, \dot{\theta}; \bar{J}) = \frac{1}{2}[A_{\alpha\beta}]\dot{\theta}^2 + \frac{1}{2}[\rho^{ab}]\bar{J}^2 + mgl(\cos \theta - 1) \quad (5.54)$$

where

$$[A_{\alpha\beta}] = [g_{\alpha\beta} - g_{\alpha a} \rho^{ab} g_{b\beta}] = \frac{1}{3}ml^2 - \frac{(\frac{1}{2}mlR \cos \theta)^2}{(\frac{1}{3}M + m) R^2 + \frac{1}{3}ml^2 \sin^2 \theta + k} \quad (5.55)$$

is the modified horizontal kinetic energy metric.

For the conservative system model, the inverted equilibrium

$$(\theta, \dot{\theta}, \dot{\phi})_e = (0, 0, 0). \quad (5.56)$$

is stable provided $E_{\tau,\sigma,\rho}$ is definite as a function of θ and $\dot{\theta}$. Define the amended potential

$$V_\mu(\theta) = mgl(\cos \theta - 1) + \frac{1}{2} \frac{\bar{J}^2}{(\frac{1}{3}M + m) R^2 + \frac{1}{3}ml^2 \sin^2 \theta + k}.$$

The equilibrium (5.56) will be stable provided

$$\text{sign}[A_{\alpha\beta}]_e = \text{sign} \left(\frac{\partial^2 V_\mu}{\partial \theta^2} \right)_e. \quad (5.57)$$

Since V_μ has a maximum at the equilibrium of interest, the right-hand side of (5.57) is

negative. Therefore k must be chosen to make $[A_{\alpha\beta}] < 0$ at the equilibrium. Now,

$$[A_{\alpha\beta}]_e = \frac{1}{3}ml^2 \left(\frac{\left(\frac{1}{3}M + m\right) R^2 + k - \frac{3}{4}mR^2}{\left(\frac{1}{3}M + m\right) R^2 + k} \right)$$

is negative provided

$$-\left(\frac{1}{3}M + m\right) R^2 < k < -\left(\frac{1}{3}M + \frac{1}{4}m\right) R^2.$$

Define a new control parameter \bar{k} and let

$$k = -\left(\frac{1}{3}M + m\right) R^2 + \frac{\bar{k} - 1}{\bar{k}} \left(\frac{3}{4}mR^2\right). \quad (5.58)$$

The stability condition then becomes $\bar{k} > 1$.

Substituting \bar{k} and simplifying, the horizontal metric $A_{\alpha\beta}$ becomes

$$[A_{\alpha\beta}] = \frac{1}{3}ml^2 \left(\frac{\left(\frac{1}{3}ml^2 - \frac{3}{4}mR^2\right) \sin^2 \theta - \frac{1}{\bar{k}} \frac{3}{4}mR^2}{\frac{1}{3}ml^2 \sin^2 \theta + \frac{\bar{k}-1}{\bar{k}} \left(\frac{3}{4}mR^2\right)} \right).$$

When $\bar{k} > 1$, $A_{\alpha\beta}$ is negative for all $\theta \in (-\bar{\theta}, \bar{\theta})$ where

$$\bar{\theta} = \sin^{-1} \sqrt{\left(\frac{1}{\bar{k}}\right) \left(1 + \left(\frac{2l}{3R}\right)^2\right)^{-1}}.$$

When $\theta = \pm\bar{\theta}$, $A_{\alpha\beta}$ becomes zero and the control law (5.51) becomes singular. Thus $\bar{\theta}$ places a physical limit on the region of attraction of the stabilizing control law. As noted in [16], the value of $\bar{\theta}$ approaches $\frac{\pi}{2}$ in the limit that $\bar{k} \rightarrow 1$ and $l/R \rightarrow 0$.

As shown in Appendix F, linear damping provides a very accurate model of friction in the pendulum link of the experimental apparatus. The azimuthal damping is more accurately

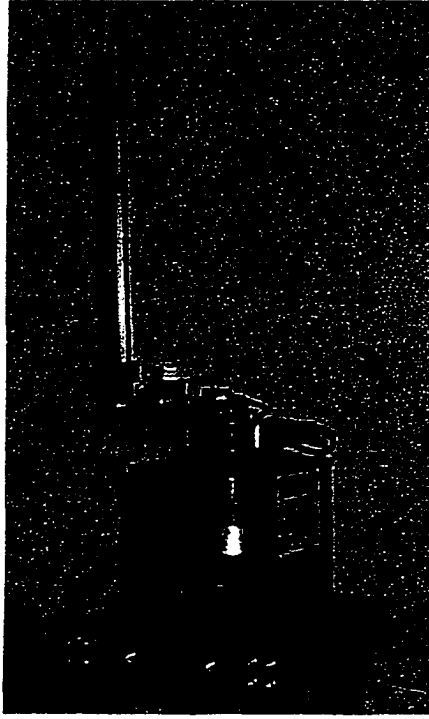


Figure 5.6: Experimental apparatus.

characterized by a Coulomb model, though we assume that this damping too is linear in velocity. Including the friction model and a dissipative feedback torque u_{diss} , the open-loop equations (5.50) become

$$\begin{aligned} \frac{d}{dt} \frac{\partial L}{\partial \dot{\theta}} - \frac{\partial L}{\partial \theta} &= -d_{\theta} \dot{\theta} \\ \frac{d}{dt} \frac{\partial L}{\partial \dot{\phi}} &= -d_{\phi} \dot{\phi} + u_{cL} + u_{\text{diss}} \end{aligned} \quad (5.59)$$

where $d_{\theta} > 0$ and $d_{\phi} > 0$. In the notation of Theorem 5.2.4, define

$$\bar{d}_x^{ab} = \bar{d}_{\theta} g^{ab} \quad \text{and} \quad \bar{d}_J^{ab} = \bar{d}_J g^{ab}$$

where \bar{d}_θ and \bar{d}_J are dissipative control gains. Choosing

$$\begin{aligned} u_{\text{diss}} &= d_\phi \dot{\phi} + [g_{ab} \bar{d}_x^{bc} g_{c\beta}] \dot{\theta} - [D_{ab} \rho^{bc} g_{cd} \bar{d}_J^{de}] \bar{J} \\ &= d_\phi \dot{\phi} + \bar{d}_\theta [g_{\alpha b}] \dot{\theta} - \bar{d}_J [D_{ab} \rho^{bc}] \bar{J} \end{aligned}$$

with $\bar{d}_\theta \geq 0$ and $\bar{d}_J > 0$ exponentially stabilizes the equilibrium (5.56). Note that the dissipative control law attempts to exactly cancel the damping in the controlled direction. While exact cancellation is practically impossible, the exponential stability result of Theorem 5.2.4 ensures a degree of robustness to modeling errors.

Figure 5.6 shows the experimental apparatus. As discussed in Appendix F, the system is well-modeled by the equations developed in this section with the parameter values

$$\begin{aligned} M &= 0.259 \text{ kg}, & R &= 0.211 \text{ m}, & d_\phi &= 0.0096 \text{ Nms}, \\ m &= 0.130 \text{ kg}, & l &= 0.332 \text{ m}, & d_\theta &= 0.00015 \text{ Nms}. \end{aligned}$$

Figure 5.7 shows the experimental results for the control parameters

$$\bar{k} = 2, \quad \bar{d}_\theta = 10 \text{ s}^{-1}, \quad \bar{d}_J = 5 \text{ s}^{-1}.$$

Initially, the pendulum is very near the feedback-stabilized inverted equilibrium. At approximately 2 seconds, the pendulum is perturbed. The system undergoes a damped oscillation, converging once again to near-equilibrium within about 2 seconds.

One discrepancy between the experiment and simulations is a slow, steady drift in the ϕ direction which is apparent in the latter seconds of the experiment shown in Figure 5.7. One explanation is that the symmetry axis of the apparatus is not truly vertical resulting in a bias in the measurement of θ . Any such bias would naturally result in some drift in the ϕ

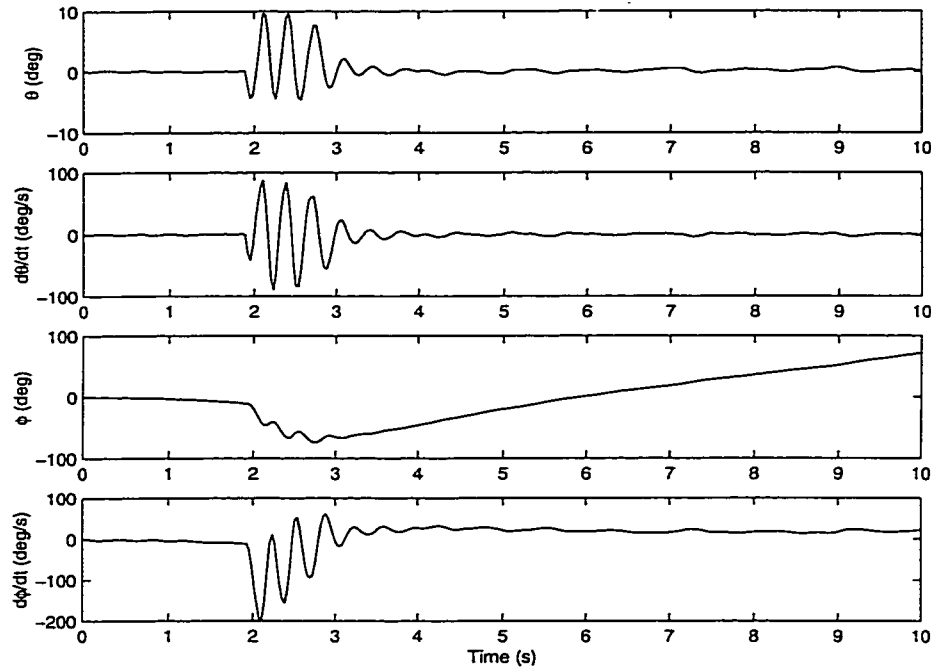


Figure 5.7: Experimental results.

direction. One might reasonably expect drift since the control law preserves the azimuthal symmetry of the system. To eliminate drift, one might employ an additional control torque which breaks the symmetry as described in [10].

5.3 Dissipation and Euler-Poincaré Systems

Recall that in Chapter 4, drag on the feedback-controlled underwater vehicle was shown to enhance stability of steady, long-axis translation. In this section, we consider the effect of physical damping on an entire class of Euler-Poincaré systems which have been stabilized by the method of controlled Lagrangians [18]. We search for a dissipative feedback control law to asymptotically stabilize a closed-loop equilibrium which is stable for a conservative system model. Our approach is similar in spirit to that of Chapter 4. We use a Lyapunov function for the conservative, closed-loop system to study the effect of physical damping and to design the feedback dissipation.

The systems considered here have as their configuration space a product of Lie groups $Q = H \times G$ and they exhibit full symmetry under the actions of H and G . While it is still required that the r -dimensional Lie group G be Abelian, the n -dimensional group H may generally be non-Abelian. Because of the symmetry, the dynamics may be described in a reduced velocity phase space isomorphic to $\mathfrak{h} \oplus \mathfrak{g}$, where \mathfrak{h} and \mathfrak{g} are the Lie algebras of H and G , respectively. Let η^α (where $\alpha \in \{1, 2, \dots, n\}$) be a component of the velocity $\eta \in \mathfrak{h}$ and let $\dot{\theta}^a$ (where $a \in \{1, 2, \dots, r\}$) be a component of the velocity $\dot{\theta} \in \mathfrak{g}$. Define the reduced Lagrangian

$$l(\eta^\alpha, \dot{\theta}^a) = \frac{1}{2}g_{\alpha\beta}\eta^\alpha\eta^\beta + g_{ab}\eta^\alpha\dot{\theta}^b + \frac{1}{2}g_{ab}\dot{\theta}^a\dot{\theta}^b, \quad (5.60)$$

where $g_{\alpha\beta}$, g_{ab} , and $g_{\alpha b}$ are *constant* components of the kinetic energy metric tensor. In the absence of generalized forces other than the control, the open-loop equations are the Euler-Poincaré equations:

$$\frac{d}{dt} \frac{\partial l}{\partial \eta^\alpha} = c_{\alpha\gamma}^\beta \eta^\gamma \frac{\partial l}{\partial \eta^\beta} \quad (5.61)$$

$$\frac{d}{dt} \frac{\partial l}{\partial \dot{\theta}^a} = u_a. \quad (5.62)$$

The coefficients $c_{\alpha\gamma}^\beta$ represent the Lie algebra structure constants for \mathfrak{h} .

Recall that in the Lie-Poisson (Hamiltonian) setting, a Casimir is a function of the momenta which has its gradient in the null space of the Poisson tensor. Define the momentum conjugate to η^α ,

$$M_\alpha = \frac{\partial l}{\partial \eta^\alpha}. \quad (5.63)$$

In the Euler-Poincaré setting, a Casimir $C^k(M_\alpha)$ satisfies

$$\frac{d}{dt}C^k = \frac{\partial C^k}{\partial M_\alpha} \left(\frac{d}{dt}M_\alpha \right) = \frac{\partial C^k}{\partial M_\alpha} \left(c_{\alpha\gamma}^\beta \eta^\gamma \frac{\partial l}{\partial \eta^\beta} \right) = 0.$$

The Casimirs C^k of the non-Abelian group dynamics are conserved for any choice of control. Physically, Casimirs correspond to inertial conservation laws. Since the control acts on the shape space G , which represents internal degrees of freedom, it does not affect the total system momentum. Casimirs are thus conserved under any choice of control.

For systems described by equations (5.61) and (5.62), one is often interested in the stability of a relative equilibrium

$$(\eta^\alpha, \dot{\theta}^a) = (\eta_e^\alpha, \dot{\theta}_e^a)$$

of the uncontrolled dynamics, where η_e^α is nonzero. In terms of the method of controlled Lagrangians, this problem is distinct from the problems considered in Section 5.2.

The method of controlled Lagrangians provides a control-dependent modification of the kinetic energy metric and a choice of control which preserves the Lagrangian structure in the closed-loop system. In this case, one chooses a modified reduced Lagrangian $l_{\tau,\sigma,\rho}$ and a control u_a such that

$$\frac{d}{dt} \frac{\partial l_{\tau,\sigma,\rho}}{\partial \eta^\alpha} = c_{\alpha\gamma}^\beta \eta^\gamma \frac{\partial l_{\tau,\sigma,\rho}}{\partial \eta^\beta} \tag{5.64}$$

$$\frac{d}{dt} \frac{\partial l_{\tau,\sigma,\rho}}{\partial \dot{\theta}^a} = 0. \tag{5.65}$$

Choosing the modified energy in such a way that

$$\frac{\partial l}{\partial \eta^\alpha} = \frac{\partial l_{\tau,\sigma,\rho}}{\partial \eta^\alpha} \quad (5.66)$$

leads to “matching” of equations (5.61) and (5.64), as in equation (5.11). The reduced controlled Lagrangian is

$$\begin{aligned} l_{\tau,\sigma,\rho}(\eta^\alpha, \dot{\theta}^a) &= l(\eta^\alpha, \dot{\theta}^a + \tau_\alpha^a \eta^\alpha) + \frac{1}{2} \sigma_{ab} \tau_\alpha^a \tau_\beta^b \eta^\alpha \eta^\beta \\ &\quad + \frac{1}{2} \varpi_{ab} (\dot{\theta}^a + (g^{ac} g_{c\alpha} + \tau_\alpha^a) \eta^\alpha) (\dot{\theta}^b + (g^{bd} g_{d\beta} + \tau_\beta^b) \eta^\beta) \end{aligned} \quad (5.67)$$

where $\varpi_{ab} = \rho_{ab} - g_{ab}$ [17]. Recall from Section 5.1.3 the Euler-Poincaré matching conditions:

$$\tau_\alpha^a = -\sigma^{ab} g_{b\alpha} \quad \text{and} \quad \sigma^{ab} + \rho^{ab} = g^{ab} \quad (5.68)$$

where ρ_{ab} and σ_{ab} are chosen constant to preserve symmetry. Also recall from (5.20) that these conditions lead to the controlled Lagrangian

$$l_{\tau,\sigma,\rho}(\eta^\alpha, \dot{\theta}^a) = \frac{1}{2} g_{\alpha\beta} \eta^\alpha \eta^\beta + g_{\alpha b} \eta^\alpha \dot{\theta}^b + \frac{1}{2} \rho_{ab} \dot{\theta}^a \dot{\theta}^b. \quad (5.69)$$

One may check that the control law (5.19) which leads to the closed-loop equations (5.64) and (5.65) may also be written as

$$\begin{aligned} u_a &= k_a^\alpha \left(\frac{d}{dt} \frac{\partial l}{\partial \eta^\alpha} \right) \\ &= k_a^\alpha c_{\alpha\beta}^\gamma \eta^\beta \frac{\partial l}{\partial \eta^\gamma} \end{aligned} \quad (5.70)$$

where k_a^α is defined in (5.30). Because of its role in the feedback control law (5.70), k_a^α may

be thought of as a control gain, replacing the previously free parameter ρ_{ab} . Equation (5.70) is often a more convenient expression of the control law than (5.19).

Define the controlled momentum

$$\bar{J}_a = \frac{\partial l_{\tau,\sigma,\rho}}{\partial \dot{\theta}^a} = g_{a\alpha} \eta^\alpha + \rho_{ab} \dot{\theta}^b. \quad (5.71)$$

Written in terms of η^α and \bar{J}_a , the controlled energy takes the block diagonal form

$$E_{\tau,\sigma,\rho}(\eta^\alpha, \bar{J}_a) = \frac{1}{2} A_{\alpha\beta} \eta^\alpha \eta^\beta + \frac{1}{2} \rho^{ab} \bar{J}_a \bar{J}_b, \quad (5.72)$$

where the horizontal kinetic energy metric is

$$A_{\alpha\beta} = g_{\alpha\beta} - g_{a\alpha} \rho^{ab} g_{b\beta}. \quad (5.73)$$

Remark 5.3.1 *The control u_a in equation (5.62) leaves considerable freedom in matching this equation to a desired closed-loop equation such as equation (5.65). Choosing the right-hand side of (5.65) to be zero is somewhat natural in the conservative setting, since this choice conserves \bar{J}_a . Conservation laws simplify stability analysis for the closed-loop system. The choice (5.65) of closed-loop θ^a -dynamics is not unique, however. For example, one might use control to impose Euler-Poincaré equations for some m -dimensional, non-Abelian Lie group with structure constants \bar{c}_{ad}^b (where m is the dimension of the original Lie group G):*

$$\frac{d}{dt} \frac{\partial l_{\tau,\sigma,\rho}}{\partial \dot{\theta}^a} = \bar{c}_{ad}^b \dot{\theta}^d \frac{\partial l_{\tau,\sigma,\rho}}{\partial \dot{\theta}^b}. \quad (5.74)$$

One might imagine a situation where the resulting closed-loop phase space structure is more useful than that due to (5.65). We call this structure-modifying feedback control. (See also

Remark 4.1.12 and [13], [70].)

Rather than pursue the idea of structure-modifying feedback, we continue as in Section 5.2 studying the effect of physical and feedback dissipation on the closed-loop dynamics under the control law given by the method of controlled Lagrangians.

5.3.1 The Effect of Generalized Forces on the Modified Energy

Assume that the control law u_a has been chosen as indicated in (5.70) for the conservative system model. Further, assume that there is a function

$$E_{\bar{\Phi}}(\eta^\alpha, \bar{J}_a) = \frac{1}{2}A_{\alpha\beta}\eta^\alpha\eta^\beta + \frac{1}{2}\rho^{ab}\bar{J}_a\bar{J}_b + \bar{\Phi}(C^k, \bar{J}_a). \quad (5.75)$$

which has a maximum at some desired relative equilibrium

$$(\eta^\alpha, \dot{\theta}^a) = (\eta_e^\alpha, \dot{\theta}_e^a). \quad (5.76)$$

One method of generating such a function is the energy-Casimir method, which imposes conditions on the control gains and on the equilibrium values of the first and second partial derivatives of $\bar{\Phi}$. To illustrate the idea, we proceed with the first step of the method. That is, we seek conditions on $\bar{\Phi}$ for which the equilibrium (5.76) is a critical point of $E_{\bar{\Phi}}$. First, using the notation in [18], define the controlled momentum conjugate to η^α as

$$\begin{aligned} \bar{M}_\alpha &= \frac{\partial l_{\tau,\sigma,\rho}(\eta^\alpha, \dot{\theta}^a)}{\partial \eta^\alpha} = \frac{\partial l(\eta^\alpha, \dot{\theta}^a)}{\partial \eta^\alpha} = g_{\alpha\beta}\eta^\beta + g_{\alpha a}\dot{\theta}^a \\ &= (g_{\alpha\beta} - g_{a\alpha}\rho^{ab}g_{b\beta})\eta^\beta + g_{\alpha a}\rho^{ab}\bar{J}_b \\ &= A_{\alpha\beta}\eta^\beta + g_{\alpha a}\rho^{ab}\bar{J}_b. \end{aligned} \quad (5.77)$$

Note that $\bar{M}_\alpha = M_\alpha$ because of the Euler-Poincaré matching conditions. Recall that the Casimirs C^k depend only on \bar{M}_α ; they are Casimirs of the non-Abelian group dynamics.

For the equilibrium (5.76) to be a critical point, the first variation of $E_{\bar{\Phi}}$ must be zero at the equilibrium,

$$DE_{\bar{\Phi}}|_e \cdot (\delta\eta^\beta, \delta\bar{J}_b) = \left(\eta^\alpha A_{\alpha\beta} + \frac{\partial\bar{\Phi}}{\partial C^k} \frac{\partial C^k}{\partial \bar{M}_\alpha} A_{\alpha\beta} \right) \delta\eta^\beta + \left(\bar{J}_a \rho^{ab} + \frac{\partial\bar{\Phi}}{\partial C^k} \frac{\partial C^k}{\partial \bar{M}_\alpha} g_{\alpha a} \rho^{ab} + \frac{\partial\bar{\Phi}}{\partial \bar{J}_b} \right) \delta\bar{J}_b = 0. \quad (5.78)$$

Since the variations $\delta\eta^\alpha$ and $\delta\bar{J}_a$ are arbitrary, condition (5.78) requires that

$$\left. \frac{\partial\bar{\Phi}}{\partial C^k} \frac{\partial C^k}{\partial \bar{M}_\alpha} \right|_e = -\eta_e^\alpha \quad (5.79)$$

and that

$$\begin{aligned} 0 &= \left(\bar{J}_a \rho^{ab} + \frac{\partial\bar{\Phi}}{\partial C^k} \frac{\partial C^k}{\partial \bar{M}_\alpha} g_{\alpha a} \rho^{ab} + \frac{\partial\bar{\Phi}}{\partial \bar{J}_b} \right)_e \\ &= \left(\rho^{ba} (\bar{J}_a - g_{a\alpha} \eta^\alpha) + \frac{\partial\bar{\Phi}}{\partial \bar{J}_b} \right)_e \\ &= \left(\dot{\theta}^b + \frac{\partial\bar{\Phi}}{\partial \bar{J}_b} \right)_e. \end{aligned} \quad (5.80)$$

In the following analysis, only equilibria for which $\dot{\theta}_e^a = 0$ are considered.

Remark 5.3.2 *It is natural to consider equilibria for which $\dot{\theta}_e^a = 0$. If $\dot{\theta}_e^a \neq 0$, then friction in the internal actuator would require a steady counterforce which might be costly to maintain. Still, this condition could be relaxed in the analysis that follows, perhaps leading to a more general result.*

Continuing, one next requires that the second variation of $E_{\bar{\Phi}}$ be definite when evaluated

at the equilibrium. Often, a simple but adequate choice of $\bar{\Phi}$ is a function which is linear and quadratic in its arguments:

$$\begin{aligned} \bar{\Phi}(C^k, \bar{J}_a) = & \frac{\partial \bar{\Phi}}{\partial C^k} \Big|_e C^k + \frac{\partial \bar{\Phi}}{\partial \bar{J}_a} \Big|_e \bar{J}_a + \frac{\partial^2 \bar{\Phi}}{\partial C^k \partial C^l} \Big|_e \left(\frac{1}{2} (C^k - C_e^k)(C^l - C_e^l) \right) \\ & + \frac{\partial^2 \bar{\Phi}}{\partial C^k \partial \bar{J}_a} \Big|_e \left((C^k - C_e^k)(\bar{J}_a - \bar{J}_{ae}) \right) + \frac{\partial^2 \bar{\Phi}}{\partial \bar{J}_a \partial \bar{J}_b} \Big|_e \left(\frac{1}{2} (\bar{J}_a - \bar{J}_{ae})(\bar{J}_b - \bar{J}_{be}) \right), \end{aligned} \quad (5.81)$$

where the notation $|_e$ indicates that the term is a scalar constant determined by the energy-Casimir method. In proving stability of a given relative equilibrium, the linear terms in (5.81) ensure that the equilibrium is a critical point of $E_{\bar{\Phi}}$, while the quadratic terms provide definiteness of the second variation.

Assume that $E_{\bar{\Phi}} \leq 0$ with equality if and only if the system is at the desired equilibrium. For the conservative system, the controlled energy $E_{\tau, \sigma, \rho}$, the Casimirs C^k , and the controlled conserved quantities \bar{J}_a are all conserved. Then $\frac{d}{dt} E_{\bar{\Phi}} = 0$ and Lyapunov stability follows immediately.

More generally, suppose that the system is subject to generalized forces F_α and F_a . The open-loop equations become

$$\frac{d}{dt} \frac{\partial l}{\partial \eta^\alpha} = c_{\alpha\gamma}^\beta \eta^\gamma \frac{\partial l}{\partial \eta^\beta} + F_\alpha \quad (5.82)$$

$$\frac{d}{dt} \frac{\partial l}{\partial \theta^a} = u_a + F_a. \quad (5.83)$$

To examine the effect of physical and feedback dissipation on closed-loop stability of equilibria, consider the rate of change of $E_{\bar{\Phi}}$ due to the generalized forces F_α and F_a . While $\frac{d}{dt} E_{\bar{\Phi}} = 0$ for the conservative system, the forces F_α and F_a destroy the conservation laws. In general, the *internal* forces F_a destroy conservation of $E_{\tau, \sigma, \rho}$ and \bar{J}_a . These forces do not

affect $C^k(\tilde{M}_\alpha)$ since F_α does not enter the equation for $\frac{d}{dt}\tilde{M}_\alpha$,

$$\frac{d}{dt}\tilde{M}_\alpha = \frac{d}{dt} \frac{\partial l_{\tau,\sigma,\rho}}{\partial \eta^\alpha} = \frac{d}{dt} \frac{\partial l}{\partial \eta^\alpha} = c_{\alpha\gamma}^\beta \eta^\gamma \frac{\partial l}{\partial \eta^\beta} + F_\alpha. \quad (5.84)$$

However, the *external* forces F_α typically destroy all of the conservation laws.

Adapting equation (5.32) to the current problem gives

$$\begin{aligned} \dot{E}_{\tilde{\Phi}} &= A_{\alpha\beta} \eta^\alpha \dot{\eta}^\beta + \rho^{ab} \tilde{J}_a \dot{\tilde{J}}_b + \frac{\partial \tilde{\Phi}}{\partial C^k} \frac{\partial C^k}{\partial \tilde{M}_\alpha} \dot{\tilde{M}}_\alpha + \frac{\partial \tilde{\Phi}}{\partial \tilde{J}_a} \dot{\tilde{J}}_a \\ &= \eta^\alpha A_{\alpha\beta} B^{\beta\gamma} (F_\gamma - g_{\gamma b} g^{bc} F_c) + \tilde{J}_a D^{ab} (F_b - k_b^\beta F_\beta) + \frac{\partial \tilde{\Phi}}{\partial C^k} \frac{\partial C^k}{\partial \tilde{M}_\alpha} \dot{\tilde{M}}_\alpha + \frac{\partial \tilde{\Phi}}{\partial \tilde{J}_a} \dot{\tilde{J}}_a \end{aligned}$$

Using equation (5.31) for $\frac{d}{dt}\tilde{J}_a$ and equation (5.84) for $\frac{d}{dt}\tilde{M}_\alpha$, and noting that $\dot{E}_{\tilde{\Phi}} = 0$ when $F_\alpha = F_a = 0$, one finds that

$$\begin{aligned} \dot{E}_{\tilde{\Phi}} &= \eta^\alpha A_{\alpha\beta} B^{\beta\gamma} (F_\gamma - g_{\gamma b} g^{bc} F_c) \\ &\quad + \tilde{J}_a D^{ab} (F_b - k_b^\beta F_\beta) + \frac{\partial \tilde{\Phi}}{\partial C^k} \frac{\partial C^k}{\partial \tilde{M}_\alpha} F_\alpha + \frac{\partial \tilde{\Phi}}{\partial \tilde{J}_a} \rho_{ab} D^{bc} (F_c - k_c^\beta F_\beta) \end{aligned} \quad (5.85)$$

Assume that $\dot{\theta}_e = 0$ and that $\tilde{\Phi}$ takes the form

$$\tilde{\Phi}(C^k, \tilde{J}_a) = \Phi(C^k) + \Psi(\tilde{J}_a)$$

where Φ is linear and quadratic in its arguments and

$$\Psi(\tilde{J}_a) = \frac{1}{2\psi} \rho^{ab} \tilde{J}_a \tilde{J}_b.$$

The scalar constant ψ is chosen to satisfy conditions imposed during the stability analysis

of the conservative system model. From equation (5.85)

$$\frac{d}{dt}E_{\Phi,\Psi} = \left(\eta^\alpha A_{\alpha\beta} B^{\beta\gamma} + \frac{\partial\Phi}{\partial C^k} \frac{\partial C^k}{\partial \bar{M}_\gamma} \right) F_\gamma - \eta^\alpha g_{\alpha a} D^{ab} F_b + \left(1 + \frac{1}{\psi} \right) \bar{J}_a D^{ab} \left(F_b - k_b^\beta F_\beta \right). \quad (5.86)$$

Remark 5.3.3 (Feedback dissipation with no physical dissipation.) Consider the case in which $F_\alpha = 0$ and let $F_a = D_{ab} \rho^{bc} u_c^{\text{diss}}$ where dissipation is due only to the control u_a^{diss} . Equation (5.86) becomes

$$\frac{d}{dt}E_{\Phi,\Psi} = \left(-g_{\alpha a} \eta^\alpha + \left(1 + \frac{1}{\psi} \right) \bar{J}_a \right) D^{ab} F_b \quad (5.87)$$

$$= \left(-g_{\alpha a} \eta^\alpha + \left(1 + \frac{1}{\psi} \right) \bar{J}_a \right) \rho^{ab} u_b^{\text{diss}} \quad (5.88)$$

This is precisely the case considered in [11]. Clearly, one may choose u_a^{diss} to make $\frac{d}{dt}E_{\bar{\Phi}}$ sign semidefinite with whatever sign is required by the sign of $E_{\bar{\Phi}}$. (For example, if $E_{\bar{\Phi}} \leq 0$, as we have assumed, then one may choose u_a^{diss} to make $\frac{d}{dt}E_{\bar{\Phi}} \geq 0$.) Asymptotic stability of the desired equilibrium may then be studied in the context of LaSalle's invariance principle.

Unfortunately, the negative definite function $E_{\Phi,\Psi}$ is not generally suitable as a Lyapunov function when physical dissipation is present. Although $E_{\Phi,\Psi}$ is conserved when $F_\alpha = F_a = 0$, nonzero generalized forces destroy the conservation laws for the energy $l_{\tau,\sigma,\rho}$, the controlled momenta \bar{J}_a , and the Casimirs C^k . The typical result, similar to the problem described in Proposition 5.2.2, is that a Lyapunov function $E_{\Phi,\Psi}$ developed for a conservative system using these conservation laws will have an indefinite rate in the presence of physical damping, regardless of the choice of feedback dissipation. (The example of a spacecraft with an internal rotor, discussed in Section 5.3.2 below, verifies this observation.) Consider a function $\bar{\Phi}$ of the form (5.81). The terms linear in C^k and \bar{J}_a ensure

that the equilibrium is a critical point. The quadratic terms provide $E_{\bar{\Phi}}$ with the correct definiteness in directions where it is otherwise indefinite or definite in the wrong sense. These quadratic terms can be problematic when drag is included because they can lead to an indefinite energy rate. Alternatively, if the quadratic terms were omitted, one *might* obtain a negative semidefinite function whose rate could be made positive semidefinite by an appropriate choice of feedback dissipation. Stability might then be studied by applying LaSalle's invariance principle to this semidefinite Lyapunov function.

Suppose that a negative semidefinite energy function can be formed by removing from $\Phi(C^k)$ the terms quadratic in C^k . Define

$$\bar{\Phi}(C^k) = \left(\frac{\partial \bar{\Phi}}{\partial C^k} \right)_e C^k. \quad (5.89)$$

Assumption 5.3.4

$$\bar{E}_{\bar{\Phi}, \Psi} = \frac{1}{2} A_{\alpha\beta} \eta^\alpha \eta^\beta + \frac{1}{2} \rho^{ab} \tilde{J}_a \tilde{J}_b + \bar{\Phi}(C^k) + \Psi(\tilde{J}_a) \leq 0. \quad (5.90)$$

The goal is to find a subclass of Euler-Poincaré systems which, having been stabilized by the method of controlled Lagrangians, can be shown to be asymptotically stable in the presence of physical dissipation using a semidefinite energy function of the form (5.90).

It should be noted that assumption 5.3.4 is somewhat restrictive. The assumption holds for the spacecraft with a single internal rotor considered in Section 5.3.2 and for an underwater vehicle with three internal rotors. However, it is not always true that one obtains a semidefinite Lyapunov function by simply truncating quadratic terms from $\Phi(C^k)$. In other words, applying the first two steps of the energy-Casimir method (see page 39)

does not always yield a function which is semidefinite about the critical point.

Suppose the system is subject to physical damping described by the generalized forces $D_\alpha(\eta, \dot{\theta})$ and $D_a(\eta, \dot{\theta})$. In this setting, we will be concerned with stabilizing the relative equilibrium $(\eta, \dot{\theta})_e = (\eta_e, 0)$ which is an unstable relative equilibrium of the uncontrolled, conservative dynamics. Of course, in the presence of physical dissipation, a force must act to oppose the damping when the system is at equilibrium. Assume that there is a constant input force which is equal and opposite to the dissipative force at equilibrium. The open-loop equations of motion become

$$\begin{aligned}\frac{d}{dt} \frac{\partial l}{\partial \eta^\alpha} &= c_{\alpha\gamma}^\beta \eta^\gamma \frac{\partial l}{\partial \eta^\beta} + D_\alpha(\eta, \dot{\theta}) - D_\alpha(\eta_e, 0) \\ \frac{d}{dt} \frac{\partial l}{\partial \dot{\theta}^a} &= u_a + D_a(\eta, \dot{\theta}) - D_a(\eta_e, 0).\end{aligned}$$

Most components of the thrust term $D_\alpha(\eta_e, 0)$ will be zero. Even so, this term obviously requires some additional actuation such as a thruster. This additional control authority might be used in a more sophisticated way. For example, one might choose the thrust to be some function of the velocity. Here, however, it is assumed that the additional input is the constant force $D_\alpha(\eta_e, 0)$.

Physical dissipation can take a variety of forms and general statements are difficult to make. One may reasonably assume that drag opposes velocity,

$$\eta^\alpha D_\alpha(\eta, \dot{\theta}) \begin{cases} < 0 & \eta \neq 0, \\ = 0 & \eta = 0, \end{cases} \quad \text{and} \quad \dot{\theta}^a D_a(\eta, \dot{\theta}) \begin{cases} < 0 & \dot{\theta} \neq 0, \\ = 0 & \dot{\theta} = 0. \end{cases} \quad (5.91)$$

Assumption (5.91) includes a large class of dissipative processes. To simplify the analysis, we make the following stronger assumption on the form of drag.

Assumption 5.3.5

$$\begin{aligned}
 D_a(\eta, \dot{\theta}) &= 0 \\
 &\text{and} \\
 D_\alpha(\eta, \dot{\theta}) &= -d_{\alpha\beta}(\eta^\beta - \eta_e^\beta),
 \end{aligned} \tag{5.92}$$

where $d_{\alpha\beta}$ is a positive definite tensor.

The assumption that $D_a = 0$ is equivalent to assuming that any internal damping is cancelled through feedback. Assuming that D_α does not depend on $\dot{\theta}$ is reasonable, since $\dot{\theta}$ corresponds to internal dynamics whereas the force D_α acts externally. This linear drag model belongs to the class of damping forces known as Rayleigh dissipation. While the assumption of Rayleigh dissipation is restrictive, the results derived here should hold for more general drag models, so long as these models reflect some very basic properties of physical damping. For example, terms which are higher order in velocity may be introduced so long as drag always "opposes" velocity in the sense of (5.91).

Recall equation (5.86) for the rate of change of $E_{\bar{\Phi}, \Psi}$,

$$\begin{aligned}
 \frac{d}{dt} E_{\bar{\Phi}, \Psi} &= \left(\eta^\alpha A_{\alpha\beta} B^{\beta\gamma} + \frac{\partial \bar{\Phi}}{\partial C^k} \frac{\partial C^k}{\partial \bar{M}_\gamma} \right) (-d_{\gamma\psi}(\eta^\psi - \eta_e^\psi)) - \eta^\alpha g_{\alpha a} D^{ab} F_b \\
 &\quad + \left(1 + \frac{1}{\psi} \right) \bar{J}_a D^{ab} \left(F_b - k_b^\beta (-d_{\beta\gamma}(\eta^\gamma - \eta_e^\gamma)) \right)
 \end{aligned} \tag{5.93}$$

Assumption 5.3.6

$$C^k = \frac{1}{2} h^{k\alpha\beta} \bar{M}_\alpha \bar{M}_\beta$$

where $h^{k\alpha\beta}$ is constant and symmetric.

Assumption 5.3.6 holds for a number of systems of physical interest including the spacecraft, the underwater vehicle, and the heavy top. Substituting for the gradient of C^k in (5.93),

$$\begin{aligned} \frac{d}{dt} E_{\bar{\Phi}, \Psi} = & \\ & \left(\eta^\alpha A_{\alpha\beta} B^{\beta\gamma} + \left(\eta^\alpha A_{\alpha\beta} + \bar{J}_a \rho^{ab} g_{b\beta} \right) \frac{\partial \bar{\Phi}}{\partial C^k} h^{k\beta\gamma} - \left(1 + \frac{1}{\psi} \right) \bar{J}_a D^{ab} k_b^\gamma \right) (-d_{\gamma\psi} (\eta^\psi - \eta_e^\psi)) \\ & + \left(-\eta^\alpha g_{\alpha a} + \left(1 + \frac{1}{\psi} \right) \bar{J}_a \right) D^{ab} F_b. \end{aligned} \quad (5.94)$$

To condense notation, define

$$X_{\alpha\beta} = A_{\alpha\gamma} \left(B^{\gamma\psi} + \frac{\partial \bar{\Phi}}{\partial C^k} h^{k\gamma\psi} \right) (-d_{\psi\beta}) \quad (5.95)$$

$$Y_\alpha^a = \left(\rho^{ab} g_{b\beta} \frac{\partial \bar{\Phi}}{\partial C^k} h^{k\beta\gamma} - \left(1 + \frac{1}{\psi} \right) D^{ab} k_b^\gamma \right) (-d_{\gamma\alpha}). \quad (5.96)$$

We also make the following assumption.

Assumption 5.3.7 η_e^α is in the null space of $X_{\alpha\beta}$ and Y_α^a .

This assumption holds, for example, for the spacecraft problem considered in Section 5.3.2.

Under Assumption 5.3.7, the rate of change of $E_{\bar{\Phi}, \Psi}$ does not depend on η_e^α and

$$\frac{d}{dt} E_{\bar{\Phi}, \Psi} = \eta^\alpha X_{\alpha\beta} \eta^\beta + \eta^\alpha Y_\alpha^a \bar{J}_a + \left(-\eta^\alpha g_{\alpha a} + \left(1 + \frac{1}{\psi} \right) \bar{J}_a \right) D^{ab} F_b. \quad (5.97)$$

Consider the dissipative feedback control law

$$F_a = D_{ab} \bar{d}^{bc} \left(-g_{c\beta} \eta^\beta + \left(1 + \frac{1}{\psi} \right) \bar{J}_c \right) \quad (5.98)$$

where \bar{d}^{bc} represents a control gain. Substituting into equation (5.97) and using Assump-

tion 5.3.7 gives

$$\frac{d}{dt}E_{\bar{\Phi},\Psi} = \begin{pmatrix} [\bar{J}_a] \\ [\eta^\alpha] \end{pmatrix} \cdot \begin{pmatrix} P & Q \\ R & S \end{pmatrix} \begin{pmatrix} [\bar{J}_b] \\ [\eta^\beta] \end{pmatrix} \quad (5.99)$$

where

$$\begin{aligned} P &= \left(1 + \frac{1}{\psi}\right)^2 [\bar{d}^{ab}] \\ Q &= -\left(1 + \frac{1}{\psi}\right) [\bar{d}^{ac} g_{c\beta}] \\ R &= \left[Y_\alpha^b - \left(1 + \frac{1}{\psi}\right) g_{\alpha c} \bar{d}^{cb}\right] \\ S &= [X_{\alpha\beta} + g_{\alpha c} \bar{d}^{cd} g_{d\beta}]. \end{aligned}$$

Suppose that the dissipative feedback gain \bar{d}_{ab} is chosen to be symmetric and positive definite. Then the remaining conditions on \bar{d}_{ab} under which $\frac{d}{dt}E_{\bar{\Phi},\Psi} \geq 0$, can be obtained from the following lemma.

Lemma 5.3.8 *The square matrix*

$$\begin{pmatrix} A & B \\ C & D \end{pmatrix}$$

with $A = A^T > 0$ is positive semidefinite provided

$$(D - CA^{-1}B) + (D - CA^{-1}B)^T - B^T A^{-1}B - CA^{-1}C^T \geq 0.$$

Proof. Given vectors \mathbf{x} and \mathbf{y} of compatible size,

$$\begin{pmatrix} \mathbf{x} \\ \mathbf{y} \end{pmatrix} \cdot \begin{pmatrix} A & B \\ C & D \end{pmatrix} \begin{pmatrix} \mathbf{x} \\ \mathbf{y} \end{pmatrix} = \begin{pmatrix} \mathbf{x} \\ \mathbf{y} \end{pmatrix} \cdot \begin{pmatrix} \bar{A} & \bar{B} \\ \bar{B}^T & \bar{D} \end{pmatrix} \begin{pmatrix} \mathbf{x} \\ \mathbf{y} \end{pmatrix}$$

where

$$2 \begin{pmatrix} \bar{A} & \bar{B} \\ \bar{B}^T & \bar{D} \end{pmatrix} = \begin{pmatrix} A & B \\ C & D \end{pmatrix} + \begin{pmatrix} A & B \\ C & D \end{pmatrix}^T.$$

But $A = A^T$, so $\bar{A} = A$. One may easily verify that

$$\begin{pmatrix} x \\ y \end{pmatrix} \cdot \begin{pmatrix} \bar{A} & \bar{B} \\ \bar{B}^T & \bar{D} \end{pmatrix} \begin{pmatrix} x \\ y \end{pmatrix} = y \cdot (\bar{D} - \bar{B}^T A^{-1} \bar{B}) y + (x + A^{-1} \bar{B} y) \cdot A (x + A^{-1} \bar{B} y).$$

The latter term is positive definite. Therefore, one requires that

$$\bar{D} - \bar{B}^T A^{-1} \bar{B} = (D - CA^{-1}B) + (D - CA^{-1}B)^T - B^T A^{-1} B - CA^{-1}C^T \geq 0. \quad (5.100)$$

□

Applying Lemma 5.3.8 to the matrix in equation (5.99),

$$\begin{aligned} S - RP^{-1}Q &= \begin{bmatrix} X_{\alpha\beta} + g_{\alpha c} \bar{d}^{cd} g_{d\beta} \\ - \left(Y_{\alpha}^a - \left(1 + \frac{1}{\psi} \right) g_{\alpha c} \bar{d}^{ca} \right) \left(1 + \frac{1}{\psi} \right)^{-2} \bar{d}_{ab} \left(- \left(1 + \frac{1}{\psi} \right) \bar{d}^{bd} g_{d\beta} \right) \end{bmatrix} \\ &= \begin{bmatrix} X_{\alpha\beta} + \left(1 + \frac{1}{\psi} \right)^{-1} Y_{\alpha}^a g_{a\beta} \end{bmatrix} \\ Q^T P^{-1} Q &= \begin{bmatrix} g_{\alpha a} \bar{d}^{ab} g_{b\beta} \end{bmatrix} \\ RP^{-1}R^T &= \begin{bmatrix} Y_{\alpha}^a - \left(1 + \frac{1}{\psi} \right) g_{\alpha c} \bar{d}^{ca} \right) \left(1 + \frac{1}{\psi} \right)^{-2} \bar{d}_{ab} \left(Y_{\beta}^b - \left(1 + \frac{1}{\psi} \right) \bar{d}^{bd} g_{d\beta} \right) \\ \left(1 + \frac{1}{\psi} \right)^{-2} Y_{\alpha}^a \bar{d}_{ab} Y_{\beta}^b - \left(1 + \frac{1}{\psi} \right)^{-1} \left(Y_{\alpha}^a g_{a\beta} + g_{\alpha a} Y_{\beta}^a \right) + g_{\alpha a} \bar{d}^{ab} g_{b\beta} \end{bmatrix}. \end{aligned}$$

Substituting into condition (5.100), one obtains the following theorem.

Theorem 5.3.9 *Suppose feedback dissipation of the form (5.98) is chosen with \bar{d}_{ab} sym-*

metric and positive definite. Then $\frac{d}{dt}E_{\bar{\phi},\psi} \geq 0$ provided \bar{d}_{ab} can also be chosen to satisfy

$$\left[X_{\alpha\beta} + X_{\beta\alpha} - \left(1 + \frac{1}{\psi}\right)^{-2} Y_{\alpha}^a \bar{d}_{ab} Y_{\beta}^b + 2 \left(1 + \frac{1}{\psi}\right)^{-1} (Y_{\alpha}^a g_{a\beta} + g_{\beta\alpha} Y_{\alpha}^a) - 2g_{\alpha\alpha} \bar{d}^{ab} g_{b\beta} \right] \geq 0. \quad (5.101)$$

In the following section, Theorem 5.3.9 is applied to the example of a spacecraft with a single internal rotor actuator.

5.3.2 Example: The rigid spacecraft with one internal rotor

Consider a rigid body with an internal rotor aligned with the third principal axis of the body. The rotor spins under the influence of a control torque u . The problem of stabilizing steady intermediate axis rotation of the body using the method of controlled Lagrangians was first considered in [15] and then further in [18, 11]. The configuration space is $Q = SO(3) \times S^1$, with the first factor $H = SO(3)$ representing the spacecraft attitude and the second factor $G = S^1$ representing the rotor angle. The Lagrangian is the total kinetic energy of the system.

Open-Loop Dynamics. The reduced Lagrangian on $so(3) \times \mathbb{R}$ is

$$l(\Omega, \dot{\phi}) = \frac{1}{2} \begin{pmatrix} \Omega_1 \\ \Omega_2 \\ \Omega_3 \\ \dot{\phi} \end{pmatrix} \cdot \begin{pmatrix} \lambda_1 & 0 & 0 & 0 \\ 0 & \lambda_2 & 0 & 0 \\ 0 & 0 & \lambda_3 & J_3 \\ 0 & 0 & J_3 & J_3 \end{pmatrix} \begin{pmatrix} \Omega_1 \\ \Omega_2 \\ \Omega_3 \\ \dot{\phi} \end{pmatrix} \quad (5.102)$$

where $\Omega = (\Omega_1, \Omega_2, \Omega_3)^T$ is the angular velocity of the carrier and ϕ is the relative angle of the rotor. The rigid body moments of inertia are $I_1 > I_2 > I_3$ and the rotor moments

of inertia are $J_1 = J_2$ and J_3 . It is also convenient to define the components of the *locked* inertia, $\lambda_i = I_i + J_i$ for $i = 1, 2, 3$. Assume that $\lambda_1 > \lambda_2 > \lambda_3$. In the notation of previous sections,

$$[g_{\alpha\beta}] = \begin{pmatrix} \lambda_1 & 0 & 0 \\ 0 & \lambda_2 & 0 \\ 0 & 0 & \lambda_3 \end{pmatrix}, \quad [g_{ab}] = [g_{\alpha\beta}]^T = \begin{pmatrix} 0 \\ 0 \\ J_3 \end{pmatrix}, \quad [g_{ab}] = J_3.$$

The components of body angular momentum are

$$[\tilde{M}_\alpha] = \frac{\partial l}{\partial \Omega} = \begin{pmatrix} \lambda_1 \Omega_1 \\ \lambda_2 \Omega_2 \\ \lambda_3 \Omega_3 + J_3 \dot{\phi} \end{pmatrix}.$$

The momentum conjugate to ϕ is

$$\frac{\partial l}{\partial \dot{\phi}} = l_3 = J_3(\Omega_3 + \dot{\phi}).$$

With a control torque u acting on the internal rotor, the equations of motion are

$$\begin{aligned} \frac{d}{dt} \frac{\partial l}{\partial \Omega} &= -\hat{\Omega} \frac{\partial l}{\partial \Omega} \\ \frac{d}{dt} \frac{\partial l}{\partial \dot{\phi}} &= u. \end{aligned}$$

A Casimir for the system is the magnitude of the total angular momentum,

$$C = \frac{1}{2} \frac{\partial l}{\partial \Omega} \cdot \frac{\partial l}{\partial \Omega} = \frac{1}{2} \left((\lambda_1 \Omega_1)^2 + (\lambda_2 \Omega_2)^2 + (\lambda_3 \Omega_3 + J_3 \dot{\phi})^2 \right). \quad (5.103)$$

The Controlled Lagrangian System. Since the Abelian group $G = S^1$ is one-dimensional, g_{ab} , σ_{ab} and ρ_{ab} are all scalars. Given that $[g_{ab}] = J_3$, we let $[\sigma_{ab}] = \sigma J_3$ and $[\rho_{ab}] = \rho J_3$ where σ and ρ are dimensionless scalars. For matching, ρ should satisfy

$$\frac{1}{\sigma J_3} + \frac{1}{\rho J_3} = \frac{1}{J_3}, \quad \text{i.e.} \quad \sigma = \frac{\rho}{\rho - 1}. \quad (5.104)$$

The controlled Lagrangian is

$$l_{\tau,\sigma,\rho}(\Omega, \dot{\phi}) = \frac{1}{2} (\lambda_1 \Omega_1^2 + \lambda_2 \Omega_2^2 + I_3 \Omega_3^2) + J_3 \Omega_3 \dot{\phi} + \frac{1}{2} \rho J_3 \dot{\phi}^2. \quad (5.105)$$

Define a new control parameter k in terms of ρ ,

$$k = \left(1 + \frac{\rho}{\rho - 1} \frac{I_3}{J_3} \right)^{-1}.$$

The method of controlled Lagrangians provides the control law

$$u = u_{\text{cL}} = k(\lambda_1 - \lambda_2)\Omega_1\Omega_2 \quad (5.106)$$

which gives closed-loop equations that derive from the Lagrangian (5.105):

$$\begin{aligned} \frac{d}{dt} \frac{\partial l_{\tau,\sigma,\rho}}{\partial \Omega} &= -\hat{\Omega} \frac{\partial l_{\tau,\sigma,\rho}}{\partial \Omega} \\ \frac{d}{dt} \frac{\partial l_{\tau,\sigma,\rho}}{\partial \dot{\phi}} &= 0. \end{aligned}$$

Notice the controlled conserved quantity

$$\bar{l}_3 = \frac{\partial l_{\tau,\sigma,\rho}}{\partial \dot{\phi}} = J_3(\Omega_3 + \rho \dot{\phi}).$$

For this example

$$[A_{\alpha\beta}] = [g_{\alpha\beta} - g_{\alpha a} \rho^{ab} g_{b\beta}] = \begin{pmatrix} \lambda_1 & 0 & 0 \\ 0 & \lambda_2 & 0 \\ 0 & 0 & I_3 + \frac{\rho-1}{\rho} J_3 \end{pmatrix}.$$

Because it has units of inertia and is parameterized by ρ , define the “controlled inertia”

$$I_{C_3} = I_3 + \frac{\rho-1}{\rho} J_3.$$

Using $[A_{\alpha\beta}]$, the controlled energy may be written according to equation (5.72) as

$$l_{\tau,\sigma,\rho}(\Omega, \bar{l}_3) = \frac{1}{2} \Omega \cdot \begin{pmatrix} \lambda_1 & 0 & 0 \\ 0 & \lambda_2 & 0 \\ 0 & 0 & I_{C_3} \end{pmatrix} \Omega + \frac{\bar{l}_3^2}{2\rho J_3}.$$

Stability of Steady Intermediate-axis Rotation. Consider the equilibrium

$$\Omega_e = \begin{pmatrix} 0 \\ \bar{\Omega} \\ 0 \end{pmatrix}, \quad \dot{\phi}_e = 0, \quad (5.107)$$

where $\bar{\Omega} \neq 0$. This equilibrium corresponds to steady rotation about the intermediate axis and is unstable for the uncontrolled spacecraft.

The control law (5.106) can be shown to stabilize the equilibrium (5.107) for appropriate choices of k (equivalently, ρ). Conditions on k for stability may be found by applying the

energy-Casimir method to the augmented energy

$$E_{\Phi, \Psi}(\Omega, \bar{l}_3) = l_{\tau, \sigma, \rho}(\Omega, \bar{l}_3) + \Phi(C) + \Psi(\bar{l}_3) \quad (5.108)$$

where

$$C(\Omega, \bar{l}_3) = \frac{1}{2} \left[(\lambda_1 \Omega_1)^2 + (\lambda_2 \Omega_2)^2 + \left(I_{C_3} \Omega_3 + \frac{1}{\rho} \bar{l}_3 \right)^2 \right].$$

Let

$$\Psi(\bar{l}_3) = \frac{\bar{l}_3^2}{2\psi\rho J_3}$$

In proving nonlinear stability of the equilibrium (5.107), one first requires that it be a critical point of $E_{\Phi, \Psi}$:

$$\begin{aligned} (DE_{\Phi, \Psi})_e \cdot (\delta\Omega, \delta\bar{l}_3) = 0 = & \left([A_{\alpha\beta}] \Omega_e + \left(\frac{\partial\Phi}{\partial C} \right)_e \begin{pmatrix} \lambda_1^2 \Omega_1 \\ \lambda_2^2 \Omega_2 \\ I_{C_3} (I_{C_3} \Omega_3 + \frac{1}{\rho} \bar{l}_3) \end{pmatrix} \right) \cdot \delta\Omega \\ & + \left(\left(1 + \frac{1}{\psi} \right) \frac{\bar{l}_{3e}}{\rho J_3} + \left(\frac{\partial\Phi}{\partial C} \right)_e \frac{1}{\rho} \left(I_{C_3} \Omega_3 + \frac{1}{\rho} \bar{l}_3 \right)_e \right) \cdot \delta\bar{l}_3. \end{aligned}$$

This requirement is satisfied by choosing Φ such that

$$\left(\frac{\partial\Phi}{\partial C} \right)_e = -\frac{1}{\lambda_2}.$$

Next, one requires that the equilibrium be either a maximum or a minimum of $E_{\Phi, \Psi}$. This will be true if the matrix of the second variation of $E_{\Phi, \Psi}$ is definite when evaluated at the

equilibrium. The matrix of the second variation evaluated at the equilibrium is

$$\begin{pmatrix} \lambda_1 \left(1 - \frac{\lambda_1}{\lambda_2}\right) & 0 & 0 & 0 \\ 0 & (\lambda_2^2 \bar{\Omega})^2 \left(\frac{\partial^2 \Phi}{\partial C^2}\right)_e & 0 & 0 \\ 0 & 0 & I_{C_3} \left(1 - \frac{I_{C_3}}{\lambda_2}\right) & -\frac{I_{C_3}}{\lambda_2 \rho} \\ 0 & 0 & -\frac{I_{C_3}}{\lambda_2 \rho} & \left(1 + \frac{1}{\psi}\right) \frac{1}{\rho J_3} - \frac{1}{\lambda_2} \left(\frac{1}{\rho}\right)^2 \end{pmatrix}. \quad (5.109)$$

Since the first diagonal element is negative, the matrix must be negative definite for $E_{\Phi, \psi}$ to be a Lyapunov function. The second diagonal element is negative provided one chooses Φ such that

$$\left(\frac{\partial^2 \Phi}{\partial C^2}\right)_e < 0.$$

The third diagonal element is negative if

$$k > 1 - \frac{I_3}{\lambda_2} \quad (k \neq 1).$$

If $1 - \frac{I_3}{\lambda_2} < k < 1$, then I_{C_3} is positive. If $k > 1$, then I_{C_3} is negative. In either case, the third diagonal element in the matrix of the second variation is negative. Assume that $k > 1$, which corresponds to choosing ρ such that

$$-\frac{J_3}{I_3} < \frac{\rho}{\rho - 1} < 0 \quad \text{or} \quad 0 < \rho < \frac{J_3}{J_3 + I_3}.$$

The final condition for the second variation evaluated at equilibrium to be negative definite is that ψ be chosen to satisfy

$$\left(1 + \frac{1}{\psi}\right) < \frac{J_3}{\rho(\lambda_2 - I_{C_3})} \quad (5.110)$$

Assuming k and ψ are chosen according to the requirements above, a negative definite Lyapunov function for the equilibrium (5.107) is

$$E_{\Phi, \Psi}(\Omega, \tilde{l}_3) = l_{\tau, \sigma, \rho}(\Omega, \tilde{l}_3) - \frac{1}{\lambda_2} C + \Phi_e^{11} \frac{1}{2} (C - C_e)^2 + \frac{\tilde{l}_3^2}{2\psi\rho J_3},$$

where

$$\Phi_e^{11} < 0.$$

As was shown in [11], an appropriate choice of feedback dissipation leads to asymptotic stability, in the conservative setting. While a spacecraft is arguably free from external damping, consider the effect of drag as a simple illustration of the ideas developed in Section 5.3.1.

The Effect of External Damping. Now, assume that the spacecraft is subject to an external damping torque $-D\Omega$ where $D = \text{diag}(d_1, d_2, d_3) > 0$. Also, assume that an external “propulsive” torque $D\Omega_e$ acts on the spacecraft. The revised open-loop equations of motion are

$$\frac{d}{dt} \frac{\partial l}{\partial \Omega} = -\hat{\Omega} \frac{\partial l}{\partial \Omega} - D(\Omega - \Omega_e) \quad (5.111)$$

$$\frac{d}{dt} \frac{\partial l}{\partial \dot{\phi}} = u. \quad (5.112)$$

Choose the new control law

$$u = u_{cL} + u_{\text{diss}} \quad (5.113)$$

where u_{cL} is given by (5.106) and u_{diss} is a dissipative feedback term to be chosen.

Because the rate of change of $E_{\Phi, \Psi}$ is indefinite regardless of the choice of feedback dissipation, $E_{\Phi, \Psi}$ cannot be a Lyapunov function. (See Remark 5.3.11.) Consider instead

the negative semidefinite function

$$\bar{E}_{\bar{\Phi}, \Psi} = l_{\tau, \sigma, \rho}(\eta^\alpha, \bar{J}_a) + \bar{\Phi}(C) + \Psi(\bar{l}_3). \quad (5.114)$$

where

$$\bar{\Phi}(C) = -\frac{1}{\lambda_2} C.$$

In accordance with Assumption 5.3.6, we may write $C = \frac{1}{2} h^{1\alpha\beta} \bar{M}_\alpha \bar{M}_\beta$ where

$$[h^{1\alpha\beta}] = \mathcal{I}.$$

According to definitions (5.95) and (5.96),

$$\begin{aligned} [X_{\alpha\beta}] &= \begin{pmatrix} \lambda_1 & 0 & 0 \\ 0 & \lambda_2 & 0 \\ 0 & 0 & I_{C_3} \end{pmatrix} \left[\begin{pmatrix} \frac{1}{\lambda_1} & 0 & 0 \\ 0 & \frac{1}{\lambda_2} & 0 \\ 0 & 0 & \frac{1}{\lambda_3} \end{pmatrix} - \frac{1}{\lambda_2} \mathcal{I} \right] (-D) \\ &= \text{diag} \left(-\left(1 - \frac{\lambda_1}{\lambda_2}\right) d_1, 0, -I_{C_3} \left(\frac{1}{\lambda_3} - \frac{1}{\lambda_2}\right) d_3 \right) \end{aligned}$$

and

$$\begin{aligned} [Y_\alpha^a] &= \left(0, 0, -\frac{1}{\rho\lambda_2} - \left(1 + \frac{1}{\psi}\right) \frac{\rho-1}{\rho} \frac{1}{I_3} \right) (-D) \\ &= \left(0, 0, \left(\frac{1}{\rho\lambda_2} + \left(1 + \frac{1}{\psi}\right) \frac{\rho-1}{\rho I_3}\right) d_3 \right) \end{aligned}$$

As required by Assumption 5.3.7, Ω_e is in the null space of $[X_{\alpha\beta}]$ and $[Y_\alpha^a]$.

Define the dissipative feedback gain

$$[\bar{d}_{ab}] = \frac{J_3}{\bar{d}}$$

where \bar{d} is a scalar gain. According to (5.98), let

$$\begin{aligned} u_{\text{diss}} &= \left[D_{ab} \bar{d}^{bc} \left(-g_{c\beta} \eta^\beta + \left(1 + \frac{1}{\psi} \right) \bar{J}_c \right) \right] \\ &= \left(\frac{1}{J_3} + \frac{\rho - 1}{\rho} \frac{1}{I_3} \right)^{-1} \frac{\bar{d}}{J_3} \left(-J_3 \Omega_3 + \left(1 + \frac{1}{\psi} \right) \bar{l}_3 \right). \end{aligned} \quad (5.115)$$

Theorem 5.3.9 gives conditions on the dissipative feedback gain \bar{d} for asymptotic stability.

In Appendix G, it is shown that choosing

$$\bar{d} = \left(\frac{\left(\frac{1}{\rho \lambda_2} + \left(1 + \frac{1}{\psi} \right) \frac{\rho - 1}{\rho} \frac{1}{I_3} \right)^2}{\left(1 + \frac{1}{\psi} \right)^2 \left(-\frac{I_{C_3}}{J_3} \left(\frac{1}{\lambda_3} - \frac{1}{\lambda_2} \right) + 2 \left(\frac{1}{\left(1 + \frac{1}{\psi} \right) \rho \lambda_2} + \frac{\rho - 1}{\rho} \frac{1}{I_3} \right) \right)} \right) d_3 > 0 \quad (5.116)$$

with

$$0 < 1 + \frac{1}{\psi} < \min \left(-\frac{I_3}{(\rho - 1)\lambda_2}, \frac{J_3}{\rho(\lambda_2 - I_{C_3})} \right) \quad (5.117)$$

makes $\dot{E}_{\bar{\Phi}, \bar{\Psi}} \geq 0$.

LaSalle's invariance principle is applicable to systems with semidefinite Lyapunov functions. However, the task of finding a trapping region is hindered by the semidefiniteness; one may no longer define a compact set simply by bounding the value of the Lyapunov function. For this example, however, one may find a compact, positively invariant set by using a physical argument similar to the argument used to define the set B_2 on page 107. Since drag increases linearly with angular velocity and the propulsive torque is constant, the magnitude of body angular rate $\|\Omega\|$ must be bounded. The Casimir $C = \frac{1}{2} \left\| \frac{\partial l}{\partial \Omega} \right\|^2$ may

be used to define a (noncompact) positively invariant region whose boundary is determined by this “maximum sustainable angular rate.” Another (noncompact) positively invariant region may be defined by bounding the value of $\bar{E}_{\bar{\Phi},\Psi}$. The intersection of these two sets is compact and positively invariant. Thus, LaSalle’s principle may be applied within this region.

Examining the dynamics on the set where $\frac{d}{dt}\bar{E}_{\bar{\Phi},\Psi} = 0$, one finds that

$$\lambda_2 \dot{\Omega}_2 = -d_2(\Omega_2 - \bar{\Omega}).$$

The largest invariant set within the set where $\frac{d}{dt}\bar{E}_{\bar{\Phi},\Psi} = 0$ contains only the desired equilibrium (5.107). Thus, one may conclude that the equilibrium is asymptotically stable. In fact, since the trapping region determined by the method outline above is radially unbounded, one may conclude global asymptotic stability.

Theorem 5.3.10 (Global Asymptotic Stability of Steady Intermediate Axis Rotation with Drag) *Consider the control law (5.113) with u_{diss} given by (5.115). If $k > 1$, \bar{d} satisfies condition (5.116) and ψ satisfies condition (5.117), the equilibrium (5.107) is globally asymptotically stable.*

Remark 5.3.11 *If one considers the original negative definite function $E_{\Phi,\Psi}$ rather than $\bar{E}_{\bar{\Phi},\Psi}$, one finds that $\frac{d}{dt}E_{\Phi,\Psi}$ is indefinite. As a simple illustration of this fact, assume that at an instant $\Omega_1 = \Omega_3 = 0$ and $\bar{l}_3 = 0$. Then, at that instant,*

$$\frac{d}{dt}E_{\Phi,\Psi} = \left(\frac{\partial^2 \Phi}{\partial C^2} \right)_e (C - C_e)(\lambda_2 \Omega_2)(-d_2(\Omega_2 - \bar{\Omega})).$$

Since $(C - C_e)(\Omega_2 - \bar{\Omega}) > 0$ in this special case, the sign of $\frac{d}{dt}E_{\Phi,\Psi}$ depends on the sign of

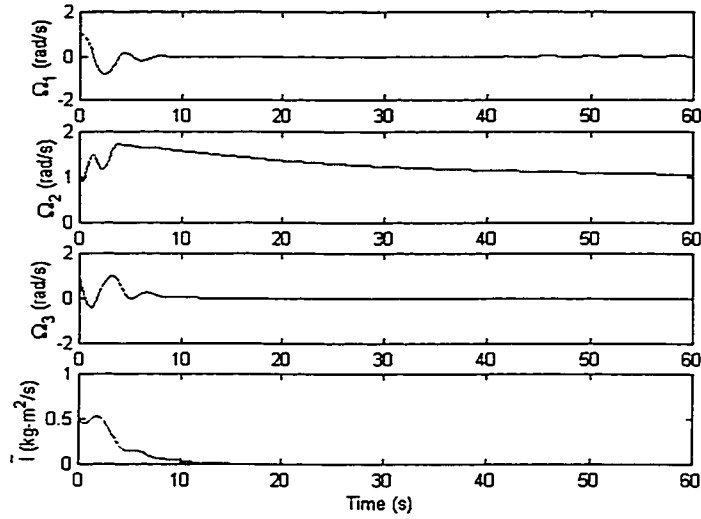


Figure 5.8: Closed-loop spacecraft response to an initial perturbation.

Ω_2 . Therefore, $\frac{d}{dt} E_{\Phi, \Psi}$ is indefinite under the influence of drag, as modeled.

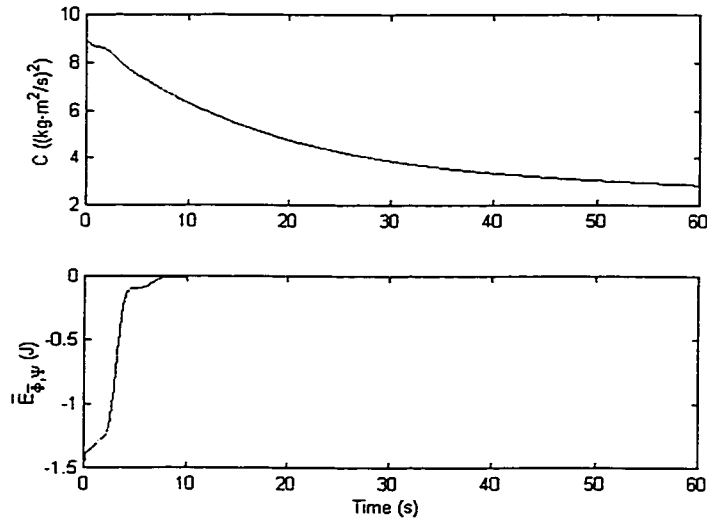


Figure 5.9: The Casimir and Lyapunov function.

The stability result of Theorem 5.3.10 is confirmed in the simulation shown in Figure 5.8. Figure 5.9 shows the time history of the Casimir C and the semidefinite Lyapunov function $\bar{E}_{\Phi, \Psi}$. The parameters used in the simulation were to reflect the assumed principal inertia

ordering, but are otherwise arbitrary:

$$I_1 = 3 \text{ kg m}^2, \quad I_2 = 2 \text{ kg m}^2, \quad I_3 = 1 \text{ kg m}^2,$$

$$J_1 = J_2 = 0.25 \text{ kg m}^2, \quad J_3 = 0.5 \text{ kg m}^2.$$

The physical damping coefficients were $d_1 = d_2 = d_3 = 0.1 \text{ kg m}^2/\text{s}$. The remaining parameters were chosen as

$$k = 2.5 (\rho = 0.23), \quad \psi = -1.1, \quad \bar{d} = 1.5.$$

The desired equilibrium was steady rotation about the intermediate axis (the 2-axis) at 1 rad/s. (Once again, this choice was arbitrary.) The initial condition for the simulation was

$$\Omega_0 = (1, 1, 1) \text{ rad/s} \quad \bar{l}_0 = 0.5 \text{ kgm}^2/\text{s}.$$

As is evident in the simulation results of Figure 5.8, the perturbations in Ω_1 , Ω_3 , and \bar{l} decay within ten seconds. Once the spacecraft is rotating purely about its intermediate axis, the dynamics are governed by the linear damping and the constant propulsive torque. Additional control authority over the propulsive torque could produce even faster convergence to the equilibrium spin rate $\Omega_2 = 1 \text{ rad/s}$.

Chapter 6

Conclusions and Future Work

The principal, unifying theme for this work is feedback stabilization from a geometric mechanical perspective. The idea of reduction by symmetry leads to the low-dimensional model of an underwater vehicle with rotors used in Chapters 3 and 4. The first step in the control design, originally based on the insightful work of Krishnaprasad [40] and Bloch *et al* [13], may be derived using the elegant idea of kinetic energy shaping, i.e., the method of controlled Lagrangians [17]. Proof of stability via the energy-Casimir method and Lyapunov-based design of feedback dissipation are also geometric in nature.

A secondary theme arises from a concern over the effect of drag on the underwater vehicle stabilization results. The question about the effect of physical dissipation in this particular system led to the more general inquiry, described in Chapter 5, into the effect of damping on controlled Lagrangian systems.

In Section 6.1, we summarize the results presented here. Section 6.2 describes a few ideas for future investigation.

6.1 Summary

Leonard [42] studied the dynamics of ellipsoidal underwater vehicles modeled using Kirchhoff's equations for a rigid body in a perfect fluid. Stability criteria for various translational relative equilibria gave conditions on angular rate and CG location for nonlinear stability. Leonard and Woolsey [45] later considered the possibility of providing gyroscopic stability using an internal rotor rather than by spinning the body. Since these predictions were developed assuming an inviscid fluid, concern arose over the effect of viscosity. Chapter 3 reviews the equilibria and their predicted stability properties and also describes an experimental investigation of the criteria. The experiments involved launching a bottom-heavy prolate spheroid with an internal rotor along its symmetry axis in the direction of gravity. While the critical parametric conditions for stability were not finely resolved, the experiments indicate that the stability conditions based on the ideal fluid model are somewhat conservative. This result is physically reasonable. One would expect flow separation on the aft, leeward side of a prolate spheroid whose symmetry axis is slightly misaligned with the flow. The low-pressure, separated flow would tend to realign the symmetry axis with the flow. (This viscous effect alone is not enough, however, to overcome the destabilizing fluid moment predicted by potential flow theory. Thus, stability requires some other mechanism such as a low CG or gyroscopic stabilization.)

In Chapter 4, a control law is proposed for an underwater vehicle with three internal rotors as actuators. The development takes place in three stages:

1. Stabilize a conservative model of the system by shaping kinetic energy,
2. Add feedback dissipation to achieve asymptotic stability,
3. Examine the effect of physical dissipation to ensure good performance.

The first step involves shaping the kinetic energy of the closed-loop system by effectively modifying the system's inertia. Steady long-axis translation is stabilized by choosing control gains to make the modified inertia negative. The second step follows naturally from the constructive Lyapunov analysis used to prove stability in the first step. Prior insights from [31] and new analysis indicate choices of control gains which expand the estimated region of attraction. Furthermore, simulations suggest that the region of attraction estimates are conservative. Because physical damping is omitted in this step, the dynamics evolve on an invariant surface defined by the initial condition. Steady long-axis translation is shown to be asymptotically stable restricted to the appropriate level set; for example, the final velocity of the vehicle is dictated by the initial translational momentum. The third step involves a general model for the damping force and torque on an ellipsoidal underwater vehicle which is presented in Chapter 3. It is notable that this drag model contains, as a special case, a common model cited in [29]. One effect of damping on the vehicle dynamics is to destroy conservation laws used to construct the Lyapunov function in the first step. Therefore, a modified semidefinite Lyapunov function is introduced by truncating terms from the previous Lyapunov function. Proving asymptotic stability with a semidefinite Lyapunov function is complicated by the difficulty of finding a trapping region and the necessity of examining the "zero dynamics," i.e., the dynamics on the set where the Lyapunov rate is zero. In the case of coincident CG and CB, these difficulties are overcome resulting in a global asymptotic stability result. In the case of noncoincident centers, we resort to local analysis in both the second and third steps, resulting in locally exponentially stabilizing control laws.

Chapter 5 describes a more general inquiry into the effect of damping on controlled Lagrangian systems. We first consider "balance systems" for which the desired equilibrium

is a maximum of the potential energy. Stabilization involves modifying the kinetic energy metric, often by making the closed-loop energy metric negative in certain directions, so that the equilibrium is a maximum of an energy-based Lyapunov function. Concern for the effect of damping is quite natural, considering the nature of the control law. The analysis indicates that, while damping in the unactuated directions is beneficial in the sense that it tends to asymptotically stabilize the unactuated dynamics, damping in the controlled directions can destabilize. Fortunately, however, damping in these directions can be directly compensated for. Thus, a suitable choice of feedback dissipation leads to asymptotic stability of the desired equilibrium. The results were demonstrated in simulation and experimentally. We also considered the effect of damping on relative equilibria of Euler-Poincaré (reduced Lagrangian) systems which have been stabilized using the method of controlled Lagrangians. Sufficient conditions were suggested for asymptotic stability in the presence of linear damping.

6.2 Future Work

Feedback structure modification. It was noted in Remark 4.1.12 that a truncated version of the control law used for a vehicle with coincident CG and CB leads to an almost Poisson closed-loop system with the same modified Hamiltonian and a modified structure. Similarly, as described in Remark 4.2.2, for a vehicle with noncoincident CG and CB, omitting the gravitational term from the feedback control law derived using the method of controlled Lagrangians leads to an almost Poisson closed-loop system with a modified kinetic energy, a modified potential energy, and a modified structure.

The idea of modifying structure through feedback generalizes the idea of energy modification and, within the framework of the method of controlled Lagrangians, might potentially

lead to broader conditions for closed-loop stability. Furthermore, there may be physical reasons why a feedback-modified structure is more appealing than the uncontrolled structure. In [13], for example, the configuration space of a spacecraft with three internal rotors was modified through feedback to resemble the configuration space of a heavy top. This idea relates directly to that of Leonard [43], in which a system's symmetry is intentionally broken through feedback in order to stabilize in those symmetry directions.

Robustness of the method of controlled Lagrangians to unmodeled dynamics.

This problem was suggested by Jerrold Marsden out of a concern that the stabilizing control laws based on low-dimensional models of physical systems might excite higher-order modes leading to instability. To study robustness, "unmodeled dynamics" may be introduced through additional kinetic and potential energy terms in the original Lagrangian. For example, one may consider a first-order model of a flexible pendulum link by replacing a rigid link with two rigid links pinned with a stiff torsion spring. (See Figure 6.1.) The Lagrangian describing this system involves an additional kinetic energy term, corresponding to the additional link, and an additional potential energy term corresponding to the torsion spring. The method may be considered "robust to unmodeled dynamics" if the control law derived for the rigid link also stabilizes the flexible link without exciting the bending mode. Preliminary investigation and simulations of this type of system indicates that unmodeled dynamics are not problematic.

Experiments with internally actuated underwater vehicles. Given the practical motivation for the work presented here, a quite natural next step is to test these ideas experimentally. One application of a laboratory scale underwater vehicle with rotors would be to investigate spacecraft attitude control using reaction wheels. Similar programs in experimental spacecraft control have focused on spacecraft with external actuators. The

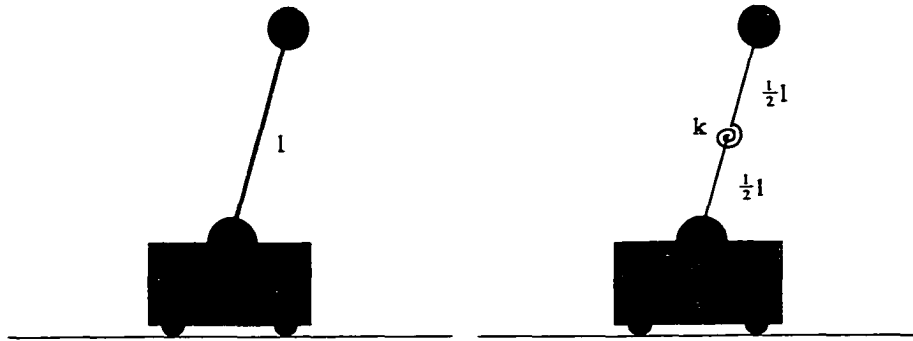


Figure 6.1: First order approximation of a flexible pendulum.

spacecraft are simulated using neutrally buoyant underwater vehicles with propellers. (See, for example, the University of Maryland Space Systems Laboratory's Supplemental Camera and Maneuvering Platform (SCAMP), described in [5].) A more ambitious experimental program would investigate the use of internal rotors to control a steadily translating underwater vehicle, as described in this dissertation. The experimental results described in Section 3, where a small internal rotor was used to provide gyroscopic stability to a translating, prolate spheroid, demonstrate the possible practical viability of using internal rotors on underwater vehicles. It is anticipated that internal rotors would be particularly useful for vehicles moving at low velocity, perhaps in a highly disturbed environment, such as a coastal region. Such an environment could be simulated at laboratory scale with relative ease and the merits of such a scheme could be effectively evaluated.

Appendix A

Discussion of Kirchhoff's Equations

Consider a rigid body B of arbitrary shape immersed in an inviscid, incompressible fluid which is itself contained in some envelope \mathcal{E} . Let \mathbf{u} denote the velocity of the fluid at a point with respect to some coordinate frame fixed in space. The motion of the fluid bounded between B and \mathcal{E} is called *irrotational* if the *vorticity* $\nabla \times \mathbf{u}$ is zero at every point in the fluid. In this case, the motion of any infinitesimal volume of fluid is described by a combination of pure translation and pure strain; there is no rotational component. Suppose that a closed curve denoted ∂A is drawn within the fluid and that this curve completely bounds a surface A (see Figure A.1). The *circulation* of the fluid about the circuit ∂A is defined as

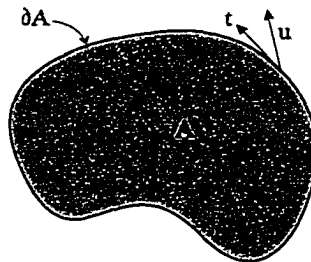


Figure A.1: Circulation.

$$\Gamma = \int_{\partial A} \mathbf{u} \cdot \mathbf{t} \, ds$$

where s denotes arclength along the curve and \mathbf{t} denotes the unit tangent vector tangent to the curve. By Stokes' theorem,

$$\Gamma = \iint_A (\nabla \times \mathbf{u}) \cdot \mathbf{n} \, dA$$

where dA represents a differential area element of the surface A and \mathbf{n} denotes a unit vector normal to that element. The fluid motion is irrotational if $\Gamma = 0$ about every circuit ∂A that can be drawn in the fluid. Kelvin's circulation theorem states that, in the absence of nonconservative forces, Γ remains constant. Thus if the fluid motion is initially irrotational, it will always be so.

The free, irrotational motion of an ideal fluid in a simply-connected region is described by a single-valued velocity potential ϕ :

$$\mathbf{u} = -\nabla\phi. \tag{A.1}$$

Lamb [41] gives the following physical interpretation for the velocity potential: "Any actual state of motion of a liquid, for which a (single-valued) velocity potential (ϕ) exists, could be produced instantaneously from rest by the application of a properly chosen system of impulsive pressures"

$$\rho\phi + C,$$

where ρ is the fluid density and C is an arbitrary constant. (The additive constant has no effect on the fluid motion since it represents a uniformly applied impulsive pressure.) The condition for continuity of an incompressible fluid is that $\nabla \cdot \mathbf{u} = 0$ everywhere in the fluid.

If the fluid motion derives from a velocity potential, continuity implies that

$$\nabla^2 \phi = 0 \tag{A.2}$$

throughout the fluid. Considering the conditions for solubility of Laplace's equation, the velocity potential is completely determined (up to an additive constant) when ϕ , $\nabla\phi \cdot \mathbf{n}$, or some combination is given over the bounding surfaces \mathcal{E} and \mathcal{B} . (Following convention, \mathbf{n} denotes the unit normal vector to the surface directed *into* the fluid.) If the envelope \mathcal{E} extends to infinity, it is sufficient to require that the velocity be zero there. In this case, too, the fluid motion is completely determined.

Let \mathcal{E}/\mathcal{B} denote the fluid volume. Recalling equation (A.1) for the fluid velocity, assuming that ϕ satisfies (A.2), and applying the divergence theorem to the quantity $\mathbf{u}\phi$ gives

$$\iiint_{\mathcal{E}/\mathcal{B}} \|\nabla\phi\|^2 dV = - \iint_{\mathcal{E}} \phi \nabla\phi \cdot \mathbf{n} dA - \iint_{\mathcal{B}} \phi \nabla\phi \cdot \mathbf{n} dA. \tag{A.3}$$

The kinetic energy of the fluid is

$$T_f = \frac{1}{2} \iiint_{\mathcal{E}/\mathcal{B}} \rho \|\mathbf{u}\|^2 dV, \tag{A.4}$$

so premultiplying both sides of equation (A.3) by $\frac{1}{2}\rho$ reveals an energy balance,

$$T_f = -\frac{1}{2}\rho \left(\iint_{\mathcal{E}} \phi \nabla\phi \cdot \mathbf{n} dA + \iint_{\mathcal{B}} \phi \nabla\phi \cdot \mathbf{n} dA \right). \tag{A.5}$$

According to Lamb's interpretation of the velocity potential, the right-hand side of (A.5) represents the work done by the system of impulsive pressures which, applied at the bounding surfaces, would effect the actual fluid motion from a state of rest.

Of particular interest is the case in which the rigid body \mathcal{B} moves through the fluid under no influence other than that of the fluid. In this case, the “work” done by the rigid body on the fluid, i.e., the right-hand side of (A.5), takes a simple form. By treating the body and the fluid as one combined dynamical system, the partial differential equations which describe the more general problem of rigid body motion in a fluid reduce to a finite set of ordinary differential equations and, as Lamb remarks, “the troublesome calculation of the effect of the fluid pressures on the surfaces of the solids is avoided.”

Suppose that the surface of the envelope \mathcal{E} is infinitely far from the rigid body \mathcal{B} in all directions. Fix a coordinate frame to \mathcal{B} and suppose that the body moves with translational velocity $\mathbf{v} = [v_1, v_2, v_3]^T$ and angular velocity $\boldsymbol{\Omega} = [\Omega_1, \Omega_2, \Omega_3]^T$, both written with respect to the moving coordinate frame. (See Figure A.2.) Consider the problem of finding a

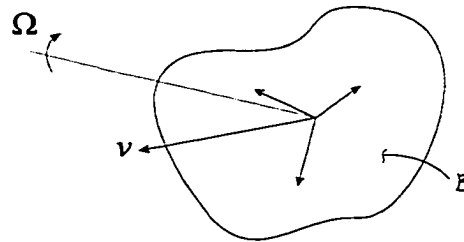


Figure A.2: Rigid body in a fluid.

velocity potential ϕ which satisfies Laplace’s equation (A.2) subject to the conditions that

1. the fluid velocity normal to the surface of \mathcal{B} at a point is equal to the normal velocity of the surface at that point.
2. the fluid is at rest infinitely far from \mathcal{B} .

Tangential motion of the fluid at the body’s surface is allowed but is not prescribed. Kirch-

hoff found that the solution takes the form

$$\phi = \mathbf{v} \cdot \boldsymbol{\phi} + \boldsymbol{\Omega} \cdot \boldsymbol{\chi} \quad (\text{A.6})$$

where the components of $\boldsymbol{\phi} = [\phi_1, \phi_2, \phi_3]^T$ and $\boldsymbol{\chi} = [\chi_1, \chi_2, \chi_3]^T$ depend only on the shape of \mathcal{B} . Let \mathbf{x} denote the position of a point on the surface of the rigid body relative to the body-fixed coordinate frame. The boundary condition at the surface of \mathcal{B} becomes

$$-\nabla\phi \cdot \mathbf{n} = (\mathbf{v} + \boldsymbol{\Omega} \times \mathbf{x}) \cdot \mathbf{n}. \quad (\text{A.7})$$

Each component of $\boldsymbol{\phi}$ and $\boldsymbol{\chi}$ must satisfy equation (A.2) independently, subject to the relevant boundary condition on \mathcal{B} implied by equation (A.7) with ϕ given by (A.6):

$$-\nabla\phi \cdot \mathbf{n} = - \begin{pmatrix} \nabla\phi_1 \cdot \mathbf{n} \\ \nabla\phi_2 \cdot \mathbf{n} \\ \nabla\phi_3 \cdot \mathbf{n} \end{pmatrix} = \mathbf{n} \quad \text{and} \quad -\nabla\boldsymbol{\chi} \cdot \mathbf{n} = - \begin{pmatrix} \nabla\chi_1 \cdot \mathbf{n} \\ \nabla\chi_2 \cdot \mathbf{n} \\ \nabla\chi_3 \cdot \mathbf{n} \end{pmatrix} = \boldsymbol{\chi} \times \mathbf{n}.$$

According to Lamb, Lord Kelvin defines the ‘impulse’ of the body-fluid system at an instant to be the impulsive force and couple required to instantaneously generate the body and fluid’s motion from rest. Lamb shows that the component of impulse due to the pressure at the infinite boundary \mathcal{E} vanishes and that the variation in system impulse is therefore given entirely by the time integral of the external forces acting on the rigid body. The system impulse thus behaves “in exactly the same way as the momentum of a finite dynamical system.”

Let $\mathbf{P} = [P_1, P_2, P_3]^T$ and $\boldsymbol{\Pi} = [\Pi_1, \Pi_2, \Pi_3]^T$ represent the impulsive force and couple, respectively, written with respect to the body-fixed coordinate frame. Also, let $\mathcal{F}_{\text{other}}$ and

$\mathcal{T}_{\text{other}}$ represent an external force and torque acting on the rigid body. As Lamb shows by considering infinitesimal motions of the body-fluid system, the impulse varies according to the equations

$$\dot{\Pi} = \Pi \times \Omega + P \times v + \mathcal{T}_{\text{other}}$$

$$\dot{P} = P \times \Omega + \mathcal{F}_{\text{other}}$$

Since the integral over \mathcal{E} vanishes, the kinetic energy of the fluid (A.5) becomes

$$T_f = -\frac{1}{2}\rho \left(\iint_B \phi \nabla \phi \cdot \mathbf{n} \, dA \right). \quad (\text{A.8})$$

Substituting the expression (A.6) for the velocity potential ϕ into (A.8) gives

$$T_f = \frac{1}{2} \begin{pmatrix} v \\ \Omega \end{pmatrix} \cdot \begin{pmatrix} M_f & D_f^T \\ D_f & I_f \end{pmatrix} \begin{pmatrix} v \\ \Omega \end{pmatrix} \quad (\text{A.9})$$

where the square matrix is a constant, symmetric, positive definite matrix whose entries depend only upon the density of the fluid and the shape of the body \mathcal{B} . For example,

$$\begin{aligned} M_{f_{11}} &= -\rho \iint_B \phi_1 \nabla \phi_1 \cdot \mathbf{n} \, dS \\ &= \rho \iint_B \phi_1 (\mathbf{n} \cdot \mathbf{e}_1) \, dS, \end{aligned}$$

where the latter equality arises from the boundary condition (A.7). The expression (A.9) for the fluid kinetic energy holds formally for bodies \mathcal{B} of arbitrary shape. Naturally, the complexity of the integrals defining the components of M_f , D_f , and I_f depends on the complexity of the shape of the body and on the choice of body-fixed coordinate frame.

Let T_{rb} denote the kinetic energy of the rigid body. It is assumed that the mass of the body, say m , is equal to the mass of the displaced fluid so that the body is neutrally buoyant. The location of the mass center of \mathcal{B} with respect to the body-fixed coordinate frame is given by \boldsymbol{r} . Let \boldsymbol{I}_{rb} denote the rigid body inertia tensor computed with respect to the body-fixed frame. Then the kinetic energy of the rigid body alone is

$$T_{rb} = \frac{1}{2} \begin{pmatrix} \boldsymbol{v} \\ \boldsymbol{\Omega} \end{pmatrix} \cdot \begin{pmatrix} m\boldsymbol{\mathcal{I}} & -m\hat{\boldsymbol{r}} \\ m\hat{\boldsymbol{r}} & \boldsymbol{I}_{rb} \end{pmatrix} \begin{pmatrix} \boldsymbol{v} \\ \boldsymbol{\Omega} \end{pmatrix}. \quad (\text{A.10})$$

The total system energy is

$$T = T_{rb} + T_f = \frac{1}{2} \begin{pmatrix} \boldsymbol{v} \\ \boldsymbol{\Omega} \end{pmatrix} \cdot \begin{pmatrix} \boldsymbol{M} & \boldsymbol{D}^T \\ \boldsymbol{D} & \boldsymbol{I} \end{pmatrix} \begin{pmatrix} \boldsymbol{v} \\ \boldsymbol{\Omega} \end{pmatrix} \quad (\text{A.11})$$

where

$$\begin{aligned} \boldsymbol{M} &= \boldsymbol{M}_f + m\boldsymbol{\mathcal{I}} \\ \boldsymbol{D} &= \boldsymbol{D}_f + m\hat{\boldsymbol{r}} \\ \boldsymbol{I} &= \boldsymbol{I}_f + \boldsymbol{I}_{rb}. \end{aligned} \quad (\text{A.12})$$

Lamb shows that the system impulse is related to the rigid body velocity according to

$$P_i = \frac{\partial T}{\partial v_i} \quad \text{and} \quad \Pi_i = \frac{\partial T}{\partial \Omega_i} \quad (\text{A.13})$$

for $i = 1, 2,$ and 3 . In terms of the system impulse, the total kinetic energy is

$$T = \frac{1}{2} \begin{pmatrix} \mathbf{P} \\ \mathbf{\Pi} \end{pmatrix} \cdot \begin{pmatrix} \mathbf{M} & \mathbf{D}^T \\ \mathbf{D} & \mathbf{I} \end{pmatrix}^{-1} \begin{pmatrix} \mathbf{P} \\ \mathbf{\Pi} \end{pmatrix}. \quad (\text{A.14})$$

Lamb points out several simplifications of the generalized inertia tensor. For example, one may always rotate the body coordinate axes such that \mathbf{M} becomes diagonal. Furthermore, writing \mathbf{D} as the sum of a symmetric and a skew-symmetric matrix, one may eliminate the skew-symmetric contribution by shifting the coordinate origin. Thus the number of coefficients required to define the generalized inertia reduces from twenty-one to fifteen. Further simplifications follow for particular body shapes. In particular, Lamb discusses bodies having one or more planes of symmetry, one or more axes of symmetry, and a special type of "helical" symmetry illustrated by a ship's propeller. An ellipsoid with uniformly distributed mass is an example of a body with three planes of symmetry. Choosing coordinate axes fixed to the ellipsoid principal axes, one finds that $\mathbf{M} = \text{diag}(m_1, m_2, m_3)$, $\mathbf{D} = \mathbf{0}$, and $\mathbf{I} = \text{diag}(I_1, I_2, I_3)$. Even if the ellipsoid mass is not uniformly distributed, one obtains such simplifications for the added mass and inertia matrices \mathbf{M}_f , \mathbf{D}_f , and \mathbf{I}_f .

Appendix B

Proof of Theorem 4.1.2

Consider the function (4.10):

$$H_\Phi = H_K(\mathbf{\Pi}, \mathbf{P}, \zeta) + \Phi(C_1, C_2, \zeta_1, \zeta_2, \zeta_3).$$

where $C_1 = \frac{1}{2}\|\mathbf{P}\|^2$ and $C_2 = \mathbf{\Pi} \cdot \mathbf{P}$. Since H_K and any smooth function Φ are conserved under the dynamics (4.6), $\dot{H}_\Phi = 0$. To be a Lyapunov function for the equilibrium

$$\mathbf{\Pi}_e = \begin{pmatrix} \Pi_1^0 \\ 0 \\ 0 \end{pmatrix}, \quad \mathbf{P}_e = \begin{pmatrix} P_1^0 \\ 0 \\ 0 \end{pmatrix}, \quad \zeta_e = \begin{pmatrix} \zeta_1^0 \\ 0 \\ 0 \end{pmatrix}, \quad (\text{B.1})$$

H_Φ must have a minimum or a maximum there. First, in order for the equilibrium to be a critical point one requires $(DH_\Phi)_e = \mathbf{0}$, where

$$\begin{aligned} DH_\Phi(\mathbf{\Pi}_e, \mathbf{P}_e, \zeta_e) \cdot (\delta\mathbf{\Pi}, \delta\mathbf{P}, \delta\zeta) &= (\mathbf{I}_K^{-1}(\mathbf{\Pi}_e - \zeta_e) + \Phi_{2|e}P_e) \cdot \delta\mathbf{\Pi} \\ &+ (\mathbf{M}^{-1}P_e + \Phi_{1|e}P_e + \Phi_{2|e}\mathbf{\Pi}_e) \cdot \delta\mathbf{P} + (-\mathbf{I}_K^{-1}(\mathbf{\Pi}_e - \zeta_e) + (\Phi_3, \Phi_4, \Phi_5)_e^T) \cdot \delta\zeta. \end{aligned} \quad (\text{B.2})$$

Φ_i is the partial derivative of Φ with respect to its i th argument. (For example, $\Phi_1 = \frac{\partial \Phi}{\partial C_1}$.)

If the function Φ satisfies

$$\begin{aligned}\Phi_1|_e &= \bar{\rho}_1 = -\frac{1}{m_1} + \frac{1}{I_{K_1}} \frac{\Pi_1^0(\Pi_1^0 - \zeta_1^0)}{P_1^0}, \\ \Phi_2|_e &= \bar{\rho}_2 = -\frac{1}{I_{K_1}} \frac{(\Pi_1^0 - \zeta_1^0)}{P_1^0}, \\ \Phi_3|_e &= \bar{\rho}_3 = \frac{\Pi_1^0 - \zeta_1^0}{I_{K_1}}, \\ \Phi_4|_e &= 0, \\ \Phi_5|_e &= 0,\end{aligned}$$

then H_Φ will have a critical point at the equilibrium (B.1).

For the critical point to be a maximum or a minimum, the second variation $D^2 H_\Phi$ must be definite when evaluated at the equilibrium. The symmetric matrix

$$\mathcal{H} = \begin{pmatrix} \mathcal{H}_{11} & \mathcal{H}_{12} & \mathcal{H}_{13} \\ \mathcal{H}_{12}^T & \mathcal{H}_{22} & \mathcal{H}_{23} \\ \mathcal{H}_{13}^T & \mathcal{H}_{23}^T & \mathcal{H}_{33} \end{pmatrix}$$

represents the matrix of the second derivative of H_Φ where

$$\mathcal{H}_{11} = I_K^{-1} + \Phi_{22} P P^T$$

$$\mathcal{H}_{12} = \Phi_2 \mathcal{I} + P(\Phi_{22} \Pi^T + \Phi_{12} P^T)$$

$$\mathcal{H}_{13} = -I_K^{-1} + P(\Phi_{23}, \Phi_{24}, \Phi_{25})$$

$$\mathcal{H}_{22} = M^{-1} + \Phi_1 \mathcal{I} + \Phi_{22} \Pi \Pi^T + \Phi_{12}(\Pi P^T + P \Pi^T) + \Phi_{11} P P^T$$

$$\mathcal{H}_{23} = P(\Phi_{13}, \Phi_{14}, \Phi_{15}) + \Pi(\Phi_{23}, \Phi_{24}, \Phi_{25})$$

$$\mathcal{H}_{33} = I_K^{-1} + \begin{pmatrix} \Phi_{33} & \Phi_{34} & \Phi_{35} \\ \Phi_{34} & \Phi_{44} & \Phi_{45} \\ \Phi_{35} & \Phi_{45} & \Phi_{55} \end{pmatrix}.$$

The scalar quantity Φ_{ij} is the second partial derivative of Φ with respect to its i th and j th arguments. (For example, $\Phi_{12} = \frac{\partial^2 \Phi}{\partial C_1 \partial C_2}$.)

If $I_{K_2} > 0$ and $I_{K_3} > 0$, the second and third principal determinants of \mathcal{H} will be positive. In this case, for $D^2 H_\Phi$ to be definite when evaluated at the equilibrium (B.1), it must be positive definite. If all principal determinants of \mathcal{H}_e are positive, then the equilibrium will be a minimum of H_Φ . Checking principal determinants, one finds that all principal determinants of \mathcal{H}_e are positive if for $i = 2$ and $i = 3$

$$\frac{1}{I_{K_1}} \left(\frac{1}{I_{K_i}} - \frac{1}{I_{K_1}} \right) \left(\frac{\Pi_1^0 - \zeta_1^0}{P_1^0} \right)^2 + \frac{1}{I_{K_1} I_{K_i}} \frac{(\Pi_1^0 - \zeta_1^0) \zeta_1^0}{(P_1^0)^2} > \frac{1}{I_{K_i}} \left(\frac{1}{m_1} - \frac{1}{m_i} \right) \quad (\text{B.3})$$

and Φ satisfies:

$$\begin{aligned} \Phi_{11}|_e &= \rho_1 > -\frac{1}{(P_1^0)^2} \left(\frac{1}{m_1} + \bar{\rho}_1 + 3\rho_3(\Pi_1^0)^2 + 2\bar{\rho}_2 \left(\frac{\Pi_1^0}{P_1^0} \right) \right), \\ \Phi_{12}|_e &= \rho_2 = -\bar{\rho}_2 \frac{1}{(P_1^0)^2} - \rho_3 \left(\frac{\Pi_1^0}{P_1^0} \right), \\ \Phi_{22}|_e &= \rho_3 > -\frac{1}{I_{K_1}} \frac{1}{(P_1^0)^2}, \\ \Phi_{33}|_e &= \rho_{3.5} > \frac{\rho_3 (P_1^0)^2}{1 - \rho_3 I_{K_1} (P_1^0)^2}, \\ \Phi_{44}|_e &= \rho_4 > \frac{m_2 \bar{\rho}_2^2}{1 - m_2 I_{K_2} \bar{\rho}_2^2}, \\ \Phi_{55}|_e &= \rho_5 > \frac{m_3 \bar{\rho}_2^2}{1 - m_3 I_{K_3} \bar{\rho}_2^2} \end{aligned}$$

with all other second partial derivatives of Φ equal to zero. Note that these conditions only

apply to Φ at one point, the equilibrium. Otherwise, Φ is completely free.

If, instead, K is chosen such that $I_{K_2} < 0$ and $I_{K_3} < 0$, then the equilibrium (B.1) will be a *maximum* provided the conditions on Φ stated above are satisfied *with all of the inequalities reversed*.

Thus, if $\text{sign}(I_{K_2}) = \text{sign}(I_{K_3})$ and condition (B.3) is satisfied, there exists a Lyapunov function proving stability of the equilibrium (B.1).

Referring to condition (B.3), note that stability in the special case that $\Omega_1^0 = 0$ requires that $I_{K_2} < 0$ and $I_{K_3} < 0$. Therefore, if $\Omega_1^0 = 0$, the stabilized equilibrium must be a maximum. The constants $\bar{\rho}_1, \bar{\rho}_2$, and $\bar{\rho}_3$ simplify, in this case, to

$$\bar{\rho}_1 = -\frac{1}{m_1}, \quad \bar{\rho}_2 = \bar{\rho}_3 = 0.$$

Thus, the conditions on the constants ρ_1, ρ_2, ρ_4 , and ρ_5 simplify to

$$\rho_1 < -3\rho_3 \left(\frac{\Pi_1^0}{P_1^0} \right)^2, \quad \rho_2 = -\rho_3 \left(\frac{\Pi_1^0}{P_1^0} \right), \quad \rho_4 < 0, \quad \rho_5 < 0.$$

These conditions are satisfied by the choice of constants $\rho_1, \rho_2, \rho_3, \rho_4$, and ρ_5 in the proof of Corollary 4.1.3.

Appendix C

Translational Relative Equilibria: Noncoincident Centers

Recall the equations of motion for a vehicle with $r \neq 0$,

$$\dot{\Pi} = \Pi \times \Omega + P \times v + r \times mg\Gamma$$

$$\dot{P} = P \times \Omega$$

$$\dot{\Gamma} = \Gamma \times \Omega$$

$$\dot{\zeta} = 0.$$

Consider only the case $\Omega \equiv 0$. In this case, $\dot{P} = 0$ and $\dot{\Gamma} = 0$. Also, since $\dot{\Omega} = 0$,

$$A_k(\dot{\Pi} - \dot{\zeta}) + B_k^T \dot{P} = A_k \dot{\Pi} = 0.$$

The matrix A_k is full rank, so $\dot{\Pi} = 0$. The system must therefore be at equilibrium with

$$P_e \times v_e + r \times mg\Gamma_e = 0. \tag{C.1}$$

Before stating the explicit equilibria, we note that $\mathbf{r} \cdot (\mathbf{P}_e \times \mathbf{v}_e) = 0$ so that there is no component of the equilibrium "fluid torque" $\mathbf{P} \times \mathbf{v}$ in the direction of the CG. Now, from equation (C.1) we have

$$\begin{aligned}\Gamma_e &= \delta \mathbf{r} + \frac{1}{m g \mathbf{r} \cdot \mathbf{r}} \mathbf{r} \times (\mathbf{P}_e \times \mathbf{v}_e) \\ &= \delta \mathbf{r} + \frac{1}{m g \mathbf{r} \cdot \mathbf{r}} \mathbf{r} \times (\mathbf{P}_e \times M^{-1} \mathbf{P}_e)\end{aligned}$$

where $|\delta|$ is determined from the identity $\|\Gamma\|^2 = 1$. To verify this, we substitute Γ_e into equation (C.1) and use the vector identity

$$\mathbf{a} \times (\mathbf{b} \times \mathbf{c}) = (\mathbf{a} \cdot \mathbf{c})\mathbf{b} - (\mathbf{a} \cdot \mathbf{b})\mathbf{c}.$$

We find that

$$\begin{aligned}0 &= \mathbf{P}_e \times M^{-1} \mathbf{P}_e + \mathbf{r} \times m g \left(\delta \mathbf{r} + \frac{1}{m g \mathbf{r} \cdot \mathbf{r}} \mathbf{r} \times (\mathbf{P}_e \times M^{-1} \mathbf{P}_e) \right) \\ &= \mathbf{P}_e \times M^{-1} \mathbf{P}_e + \frac{1}{\mathbf{r} \cdot \mathbf{r}} (\mathbf{r} \cdot (\mathbf{P}_e \times M^{-1} \mathbf{P}_e) \mathbf{r} - \mathbf{r} \cdot \mathbf{r} (\mathbf{P}_e \times M^{-1} \mathbf{P}_e)) \\ &= \mathbf{P}_e \times M^{-1} \mathbf{P}_e - \mathbf{P}_e \times M^{-1} \mathbf{P}_e.\end{aligned}$$

Choosing $\mathbf{r} = \gamma \mathbf{e}_3$ gives

$$\Gamma_e = \delta \gamma \mathbf{e}_3 + \frac{1}{m g \gamma} \mathbf{e}_3 \times (\mathbf{P}_e \times M^{-1} \mathbf{P}_e). \quad (\text{C.2})$$

Notice that

$$\mathbf{e}_3 \cdot (\mathbf{P}_e \times M^{-1} \mathbf{P}_e) = \left(\frac{1}{m_2} - \frac{1}{m_1} \right) P_1^0 P_2^0$$

where P_i^0 is the i th component of \mathbf{P}_e . Thus, either $P_1^0 = 0$ or $P_2^0 = 0$ at an equilibrium for

which $\Omega \equiv 0$. Recall from Section (4.2) that

$$\begin{pmatrix} \Pi - \zeta \\ P \end{pmatrix} = \begin{pmatrix} (\mathcal{I} - K)^{-1} & -K(\mathcal{I} - K)^{-1}(m\hat{r})M^{-1} \\ 0 & \mathcal{I} \end{pmatrix}^{-1} \begin{pmatrix} \bar{I} & m\hat{r} \\ -m\hat{r} & M \end{pmatrix} \begin{pmatrix} \Omega \\ v \end{pmatrix}.$$

One therefore obtains the following two five-parameter families of relative equilibria for which $\Omega \equiv 0$:

$$\Pi_e = (m\gamma\widehat{e}_3)M^{-1}P_e + \zeta_e, \quad P_e = P_i^0 e_i + P_3^0 e_3, \quad \zeta_e = \zeta_1^0 e_1 + \zeta_2^0 e_2 + \zeta_3^0 e_3$$

$$\text{and} \quad \Gamma_e = \pm \sqrt{1 - \left(\left(\frac{1}{m_3} - \frac{1}{m_i} \right) \frac{P_i^0 P_3^0}{mg\gamma} \right)^2} e_3 + \left(\frac{1}{m_3} - \frac{1}{m_i} \right) \frac{P_i^0 P_3^0}{mg\gamma} e_i, \quad i = 1, 2. \quad (\text{C.3})$$

The five equilibrium parameters are $\zeta_1^0, \zeta_2^0, \zeta_3^0$ and P_i^0 and P_3^0 and the two families are given by $i = 1$ or 2 . Obviously, we must require that

$$1 - \left(\left(\frac{1}{m_3} - \frac{1}{m_i} \right) \frac{P_i^0 P_3^0}{mg\gamma} \right)^2 > 0 \quad (\text{C.4})$$

in order for (C.3) to be an equilibrium.

If $P_1^0 = P_2^0 = 0$, then the vehicle moves along its 3-axis parallel to the direction of gravity and $C_3 = P_3^0$. If $P_3^0 = 0$, then the vehicle moves along its i -axis orthogonal to the direction of gravity and $C_3 = 0$. To characterize more general equilibria, it is useful to replace the equilibrium parameters P_i^0 and P_3^0 with the conserved quantities C_1 and C_3 . For $i = 1$ and 2 , we have

$$C_1 = \frac{1}{2} P_e \cdot P_e = \frac{1}{2} \left((P_i^0)^2 + (P_3^0)^2 \right) \quad (\text{C.5})$$

$$C_3 = \Gamma_e \cdot P_e = \pm \sqrt{1 - \left(\left(\frac{1}{m_3} - \frac{1}{m_i} \right) \frac{P_i^0 P_3^0}{mg\gamma} \right)^2} P_3^0 + \left(\frac{1}{m_3} - \frac{1}{m_i} \right) \frac{P_i^0 P_3^0}{mg\gamma} P_i^0. \quad (\text{C.6})$$

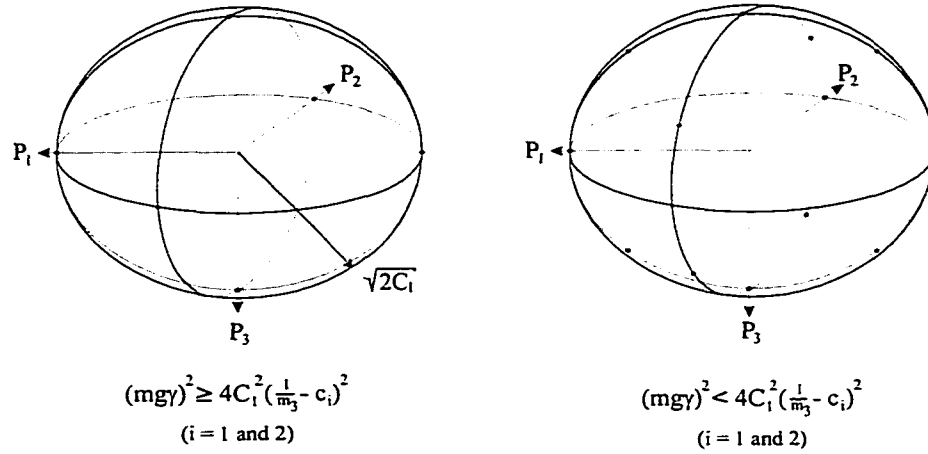


Figure C.1: Equilibrium values of P given Π_e , and C_1 with $C_3 = 0$.

Substituting (C.5) into (C.6) gives the following implicit equation for P_i^0 ,

$$\left(\frac{C_3}{\pm \sqrt{2C_1 - (P_i^0)^2}} - \left(\frac{1}{m_3} - \frac{1}{m_i} \right) \frac{(P_i^0)^2}{mg\gamma} \right)^2 = 1 - \left(\left(\frac{1}{m_3} - \frac{1}{m_i} \right) \frac{P_i^0}{mg\gamma} \right)^2 (2C_1 - (P_i^0)^2). \quad (\text{C.7})$$

Equation (C.7) is quartic in P_i^0 so there are at most four real values for P_i^0 given C_1 and C_3 . Of particular interest is the case where $C_3 = 0$ because this value corresponds to the equilibrium describing pure long axis translation in the horizontal plane. Indeed, if $P_3^0 = 0$ then equation (C.5) gives two solutions for P_i^0 corresponding to “forward” and “reverse” translation along the i th principal axis where $i = 1$ or 2 . Alternatively, if $P_3^0 \neq 0$ and $C_3 = 0$ then equation (C.7) leads to

$$1 = 2C_1 \left(\left(\frac{1}{m_3} - \frac{1}{m_i} \right) \frac{P_i^0}{mg\gamma} \right)^2.$$

It follows that

$$P_i^0 \in \left\{ \pm \sqrt{2C_1}, \pm \frac{mg\gamma}{\sqrt{2C_1} \left(\frac{1}{m_3} - \frac{1}{m_i} \right)} \right\}. \quad (\text{C.8})$$

The latter two solutions correspond to physical equilibria if and only if

$$0 < 2C_1 - (P_i^0)^2 = 2C_1 - \left(\frac{mg\gamma}{\sqrt{2C_1} \left(\frac{1}{m_3} - \frac{1}{m_i} \right)} \right)^2.$$

Combining this condition with condition (C.4), one finds that “gliding equilibria” can occur if and only if

$$0 < \left(\frac{mg\gamma}{2C_1 \left(\frac{1}{m_3} - \frac{1}{m_i} \right)} \right)^2 < 1. \quad (\text{C.9})$$

Thus, if the translational momentum (i.e., C_1) is large or the CG is not very far from the CB these equilibria exist.

A reasonable goal is to asymptotically stabilize the equilibrium corresponding to $i = 1$ and $P_3^0 = 0$ with as large a region of attraction as possible. The region of attraction will be limited by the proximity of the nearest neighboring equilibrium. If γ is chosen large enough that condition (C.9) is *not* satisfied, then some of the neighboring equilibria will be eliminated. (Translation along the 2 and 3-axis remain as equilibria.) Therefore, one might require that

$$(mg\gamma)^2 \geq \left(2C_1 \left(\frac{1}{m_3} - \frac{1}{m_i} \right) \right)^2, \quad i = 1, 2. \quad (\text{C.10})$$

The translational component \mathbf{P}_e of relative equilibria for the underwater vehicle can be depicted on a sphere of radius $\sqrt{2C_1}$. In Figure C.1, the various values of \mathbf{P}_e are indicated in the special case that $C_3 = 0$. Shown on the left is the case where condition (C.10) is satisfied; on the right is the case where the condition is not satisfied. (Note: The spheres in Figure C.1 do *not* represent leaves of a foliation of phase space. Coadjoint orbits for the Hamiltonian system (4.66) are generically six-dimensional.)

Appendix D

Dissipative Gains for Theorem 4.2.4.

Recall that the characteristic polynomial of the linearized system (4.87) is

$$\lambda^3(\lambda^2 + \mu_1\lambda + \mu_2)(\lambda^4 + \mu_3\lambda^3 + \mu_4\lambda^2 + \mu_5\lambda + \mu_6) \quad (\text{D.1})$$

where

$$\begin{aligned} \mu_1 &= -a_2(1-k)k_{d_2} \\ \mu_2 &= a_2 \left(mg\gamma - (1-k) \left(\frac{1}{m_1} - \frac{1}{m_3} \right) (P_1^0)^2 \right) \\ \mu_3 &= -(1-k) \left(\frac{k_{d_3}}{I_3} + a_1 k_{d_1} \right) \\ \mu_4 &= -\frac{1-k}{I_3} \left(\frac{1}{m_1} - \frac{1}{m_2} \right) (P_1^0)^2 \\ &\quad + a_1 \frac{(1-k)^2}{I_3} \left((m\gamma)^2 \left(\frac{1}{m_1} - \frac{1}{m_2} \right)^2 (P_1^0)^2 + k_{d_1} k_{d_3} \right) + a_1 mg\gamma \\ \mu_5 &= -a_1 \frac{1-k}{I_3} \left(-(1-k)k_{d_1} \left(\frac{1}{m_1} - \frac{1}{m_2} \right) (P_1^0)^2 + (m\gamma)k_{d_3} \right) \\ \mu_6 &= -a_1(mg\gamma) \frac{1-k}{I_3} \left(\frac{1}{m_1} - \frac{1}{m_2} \right) (P_1^0)^2. \end{aligned}$$

In addition to requiring that each coefficient μ_3, μ_4, μ_5 , and μ_6 be positive, the Routh-Hurwitz criterion requires that

$$\mu_3\mu_4 - \mu_5 > 0 \quad (\text{D.2})$$

$$\mu_3\mu_4\mu_5 - \mu_5^2 - \mu_6\mu_3^2 > 0. \quad (\text{D.3})$$

To simplify notation, make the following substitutions:

$$\bar{U} = mg\gamma, \quad \bar{T} = \left(\frac{1}{m_1} - \frac{1}{m_2} \right) (P_1^0)^2, \quad I_{k_3} = \frac{I_3}{1-k}.$$

Then

$$\begin{aligned} \mu_4 &= \left(\frac{a_1}{I_{k_3}} \right) \left(\bar{U}I_{k_3} - \frac{\bar{T}}{a_1} + (1-k) \left((m\gamma)^2 \left(\frac{1}{m_1} - \frac{1}{m_2} \right) \bar{T} + k_{d_1}k_{d_3} \right) \right) \\ \mu_5 &= -\frac{a_1}{I_{k_3}} \left(-(1-k)k_{d_1}\bar{T} + k_{d_3}\bar{U} \right) \\ \mu_6 &= -\frac{a_1}{I_{k_3}} \bar{T}\bar{U}. \end{aligned}$$

Substituting into condition (D.2) and multiplying by $(I_{k_3}/a_1) < 0$ gives

$$\begin{aligned} 0 &> \\ & - \left(\frac{k_{d_3}}{I_{k_3}} + (1-k)a_1k_{d_1} \right) \left(\bar{U}I_{k_3} - \frac{\bar{T}}{a_1} + (1-k) \left((m\gamma)^2 \left(\frac{1}{m_1} - \frac{1}{m_2} \right) \bar{T} + k_{d_1}k_{d_3} \right) \right) + \bar{T}\bar{U} \\ &= \frac{k_{d_3}\bar{T}}{I_{k_3}a_1} - (1-k)I_{k_3}k_{d_1}\bar{U} - (1-k) \left(\frac{k_{d_3}}{I_{k_3}} + (1-k)a_1k_{d_1} \right) \cdot \\ & \quad \left((m\gamma)^2 \left(\frac{1}{m_1} - \frac{1}{m_2} \right) \bar{T} + k_{d_1}k_{d_3} \right). \end{aligned}$$

This condition is automatically satisfied for $k > 1$, $\gamma > 0$ and $\mathbf{K}_d > \mathbf{0}$.

Condition (D.3) may be rewritten

$$\left(\frac{\mu_5}{\mu_3}\right)^2 - \mu_4 \left(\frac{\mu_5}{\mu_3}\right) + \mu_6 < 0. \quad (\text{D.4})$$

There is a range of μ_5/μ_3 for which (D.4) is satisfied provided

$$\begin{aligned} 0 &< \mu_4^2 - 4\mu_6 \\ &= \left(\frac{a_1}{I_{k_3}}\right)^2 \left(\bar{U}I_{k_3} - \frac{\bar{T}}{a_1} + (1-k) \left((m\gamma)^2 \left(\frac{1}{m_1} - \frac{1}{m_2} \right) \bar{T} + k_{d_1}k_{d_3} \right) \right)^2 + 4 \left(\frac{a_1}{I_{k_3}}\right) \bar{T}\bar{U} \\ &= \left(\frac{a_1}{I_{k_3}}\right)^2 \left(\left(\bar{U}I_{k_3} + \frac{\bar{T}}{a_1} \right)^2 + 2 \left(\bar{U}I_{k_3} - \frac{\bar{T}}{a_1} \right) (1-k) \left((m\gamma)^2 \left(\frac{1}{m_1} - \frac{1}{m_2} \right) \bar{T} + k_{d_1}k_{d_3} \right) \right. \\ &\quad \left. + (1-k)^2 \left((m\gamma)^2 \left(\frac{1}{m_1} - \frac{1}{m_2} \right) \bar{T} + k_{d_1}k_{d_3} \right)^2 \right). \end{aligned}$$

This condition is also satisfied under the existing conditions on k , γ , and \mathbf{K}_d . Condition (D.4) is satisfied when

$$\mu_4 - \sqrt{\mu_4^2 - 4\mu_6} < 2 \left(\frac{\mu_5}{\mu_3}\right) < \mu_4 + \sqrt{\mu_4^2 - 4\mu_6}. \quad (\text{D.5})$$

Inequality (D.5) gives implicit conditions on the control parameters. Provided these conditions do not contradict the previous stability conditions, the equilibrium (4.82) is locally exponentially stable. Rather than solve (D.5) for explicit conditions (which would be rather messy), require that the control parameters k_{d_1} , and k_{d_3} be chosen such that

$$\mu_4 - 2 \left(\frac{\mu_5}{\mu_3}\right) = 0. \quad (\text{D.6})$$

Clearly this choice satisfies (D.5). It is a conservative choice in the sense that a small error in the parameters will not violate condition (D.5). (Given error bounds on the parameter

estimates which define the control gains, one could check that (D.5) is satisfied for parameter values within an expected range.)

Expanding equation (D.6), one obtains an equation cubic in k_{d_1} and k_{d_3} ,

$$0 = \left(\frac{k_{d_3}}{I_{k_3}} + (1-k)a_1k_{d_1} \right) \left(I_{k_3}\tilde{U} - \frac{\tilde{T}}{I_{k_3}} + (1-k) \left(k_{d_1}k_{d_3} + (m\gamma)^2 \left(\frac{1}{m_1} - \frac{1}{m_2} \right) \tilde{T} \right) \right) + 2((1-k)k_{d_1}\tilde{T} - k_{d_3}\tilde{U}) \quad (\text{D.7})$$

Using k_{d_1} as a free parameter, one may solve for k_{d_3} numerically. In the interest of obtaining an explicit condition, one may observe that, in the limit that k_{d_1} and k_{d_3} are small enough, the cubic terms in (D.7) are negligible and only linear terms remain. If one chooses k_{d_1} and k_{d_3} small and satisfying

$$\frac{k_{d_1}}{k_{d_3}} = \left(\frac{1}{a_1 I_{k_3}} \right) \frac{a_1 I_{k_3} \tilde{U} + \tilde{T} - (1-k)a_1(m\gamma)^2 \left(\frac{1}{m_1} - \frac{1}{m_2} \right) \tilde{T}}{a_1 I_{k_3} \tilde{U} + \tilde{T} + a_1(m\gamma)^2 \left(\frac{1}{m_1} - \frac{1}{m_2} \right) \tilde{T}} \quad (\text{D.8})$$

(assuming the denominator is nonzero) then (D.7) is satisfied approximately. Verifying that (D.5) is satisfied, one finds that the roots of the quartic polynomial (D.1) all have negative real part.

Appendix E

Identities Concerning the Method of Controlled Lagrangians

E.1 Modified Metric Under General Matching Conditions

Recall equation (5.11) for the controlled Lagrangian,

$$L_{\tau,\sigma,\rho}(x^\alpha, \dot{x}^\alpha, \dot{\theta}^a) = L(x^\alpha, \dot{x}^\alpha, \dot{\theta}^a \\ + \tau_\alpha^a \dot{x}^\alpha) + \frac{1}{2} \sigma_{ab} \tau_\alpha^a \tau_\beta^b \dot{x}^\alpha \dot{x}^\beta + \frac{1}{2} \varpi_{ab} \left(\dot{\theta}^a + (g^{ac} g_{c\alpha} + \tau_\alpha^a) \dot{x}^\alpha \right) \left(\dot{\theta}^b + (g^{bd} g_{d\beta} + \tau_\beta^b) \dot{x}^\beta \right)$$

Using the matching condition GM-1,

$$\tau_\alpha^b = -\sigma^{ab} g_{b\alpha},$$

the controlled Lagrangian may be rewritten

$$L_{\tau,\sigma,\rho}(x^\alpha, \dot{x}^\alpha, \dot{\theta}^a)$$

$$\begin{aligned}
&= \frac{1}{2}g_{\alpha\beta}\dot{x}^\alpha\dot{x}^\beta + g_{\alpha\alpha}\dot{x}^\alpha(\dot{\theta}^a - \sigma^{ac}g_{c\beta}\dot{x}^\beta) + \frac{1}{2}g_{ab}(\dot{\theta}^a - \sigma^{ac}g_{c\alpha}\dot{x}^\alpha)(\dot{\theta}^b - \sigma^{bd}g_{d\beta}\dot{x}^\beta) \\
&\quad + \frac{1}{2}g_{\alpha\alpha}\sigma^{ab}g_{b\beta}\dot{x}^\alpha\dot{x}^\beta + \frac{1}{2}\varpi_{ab}\left(\dot{\theta}^a + (g^{ac} - \sigma^{ac})g_{c\alpha}\dot{x}^\alpha\right)\left(\dot{\theta}^b + (g^{bd} - \sigma^{bd})g_{d\beta}\dot{x}^\beta\right) - V(x^\alpha) \\
&= \frac{1}{2}\left(g_{\alpha\beta} - 2g_{\alpha\alpha}\sigma^{ab}g_{b\beta} + g_{\alpha\alpha}\sigma^{ab}g_{bc}\sigma^{cd}g_{d\beta} + g_{\alpha\alpha}\sigma^{ab}g_{b\beta}\right. \\
&\quad \left.+ g_{\alpha\alpha}(g^{ab} - \sigma^{ab})(\rho_{bc} - g_{bc})(g^{cd} - \sigma^{cd})g_{d\beta}\right)\dot{x}^\alpha\dot{x}^\beta \\
&\quad + \dot{x}^\alpha\dot{\theta}^a\left(g_{\alpha\alpha} - g_{\alpha b}\sigma^{bc}g_{ca} + g_{\alpha b}(g^{bc} - \sigma^{bc})(\rho_{ca} - g_{ca})\right) + \frac{1}{2}\dot{\theta}^a\dot{\theta}^b(g_{ab} + \rho_{ab} - g_{ab}) - V(x^\alpha).
\end{aligned}$$

Simplifying the latter two terms above gives the controlled Lagrangian (5.11) with

$$\begin{aligned}
(g_{\tau,\sigma,\rho})_{\alpha\beta} &= g_{\alpha\beta} + g_{\alpha c}\sigma^{cd}(g_{de} - \sigma_{de})\sigma^{ef}g_{f\beta} + g_{\alpha c}(g^{cd} - \sigma^{cd})(\rho_{de} - g_{de})(g^{ef} - \sigma^{ef})g_{f\beta} \\
(g_{\tau,\sigma,\rho})_{\alpha b} &= g_{\alpha c}(g^{cd} - \sigma^{cd})\rho_{db} \\
(g_{\tau,\sigma,\rho})_{ab} &= \rho_{ab}.
\end{aligned}$$

To find the horizontal component of the kinetic energy metric, we “complete the square” as in Section 5.1.1.

$$\begin{aligned}
&\frac{1}{2}(g_{\tau,\sigma,\rho})_{\alpha\beta}\dot{x}^\alpha\dot{x}^\beta + (g_{\tau,\sigma,\rho})_{\alpha b}\dot{x}^\alpha\dot{\theta}^b + \frac{1}{2}(g_{\tau,\sigma,\rho})_{ab}\dot{\theta}^a\dot{\theta}^b = \\
&\quad \frac{1}{2}\left(g_{\alpha\beta} + g_{\alpha c}\sigma^{cd}(g_{de} - \sigma_{de})\sigma^{ef}g_{f\beta} + g_{\alpha c}(g^{cd} - \sigma^{cd})(\rho_{de} - g_{de})(g^{ef} - \sigma^{ef})g_{f\beta}\right)\dot{x}^\alpha\dot{x}^\beta \\
&\quad - \frac{1}{2}\rho_{ab}\left((g^{ac} - \sigma^{ac})g_{c\alpha}\dot{x}^\alpha\right)\left((g^{bd} - \sigma^{bd})g_{d\beta}\dot{x}^\beta\right) \\
&\quad + \rho_{ab}\left(\frac{1}{2}\dot{\theta}^a\dot{\theta}^b + (g^{bc} - \sigma^{bc})g_{c\alpha}\dot{\theta}^a\dot{x}^\alpha + \frac{1}{2}\left((g^{ac} - \sigma^{ac})g_{c\alpha}\dot{x}^\alpha\right)\left((g^{bd} - \sigma^{bd})g_{d\beta}\dot{x}^\beta\right)\right)
\end{aligned}$$

Recall that the controlled momentum conjugate to θ^a is given by

$$\bar{J}_a = \frac{\partial L_{\tau,\sigma,\rho}}{\partial \dot{\theta}^a} = \rho_{ab}\left(\dot{\theta}^a + (g^{bc} - \sigma^{bc})g_{c\alpha}\dot{x}^\alpha\right).$$

Substituting above gives

$$\frac{1}{2}(g_{\tau,\sigma,\rho})_{\alpha\beta}\dot{x}^\alpha\dot{x}^\beta + (g_{\tau,\sigma,\rho})_{\alpha b}\dot{x}^\alpha\dot{\theta}^b + \frac{1}{2}(g_{\tau,\sigma,\rho})_{ab}\dot{\theta}^a\dot{\theta}^b = \frac{1}{2}A_{\alpha\beta}\dot{x}^\alpha\dot{x}^\beta + \frac{1}{2}\rho^{ab}\bar{J}_a\bar{J}_b \quad (\text{E.1})$$

where $A_{\alpha\beta}$ is the coordinate expression for g_σ , the horizontal component of the kinetic energy metric:

$$\begin{aligned} A_{\alpha\beta} &= g_{\alpha\beta} + g_{\alpha a}\sigma^{ab}(g_{bc} - \sigma_{bc})\sigma^{cd}g_{d\beta} + g_{\alpha a}(g^{ab} - \sigma^{ab})(\rho_{bc} - g_{bc})(g^{cd} - \sigma^{cd})g_{d\beta} \\ &\quad - g_{\alpha a}(g^{ab} - \sigma^{ab})\rho_{bc}(g^{cd} - \sigma^{cd})g_{d\beta} \\ &= g_{\alpha\beta} + g_{\alpha a}\sigma^{ab}(g_{bc} - \sigma_{bc})\sigma^{cd}g_{d\beta} - g_{\alpha a}(g^{ab} - \sigma^{ab})g_{bc}(g^{cd} - \sigma^{cd})g_{d\beta} \\ &= g_{\alpha\beta} + g_{\alpha a}\sigma^{ab}g_{bc}\sigma^{cd}g_{d\beta} - g_{\alpha a}\sigma^{ab}g_{b\beta} - g_{\alpha a}g^{ab}g_{b\beta} + 2g_{\alpha a}\sigma^{ab}g_{b\beta} - g_{\alpha a}\sigma^{ab}g_{bc}\sigma^{cd}g_{d\beta} \\ &= g_{\alpha\beta} - g_{\alpha a}(g^{ab} - \sigma^{ab})g_{b\beta}. \end{aligned}$$

E.2 Identities for $B_{\alpha\beta}$ and B_{ab} .

Recall that

$$\begin{pmatrix} g_{\alpha\beta} & g_{\alpha b} \\ g_{a\beta} & g_{ab} \end{pmatrix}^{-1} = \begin{pmatrix} B^{\alpha\beta} & -B^{\alpha\gamma}g_{\gamma c}g^{cb} \\ -B^{ac}g_{c\gamma}g^{\gamma\beta} & B^{ab} \end{pmatrix}.$$

Then, by construction,

$$g_{\alpha\beta}B^{\beta\gamma} - g_{\alpha b}B^{bd}g_{d\delta}g^{\delta\gamma} = \delta_\alpha^\gamma \quad (\text{E.2})$$

$$-g_{\alpha\beta}B^{\beta\delta}g_{\delta d}g^{dc} + g_{\alpha b}B^{bc} = 0 \quad (\text{E.3})$$

$$g_{a\beta}B^{\beta\gamma} - g_{ab}B^{bd}g_{d\delta}g^{\delta\gamma} = 0 \quad (\text{E.4})$$

$$-g_{a\beta}B^{\beta\delta}g_{\delta d}g^{dc} + g_{ab}B^{bc} = \delta_a^c. \quad (\text{E.5})$$

Using equation (E.2), we may write $B^{\alpha\beta}$ in terms of B^{ab} ,

$$B^{\alpha\beta} = g^{\alpha\beta} + g^{\alpha\gamma} g_{\gamma a} B^{ab} g_{b\delta} g^{\delta\beta}. \quad (\text{E.6})$$

Similarly, using equation (E.5), we may write

$$B^{ab} = g^{ab} + g^{ac} g_{c\alpha} B^{\alpha\beta} g_{\beta d} g^{db}. \quad (\text{E.7})$$

E.3 Proof of Proposition 5.2.2.

Recall the assumption that, at an instant,

$$\bar{J}_a = \left(1 + \frac{1}{\psi}\right)^{-1} D_{ab} g^{bc} g_{c\alpha} B^{\alpha\beta} A_{\beta\gamma} \dot{x}^\gamma$$

so that

$$\dot{E}_{\tau,\sigma,\rho,\psi} = \dot{x}^\alpha A_{\alpha\beta} B^{\beta\gamma} \left(\delta_\gamma^\psi - g_{\gamma a} g^{ab} k_b^\psi\right) F_\psi \quad (\text{E.8})$$

Here, we show that

$$\delta_\alpha^\beta - g_{\alpha a} g^{ab} k_b^\beta = B_{\alpha\gamma} A^{\alpha\beta}.$$

First, observe that

$$\begin{aligned} \left(\delta_\alpha^\beta + g_{\alpha a} D^{ab} k_b^\beta\right) \left(\delta_\beta^\gamma - g_{\beta c} g^{cd} k_d^\gamma\right) &= \delta_\alpha^\gamma - g_{\alpha a} \left(g^{ab} - D^{ab} + D^{ac} k_c^\psi g_{\psi b}\right) k_b^\gamma \\ &= \delta_\alpha^\gamma - g_{\alpha a} \left(g^{ab} - D^{ab} + \sigma^{ac} g_{c\delta} B^{\delta\psi} g_{\psi b}\right) k_b^\gamma \\ &= \delta_\alpha^\gamma. \end{aligned}$$

Thus

$$\begin{aligned}(\delta_{\alpha}^{\beta} - g_{\alpha a} g^{ab} k_b^{\beta}) &= (\delta_{\alpha}^{\beta} + g_{\alpha a} D^{ab} k_b^{\beta})^{-1} \\ &= \left((B_{\beta\gamma} + g_{\beta a} \sigma^{ab} g_{b\gamma}) B^{\gamma\alpha} \right)^{-1} \\ &= B_{\alpha\gamma} A^{\gamma\beta}.\end{aligned}$$

Substituting into equation (E.8) gives

$$\dot{E}_{\tau,\sigma,\rho,\psi} = \dot{x}^{\alpha} F_{\alpha}. \quad (\text{E.9})$$

Appendix F

Experimental Rotary Arm Pendulum

The parameter values for the experimental apparatus described in Section 5.2.3 are

$$M = 0.259 \text{ kg}, \quad R = 0.211 \text{ m}, \quad m = 0.130 \text{ kg}, \quad l = 0.332 \text{ m}.$$

The effect of physical dissipation in the pendulum link and in the rotor arm was identified experimentally. Friction in the pendulum link is well-approximated by a viscous friction model,

$$F_\theta = -d_\theta \dot{\theta} \tag{F.1}$$

where

$$d_\theta = 0.00015 \text{ kgM}^2/\text{s}.$$

Figure F.1 compares the free response of the pendulum link to an initial displacement, with the rotor arm locked in place, to a simulated response to the same initial condition. The damping model in equation (F.1) is used in the simulation. As can be seen in the figure, the damping model gives a slight error in phase and velocity, but predicts amplitude well. (Note: In Figure F.1, $\theta = 0$ corresponds to the pendulum hanging vertically down.)

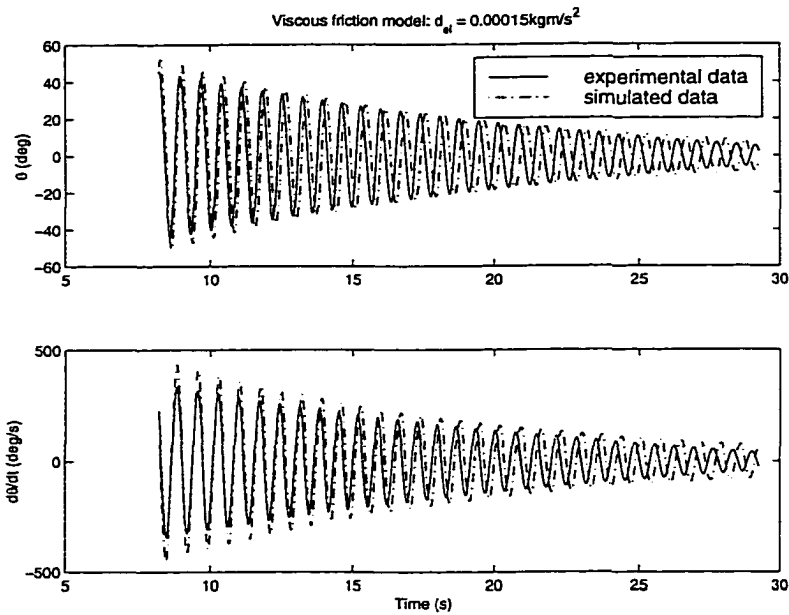


Figure F.1: Elevation response to initial perturbation.

Though viscous friction provides a good model of damping in the pendulum link, it was found that damping in the azimuthal direction is best approximated by a Coulomb friction model,

$$F_{\phi} = -d_{\phi} \text{sign}(\dot{\phi}) \quad (\text{F.2})$$

where

$$d_{\phi} = 0.0096 \text{ kgm}^2/\text{s}.$$

Figure F.2 compares simulation with experiment. The plot shows the initial condition response of the pendulum rotor arm (without the pendulum link) to an initial velocity as well as a simulated response to the same initial conditions using the damping model in equation (F.2). The Coulomb friction model matches the physical response very well, except for a slight “one per rev” oscillation in the azimuthal velocity..

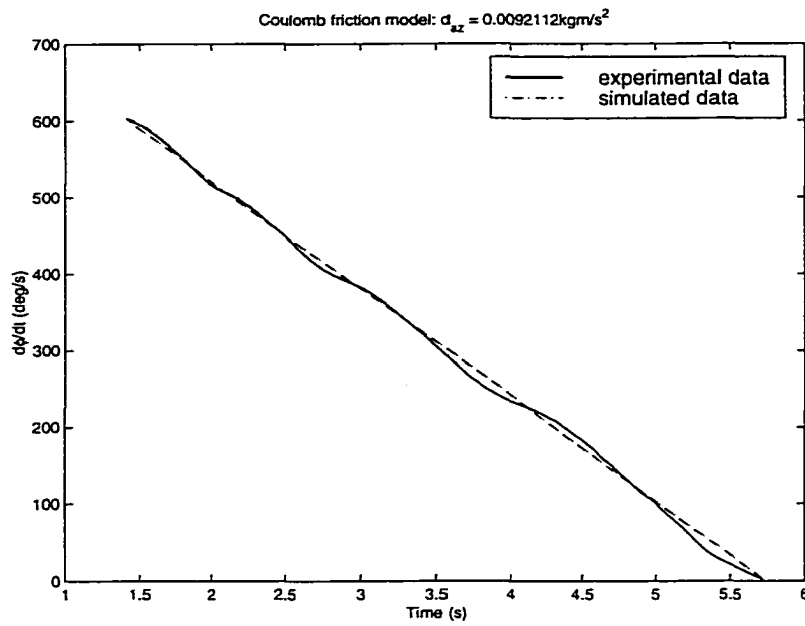


Figure F.2: Azimuthal velocity response to initial perturbation.

Appendix G

Computations for Spacecraft Example.

In Section 5.3.2, we design feedback dissipation to drive the negative semidefinite function $\bar{E}_{\bar{\Phi}, \Psi}$ to its maximum value. To conclude that $\dot{\bar{E}}_{\bar{\Phi}, \Psi} \geq 0$ under the influence of external and feedback dissipation, one requires that $\bar{d} > 0$ and that

$$\begin{aligned}
 0 &\leq \left[X_{\alpha\beta} - \frac{1}{2} \left(1 + \frac{1}{\psi}\right)^{-2} Y_{\alpha}^a \bar{d}_{ab} Y_{\beta}^b + \left(1 + \frac{1}{\psi}\right)^{-1} (Y_{\alpha}^a g_{a\beta} + g_{\beta a} Y_{\alpha}^a) - g_{\alpha a} \bar{d}^{ab} g_{b\beta} \right] \\
 &= \text{diag} \left(-\left(1 - \frac{\lambda_1}{\lambda_2}\right) d_1, 0, -I_{C_3} \left(\frac{1}{\lambda_3} - \frac{1}{\lambda_2}\right) d_3 \right) \\
 &\quad - \frac{J_3}{2\bar{d}} \left(\left(1 + \frac{1}{\psi}\right)^{-1} \frac{1}{\rho\lambda_2} + \frac{\rho-1}{\rho I_3} \right)^2 d_3^2 \mathbf{e}_3 \mathbf{e}_3^T \\
 &\quad + 2J_3 \left(\frac{1}{\rho\lambda_2} + \left(1 + \frac{1}{\psi}\right) \frac{\rho-1}{\rho I_3} \right) d_3 \mathbf{e}_3 \mathbf{e}_3^T + J_3 \bar{d} \mathbf{e}_3 \mathbf{e}_3^T. \tag{G.1}
 \end{aligned}$$

The first element of the diagonal matrix on the right-hand side of (G.1) is positive and the second is zero. The third diagonal element may be written

$$J_3 \bar{d} \left\{ -\frac{1}{2} \left(\frac{\beta + \alpha\delta}{\alpha} \right)^2 x^2 + \left(\gamma + \frac{2}{\alpha} (\beta + \alpha\delta) \right) x - 1 \right\} \tag{G.2}$$

where

$$\begin{aligned}\alpha &= 1 + \frac{1}{\psi}, \\ \beta &= \frac{1}{\rho\lambda_2}, \\ \delta &= \frac{\rho - 1}{\rho} \frac{1}{I_3}, \\ \gamma &= -\frac{I_{C_3}}{J_3} \left(\frac{1}{\lambda_3} - \frac{1}{\lambda_2} \right) > 0, \\ x &= \frac{d_3}{d}.\end{aligned}$$

Choosing the control gain $k > 1$ (which defines ρ) and choosing ψ according to condition (5.110) gives

$$\alpha < \frac{J_3}{\rho(\lambda_2 - I_{C_3})}, \quad \beta > 0, \quad \delta < 0, \quad \gamma > 0.$$

There is a range of x such that the expression (G.2) is positive only if the discriminant of the term quadratic in x is positive. This discriminant may be written

$$\begin{aligned}\gamma^2 + \frac{4}{\alpha}\gamma(\beta + \alpha\delta) + \left(\frac{4}{\alpha^2} - \frac{2}{\alpha^2} \right) (\beta + \alpha\delta)^2 \\ = \left(\gamma \pm \frac{\sqrt{2}}{\alpha}(\beta + \alpha\delta) \right)^2 + \left(\frac{4 \mp 2\sqrt{2}}{\alpha} \right) \gamma(\beta + \alpha\delta).\end{aligned}\quad (\text{G.3})$$

Suppose that α is chosen negative. Then the latter term in (G.3) is negative and the discriminant may or may not be positive. Suppose that α is chosen positive (subject to condition (5.110)). Then choosing α to satisfy

$$\alpha < \min \left(-\frac{\beta}{\delta}, \frac{J_3}{\rho(\lambda_2 - I_{C_3})} \right) \quad (\text{G.4})$$

makes the discriminant positive so that there is some range of x within which the expres-

sion (G.2) is positive. The roots of (G.2) are

$$x_{\pm} = -\left(\frac{\alpha}{\beta + \alpha\delta}\right)^2 \left[-\left(\gamma + \frac{2}{\alpha}(\beta + \alpha\delta)\right) \pm \sqrt{\left(\gamma + \frac{2}{\alpha}(\beta + \alpha\delta)\right)^2 - \frac{2}{\alpha^2}(\beta + \alpha\delta)^2} \right]. \quad (\text{G.5})$$

Any value of x lying between these two roots makes (G.2) positive. Furthermore, x is positive in this range, so a positive value of \bar{d} corresponds to any choice of $x \in (x_-, x_+)$. A reasonable choice of x is the one which maximizes (G.2):

$$x = \frac{d_3}{\bar{d}} = \frac{\alpha^2 \left(\gamma + \frac{2}{\alpha}(\beta + \alpha\delta)\right)}{(\beta + \alpha\delta)^2} \quad (\text{G.6})$$

Bibliography

- [1] R. Abraham and J.E. Marsden. *Foundations of Mechanics*. Addison-Wesley, Reading, MA, 2nd edition, 1987.
- [2] R. Abraham, J.E. Marsden, and T.S. Ratiu. *Manifolds, Tensor Analysis, and Applications*. Springer-Verlag, New York, NY, 2nd edition, 1988.
- [3] H. J. Allen. Estimation of the forces and moments acting on inclined bodies of revolution of high fineness ratio. *NACA RM A9126*, 1949.
- [4] H. J. Allen and E. W. Perkins. A study of effects of viscosity on flow over slender inclined bodies of revolution. *NACA Report 1048*, 1951.
- [5] D. E. Anderson, C. A. Buck, and R. Cohen. Applications of free-flying cameras for spaced-based operations. In *SAE/AIAA International Conference on Environmental Systems*, Friedrichshafen, Germany, June 1994.
- [6] V.I. Arnold. *Mathematical Methods of Classical Mechanics*. Springer-Verlag, New York, NY, 2nd edition, 1989.
- [7] A. Ashford. *If I Found a Wistful Unicorn*. Peachtree Publishers, Ltd., Atlanta, 1978. Illustrations by Bill Drath.

- [8] A. Astolfi, D. Chhabra, and R. Ortega. Asymptotic stabilization of selected equilibria of the underactuated Kirchhoff's equations. In *Proc. American Control Conference*, Washington, D.C., June 2001. To appear.
- [9] R. Bellman. *Introduction to Matrix Analysis*. McGraw-Hill Book Company, Inc., New York, NY, 1960.
- [10] A. M. Bloch, D.E. Chang, N. E. Leonard, and J. E. Marsden. Controlled Lagrangians and the stabilization of mechanical systems II: Potential shaping and tracking. *IEEE Transactions on Automatic Control*, 2000. Submitted.
- [11] A. M. Bloch, D.E. Chang, N. E. Leonard, J. E. Marsden, and C. Woolsey. Asymptotic stabilization of Euler-Poincaré mechanical systems. In N. E. Leonard and R. Ortega, editors, *Lagrangian and Hamiltonian Methods for Nonlinear Control*, pages 51–56, Princeton, NJ, March 2000. Pergamon Press.
- [12] A. M. Bloch, P. S. Krishnaprasad, J. E. Marsden, and T. Ratiu. Dissipation induced instabilities. *Ann. Inst. H. Poincaré, Analyse Nonlinéaire*, 11:37–90, 1994.
- [13] A. M. Bloch, P. S. Krishnaprasad, J. E. Marsden, and G. Sánchez de Alvarez. Stabilization of rigid body dynamics by internal and external torques. *Automatica*, 28(4):745–756, 1992.
- [14] A. M. Bloch, N. E. Leonard, and J. E. Marsden. Stabilization of mechanical systems using controlled Lagrangians. In *Proc. IEEE Conf. Decision and Control*, pages 2356–2361, San Diego, CA, December 1997.

- [15] A. M. Bloch, N. E. Leonard, and J. E. Marsden. Matching and stabilization by the method of controlled Lagrangians. In *Proc. IEEE Conf. Decision and Control*, pages 1446–1451, Tampa, FL, December 1998.
- [16] A. M. Bloch, N. E. Leonard, and J. E. Marsden. Stabilization of the pendulum on a rotor arm by the method of controlled Lagrangians. In *Proc. Int. Conf. on Robotics and Automation*, pages 500–505, IEEE, 1999.
- [17] A. M. Bloch, N. E. Leonard, and J. E. Marsden. Controlled Lagrangians and the stabilization of mechanical systems I: The first matching theorem. *IEEE Transactions on Automatic Control*, 2000. In press.
- [18] A. M. Bloch, N. E. Leonard, and J. E. Marsden. Controlled Lagrangians and the stabilization of Euler-Poincaré mechanical systems. *International Journal of Robust and Nonlinear Control*, 2000. In press.
- [19] W.M. Boothby. *An Introduction to Differential Manifolds and Riemannian Geometry*. Academic Press, 2nd edition, 1986.
- [20] R. W. Brockett. Control theory and analytic mechanics. In R. W. Brockett, R. S. Millman, and H. J. Sussmann, editors, *Volume VII of Lie Groups: History, Frontiers, and Applications*, pages 1–49, Brookline, MA, 1976. Math Sci Press.
- [21] F. Bullo. Stabilization of relative equilibria for underactuated systems on riemannian manifolds. *Automatica*, 36(12), December 2000. To appear.
- [22] A. Cannas da Silva and A. Weinstein. *Geometric Models for Noncommutative Algebras*. American Mathematical Society, 1999.

- [23] L. Cesari. *Asymptotic Behavior and Stability Problems in Ordinary Differential Equations*. Springer-Verlag, New York, 3rd edition, 1971.
- [24] D. E. Chang and J. E. Marsden. Asymptotic stabilization of the heavy top using controlled Lagrangians. In *Proc. 39th IEEE Conf. Decision and Control*, Sydney, Australia, December 2000. To appear.
- [25] T.B. Curtin, J.G. Bellingham, Catipovic J., and D. Webb. Autonomous oceanographic sampling networks. *Oceanography*, 6:86–94, 1993.
- [26] E. A. Eichelbrenner. Décollement laminaire en trois dimensions sur un obstacle fini. *La Recherche Aeronautique: ONERA Publication No. 89*, 1957.
- [27] E. A. Eichelbrenner and A. Oudart. Méthode de calcul de la couche limite tridimensionnelle: Application à un corps fuselé incliné sur le vent. *La Recherche Aeronautique: ONERA Publication No. 76*, 1955.
- [28] B. S. Fadnis. Boundary layer on rotating spheroids. *Zeitschrift fur Angewandte Mathematik und Physik V*, 1954.
- [29] T. Fossen. *Guidance and Control of Ocean Vehicles*. John Wiley and Sons, New York, NY, 1995.
- [30] S. F. Hoerner. *Fluid Dynamic Drag*. Published by the author, Midland Park, NJ, 1965.
- [31] P. Holmes, J. Jenkins, and N. E. Leonard. Dynamics of the Kirchhoff equations I: Coincident centers of gravity and buoyancy. *Physica D*, 118:311–342, 1998.
- [32] E. J. Hopkins. A semi-empirical method for calculating the pitching moment of bodies of revolution at low mach numbers. *NACA RM A51C14*, 1951.

- [33] N. E. Hoskin. The laminar boundary layer on a rotating sphere. *50 Jahre Grenzschichtforschung*, 1955.
- [34] S. M. Jalnapurkar and J. E. Marsden. Stabilization of relative equilibria. *IEEE Transactions on Automatic Control*, 45(8):1483–1491, 2000.
- [35] J. J. Jenkins. Autonomous underwater vehicle dynamics and motion tracking. Master's thesis, Princeton University, Princeton, NJ, June 1999.
- [36] K. Kawaguchi, T. Ura, Y. Tomoda, and H. Kobayashi. Development and sea trials of a shuttle type AUV "ALBAC". In *Proc. 8th Int. Symp. Unmanned Untethered Submersible Technology*, pages 7–13, 1993.
- [37] H. Khalil. *Nonlinear Systems*. Prentice Hall, Upper Saddle River, New Jersey, 2nd edition, 1996.
- [38] V. V. Kozlov. Heavy rigid body falling in an ideal fluid. *Izv. RAN Mekhanika Tverdogo Tela (Mechanics of Solids)*, 24(5):10–17, 1989.
- [39] V. V. Kozlov. On the fall of a heavy cylindrical solid in a liquid. *Izv. RAN Mekhanika Tverdogo Tela (Mechanics of Solids)*, 28(4):113–117, 1993.
- [40] P. S. Krishnaprasad. Lie-Poisson structures, dual-spin spacecraft and asymptotic stability. *Nonlinear Anal., Theory, Meth. & App.*, 9(10):1011–1035, 1985.
- [41] H. Lamb. *Hydrodynamics*. Dover, New York, 6th edition, 1932.
- [42] N. E. Leonard. Stability of a bottom-heavy underwater vehicle. *Automatica*, 33(3):331–346, 1997.

- [43] N. E. Leonard. Stabilization of underwater vehicle dynamics with symmetry-breaking potentials. *Systems and Control Letters*, 32:35–42, 1997.
- [44] N. E. Leonard and J. E. Marsden. Stability and drift of underwater vehicle dynamics: Mechanical systems with rigid motion symmetry. *Physica D*, 105:130–162, 1997.
- [45] N. E. Leonard and C. Woolsey. Internal actuation for intelligent underwater vehicle control. In *Proc. Tenth Yale Workshop on Adaptive and Learning Systems*, pages 295–300, New Haven, CT, 1998.
- [46] M. R. Liberzon. On the stability of motion of an axisymmetric rotating flight vehicle. *Izvestiya Akad. Nauk. SSSR, Mekhanika Tverdogo Tela (Soviet Journal of Contemporary Physics)*, 23(5):9–13, 1988.
- [47] P. Likins. Spacecraft attitude dynamics and control – a personal perspective on early developments. *Journal of Guidance, Control, and Dynamics*, 9(2):129–134, 1986.
- [48] J. H. Maddocks. On the stability of relative equilibria. *IMA Journal of Applied Mathematics*, 46:71–99, 1991.
- [49] J. E. Marsden. *Lectures on Mechanics*. Cambridge University Press, New York, New York, 1992.
- [50] J. E. Marsden and T. S. Ratiu. *Introduction to Mechanics and Symmetry*. Springer-Verlag, New York, New York, 1994.
- [51] J. E. Marsden, T. S. Ratiu, and A. Weinstein. Semidirect products and reduction in mechanics. *Transactions of the American Mathematical Society*, 281:147–177, 1984.

- [52] J. C. Martin. On the Magnus effects caused by the boundary-layer displacement thickness on the bodies of revolution at small angles of attack. *Journal of Aeronautical Science*, 24:421–429, 1957.
- [53] R.M. Murray, Z. Li, and S.S. Sastry. *A Mathematical Introduction to Robotic Manipulation*. CRC Press, Boca Raton, FL, 1994.
- [54] H. Nijmeijer and A. van der Schaft. *Nonlinear Dynamical Control Systems*. Springer, New York, NY, 1990.
- [55] K. Nomizu. *Lie Groups and Differential Geometry*. The Mathematical Society of Japan, 1956.
- [56] R. Ortega, A. Loría, P. J. Nicklasson, and H. Sira-Ramírez. *Passivity-based Control of Euler-Lagrange Systems*. Springer-Verlag, London, 1998.
- [57] R. Ortega and M. W. Spong. Stabilization of underactuated mechanical systems via interconnection and damping assignment. In N. E. Leonard and R. Ortega, editors, *Lagrangian and Hamiltonian Methods for Nonlinear Control*, pages 69–74, Princeton, NJ, March 2000. Pergamon Press.
- [58] G. Patrick. Relative equilibria of hamiltonian systems with symmetry: Linearization, smoothness, and drift. *Journal of Nonlinear Science*, 5:373–418, 1995.
- [59] W.F. Putnam, M. Maughmer, H. C. Curtiss Jr., and J. J. Traybar. Aerodynamics and hovering control of LTA vehicles. *Princeton Technical Report 1339*, 1977.
- [60] V.N. Rubanovskii. On the precessional-screw motions of a solid immersed in liquid. *Prikl. Matem. Mekhan.*, 49(2):160–165, 1985.

- [61] J. C. Simo, D. Lewis, and J. E. Marsden. Stability of relative equilibria. part I: The reduced energy-momentum method. *Archive for Rational Mechanics and Analysis*, 115:15–59, 1991.
- [62] M. Spivak. *A Comprehensive Introduction to Differential Geometry*. Publish or Perish, 1976.
- [63] A. J. van der Schaft. Stabilization of Hamiltonian systems. *Nonlinear Analysis: Theory, Methods, and Applications*, 10(10):1021–1035, 1986.
- [64] S. von Luthander and A. Rydberg. Experimentelle untersuchung über den luftwiderstand bei einerum eine mit der windrichtung parallele achse rotierenden kugel. *Zeitschrift fur Physik*, 36:552–558, 1935.
- [65] F.W. Warner. *Foundations of Differentiable Manifolds and Lie Groups*. Springer Verlag, New York, 2nd edition, 1989. Volume 94 of *GTM*.
- [66] D. C. Webb and P. J. Simonetti. The SLOCUM AUV: An environmentally propelled underwater glider. In *Proc. 11th International Symposium on Unmanned Untethered Submersible Technology*, pages 75–85, Durham, N.H., August 1999.
- [67] T. G. Wetzel and R. L. Simpson. Unsteady crossflow separation location measurements on a maneuvering 6:1 prolate spheroid. *AIAA Journal*, 36(11):2063–2071, 1998.
- [68] C. Woolsey and N. E. Leonard. Global asymptotic stabilization of an underwater vehicle using internal rotors. In *Proc. IEEE Conf. Decision and Control*, pages 2527–2532, Phoenix, AZ, December 1999.
- [69] C. Woolsey and N. E. Leonard. Underwater vehicle stabilization by internal rotors. In *Proc. American Control Conf.*, pages 3417–3421, San Diego, CA, June 1999.

- [70] C. Woolsey and N. E. Leonard. Modification of Hamiltonian structure to stabilize an underwater vehicle. In N. E. Leonard and R. Ortega, editors, *Lagrangian and Hamiltonian Methods for Nonlinear Control*, pages 175–176, Princeton, NJ, March 2000. Pergamon Press.